

**Effect of elevated atmospheric carbon
dioxide concentrations on soil
microbial processes and the soil
microbiome**

Thesis submitted in partial fulfillment
of the requirements for the degree of
Doctor rerum naturalium
(Dr. rer. nat.)

Submitted by
M. Sc. David Rosado Porto

Faculty of Agricultural Sciences, Nutritional Sciences
and Environmental Management
Institute of Applied Microbiology
Justus-Liebig-University Gießen, Germany
Gießen, 2022

PUBLICATIONS

International peer reviewed scientific publications:

Rosado-Porto, D., Ratering, S., Cardinale, M., Maisinger, C., Moser, G., Deppe, M., Müller, C., & Schnell, S. (2021). Elevated Atmospheric CO₂ Modifies Mostly the Metabolic Active Rhizosphere Soil Microbiome in the Giessen FACE Experiment. *Microbial Ecology*. <https://doi.org/10.1007/s00248-021-01791-y>

Abdullaeva, Y., Ratering, S., Ambika Manirajan, B., **Rosado-Porto, D.**, Schnell, S., & Cardinale, M. (2022). Domestication Impacts the Wheat-Associated Microbiota and the Rhizosphere Colonization by Seed- and Soil-Originated Microbiomes, Across Different Fields. *Frontiers in Plant Science*, 12(January). <https://doi.org/10.3389/fpls.2021.806915>

Publication submitted

Rosado-Porto, D., Ratering, S., Wohlfahrt, Y., Schneider, B., Glatt, A., & Schnell, S. Elevated atmospheric CO₂ concentrations caused a shift of the metabolically active microbiome in vineyard soil. Submitted to BMC Microbiology. ISSN: 1471-2180

Publication to be submitted

Rosado-Porto, D., Ratering, S., Moser, G., Deppe, M., Müller, C., & Schnell, S. Soil metatranscriptome demonstrates a shift in C, N and S metabolism of a grassland ecosystem in response to elevated atmospheric CO₂.

Sacharow, J., **Rosado-Porto, D.**, Weigel, V., Ratering, S., Rühl, M., Schnell, S., & Suarez, C. The bacterial composition shifted during cultivation steps of *Pleurotus ostreatus* analyzed by 16S rRNA gene metabarcoding.

Publications in preparation

Abdullaeva, Y., Ratering, S., Schnell, S., **Rosado-Porto, D.**, Ambika Manirajan, B., Glatt, A. & Cardinale, M. Host-dependent shifts of the inter-kingdom interactions in the wheat root microbiota during plant domestication.

Aranguren-Diaz, Y., Machado Sierra, E., Serrano, M., **Rosado-Porto, D.**, Ratering, S., & Schnell, S. Agricultural land use effect on soil microbiome from a Colombian dry Forest.

Quiroga, S., Ratering, S., **Rosado-Porto, D.**, Steffens, D., Kostner, D., & Schnell, S. The rhizosphere microbiome of *Rosa* sp. 'Flower Carpet'- Evaluation of different bacterial strains as plant-growth promoting rhizobacteria.

Poster

Rosado-Porto, D., Ratering, S., Cardinale, M., Maisinger, C., & Schnell, S. (2018) Elevated atmospheric CO₂ modifies the active rhizosphere soil microbiome in the Gi-FACE experiment. 17th International Symposium on Microbial Ecology (ISME17). Leipzig, Germany.

Other publication

Rosado-Porto, D., Bonivento-Calvo, J., Salcedo-Mendoza, S., Molina-Castillo, A., Maestre-Serrano, R., & García, A. D. C. (2021). Determinación de *E. coli* biotipo 1 y *E. coli* O157:H7 en canal de carne bovina en plantas de beneficio del departamento del Atlántico (Colombia). *Revista de Investigaciones Veterinarias Del Perú*, 32(3), e18476. <https://doi.org/10.15381/rivep.v32i3.18476>

Soto-Varela, Z. E., **Rosado-Porto, D.**, Bolívar-Anillo, H. J., González, C. P., Pantoja, B. G., Alvarado, D. E., & Anfuso, G. (2021). Preliminary microbiological coastal water quality determination along the department of Atlántico (Colombia): Relationships with beach characteristics. *Journal of Marine Science and Engineering*, 9(2), 1–17. <https://doi.org/10.3390/jmse9020122>

The present work was carried out at the Institute of Applied Microbiology, Faculty of Agricultural Sciences, Nutritional Sciences and Environmental Management, Justus-Liebig- University, Gießen during the period from June 2017 to January 2022 under the guidance of Prof. Dr. Sylvia Schnell.

I Supervisor: Prof. Dr. Sylvia Schnell

Institute of Applied Microbiology

Justus-Liebig-University

Heinrich-Buff-Ring 26-32, 35392 Gießen, Germany

II Supervisor: Prof. PhD Christoph Müller

Institute for Plant Ecology

Justus-Liebig-University

Heinrich-Buff-Ring 26, 35392 Gießen, Germany

Statement

"I declare that the dissertation here submitted is entirely my own work, written without any illegitimate help by any third party and solely with materials as indicated in the dissertation. I have indicated in the text where I have used texts from already published sources, either word for word or in substance, and where I have made statements based on oral information given to me. At all times during the investigations carried out by me and described in the dissertation, I have followed the principles of good scientific practice as defined in the "Statutes of the Justus-Liebig-University Gießen for the Safeguarding of Good Scientific Practice.

Gießen, 21.01.2022

David Rosado Porto

Table of contents

List of abbreviations _____	I
Summary _____	II
Zusammenfassung _____	III
Chapter 1 Introduction _____	1-5
1.1 Climate change, global warming and greenhouse gases _____	1-6
1.2 Free Air Carbon Dioxide Enrichment experiment (FACE) system _____	1-7
1.2.1 Giessen FACE _____	1-8
1.2.2 WineFACE _____	1-11
1.2.3 Effect of the increase of environmental CO ₂ on plants _____	1-12
1.2.4 FACE experiments on grasslands _____	1-13
1.2.5 FACE experiments on crop plants _____	1-13
1.3 Effect of eCO ₂ on Carbon and Nitrogen Cycles in terrestrial ecosystems _____	1-14
1.3.1 Increment of roots exudates and priming effect _____	1-14
1.3.2 Effect on soil microbial C and N cycles related processes _____	1-15
1.4 rRNA metagenomics: advantages and disadvantages _____	1-17
1.5 Functional metatranscriptomics _____	1-18
1.5.1 Principles, applications and limitations of functional metatranscriptomics _____	1-19
1.5.2 Software and pipelines for the analysis of functional metatranscriptome _____	1-20
1.6 Next generation sequencing data and compositionality _____	1-21
1.6.1 What are compositional data (CoDa)? _____	1-22
1.6.2 Microbiome sequencing data are compositional _____	1-23
1.6.3 Methods to deal with compositional data _____	1-23
1.6.4 Analysis of microbiome data as composition _____	1-24
1.7 Aims of the study _____	1-27
1.8 References _____	1-27
Chapter 2 Elevated atmospheric CO ₂ modifies mostly the metabolic active rhizosphere soil microbiome in the Giessen FACE experiment _____	2-42

Chapter 3 Elevated atmospheric CO ₂ concentrations caused a shift of the metabolically active microbiome in vineyard soil _____	3-59
Chapter 4 Soil metatranscriptome demonstrates a shift in C, N and S metabolisms of a grassland ecosystem in response to elevated atmospheric CO ₂ _____	4-94
Chapter 5 General discussion _____	5-128
Acknowledgements _____	5-140

List of abbreviations

aCO ₂	Ambient atmospheric CO ₂
ALR	Additive log-ratio
ASV	Amplicon sequence variant
cDNA	Complementary DNA
CLR	Centered log-ratio
C:N ratio	Carbon:Nitrogen ratio
CoDa	Compositional data
CODH	Carbon monoxide dehydrogenase
DNA	Deoxyribonucleic acid
DNRA	Dissimilatory NO ₃ ⁻ reduction to NH ₄ ⁺
eCO ₂	Elevated atmospheric CO ₂
FACE	Free Air Carbon Dioxide Enrichment experiment
GHG	Greenhouse gases
Gi-FACE	Giessen FACE
Gt	Gigatons
HTS	High-throughput sequencing
ILR	Isometric log-ratio
IPCC	Intergovernmental Panel on Climate Change
KEGG	Kyoto Encyclopedia of Genes and Genomes
LR	Pairwise log-ratio
mRNA	Messenger RNA
NGS	Next-generation sequencing
NMDS	Non-metric multidimensional scaling
ORF	Open Reading Frame
PCA	Principal component
PCC/ACC	Propionyl-CoA/acetyl-CoA carboxylase
PCoA	Principal co-ordinate
PCR	Polymerase chain reaction
PERMANOVA	Permutational Multivariate Analysis of Variance Using Distance Matrices
PLR	Pivot log-ratio
ppbV	Parts per billion volume
ppmV	Parts per million volume
qPCR	Quantitative PCR
RDA	Redundancy analysis
RNA	Ribonucleic acid
rRNA	Ribosomal RNA
RuBisCo	Ribulose-1,5-bisphosphate carboxylase-oxygenase
SLR	Summated (amalgamated) log-ratio
SOC	Soil organic carbon
SOM	Soil organic matter
TAB	Total aboveground biomass

Summary

Climate change due to the increment of atmospheric concentrations of CO₂ has had several impacts on different ecosystems around the world. Among the effects of elevated CO₂ (eCO₂) on soil ecosystems are its consequences on plant metabolism, which include the increase of plant photosynthetic rates, carbon inputs into soil and root exudation. Due to around 21% of photosynthetically fixed carbon is transferred to soil rhizosphere, eCO₂ has a direct impact on soil microorganisms and the microbial processes that are regulated by them. Therefore, in this work it was analyzed the effects of eCO₂ on the soil microbiome and the soil microbial processes at two Free Air Carbon Dioxide Enrichment experiment (FACE) systems in Hessen, Germany. The Giessen FACE and the Geisenheim VineyardFACE, being the first one located at a grassland field with a long-term exposure to eCO₂ and the latter one situated at vineyard and with a midterm exposure to eCO₂. The soil microbiome was analyzed by high-throughput sequencing methods for the assessment of soil active microorganisms through the analysis of 16S rRNA and mRNA, for taxonomical and functional metagenomics approaches, respectively. Alongside, it was measured the soil microbial activity assessing soil respiration activity, real time qPCR for 16S rRNA and functional genes, soil gas fluxes and soil chemical parameters.

The 16S rRNA results from both facilities demonstrated that eCO₂ treatments were significantly different from the ambient CO₂ ones and areas under higher plant influence were the most affected by eCO₂. Furthermore, 16S rRNA qPCR analyses indicated in the Giessen FACE an increment in the number of active bacteria, oppositely to Geisenheim Vineyard FACE where occurred a decrease of the copy numbers of bacterial 16S rRNA, nonetheless at both sites the total soil activity was augmented in the eCO₂ treatments. Moreover, differential abundance analyses showed that several microbial taxa were significantly affected, either positively or negatively because of eCO₂, being many of these taxa directly involved in the cycling of soil nutrients. Additionally, the analysis of functional genes by qPCR and functional metatranscriptomic approaches indicated affectations in the microbial processes involved in nitrogen (N) and carbon (C) cycles. The data obtained at both sites indicated a lessening of the nitrogen fixation process under eCO₂, suggesting that soil microorganisms are mining the soil organic matter (SOM) in order to fulfill their higher requirements for N due to a higher supply of C at eCO₂ concentrations. Moreover, functional metatranscriptomics from the Giessen FACE showed an increase in carbohydrates and amino acids metabolisms, alongside the augmentation of genes for the degradation of cellulose, chitin and lignin. Concerning

nitrogen cycle, it observed a shift in the metabolism of nitrate (NO_3^-) reduction, with an increment of dissimilatory NO_3^- reduction to ammonium (NH_4^+) (DNRA) pathway and an impairment of denitrification process which explains the increment of N_2O emissions observed in the Giessen FACE.

In general, the results obtained in the present work, demonstrated that eCO_2 and climate change have significantly affected the active soil microbiome at two different ecosystems with different lengths of exposure time to eCO_2 , producing significant alterations in the way that soil microorganisms are using and cycling soil elements.

Zusammenfassung

Der Klimawandel, der auf den Anstieg der CO_2 -Konzentration in der Atmosphäre zurückzuführen ist, hat verschiedene Auswirkungen auf unterschiedliche Ökosysteme in der ganzen Welt. Zu den Auswirkungen von erhöhtem atmosphärischem CO_2 (eCO_2) auf Bodenökosysteme gehören die Folgen für den Pflanzenstoffwechsel, die den Anstieg der Photosyntheseraten der Pflanzen, den Kohlenstoffeintrag in den Boden und die Wurzelexsudation umfassen. Da etwa 21% des photosynthetisch gebundenen Kohlenstoffs in die Rhizosphäre des Bodens gelangt, hat eCO_2 direkte Auswirkungen auf die Bodenmikroorganismen und die von ihnen geführten mikrobiellen Prozesse. Daher wurden in dieser Arbeit die Auswirkungen von eCO_2 auf das Bodenmikrobiom und die mikrobiellen Prozesse im Boden an zwei Free Air Carbon Dioxide Enrichment Experimenten (FACE) in Hessen, Deutschland, untersucht. Das Gießener FACE und das Geisenheimer VineyardFACE, wobei ersteres auf einem Grünlandfeld mit einer langfristigen Exposition mit eCO_2 und letzteres in einer Rebananlage mit einer mittelfristigen Exposition mit eCO_2 angesiedelt ist. Das Bodenmikrobiom wurde mit Hilfe von Hochdurchsatz-Sequenzierungsmethoden analysiert, um die bodenaktiven Mikroorganismen durch die Analyse von 16S rRNA und mRNA für einen taxonomischen bzw. funktionellen Metagenomik-ansatz zu bewerten. Daneben wurde die mikrobielle Aktivität des Bodens durch die Bewertung der Bodenatmungsaktivität, Echtzeit-qPCR für 16S rRNA und funktionelle Gene, Bodengasflüsse und bodenchemische Parameter gemessen.

Die 16S rRNA-Ergebnisse aus beiden Anlagen zeigten, dass sich die eCO_2 -Behandlungen signifikant von denen mit normalem atmosphärischem CO_2 unterschieden und dass die Bereiche mit höherem Pflanzeneinfluss am stärksten von eCO_2 betroffen waren. Darüber hinaus zeigten 16S rRNA qPCR-Analysen im Gießener

FACE eine Zunahme der Anzahl aktiver Bakterien, im Gegensatz zum Geisenheimer Vineyard-FACE, wo eine Abnahme der Kopienzahlen der bakteriellen 16S rRNA auftrat, nichtsdestotrotz war an beiden Standorten die gesamte Bodenaktivität bei den eCO₂-Behandlungen erhöht. Darüber hinaus zeigten Analysen der differentiellen Abundanz, dass mehrere mikrobielle Taxa durch eCO₂ entweder positiv oder negativ beeinflusst wurden, da viele dieser Taxa direkt in den Nährstoffkreislauf des Bodens eingebunden sind. Die Analyse funktioneller Gene mittels qPCR und funktioneller Metatranskriptomik deutete Beeinträchtigungen von mikrobiellen Prozessen an, die am Stickstoff- und Kohlenstoffkreislauf beteiligt sind. Die an beiden Standorten gewonnenen Daten wiesen auf eine Verringerung der Stickstofffixierung unter eCO₂ hin, was darauf hindeutet, dass die Bodenmikroorganismen die organische Bodensubstanz (SOM) abbauen, um ihren höheren Bedarf an Stickstoff zu decken, da bei eCO₂-Konzentrationen eine größere Verfügbarkeit von Kohlenstoff besteht. Darüber hinaus zeigte die funktionelle Metatranskriptomik des Gießener FACE eine Zunahme des Kohlenhydrat- und Aminosäurestoffwechsels sowie eine Zunahme von Genen für den Abbau von Zellulose, Chitin und Lignin. Was den Stickstoffkreislauf betrifft, so wurde eine Verschiebung im Stoffwechsel der Nitrat (NO₃⁻)-Reduktion beobachtet, mit einer Zunahme des dissimilatorischen NO₃⁻-Reduktionswegs zu Ammonium (NH₄⁺) (DNRA) und einer Verminderung des Denitrifikationsprozesses, was die in der Gießener FACE beobachtete Zunahme der N₂O-Emissionen erklärt.

Generell zeigen die Ergebnisse der vorliegenden Arbeit, dass eCO₂ und der Klimawandel das aktive Bodenmikrobiom in zwei verschiedenen Ökosystemen mit unterschiedlich langer Exposition mit eCO₂ signifikant beeinflusst haben, was zu signifikanten Veränderungen in der Art und Weise führt, wie Bodenmikroorganismen Bodenelemente nutzen und umsetzen.

Chapter 1 Introduction

1.1 Climate change, global warming and greenhouse gases

Over the last five decades anthropogenic greenhouse gas (GHG) emissions have steadily increased, with larger absolute values between 2000 and 2019 (IPCC, 2014, 2021). Atmospheric carbon dioxide (CO₂) accounts for a great proportion of GHG emissions, and it has been demonstrated that its concentrations in the year 2019 were the highest in the last 2 million years (DOE.2020, 2020; IPCC, 2021). Moreover, the Intergovernmental Panel on Climate Change (IPCC) also has described in its synthesis report from 2014, that not only CO₂ emissions, but the atmospheric levels of other GHG as methane (CH₄), and nitrous oxide (N₂O) are the highest in history since the pre-industrial era (Fig. 1a) (IPCC, 2014). Besides, *The Physical Science Basis* IPCC report from 2021 indicated that since 2011 GHG concentrations have continued to increase in the atmosphere, reaching annual averages of 410 parts per million volume (ppmV) for CO₂, 1866 parts per billion volume (ppbV) for CH₄, and 332 ppbV for N₂O in 2019, which represented a rise of 47%, 156% and 23% respectively, in comparison with their values from 1750 (IPCC, 2021). Taking into account the different sources that contribute to GHG emissions, fossil fuel combustion and industrial processes are responsible for about 78% of the total GHG (Fig. 1b). Furthermore, according to the IPCC, economic and population growth have been the most important drivers of rises in atmospheric CO₂ concentrations from fossil fuel combustion (IPCC, 2014).

First assessments on the contribution of atmospheric CO₂ to the global greenhouse effect were performed in the 19th century by Arrhenius, who also hypothesized about the relation between atmospheric CO₂ concentrations and long-term variations in climatic conditions (Arrhenius, 1986). Decades later, observations of atmospheric CO₂ from the 1950s to the 1960s indicated the seasonal cycle in CO₂ concentration and that it was steadily increasing. Moreover, this increase was most likely due to human activities, and the consequences for climate could be severe (Baes et al., 1977; DOE.2020, 2020). Additionally, between 1850 and 2019, cumulative anthropogenic CO₂ emissions to the atmosphere were 2390 ± 240 Gt CO₂ (IPCC, 2021).

A clear outcome of the increment of GHG is the warming of the global climate system, demonstrated by a near-linear relationship between cumulative anthropogenic CO₂ emissions and the global warming they cause. Each 1000 Gt CO₂ of cumulative CO₂ emissions cause an increment of 0.27°C to 0.63°C in global surface temperature with a best estimate of 0.45°C (Fig. 1c) (IPCC, 2021). Furthermore, each of the last four decades have been successively warmer at the Earth's surface than any preceding

decade since 1850, in which during the 21st century, global average surface temperature in 2001–2020 and 2011–2020 were 0.99°C and 1.09°C respectively higher in comparison with 1850–1900 period (IPCC, 2021).

The aforementioned has caused the warming of the atmosphere and oceans, diminishing of snow and ice amounts, rise of sea level, alterations of precipitation patterns and changes in hydrological systems, which has affected water resources in terms of quantity and quality. As consequence, many terrestrial, freshwater and marine species have shifted their geographic ranges, seasonal activities, migration patterns, abundances and species interactions in response to ongoing climate change. Likewise, in many regions negative impacts of climate have been observed on crop yields (IPCC, 2014, 2021).

1.2 Free Air Carbon Dioxide Enrichment experiment (FACE) system

Different methodologies have been used to assess the effects of elevated atmospheric CO₂ (eCO₂) levels on soil ecosystems, with the free-air CO₂ enrichment (FACE) experiment as one of these approaches. The FACE technology was first developed in the United States of America (USA) by Brookhaven National Laboratory (BNL) for use in an agricultural setting and it consisted of large-scale plots ringed by towers, with a network of pipes or plenums near the ground in such a design as to provide eCO₂, to the ambient air of the plants, which allows for the manipulation of CO₂ levels inside the plots (DOE.2020, 2020; Lewin et al., 1994). The object is to avoid the need for an enclosure or chamber around the plants. The major differences between FACE and either outdoor controlled environment chambers or open top chambers, the closest alternatives, are that FACE eliminates the following chamber effects: (1) reduction of the solar radiation environment, and (2) unnatural wind flow, turbulence, and micrometeorological patterns (Drake et al., 1985).

At this first FACE facility eCO₂, combined with manipulations of water and nitrogen supply, were conducted from 1989 to 1999 in Maricopa, Ariz., with cotton, wheat, and sorghum (Hendrey et al., 1993; Lewin et al., 1994). Since then, FACE experiments have spanned for four decades during which global ambient CO₂ (aCO₂) has risen from <360 ppmV to >410 ppmV and have permitted to evaluate the effects of eCO₂ on several terrestrial ecosystems, diverse vegetation types and biomes across the globe (Ainsworth & Long, 2021; Butterly et al., 2015; DOE.2020, 2020; Lewin et al., 1994; Mollah et al., 2009; Norby, 2011) (Table 1).

In the State of Hessen, Germany, the FACE systems at the Justus-Liebig-University Giessen (JLU) and the Geisenheim University of Applied Sciences (HSGM), have been running since 1998 and 2014, respectively. Aiming to investigate both short and long-term changes of an increased atmospheric CO₂ concentration (conditions predicted for approx. 2050) on the agro-ecosystems grassland, field vegetables, viticulture as well as fruit and shrubbery.

1.2.1 Giessen FACE

The effects of eCO₂ levels on a tempered grassland ecosystem have been studied in the Giessen FACE (Gi-FACE), which has been operating continuously since 1998, becoming a good predictor of the consequences of eCO₂ on this ecosystem. The Gi-FACE study is located at 50°32'N and 8°41.3'E near Giessen, Germany, at an elevation of 172 m above sea level. It consists of three pairs of rings with a diameter of 8 m; each pair consists of an ambient and an eCO₂ treatment ring (Jäger et al., 2003) (Fig. 2). Since May 1998 until present, eCO₂ rings have been continuously enriched by 20% above aCO₂ concentrations during daylight hours. Ambient and elevated CO₂ rings are separated by at least 20 m, and each pair is placed at the vertices of an equilateral triangle. The presence of a slight slope within the experimental site (between 0.5 and 3.5°) place the rings on a moisture gradient, such that pair 1 has the lowest mean moisture content (38.8% ± 10.2%) and pair 2 has the highest mean moisture content (46.1% ± 13.2%), whereas pair 3 is intermediate (40.7% ± 11%) (de Menezes et al., 2016; Jäger et al., 2003). The average annual air temperature and precipitation are 9.4 °C and 580 mm, respectively.

The vegetation is an *Arrhenatheretum elatioris* Br.Bl. *Filipendula ulmaria* subcommunity, dominated by *Arrhenatherum elatius*, *Galium album* and *Geranium pratense*. At least 12 grass species, 15 non-leguminous herbs and up to 5 legumes with small biomass contributions (<5%) are present within a single plot (Andresen et al., 2018). The experimental field has not been ploughed for more than 100 years. It has received N fertilization in form of granular mineral calcium-ammonium-nitrate (40 kg N ha⁻¹ year⁻¹) once a year since 1995 and has been mown twice a year since 1993. The soil at the Gi-FACE site is classified as Fluvic Geysol; its texture is a sandy clay loam over a clay layer, with pH= 6.2 and average C and N contents of 4.5% and 0.45%, respectively, as measured in 2001 (Jäger et al., 2003).

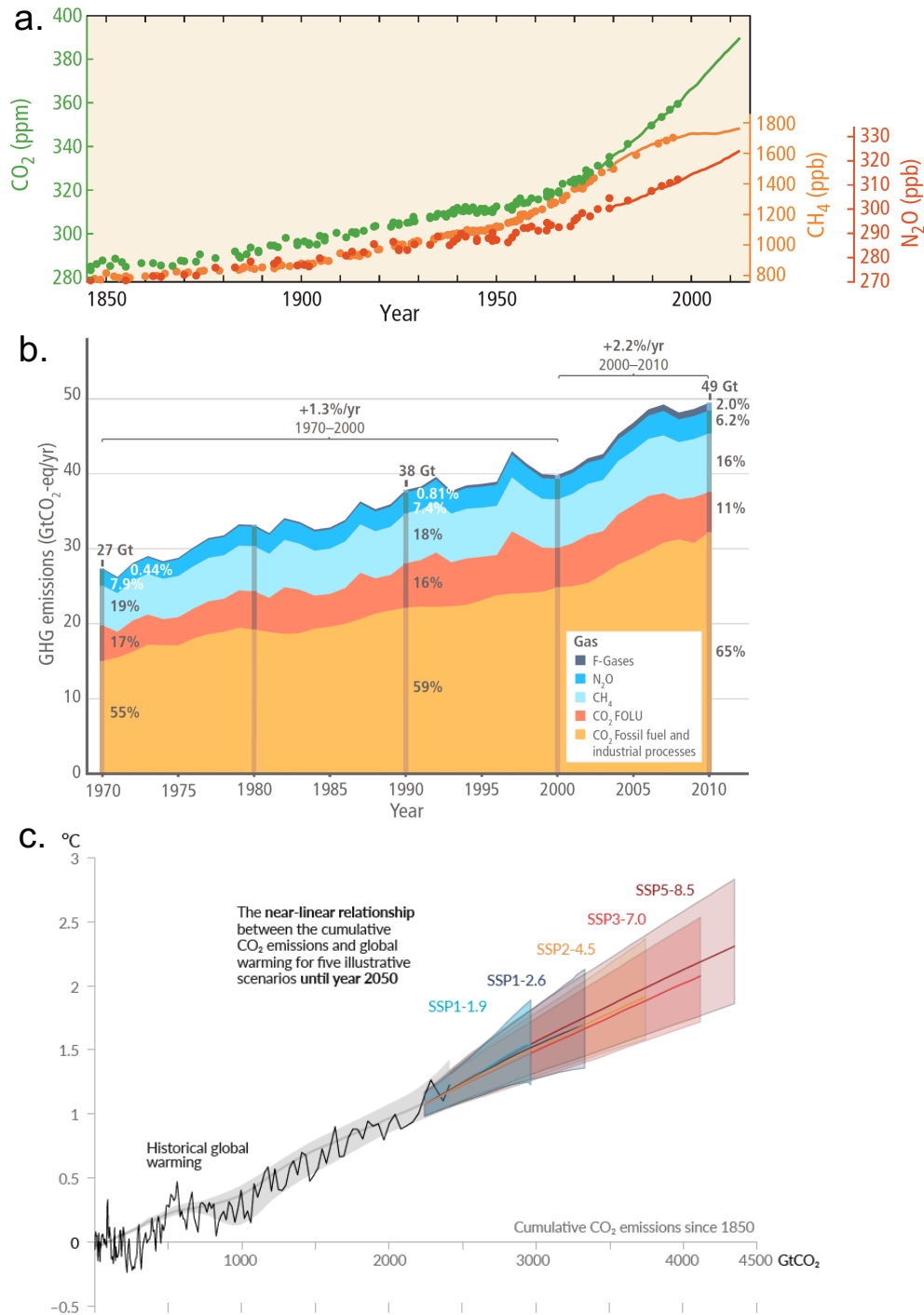


Figure 1. (a) Observed changes in atmospheric greenhouse gas concentrations of carbon dioxide (CO₂, green), methane (CH₄, orange), and nitrous oxide (N₂O, red). (b) Total annual anthropogenic greenhouse gas (GHG) emissions for the period 1970 to 2010 by gases: CO₂ from fossil fuel combustion and industrial processes; CO₂ from Forestry and Other Land Use (FOLU); methane (CH₄); nitrous oxide (N₂O); fluorinated gases (F-gases). (c) Increment in observed global surface temperature (grey range) and projected increment of global surface temperature (colored range) as a function of cumulative CO₂ emissions in Gt CO₂ from 1850 to 2019 (IPCC, 2014, 2021).

Table 1. Summary of some long-term global FACE experiments.

Name	Country	Coordinates	Running time	CO ₂ concentration	Another controlled env. Factor	Number of plots	Vegetation	Reference
Maricopa FACE	Maricopa, Ariz, USA	33°05'N, 111°59'W	1989–1999	Ambient +0, ambient +200 ppmV	-----	8	Cotton, Wheat, and Sorghum	(Hendrey et al., 1993; Lewin et al., 1994)
Duke FACE	Chapel Hill, North Carolina, USA	35°59'N, 79°06'W	1994–2011	Ambient +0, ambient +200 ppmV	-----	6	Loblolly Pine (<i>Pinus taeda</i>)	(McCarthy et al., 2010)
Nevada Desert FACE	Mojave Desert, Nevada, USA	36°49'N, 115°55'W	1997–2007	Ambient 375 ppmV, Elevated 550 ppmV	-----	9	Desert Scrub	(Evans et al., 2014)
Oak Ridge National Laboratory FACE	Oak Ridge, Tennessee, USA	35°54'N, 84°20'W	1997–2009	Ambient 396 ppmV, Elevated 547 ppmV	-----	6	Sweetgum (<i>Liquidambar styraciflua</i>)	(Norby et al., 2010)
Rhineland FACE	Rhineland, Wisconsin, USA	45°41'N, 89°38'W	1997–2009	Ambient 354 ppmV, Elevated 539 ppmV	O ₃ about 1.5 × ambient	12	Northern Hardwoods	(Burton et al., 2014)
Giessen FACE	Giessen, Hessen, Germany	50°32'N, 8°41.3'E	1998-present	Ambient 388 ppmV, Elevated 490 ppmV	-----	6	Temperated grassland	(Jäger et al., 2003)
AGFACE	Horsham, Victoria, Australia	36°45'07''S, 142°06'52''E	2007-2018	Ambient 370 ppmV, Elevated 550 ppmV	Water level Nitrogen	16	Wheat (<i>Triticum aestivum</i> L.)	(Mollah et al., 2009)
Maize FACE	Braunschweig, Lower Saxony, Germany	52°18'N, 10°26'E	2009-2012	Ambient 385 ppmV, Elevated 600 ppm	Rainfall	6	Maize (<i>Zea mays</i> L., cv. "Romario")	(Erbs et al., 2012)
SoilFACE	Horsham, Victoria, Australia	36°44'57''S, 142°06'50''E	2009-2018	Ambient 370 ppmV, Elevated 550 ppm	Nitrogen fertilization	8	Wheat (<i>Triticum aestivum</i> L.) and field pea (<i>Pisum sativum</i> L.)	(Butterly et al., 2015)
EucFACE	Richmond, New South Wales, Australia	-33.618°, 150.738°	2012-present	Ambient +0, ambient +150 ppmV	-----	6	Dry Eucalyptus forest	(Crous et al., 2015)
Geisenheim WineFACE	Geisenheim, Hessen, Germany	49°59'N, 7°57'E	2014-present	Ambient 409 ppmV, Elevated 483 ppm	-----	6	<i>Vitis vinifera</i> cv. Cabernet Sauvignon cv. Riesling	(Reineke & Selim, 2019; Wohlfahrt et al., 2018)
AmazonFACE	North of Manaus, Brazil	-2.596°, -60.208°	2016-present	Ambient +0, ambient +200 ppmV	-----	2, expanding to 8	Broadleaf evergreen rainforest	(Lapola & Norby, 2014)E

BIFoR-FACE	Staffordshire, Central England, UK	52.801°,- 2.301°	2016- present	Ambient +0, ambient +150 ppmV	-----	9	Deciduous coppice with standards woodland	(Butterly et al., 2015)
------------	--	---------------------	------------------	-------------------------------------	-------	---	---	----------------------------



Figure 2. Air view of Giessen FACE experimental site. E: elevated CO₂ ring, A: ambient CO₂ ring. Google Earth Pro Image (2021).

1.2.2 WineFACE

The Geisenheim VineyardFACE facility is located at Hochschule Geisenheim University, Germany (49°59'N, 7°57'E; 96 m above sea level) in the German wine growing region Rheingau on the banks of river Rhine and it has been functioning since 2014. Geisenheim has a temperate oceanic climate (Köppen-Geiger classification: Cfb) with mild winters and warm summers. The mean annual temperature is 10.5 °C and total annual precipitation averages 543.1 mm (long-term average from 1981 to 2010). The soil at the experimental site is characterized as low-carbonate loamy sand to sandy loam. The VineyardFACE consists of three ring pairs each with an inner diameter of 12 m, of which three are under eCO₂ and three under aCO₂ concentration (Fig. 3). Within eCO₂ rings air was enriched during daylight hours to approximately 18% above the aCO₂. Within VineyardFACE rings, vines of *Vitis vinifera* L. cv. Riesling (clone 198–30 Gm) grafted on rootstock SO4 (clone 47 Gm) and cv. Cabernet Sauvignon (clone 170) grafted on rootstock 161–49 Couderc, respectively, were planted in April 2012 as one-year-old

potted plants. Each ring contains seven rows of cv. Riesling and cv. Cabernet Sauvignon plants, which were planted alternately across a central divide. Vines were planted with a spacing of 0.9 m within rows and 1.8 m between rows, with a north-south orientation. Cover crop consisted of Freudenberger WB 130 mulch mixture III (10% *Lolium perenne*, 50% *Festuca rubra* and 40% *Poa pratensis*) and has been sowed to every second inter-row, while every other second inter-row was ploughed once in spring and was largely bare or covered with spontaneous vegetation (Reineke & Selim, 2019; Wohlfahrt et al., 2018).

1.2.3 Effect of the increase of environmental CO₂ on plants

In general terms, eCO₂ concentration has several consequences on plants, such as increased growth in C3, C4 and CAM plants by 41%, 22%, and 15%, respectively (He et al., 1995; Idso, 1994); increased plant yield (Kimball, 1983); decreased evapotranspiration of both C3 (Owensby et al., 1997) and C4 plants (Kimball, 2016); augmented photosynthetic capacity (Habash et al., 1995; P. He et al., 1995; Johnson & Pregitzer, 2007); increased below-ground biomass (Jongen et al., 1995).

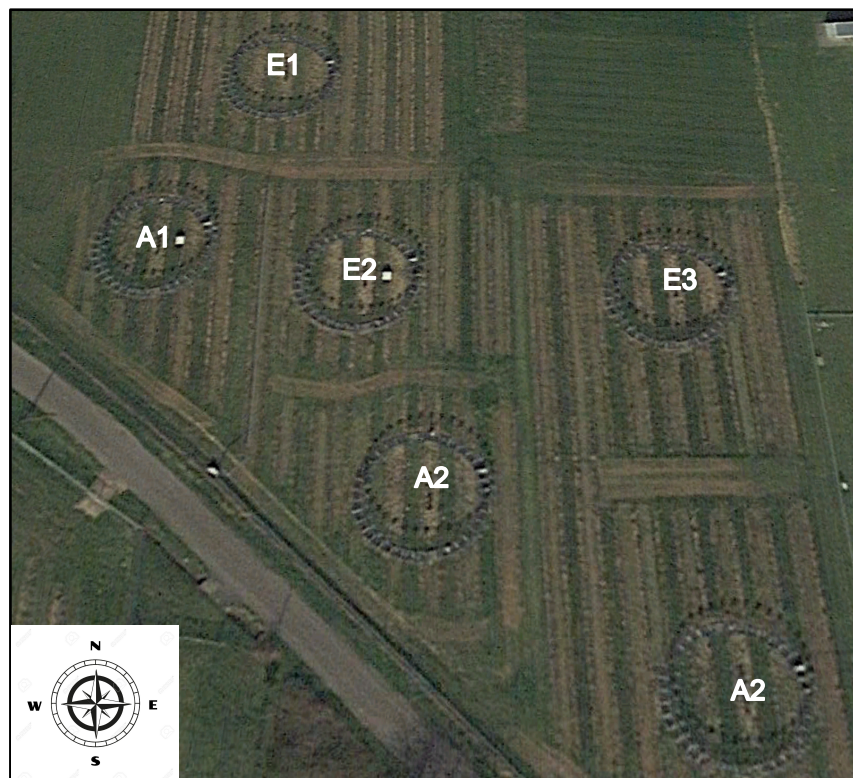


Figure 3. Air view of Geisenheim Wine FACE experimental site. E: elevated CO₂ ring, A: ambient CO₂ ring. Google Earth Pro Image (2021).

1.2.4 FACE experiments on grasslands

At the different FACE experiments around the globe the effects of eCO₂ on different types of plants have been demonstrated. In grassland ecosystems the assessment of plant responses to eCO₂ have indicated different results, which vary depending on several environmental factors. At a grassland prairie FACE, the effect of eCO₂ combined with elevated temperature and the elevation of the field, produced an increment of aboveground biomass in the first three years, but later root biomass was stronger affected than aboveground biomass (Carrillo et al., 2014; Mueller et al., 2016; Zelikova et al., 2014). At the BioCON experiment and the TasFACE above and below grass biomass had positive responses to eCO₂, but also precipitations (Hovenden et al., 2014; Reich et al., 2014). Furthermore, Californian grassland (Jasper Ridge FACE) showed a weak response of aboveground biomass, with the CO₂ response being independent on precipitation and temperature (Dukes et al., 2005; Zhu et al., 2016).

At the Giessen FACE experiment it was reported that the total aboveground biomass (TAB) was significantly increased under eCO₂. Furthermore, the different plant functional groups (grasses, forbs and legumes), had different responses through time. Initially suggesting a suppression of the forbs by grasses under eCO₂, and later converging to a positive CO₂ effect. Additionally, it was described that extreme climatic events combined with eCO₂ impact significantly the plant composition in this ecosystem (Andresen et al., 2018).

1.2.5 FACE experiments on crop plants

Largely, at the different FACEs assessing crop plants as cotton, wheat, ryegrass, rice, barley (C₃ plant), sorghum and maize (C₄ plant) diverse responses have been documented. One usual response to eCO₂ is a partial stomatal closure with a reduction in stomatal conductance to water vapor, which slows the loss rate of water from the leaves or transpiration (Ainsworth & Rogers, 2007; Kimball, 2016). Regarding shoot biomass in C₃ plants, it was observed an increase, contrasting with C₄ plants, which had little or no increase of shoot biomass (DOE.2020, 2020; Kimball, 2016; Taylor et al., 2006). One important aspect concerning crop plants is their agricultural yield. In C₃ grasses (wheat, rice, and barley), it has been reported an increase of crop yield with plenty N and H₂O, and under N limited conditions. On the contrary C₄ grass grain crops (sorghum and maize), have shown slightly negative average response to eCO₂ (Ainsworth & Long, 2017, 2021; Kimball, 2016).

At the Geisenheim VineyardFACE it has been reported by Wohlfahrt et al. (2018) that under eCO₂ conditions the varieties Riesling and Cabernet Sauvignon presented higher net photosynthesis rates of 32% and 28% respectively. Similarly, it has been demonstrated that under both scenarios eCO₂ plus reduced water availability and eCO₂ plus elevated ambient temperature grapevines presented higher net photosynthetic rates (da Silva et al., 2017; Edwards et al., 2017). Additionally, eCO₂ has been proven to affect berry and must properties, increasing berry weights, lateral leaf area, summer pruning fresh weight and yield; and altering malic and tartaric acids concentration (Kizildeniz et al., 2018; Wohlfahrt et al., 2020). Furthermore, future CO₂ concentrations might alter the way and magnitude of interactions between plants and herbivorous insects, as it was demonstrated by Reineke et al. (2019), who described that grapevine plants presented different transcriptional patterns as a response to herbivorous insect *Lobesia botrana* under eCO₂ compared to ambient concentrations.

1.3 Effect of eCO₂ on Carbon and Nitrogen Cycles in terrestrial ecosystems

Terrestrial ecosystems act as a “sink” for a significant portion of this carbon, removing and sequestering it from the atmosphere (DOE.2020, 2020). Likewise, global terrestrial soil organic carbon (SOC) pool is the largest terrestrial carbon (C) pool and constitutes a C stock that is more than twice the size of the atmospheric CO₂-C pool (IPCC, 2014; Vestergard et al., 2016)

Consequently, even relatively moderate fluctuations in net C exchange between soil and atmosphere impact the CO₂ concentration in the atmosphere profoundly. Hence, the response of terrestrial ecosystems to increasingly higher concentrations of CO₂ under a changing climate has important implications for the global carbon cycle. (Vestergard et al., 2016).

1.3.1 Increment of roots exudates and priming effect

Input of fresh plant carbon (C) and nitrogen (N) availability can potentially alter SOC decomposition, which are expected to change with rising CO₂ levels. Elevated atmospheric CO₂ increases efflux amounts of total soluble sugars, amino acids, phenolic acids, and organic acids in the root exudates (Dong et al., 2021; Jia et al., 2014; Phillips et al., 2012). Therefore, the supply of fresh plant derived C into the soil matrix due to eCO₂ may accelerate the decomposition of SOC and decrease soil C stocks (Blagodatskaya & Kuzyakov, 2008; Fontaine et al., 2004); a phenomenon known as “the

priming effect". This alteration of increased decomposition of SOC has been reported in grasslands (Liu et al., 2017; Vestergard et al., 2016), forests (Liu et al., 2017; Phillips et al., 2012; Qiao et al., 2014) and crop fields (Trivedi et al., 2016)

Several studies have demonstrated that eCO₂ changes C turnover dynamics of different fractions of SOM. The extent of priming seems to depend on the concentration of labile C inputs, with no or low priming at low concentrations and gradually increasing priming with increasing concentrations (Blagodatskaya & Kuzyakov, 2008) until reaching saturation point (Liu et al., 2017; Vestergard et al., 2016). Additionally, the sensitivity of priming in response to C input varies depending on the type of soil and elevation (Liu et al., 2017). For instance, it has been reported that greater priming occurs in low nutrient soils compared to high nutrient soils (Dimassi et al., 2014). In contrast, similar magnitudes of priming were detected in soils with different nutrients (Qiao et al., 2014). Soils with higher soil C and C:N ratio exhibited higher priming in some soils (Qiao et al., 2014) but lower priming in others (Dimassi et al., 2014; Qiao et al., 2014).

Nevertheless, it seems that eCO₂ induces in greater amounts the decomposition of older soil C (Niklaus & Falloon, 2006; Van Groenigen et al., 2005; Vestergard et al., 2016; Xie et al., 2005). Furthermore, Vestergard et al. (2016), reported that C assimilated in eCO₂ conditions is decomposed in the soil basal respiration and enhanced the formation of coarse particulate SOM (fresh SOM) and decreased the fraction of physically protected SOM (old SOM).

1.3.2 Effect on soil microbial C and N cycles related processes

Regarding the study of the impact of eCO₂ on the microbiome composition and microbial processes, they have been thoroughly analyzed in the different systems all over the world. As result diverse reports have described several changes in microbiome structures, genes and microorganisms involved in the different steps of C and N cycles. In this sense and considering that nearly up to 21% of all photosynthetically fixed carbon is transferred to the rhizosphere, roots and root exudates exert a strong influence on the composition and biomass of soil microbiome (Li et al., 2013; Walker et al., 2003). Thus, eCO₂ augments the rates of organic carbon as energy sources, through the enhancement of microbial degradation of soil SOC (Dong et al., 2021) and the microbial succession that follows is accompanied by activation of various, previously dormant microorganisms that respond specifically to the added substrate (Blagodatskaya & Kuzyakov, 2008; Di Lonardo et al., 2017). Likewise, Eisenhauer et al. (2017) has

described that bacterial and fungal biomass are positive correlated with root biomass and root exudates. Hence, the relationship between C input and priming might be affected by the size of microbial biomass present in the soil (Blagodatskaya & Kuzyakov, 2008).

With the increased soil C content, it is likely that the microbial N demand increases, consequently the enhanced priming and mineralization of SOC results in an increment of microbial N mining. Thus, due to the fact that old SOM pools contain significant physically and chemically protected N stocks, the priming effect is a response to the labile C supply by which microorganisms gain access to a reservoir of N to meet their enhanced N demand under conditions of plenty C supply (Derrien et al., 2014; Liu et al., 2017; Vestergard et al., 2016). The aforementioned has been described by Müller et al. (2009), who reported that under eCO₂ mineralization of labile organic N became more important. Also occurs an increment in the dissimilatory NO₃⁻ reduction to NH₄⁺ (DNRA) and in the immobilization of NH₄⁺ and NO₃⁻ (Müller et al., 2009).

Furthermore, alterations in N cycle due to eCO₂ conditions have been also described by Kammann et al. (2008), who indicated an increment of N₂O (a potent greenhouse gas) emissions. Likewise, Moser et al. (2018) reported that, N₂O emissions were 1.79-fold higher, and that the linear interpolations showed a 2.09-fold, 1.64-fold and 1.66-fold increase in N₂O emissions from denitrification, nitrification and heterotrophic nitrification respectively. As outcome, alterations in N cycle induces significant changes in soil biogeochemical characteristics in the rhizosphere, such as NO₃⁻, available K⁺, soil microbial biomass carbon (SMBC) and available PO₄²⁻ (Yu et al., 2016).

Also, the abundance of genes involved in labile C degradation and C and N fixation, as Ribulose-1,5-bisphosphate carboxylase-oxygenase (RuBisCo), carbon monoxide dehydrogenase (CODH), propionyl-CoA/acetyl-CoA carboxylase (PCC/ACC), *nifH* and *nirS* genes were significantly increased under eCO₂ (Xu et al., 2013). He et al. (2014) and Xiong et al. (2015) have reported a shift of soil microbial communities under eCO₂ in a soybean and a maize agro-ecosystems, respectively. These changes included stimulation of key functional genes involved in carbon fixation and degradation, nitrogen fixation, denitrification, methane metabolism and phosphorus cycling. Song et al. (2012) described that community composition of soil microbiota associated with *Phytolacca americana* and *Amaranthus cruentus* roots were significantly affected by eCO₂ and numbers of bacteria and fungi, as well as microbial C and N in the rhizosphere soils of both species, were higher at eCO₂. Simonin et al. (2015) reported that shoot biomass,

root biomass, and soil respiration were increased under eCO₂ and N supply, and these variables were positively correlated with ammonia-oxidizing bacteria abundance. Le Roux et al. (2016) described that potential nitrite oxidation rate was enhanced in soil by eCO₂. More recently, Bei et al. (2019) showed that eCO₂ had significant effects on the functional expression associated to both rhizosphere microbiomes and plant roots; and that abundances of *Eukarya* relative to *Bacteria* were significantly decreased.

Oppositely to the aforementioned studies, other reports have shown small or no effects of eCO₂ on soil microbiome structure and activity, as Marhan et al. (2011) who described that abundances of total 16S rRNA genes and nitrate-reducing bacteria were not influenced by CO₂ but by sampling date and depth. Dunbar et al. (2014) described that neither bacterial nor fungal community structure nor composition were altered under eCO₂. Pujol Pereira et al. (2013) did not find any significant effects of eCO₂ on bacterial abundance, soil C, and N concentrations. Regan et al. (2011) described that extractable organic carbon, dissolved organic nitrogen, NH₄⁺, NO₃⁻, and abundances of genes involved in ammonia oxidation and denitrification depended more on soil depth and moisture gradient than on eCO₂. Similarly, de Menezes et al. (2016) described that increases in atmospheric CO₂ may cause only minor changes in soil bacterial community composition and that functional responses of the soil community are due to factors like soil moisture rather than CO₂ concentration. Brenzinger et al. (2017) reported that the abundance and composition of microbial communities in the top soil under eCO₂ presented only small differences from soil under aCO₂, concluding that +20% CO₂ had little to no effect on the overall microbial community involved in N-cycling.

1.4 rRNA metagenomics: advantages and disadvantages

The use of rRNA instead of DNA to assess the structure and composition of microbiome in metagenomic studies provides an ideal tool to study the microbial populations that actively participate in various ecological processes (Sharma & Sharma, 2018). Some drawbacks regarding the use of DNA are that after a cell dies, amplifiable extracellular DNA can remain in soils for weeks to years and may obscure DNA-based estimates of the diversity and structure of soil microbial communities (Dlott et al., 2015; Morrissey et al., 2015). Moreover, it has been reported by Carini et al. (2016) that DNA from dead cells or free DNA represented a large fraction of microbial DNA in many soils, comprising approximately 40.7% and 40.5% of amplifiable prokaryotic 16S rRNA genes and fungal ITS amplicons, respectively. Therefore, DNA depending studies may overestimate the richness of the soil microbiome by up to 55% for prokaryotes and 52% for fungi (Carini

et al., 2016) and in consequence may hide the active microorganisms that are involved in soil microbial processes

Moreover, an argument in favor of the use of rRNA is that it has been demonstrated that ribosome numbers are correlated to the metabolic activity of bacteria (Felske et al., 1996) and different studies showed using this approach, that the active organisms instead of the dormant ones are assessed (Duineveld et al., 2001; Hoshino & Matsumoto, 2007; Hunt et al., 2013). Additionally, metatranscriptomic results reported by Bei et al. (2019), demonstrated that RNA instead of DNA is a better predictor of microbiome composition and activity in soils.

However, RNA metabarcoding has its limitations as well, mainly due to the fact that RNA conversion to cDNA requires the use of a reverse transcriptase which lacks proofreading activity, creating point mutations in some of the cDNA sequences (Houseley & Tollervey, 2010). Reverse transcriptase also regularly performs template switching, which can lead to the production of chimeric cDNA sequences and the creation of shortened isoform sequences from intramolecular template switching (Cocquet et al., 2006; Laroche et al., 2017). Nevertheless, these limitations can be minimized by using a Moloney murine leukemia virus reverse transcriptase (MMLV-RT) derivative combined with a *Escherichia coli* DNA polymerase III ϵ subunit which lowers the reverse transcription error rate by threefold, and the resulting cDNA is amplified with a proofreading DNA polymerase which produces up to eightfold fewer errors (Arezi & Hogrefe, 2007).

1.5 Functional metatranscriptomics

Profiling the small ribosome subunit 16S gene (16S rRNA gene), referred also as taxonomical metagenomics, has been widely utilized for the study and the description of microbial communities' composition in several environments (Bashiardes et al., 2016; Bikel et al., 2015). However, taxonomical metagenomics approaches have a very limited role in revealing the microbial activity measured by gene expression. An alternative to this would be the use of techniques like quantitative PCR (qPCR) to quantify gene expression in natural samples, although these are limited usually to measurement of a small number of known genes (Frias-lopez et al., 2008).

The functional metatranscriptomic shotgun sequencing (mRNAseq) provides the access to the metatranscriptome of the microbiome allowing the profiling of the active microbial community under different conditions. It is based on direct sequencing of mRNA, which is more likely to analyze the alive and active microbiome populations (Bei et al., 2019;

Moran et al., 2013). Moreover, metatranscriptomics reveals community responses simultaneously across all three domains of life (*Archaea*, *Bacteria*, and *Eukarya*) due to random-primed cDNA synthesis (Sharma & Sharma, 2018). Data from functional metatranscriptome analyses, thus, complement taxonomical metagenomics data by elucidating accurately which genes are transcribed and to what extent, thereby enabling to demonstrate the functions from a potential range of microorganisms (Franzosa et al., 2014). From such functional data, active metabolic pathways can be identified in the bacterial communities and can be associated to particular environmental conditions. Therefore, metatranscriptomics offers a more informative perspective compared with metagenomics, as it can reveal details about populations that are transcriptionally active (Bashiardes et al., 2016).

1.5.1 Principles, applications and limitations of functional metatranscriptomics

Usually, a functional metatranscriptomics analysis involves isolation of total RNA from the sample matrix and depending on the target taxonomical group (*Bacteria*, *Archaea*, or *Eukarya*) different procedures are applied for the isolation of mRNA. In eukaryotes, mRNA can be selected by synthesizing cDNA using oligo-d(T) primers, and taking advantage of the poly-A tail characterizing mRNA species (Belstrøm et al., 2017; Frias-lopez et al., 2008; Ogura et al., 2011). However, in contrast to eukaryotic mRNA, prokaryotic mRNA lacks a poly-A tail, making its selection during cDNA synthesis inapplicable (Bashiardes et al., 2016). One approach for the removal of rRNA is the use of probes targeting specific rRNA regions that are attached to magnetic beads followed by their removal with the use of a magnet (He et al., 2015; Mann et al., 2018; Peano et al., 2013; Sharma & Sharma, 2018). What is left after these depletions methods is an enriched population of mRNAs that are representative of transcriptionally active genes. For massively parallel sequence analysis, these RNAs are fractionated, cDNA is synthesized, and adapters are ligated to the cDNA ends generating a library that is amplified and then sequenced. Sequence reads are mapped to reference genomes, and the expressed genes are identified by comparison against several data bases (Fig. 4) (Section 1.5.2.).

Functional metatranscriptomics has been applied to characterize a wide range of environments. It has been utilized to analyze seawater and coastal environments (Cabral et al., 2018; Frias-lopez et al., 2008; Moran et al., 2013; Ogura et al., 2011; Wu et al., 2013), soil under the influence of different stressors (Bei et al., 2019; Sharma & Sharma, 2018), extreme environments (Chen et al., 2015; He et al., 2015), human microbiome (Belstrøm et al., 2017; Franzosa et al., 2014) and rumen microbiome (Mann et al., 2018)

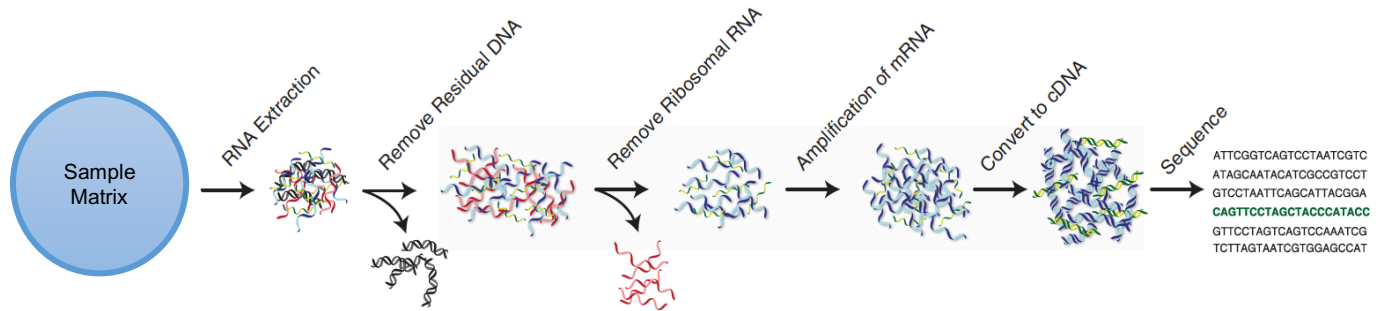


Figure 4. Schematic workflow of functional metatranscriptomics analysis (Moran et al., 2013).

There are several technical issues regarding the application of functional metatranscriptomics: (1) the collection and storage procedures to preserve the RNA of the sample, (2) the limitation to obtain high-quality and sufficient quantity of RNA, (3) the mRNA enrichment procedures by removing rRNAs which represent over 90% of the total RNA, (4) the average useful life of mRNA leads to difficulty in the detection of rapid and short-term responses to environmental changes, (5) the transcriptome databases are insufficient. Furthermore, as with all methods involving RNA manipulation, the challenge of avoiding degradation by contaminating ribonucleases needs to be handled mostly by the use of RNase inhibitors (Bikel et al., 2015). Additional problems during the reverse transcription process to synthesize cDNA, were addressed in section 1.4.

1.5.2 Software and pipelines for the analysis of functional metatranscriptome

Bioinformatics pipelines analyze the data obtained from a metatranscriptomic experiment in different ways and they vary in terms of capacities and approaches. However, they could be classified in two large groups: The first group comprises platforms and tools that map sequence reads to reference genomes and genes and consequently rely on the direct annotation of the raw reads. Within this classification are included pipelines as MG-RAST (Meyer et al., 2008), Anvi'o (Eren et al., 2015), FMAP (Kim et al., 2016) and SAMSA2 (Westreich et al., 2018). The second group includes the ones which perform *de novo* assembly of new transcriptomes, as IMP (Narayanasamy et al., 2016) and SqueezeMeta (Tamames & Puente-Sánchez, 2019).

Regarding the use of raw reads, there are some disadvantages, mainly due to the fact that they are based on homology searches for millions of sequences against huge reference databases, which exclude reads from uncultured species and/or divergent strains which are discarded during data analysis, thereby resulting in the loss of potentially useful

information; and additionally they usually require very large CPU usage (Narayanasamy et al., 2016; Sunagawa et al., 2013; Tamames & Puente-Sánchez, 2019). Some of these tools are web-based, such as MG-RAST (Meyer et al., 2008), which allows to perform analyses without the need for local compute resources, nonetheless they depend upon a service that may become oversubscribed and slow, and mapping to custom reference data bases is not supported.

Some authors, argue that it is advisable to perform assembly because it can recover larger fragments of genomes, often comprising many genes. Having the complete sequence of a gene and its context makes its functional and taxonomic assignment much easier and more reliable (Narayanasamy et al., 2015, 2016; Tamames & Puente-Sánchez, 2019). Also, it facilitates the recovery of quasi-complete genomes via binning methods and enables linking organisms and functions, thus contributing to a much more accurate ecologic description of the community's functioning. The drawback of assembly is the formation of chimeras because of misassembling parts of different genomes, and the inability to assemble some of the reads, especially the ones from low abundance species (Tamames & Puente-Sánchez, 2019).

In summary, a standard metatranscriptomic pipeline involves reads curation, assembly (not in all cases), gene matching, and functional and taxonomic annotation of the resulting genes.

1.6 Next generation sequencing data and compositionality

Sanger sequencing served as the primary sequencing tool during several years, making possible significant accomplishments including the sequencing of the entire human genome. This sequencing method is considered as a “first-generation” technology, nevertheless since the second half of the 2000s, it has occurred a shift away this “first-generation technology” toward new technologies collectively known as next-generation sequencing (NGS), which has changed the way of thinking about scientific approaches in basic, applied and clinical research (Metzker, 2010; Quinn, Erb, et al., 2018).

Several NGS products exist, each differing in the sample preparation and chemistry used, although they all work by determining the base order from a population of fragmented nucleotide sequences, such that it becomes possible to estimate the abundances of unique sequences. However, these sequence abundances are not absolute abundances because the total number of sequences measured by NGS

technology (i.e., the library size) ultimately depends on the chemistry of the assay and not the input material. Depending on the input material, NGS has many uses. These include (1) variant discovery, (2) genome assembly, (3) transcriptome assembly, (4) epigenetic and chromatin profiling, (5) metagenomic species classification or gene discovery and (6) transcript abundance quantification (Metzker, 2010; Quinn, Erb, et al., 2018).

1.6.1 What are compositional data (CoDa)?

Compositional data (CoDa) are multivariate data in which the components represent some part of a whole. They are usually recorded in closed form, summing to a constant, that is, the values for each multivariate sample are either observed as summing to a constant, usually 1 or 100%, or are expressed as values relative to a total that is irrelevant to the research objective. (Greenacre, 2021; Pawlowsky-Glahn & Egozcue, 2006). Compositional data do not exist in real Euclidean space, but rather in a sub-space known as the simplex: 3-part compositions are inside a triangle, 4-part compositions are inside a tetrahedron, and so on for higher dimensional simplexes (Aitchison, 1982, 1986; Greenacre, 2021; Pawlowsky-Glahn & Egozcue, 2006; Quinn, Erb, et al., 2018). CoDa are observed in many fields as: geochemistry (i.e. mineral compositions), ecology (i.e. relative abundances of species), biochemistry (i.e. fatty acid proportions), morphology (i.e. the shapes of living organisms), sociology (i.e. time budgets), geography (i.e. proportions of land use), political science (i.e. voting proportions), marketing (i.e. brand shares), and recently genomics and microbiome research (i.e. proportions of operational taxonomic units) (Aitchison, 2005; Greenacre, 2021)

These types of data have particular and important numerical properties that have major consequences for any statistical analysis. The properties peculiar to compositional data arises from the fact that they represent parts of some whole; therefore, they convey only relative information. Hence, they are always positive, range only from 0 to 100, or any other constant, when given in closed form and usually constrained to a constant sum. Values for components or parts in compositional data are not free to range from $-\infty$ to $+\infty$ (as unconstrained variables are). This conditions the relationships that variables have to one another, which implies that if one component increases, others must, perforce, decrease, whether or not there is a link between these components (Pawlowsky-Glahn & Egozcue, 2006). This means that the results of standard statistical analysis of the relationships between raw components or parts in a compositional dataset are clouded by spurious effects, because the constant sum constraint forces at least one covariance (and thus at least one correlation coefficient between elements) to be negative.

Consequently, if one correlation has to be negative, then none of the correlation coefficients between elements are free to range between -1 and +1 producing a bias towards negative correlations. This problem has been described under different headings: the constant-sum problem, the closure problem, the negative bias problem, the null correlation difficulty (Aitchison, 2005; Pawlowsky-Glahn & Egozcue, 2006).

1.6.2 Microbiome sequencing data are compositional

Microbial ecosystems are extremely complex and interactions within and between microbial species can profoundly impact microbiome composition in natural environments (Susin et al., 2020). Traditionally, microbiome data analysis assumes that sequencing data are equivalent to ecological representation of the taxa within a determinate environment, thus methods typically used for macro-ecology analyses are applied, including count-based strategies such as Bray-Curtis dissimilarity, zero-inflated Gaussian models and negative binomial models (Gloor et al., 2017).

However, in the case of the microbiome data, the compositional nature comes from the fact that true independence cannot be assumed in high-throughput sequencing (HTS) experiments because the sequencing instruments can deliver reads only up to its own capacity (Gloor et al., 2017). Thus, it is proper to think of these instruments as containing a fixed number of slots which must be filled. Consequently, the total read count observed in a HTS run is a fixed-size, and it represents a random sample of the relative abundance of the molecules in the underlying ecosystem (Gloor et al., 2017; Susin et al., 2020).

Furthermore, biases from sample collection, polymerase chain reaction (PCR) amplification, and the sequencing technology itself, make impossible to recover the absolute abundances of microbes from sequence counts, but the proportions of different taxa are still relevant for the analysis (Tsilimigras & Fodor, 2016).

1.6.3 Methods to deal with compositional data

John Aitchison established the foundations of a new approach to the statistical analysis of compositional data in his work from the 1980s (Aitchison, 1982, 1986). In Aitchison's approach, the paradoxes mentioned above are eliminated by not considering the original values of the compositional parts, but rather their ratios, since the ratio between the parts of the composition remain constant irrespective of what other parts are present, before or after closure (Greenacre, 2021; Pawlowsky-Glahn & Egozcue, 2006).

Nonetheless, the use of ratios for analyzing CoDa, brings with it some issues due to the nature of these kind of data, which are not coherent since the values of a subset of parts would change after closing to have unit sum, furthermore, ratios are generally compared multiplicatively. Aitchison addressed this problem by using a logarithmic transformation of the composition, which converts the ratios on a multiplicative scale to an additive scale. Thus, the log-ratio transformations (Tab. 2) take the compositional data out of the simplex into real vector space, with an additive scale, thereby complying with most standard statistical methodologies (Aitchison, 1982; Greenacre, 2021; Tsilimigras & Fodor, 2016).

Table 2. Log-ratio transformations of a composition consisting of a determined number (J) of parts (Greenacre, 2021)

Abbreviation	Name	Description
LR	Pairwise log-ratio	The log of the ratio of two parts
ALR	Additive log-ratio	A pairwise log-ratio (LR) that is one of a set of $J - 1$ ALRs having the same denominator (or numerator)
SLR	Summated (amalgamated) log-ratio	The log of the ratio of the sums (amalgamations) of two subsets of parts log-ratio
CLR	Centered log-ratio	The log of the ratio of a part and the geometric mean of all the parts; usually one of a set of J CLR, each with one of the J parts in the numerator
ILR	Isometric log-ratio	The log of the geometric means of two subsets of parts
PLR	Pivot log-ratio	The log of the ratio of a single part and the geometric mean of a subset of the parts; usually one of a set of $J - 1$ PLRs

1.6.4 Analysis of microbiome data as composition

In general, compositional data analyses begin with a log-ratio transformation, which restores much of the utility of traditional statistical analyses. However, a natural problem in using a ratio-based transformation is that one has to choose what will be in the denominator; that is to say, which value to use to normalize all the values in a sample. Aitchison considered two possible transformations. The simplest transformation is to choose one component as a reference, it is to say, a determinate taxon. Performing this type of analyses, and then correcting for multiple hypotheses is not usually realistic due to the large numbers of distinct taxa in most of metagenomic analyses. As an alternative, it is better to transform each taxon within a sample by taking the log-ratio of the counts for that taxon divided by the geometric mean of the counts of all taxa, called the centered log-ratio (clr) (Table 2) (Tsilimigras & Fodor, 2016). The clr transformed values can be

used as inputs for multivariate hypothesis testing, regression, and for model building. The clr-transformed values are scale-invariant; that is the same ratio is expected to be obtained in a sample with few read counts or an identical sample with many read counts, only the precision of the clr estimate is affected (Gloor et al., 2017; Quinn, Erb, et al., 2018).

Nonetheless, clr transformation has potential problems when applied to metagenomic data sets. This difficulty arises from extreme variability of library sizes and the great sparsity of metagenomic data sets. In a highly sparse data set, the geometric mean of all taxa can often be zero or near zero (Tsilimigras & Fodor, 2016). However, there are acceptable methods for handling with 0 count values, including the approaches of using point estimates or modeling the data as a probability distribution, implemented in the R packages *zCompositions* and *ALDEx2* respectively (Fernandes et al., 2014; Palarea-Albaladejo & Martín-Fernández, 2015; Quinn, Crowley, et al., 2018).

Beta diversity analysis using a compositional approach differs from the traditional methods for analyzing microbiome datasets, which include usually the creation of a distance matrix based of different methods as Bray-Curtis, UniFrac (both the weighted and unweighted variants), among others (Bray & Curtis, 1957; Lozupone et al., 2011). In contrast, it is used the Aitchison distance which provides a measure of distance between two D-dimensional compositions (Quinn, Erb, et al., 2018). The Aitchison distance is simply the Euclidean distance between clr-transformed compositions, this distance has scale invariance, perturbation invariance and sub-compositional dominance (Aitchison, 1982, 2005). Afterwards, the distance matrix is ordinated utilizing the variance-based compositional principal component (PCA) biplot where the relationship between inter-Operational taxonomic unit (OTU) variance and sample distance can be observed (Aitchison & Greenacre, 2002; Gloor et al., 2017; Greenacre, 2021). The compositional biplot has advantages over the ordination methods normally used in microbiome analyses, as principal co-ordinate (PCoA) and Non-metric multidimensional scaling (NMDS) plots for Beta diversity analysis. Some of these are: (1) stability of subset data, (2) analysis is not driven simply by the presence absence relationships in the data, (3) robustness against excessive sparsity (Aitchison & Greenacre, 2002; Gloor et al., 2017; Quinn, Erb, et al., 2018). However, it is important to stress, that covariances and correlations between features now exist with respect to the geometric mean reference of the log-transformed data (Aitchison & Greenacre, 2002).

In microbiome studies after the assessment of the diversity in the microbial community, it is customary to evaluate what features have changed among the groups or treatments that are being evaluated. This kind of analyses are usually referred as Differential Abundance Analysis. Currently, there are available several bioinformatic tools capable of performing such task within a compositional approach. Among these are ALDEx2 (Fernandes et al., 2014), ANCOM (Mandal et al., 2015), ANCOM-II (Kaul et al., 2017), selbal (Rivera-Pinto et al., 2018), Songbird (Morton et al., 2019), clr-lasso (Susin et al., 2020) and ANCOM-BC (Lin & Peddada, 2020). Each one of them part from the basis of performing a log-ratio transformation, although the algorithm and the way they deal with sparsity and zero counts varies from one to another.

In the case of ALDEx2 the algorithm first creates randomized instances based on the compositionally valid Dirichlet distribution. This renders the data free of zeros. Second, each of these so-called Monte Carlo (MC) instances undergoes log-ratio transformation, most usually clr or iqlr transformation. Third, conventional statistical tests (i.e. Welch's t and Wilcoxon tests for two groups; glm and Kruskal-Wallis for two or more groups) get applied to each MC instance to generate p-values (p) and Benjamini-Hochberg adjusted p-values (BH) for each feature. Fourth, these p-values and effect-sizes get averaged across all MC instances (Fernandes et al., 2014). ALDEx2 authors highlight that evidence for differential abundance can be accurately evaluated using both statistical significance and effect-size estimates because these two values respectively describe the confidence that abundance in the conditions are different, and the magnitude by which they differ. Furthermore, it has been argued that characterizing biological data in this way is more informative than decisions based upon p-value thresholds because p-values encourage acceptance or rejection of a null hypothesis rather than an explicit assessment of the evidence (Fernandes et al., 2013, 2014).

In microbiome research it is a matter of interest to elucidated who is interacting with whom, however as described in section 1.7.1., the correlation is unreliable in compositional datasets because of the negative correlation bias. Although some algorithms have been developed to evaluate microbe-microbe associations as SparCC package, available for the R programming language. SparCC replaces Pearson's correlation coefficient with an estimation of correlation based on its relationship to the log-ratio variance VLR (Friedman & Alm, 2012). The algorithm works by iteratively calculating a "basis correlation" under the assumption that the majority of pairs do not correlate (i.e. a sparse network). Another algorithm, SPIEC-EASI, assumes also that the underlying network is sparse, but bases its method on the inverse covariance matrix of

clr-transformed data (Kurtz et al., 2015). However, determining an optimal and general approach for correlation in compositional datasets is an open research problem.

1.7 Aims of the study

The increment of atmospheric CO₂ concentration affects terrestrial ecosystems, stimulating plant's above and below ground biomass and rhizodeposition of roots exudates (Section 1.1). As consequence, soil microbiome structure, composition and function are affected. Nonetheless, existing results on microbiome response to eCO₂ are in many cases contradictory or inconclusive, frequently indicating other environmental parameters as main drivers of the soil ecosystem. Furthermore, the studies conducted so far have worked mainly with DNA metabarcoding, which has several limitations when facing the assessment of microbiomes (Section 1.4). Likewise, most of current microbiome research in this area hasn't done the transition to analyze HTS data as compositional data (Section 1.6), using in many cases inadequate statistical methods to address the questions that are needed to be answered. Hence, to assess the effect eCO₂ on soil microbiome at the FACE systems in Giessen (Gi-FACE) and Geisenheim (VineyardFACE), in this work it was implemented an RNA metabarcoding approach, using either 16S rRNA metabarcoding to assess taxonomically the active microbiome structure and mRNA to address the function and changes in the expressed genes under eCO₂ conditions; and analyzing these data using a compositional data approach.

For the reasons mentioned above, the aims of the present work were: i) to assess the effect of long and mid-term eCO₂ concentrations on active soil microbiome through an rRNA-based metabarcoding approach and compositional data analysis; ii) to evaluate differences between eCO₂ and aCO₂ conditions in the vineyard and grassland soils; iii) to study how changes in soil microbiome are connected to environmental variables; iv) address changes in functional metatranscriptome due to eCO₂ conditions; v) to evaluate changes in microorganisms and genes involved in N and C cycles.

1.8 References

- Ainsworth, E. A., & Long, S. P. (2017). What have we learned from 15 years of free-air CO₂ enrichment (FACE)? A meta-analytic review of the responses of photosynthesis, canopy properties and plant production to rising CO₂. *Global Change Biology*, 23(3), 351–371. <https://doi.org/10.1029/2007JG000644>
- Ainsworth, E. A., & Long, S. P. (2021). 30 years of free-air carbon dioxide enrichment

- (FACE): What have we learned about future crop productivity and its potential for adaptation? *Global Change Biology*, 27(1), 27–49.
<https://doi.org/10.1111/gcb.15375>
- Ainsworth, E. A., & Rogers, A. (2007). The response of photosynthesis and stomatal conductance to rising [CO₂]: Mechanisms and environmental interactions. *Plant, Cell and Environment*, 30(3), 258–270. <https://doi.org/10.1111/j.1365-3040.2007.01641.x>
- Aitchison, J. (1982). The Statistical Analysis of Compositional Data. *Journal Of the Royal Statistical Society. Series B (Methodological)*, 44(2), 139–177.
<https://doi.org/10.1007/978-94-009-4109-0>
- Aitchison, J. (1986). Book review. In *The Statistical Analysis of Compositional Data* (XII). Chapman and Hall. <https://doi.org/10.1007/bf01187862>
- Aitchison, J. (2005). A Concise Guide to Compositional Data Analysis. *Proceedings of CoDaWork05*, 134. http://ima.udg.edu/Activitats/CoDaWork05/A_concise_guide_to_compositional_data_analysis.pdf
- Aitchison, J., & Greenacre, M. (2002). Biplots of compositional data. *Journal of the Royal Statistical Society. Series C: Applied Statistics*, 51(4), 375–392.
<https://doi.org/10.1111/1467-9876.00275>
- Andresen, L. C., Yuan, N., Seibert, R., Moser, G., Kammann, C. I., Luterbacher, J., Erbs, M., & Müller, C. (2018). Biomass responses in a temperate European grassland through 17 years of elevated CO₂. *Global Change Biology*, 24, 3875–3885.
<https://doi.org/10.1111/gcb.13705>
- Arezi, B., & Hogrefe, H. H. (2007). Escherichia coli DNA polymerase III ε subunit increases Moloney murine leukemia virus reverse transcriptase fidelity and accuracy of RT-PCR procedures. *Analytical Biochemistry*, 360(1), 84–91.
<https://doi.org/10.1016/j.ab.2006.10.009>
- Arrhenius, S. (1986). On the Influence of Carbonic Acid in the Air upon the Temperature of the Ground. *Philosophical Magazine and Journal of Science*, 5(41), 237–276.
- Baes, C. F., Goeller, H. E., Olson, J. S., & Rotty, R. M. (1977). Carbon dioxide and climate: the uncontrolled experiment. *American Scientist*, 65(3), 310–320.
- Bashiardes, S., Zilberman-Schapira, G., & Elinav, E. (2016). Use of metatranscriptomics in microbiome research. *Bioinformatics and Biology Insights*, 10, 19–25.
<https://doi.org/10.4137/BBI.S34610>
- Bei, Q., Moser, G., Wu, X., Müller, C., & Liesack, W. (2019). Metatranscriptomics reveals climate change effects on the rhizosphere microbiomes in European grassland. *Soil Biology and Biochemistry*, 138(July), 1–10.
<https://doi.org/10.1016/j.soilbio.2019.107604>

- Belstrøm, D., Constancias, F., Liu, Y., Yang, L., Drautz-Moses, D. I., Schuster, S. C., Kohli, G. S., Jakobsen, T. H., Holmstrup, P., & Givskov, M. (2017). Metagenomic and metatranscriptomic analysis of saliva reveals disease-associated microbiota in patients with periodontitis and dental caries. *Npj Biofilms and Microbiomes*, 3(1), 1–7. <https://doi.org/10.1038/s41522-017-0031-4>
- Bikel, S., Valdez-Lara, A., Cornejo-Granados, F., Rico, K., Canizales-Quinteros, S., Soberón, X., Del Pozo-Yauner, L., & Ochoa-Leyva, A. (2015). Combining metagenomics, metatranscriptomics and viromics to explore novel microbial interactions: Towards a systems-level understanding of human microbiome. *Computational and Structural Biotechnology Journal*, 13, 390–401. <https://doi.org/10.1016/j.csbj.2015.06.001>
- Blagodatskaya, E., & Kuzyakov, Y. (2008). Mechanisms of real and apparent priming effects and their dependence on soil microbial biomass and community structure: Critical review. *Biology and Fertility of Soils*, 45(2), 115–131. <https://doi.org/10.1007/s00374-008-0334-y>
- Bray, R. J., & Curtis, J. T. (1957). An ordination of the upland forest communities of southern Wisconsin. *Ecological Monographs*, 27(4), 325–349. <https://doi.org/10.2307/1942268>
- Brenzinger, K., Kujala, K., Horn, M. A., Moser, G., Guillet, C., Kammann, C., Müller, C., & Braker, G. (2017). Soil conditions rather than long-term exposure to elevated CO₂ affect soil microbial communities associated with N-cycling. *Frontiers in Microbiology*, 8, 1–14. <https://doi.org/10.3389/fmicb.2017.01976>
- Burton, A. J., Pregitzer, K., Percy, K., Nelson, N., Rogers, A., Nagy, J., Kubiske, M., Lindroth, R., & Zak, D. (2014). *Impacts of Interacting Elevated Atmospheric CO₂ and O₃ on the Structure and Functioning of a Northern Forest Ecosystem: Operating and Decommissioning the Aspen FACE Project*.
- Butterly, C. R., Armstrong, R., Chen, D., & Tang, C. (2015). Carbon and nitrogen partitioning of wheat and field pea grown with two nitrogen levels under elevated CO₂. *Plant and Soil*, 391(1–2), 367–382. <https://doi.org/10.1007/s11104-015-2441-5>
- Cabral, L., Pereira de Sousa, S. T., Júnior, G. V. L., Hawley, E., Andreote, F. D., Hess, M., & de Oliveira, V. M. (2018). Microbial functional responses to long-term anthropogenic impact in mangrove soils. *Ecotoxicology and Environmental Safety*, 160(January), 231–239. <https://doi.org/10.1016/j.ecoenv.2018.04.050>
- Carini, P., Marsden, P. J., Leff, J. W., Morgan, E. E., Strickland, M. S., & Fierer, N. (2016). Relic DNA is abundant in soil and obscures estimates of soil microbial diversity. *Nature Microbiology*, 2(0), 1–6. <https://doi.org/10.1038/nmicrobiol.2016.242>

- Carrillo, Y., Dijkstra, F. A., LeCain, D., Morgan, J. A., Blumenthal, D., Waldron, S., & Pendall, E. (2014). Disentangling root responses to climate change in a semiarid grassland. *Oecologia*, 175(2), 699–711. <https://doi.org/10.1007/s00442-014-2912-z>
- Chen, L. X., Hu, M., Huang, L. N., Hua, Z. S., Kuang, J. L., Li, S. J., & Shu, W. S. (2015). Comparative metagenomic and metatranscriptomic analyses of microbial communities in acid mine drainage. *ISME Journal*, 9(7), 1579–1592. <https://doi.org/10.1038/ismej.2014.245>
- Cocquet, J., Chong, A., Zhang, G., & Veitia, R. A. (2006). Reverse transcriptase template switching and false alternative transcripts. *Genomics*, 88(1), 127–131. <https://doi.org/10.1016/j.ygeno.2005.12.013>
- Crous, K. Y., Ósváldsson, A., & Ellsworth, D. S. (2015). Is phosphorus limiting in a mature Eucalyptus woodland? Phosphorus fertilisation stimulates stem growth. *Plant and Soil*, 391(1–2), 293–305. <https://doi.org/10.1007/s11104-015-2426-4>
- da Silva, J. R., Patterson, A. E., Rodrigues, W. P., Campostrini, E., & Griffin, K. L. (2017). Photosynthetic acclimation to elevated CO₂ combined with partial rootzone drying results in improved water use efficiency, drought tolerance and leaf carbon balance of grapevines (*Vitis labrusca*). *Environmental and Experimental Botany*, 134, 82–95. <https://doi.org/10.1016/j.envexpbot.2016.11.007>
- de Menezes, A. B., Müller, C., Clipson, N., & Doyle, E. (2016). The soil microbiome at the Gi-FACE experiment responds to a moisture gradient but not to CO₂ enrichment. *Microbiology*, 162, 1572–1582. <https://doi.org/10.1099/mic.0.000341>
- Derrien, D., Plain, C., Courty, P. E., Gelhaye, L., Moerdijk-Poortvliet, T. C. W., Thomas, F., Versini, A., Zeller, B., Koutika, L. S., Boschker, H. T. S., & Epron, D. (2014). Does the addition of labile substrate destabilise old soil organic matter? *Soil Biology and Biochemistry*, 76, 149–160. <https://doi.org/10.1016/j.soilbio.2014.04.030>
- Di Lonardo, D. P., De Boer, W., Klein Gunnewiek, P. J. A., Hannula, S. E., & Van der Wal, A. (2017). Priming of soil organic matter: Chemical structure of added compounds is more important than the energy content. *Soil Biology and Biochemistry*, 108, 41–54. <https://doi.org/10.1016/j.soilbio.2017.01.017>
- Dimassi, B., Mary, B., Fontaine, S., Perveen, N., Revaillet, S., & Cohan, J. P. (2014). Effect of nutrients availability and long-term tillage on priming effect and soil C mineralization. *Soil Biology and Biochemistry*, 78, 332–339. <https://doi.org/10.1016/j.soilbio.2014.07.016>
- Dlott, G., Maul, J. E., Buyer, J., & Yarwood, S. (2015). Microbial rRNA: RDNA gene ratios may be unexpectedly low due to extracellular DNA preservation in soils. *Journal of Microbiological Methods*, 115, 112–120.

- <https://doi.org/10.1016/j.mimet.2015.05.027>
- DOE.2020, U. S. (2020). *U.S. Department of Energy Free-Air CO₂ Enrichment Experiments: FACE Results, Lessons, and Legacy*.
<https://doi.org/10.2172/1615612>
- Dong, J., Hunt, J., Delhaize, E., Zheng, S. J., Jin, C. W., & Tang, C. (2021). Impacts of elevated CO₂ on plant resistance to nutrient deficiency and toxic ions via root exudates: A review. *Science of the Total Environment*, 754, 142434.
<https://doi.org/10.1016/j.scitotenv.2020.142434>
- Drake, B. G., Rogers, H. H., & Allen, L. H. (1985). Methods of exposing plants to elevated carbon dioxide. In B. R. Strain & J. D. Cure (Eds.), *Direct effects of increasing carbon dioxide on vegetation* (1st ed., pp. 11–32). United States Department of Energy.
- Duineveld, B. M., Kowalchuk, G. A., Keijzer, A., Van Elsas, J. D., & Van Veen, J. A. (2001). Analysis of bacterial communities in the rhizosphere of chrysanthemum via denaturing gradient gel electrophoresis of PCR-amplified 16S rRNA as well as DNA fragments coding for 16S rRNA. *Applied and Environmental Microbiology*, 67(1), 172–178. <https://doi.org/10.1128/AEM.67.1.172-178.2001>
- Dukes, J. S., Chiariello, N. R., Cleland, E. E., Moore, L. A., Rebecca Shaw, M., Thayer, S., Tobeck, T., Mooney, H. A., & Field, C. B. (2005). Responses of grassland production to single and multiple global environmental changes. *PLoS Biology*, 3(10). <https://doi.org/10.1371/journal.pbio.0030319>
- Dunbar, J., Gallegos-Graves, L. V., Steven, B., Mueller, R., Hesse, C., Zak, D. R., & Kuske, C. R. (2014). Surface soil fungal and bacterial communities in aspen stands are resilient to eleven years of elevated CO₂ and O₃. *Soil Biology and Biochemistry*, 76, 227–234. <https://doi.org/10.1016/j.soilbio.2014.05.027>
- Edwards, E. J., Unwin, D., Kilmister, R., Treeby, M., & Ollat, N. (2017). Multi-seasonal effects of warming and elevated CO₂ on the physiology, growth and production of mature, field grown, Shiraz grapevines. *Journal International Des Sciences de La Vigne et Du Vin*, 51(2), 127–132. <https://doi.org/10.20870/oenone.2016.0.0.1586>
- Eisenhauer, N., Lanoue, A., Strecker, T., Scheu, S., Steinauer, K., Thakur, M. P., & Mommer, L. (2017). Root biomass and exudates link plant diversity with soil bacterial and fungal biomass. *Scientific Reports*, 7, 1–8. <https://doi.org/10.1038/srep44641>
- Erbs, M., Manderscheid, R., & Weigel, H. J. (2012). A combined rain shelter and free-air CO₂ enrichment system to study climate change impacts on plants in the field. *Methods in Ecology and Evolution*, 3(1), 81–88. <https://doi.org/10.1111/j.2041-210X.2011.00143.x>

- Eren, A. M., Esen, O. C., Quince, C., Vineis, J. H., Morrison, H. G., Sogin, M. L., & Delmont, T. O. (2015). Anvi'o: An advanced analysis and visualization platform for 'omics data. *PeerJ*, 2015(10), 1–29. <https://doi.org/10.7717/peerj.1319>
- Evans, R. D., Koyama, A., Sonderegger, D. L., Charlet, T. N., Newingham, B. A., Fenstermaker, L. F., Harlow, B., Jin, V. L., Ogle, K., Smith, S. D., & Nowak, R. S. (2014). Greater ecosystem carbon in the Mojave Desert after ten years exposure to elevated CO₂. *Nature Climate Change*, 4(5), 394–397. <https://doi.org/10.1038/nclimate2184>
- Felske, A., Engelen, B., Nübel, U., & Backhaus, H. (1996). Direct ribosome isolation from soil to extract bacterial rRNA for community analysis. *Applied and Environmental Microbiology*, 62(11), 4162–4167.
- Fernandes, A. D., Macklaim, J. M., Linn, T. G., Reid, G., & Gloor, G. B. (2013). ANOVA-Like Differential Expression (ALDEx) Analysis for Mixed Population RNA-Seq. *PLoS ONE*, 8(7), e67019. <https://doi.org/10.1371/journal.pone.0067019>
- Fernandes, A. D., Reid, J. N. S., Macklaim, J. M., McMurrough, T. A., Edgell, D. R., & Gloor, G. B. (2014). Unifying the analysis of high-throughput sequencing datasets: Characterizing RNA-seq, 16S rRNA gene sequencing and selective growth experiments by compositional data analysis. *Microbiome*, 2(1), 1–13. <https://doi.org/10.1186/2049-2618-2-15>
- Fontaine, S., Bardoux, G., Abbadie, L., & Mariotti, A. (2004). Carbon input to soil may decrease soil carbon content. *Ecology Letters*, 7(4), 314–320. <https://doi.org/10.1111/j.1461-0248.2004.00579.x>
- Franzosa, E. A., Morgan, X. C., Segata, N., Waldron, L., Reyes, J., Earl, A. M., Giannoukos, G., Boylan, M. R., Ciulla, D., Gevers, D., Izard, J., Garrett, W. S., Chan, A. T., & Huttenhower, C. (2014). Relating the metatranscriptome and metagenome of the human gut. *Proceedings of the National Academy of Sciences of the United States of America*, 111(22). <https://doi.org/10.1073/pnas.1319284111>
- Frias-lopez, J., Shi, Y., Tyson, G. W., Coleman, M. L., Schuster, S. C., Chisholm, S. W., & Delong, E. F. (2008). Microbial community gene expression in ocean surface waters. *Proceedings of the National Academy of Sciences of the United States of America*, 105(10), 3805–3810. [papers2://publication/uuid/1250ACE5-E123-4C67-8BB7-4D69E7FF3767](https://doi.org/10.1073/pnas.0706001105)
- Friedman, J., & Alm, E. J. (2012). Inferring Correlation Networks from Genomic Survey Data. *PLoS Computational Biology*, 8(9), 1–11. <https://doi.org/10.1371/journal.pcbi.1002687>
- Gloor, G. B., Macklaim, J. M., Pawlowsky-Glahn, V., & Egozcue, J. J. (2017). Microbiome datasets are compositional: And this is not optional. *Frontiers in Microbiology*,

- 8(NOV), 1–6. <https://doi.org/10.3389/fmicb.2017.02224>
- Greenacre, M. (2021). Compositional data analysis. *Annual Review of Statistics and Its Application*, 8, 271–299. <https://doi.org/10.1146/annurev-statistics-042720-124436>
- Habash, D. Z., Paul, M. J., Parry, M. A. J., Keys, A. J., & Lawlor, D. W. (1995). Increased capacity for photosynthesis in wheat grown at elevated CO₂ - the relationship between electron transport and carbon metabolism. *Planta*, 197(3), 482–489. <https://doi.org/10.1007/BF00196670>
- He, P., Bader, K. P., Radunz, A., & Schmid, G. H. (1995). Consequences of high CO₂-concentrations in air on growth and gas-exchange rates in Tobacco mutants. *Zeitschrift Für Naturforschung*, 50c(11/12), 781–788.
- He, Y., Feng, X., Fang, J., Zhang, Y., & Xiao, X. (2015). Metagenome and metatranscriptome revealed a highly active and intensive sulfur cycle in an oil-immersed hydrothermal chimney in Guaymas Basin. *Frontiers in Microbiology*, 6(NOV), 1–11. <https://doi.org/10.3389/fmicb.2015.01236>
- He, Z., Xiong, J., Kent, A. D., Deng, Y., Xue, K., Wang, G., Wu, L., Van Nostrand, J. D., & Zhou, J. (2014). Distinct responses of soil microbial communities to elevated CO₂ and O₃ in a soybean agro-ecosystem. *ISME Journal*, 8(3), 714–726. <https://doi.org/10.1038/ismej.2013.177>
- Hendrey, G. R., Lewin, K. F., & Nagy, J. (1993). Free air carbon dioxide enrichment: development, progress, results. *Vegetatio*, 104–105(1), 17–31. <https://doi.org/10.1007/BF00048142>
- Hoshino, Y. T., & Matsumoto, N. (2007). DNA- versus RNA-based denaturing gradient gel electrophoresis profiles of a bacterial community during replenishment after soil fumigation. *Soil Biology and Biochemistry*, 39(2), 434–444. <https://doi.org/10.1016/j.soilbio.2006.08.013>
- Houseley, J., & Tollervey, D. (2010). Apparent non-canonical trans-splicing is generated by reverse transcriptase in vitro. *PLoS ONE*, 5(8). <https://doi.org/10.1371/journal.pone.0012271>
- Hovenden, M. J., Newton, P. C. D., & Wills, K. E. (2014). Seasonal not annual rainfall determines grassland biomass response to carbon dioxide. *Nature*, 511(7511), 583–586. <https://doi.org/10.1038/nature13281>
- Hunt, D. E., Lin, Y., Church, M. J., Karl, D. M., Tringe, S. G., Izzo, L. K., & Johnson, Z. I. (2013). Relationship between abundance and specific activity of bacterioplankton in open ocean surface waters. *Applied and Environmental Microbiology*, 79(1), 177–184. <https://doi.org/10.1128/AEM.02155-12>
- Idso, K. (1994). Plant responses to atmospheric CO₂ enrichment in the face of environmental constraints: a review of the past 10 years' research. *Agricultural and*

- Forest Meteorology*, 69(3–4), 153–203. [https://doi.org/10.1016/0168-1923\(94\)90025-6](https://doi.org/10.1016/0168-1923(94)90025-6)
- IPCC. (2014). Climate Change 2014: Synthesis Report. Contribution of Working Groups I, II and III to the Fifth Assessment Report of the Intergovernmental Panel on Climate Change. In R. K. Pachauri & L. . Meyer (Eds.), *Climate Change 2014: Synthesis Report. Contribution of Working Groups I, II and III to the Fifth Assessment Report of the Intergovernmental Panel on Climate Change*. IPCC. <https://doi.org/10.1017/CBO9781107415324>
- IPCC. (2021). Technical Summary. Contribution of Working Group I to the Sixth Assessment Report of the Intergovernmental Panel on Climate Change. In V. Masson-Delmotte, P. Zhai, A. Pirani, S. L. Connors, C. Péan, S. Berger, N. Caud, Y. Chen, L. Goldfarb, M. I. Gomis, M. Huang, K. Leitzell, E. Lonnoy, J. B. R. Matthews, T. K. Mycock, T. Waterfield, O. Yelekcy, R. Yu, & B. Zhous (Eds.), *Summary for Policymakers. In: Climate Change 2021: The Physical Science Basis. Contribution of Working Group I to the Sixth Assessment Report of the Intergovernmental Panel on Climate Change* (In Press). Cambridge University Press.
- Jäger, H. J., Schmidt, S. W., Kammann, C., Grunhage, L., Muller, C., & Hanewald, K. (2003). The University of Giessen Free-Air Carbon Dioxide Enrichment study: Description of the experimental site and of a new enrichment system. *Journal of Applied Botany-Angewandte Botanik*, 77(5–6), 117–127.
- Jia, X., Wang, W., Chen, Z., He, Y., & Liu, J. (2014). Concentrations of secondary metabolites in tissues and root exudates of wheat seedlings changed under elevated atmospheric CO₂ and cadmium-contaminated soils. *Environmental and Experimental Botany*, 107, 134–143. <https://doi.org/10.1016/j.envexpbot.2014.06.005>
- Johnson, R. M., & Pregitzer, K. S. (2007). Concentration of sugars, phenolic acids, and amino acids in forest soils exposed to elevated atmospheric CO₂ and O₃. *Soil Biology and Biochemistry*, 39(12), 3159–3166. <https://doi.org/10.1016/j.soilbio.2007.07.010>
- Jongen, M., Jones, M. B., Hebeisen, T., Blum, H., & Hendrey, G. (1995). The effects of elevated CO₂ concentrations on the root growth of *Lolium perenne* and *Trifolium repens* grown in a FACE* system. *Global Change Biology*, 1, 361–371.
- Kammann, C., Müller, C., Grünhage, L., & Jäger, H. J. (2008). Elevated CO₂ stimulates N₂O emissions in permanent grassland. *Soil Biology & Biochemistry*, 40, 2194–2205. <https://doi.org/10.1016/j.soilbio.2008.04.012>
- Kaul, A., Mandal, S., Davidov, O., & Peddada, S. D. (2017). Analysis of microbiome data

- in the presence of excess zeros. *Frontiers in Microbiology*, 8(NOV), 1–10. <https://doi.org/10.3389/fmicb.2017.02114>
- Kim, J., Kim, M. S., Koh, A. Y., Xie, Y., & Zhan, X. (2016). FMAP: Functional Mapping and Analysis Pipeline for metagenomics and metatranscriptomics studies. *BMC Bioinformatics*, 17(1), 1–8. <https://doi.org/10.1186/s12859-016-1278-0>
- Kimball, B. A. (1983). Carbon dioxide and agricultural yield: An assemblage and analysis of 430 prior observations. *Agronomy Journal*, 75(5), 779. <https://doi.org/10.2134/agronj1983.00021962007500050014x>
- Kimball, B. A. (2016). Crop responses to elevated CO₂ and interactions with H₂O, N, and temperature. *Current Opinion in Plant Biology*, 31, 36–43. <https://doi.org/10.1016/j.pbi.2016.03.006>
- Kizildeniz, T., Pascual, I., Irigoyen, J. J., & Morales, F. (2018). Using fruit-bearing cuttings of grapevine and temperature gradient greenhouses to evaluate effects of climate change (elevated CO₂ and temperature, and water deficit) on the cv. red and white Tempranillo. Yield and must quality in three consecutive growin. *Agricultural Water Management*, 202, 299–310. <https://doi.org/10.1016/j.agwat.2017.12.001>
- Kurtz, Z. D., Müller, C. L., Miraldi, E. R., Littman, D. R., Blaser, M. J., & Bonneau, R. A. (2015). Sparse and Compositionally Robust Inference of Microbial Ecological Networks. *PLoS Computational Biology*, 11(5), 1–25. <https://doi.org/10.1371/journal.pcbi.1004226>
- Lapola, D. M., & Norby, R. (2014). Assessing the effects of increased atmospheric CO₂ on the ecology and resilience of the Amazon forest. In *Science plan et implementation strategy: Vol. Amazon-FAC*.
- Laroche, O., Wood, S. A., Tremblay, L. A., Lear, G., Ellis, J. I., & Pochon, X. (2017). Metabarcoding monitoring analysis: The pros and cons of using co-extracted environmental DNA and RNA data to assess offshore oil production impacts on benthic communities. *PeerJ*, 2017(5). <https://doi.org/10.7717/peerj.3347>
- Le Roux, X., Bouskill, N. J., Niboyet, A., Barthes, L., Dijkstra, P., Field, C. B., Hungate, B. A., Lerondelle, C., Pommier, T., Tang, J., Terada, A., Tourn, M., & Poly, F. (2016). Predicting the responses of soil nitrite-oxidizers to multi-factorial global change: A trait-based approach. *Frontiers in Microbiology*, 7(MAY), 1–13. <https://doi.org/10.3389/fmicb.2016.00628>
- Lewin, K. F., Hendrey, G. R., Nagy, J., & LaMorte, R. L. (1994). Design and application of a free-air carbon dioxide enrichment facility. *Agricultural and Forest Meteorology*, 70(1–4), 15–29. [https://doi.org/10.1016/0168-1923\(94\)90045-0](https://doi.org/10.1016/0168-1923(94)90045-0)
- Li, K., Guo, X. W., Xie, H. G., Guo, Y., & Li, C. (2013). Influence of root exudates and residues on soil microecological environment. *Pakistan Journal of Botany*, 45(5),

1773–1779.

- Lin, H., & Peddada, S. Das. (2020). Analysis of compositions of microbiomes with bias correction. *Nature Communications*, 11(1), 1–11. <https://doi.org/10.1038/s41467-020-17041-7>
- Liu, X. J. A., Sun, J., Mau, R. L., Finley, B. K., Compson, Z. G., van Gestel, N., Brown, J. R., Schwartz, E., Dijkstra, P., & Hungate, B. A. (2017). Labile carbon input determines the direction and magnitude of the priming effect. *Applied Soil Ecology*, 109, 7–13. <https://doi.org/10.1016/j.apsoil.2016.10.002>
- Lozupone, C., Lladser, M. E., Knights, D., Stombaugh, J., & Knight, R. (2011). UniFrac: An effective distance metric for microbial community comparison. *ISME Journal*, 5(2), 169–172. <https://doi.org/10.1038/ismej.2010.133>
- Mandal, S., Van Treuren, W., White, R. A., Eggesbø, M., Knight, R., & Peddada, S. D. (2015). Analysis of composition of microbiomes: a novel method for studying microbial composition. *Microbial Ecology in Health & Disease*, 26(0), 1–7. <https://doi.org/10.3402/mehd.v26.27663>
- Mann, E., Wetzels, S. U., Wagner, M., Zebeli, Q., & Schmitz-Esser, S. (2018). Metatranscriptome sequencing reveals insights into the gene expression and functional potential of rumen wall bacteria. *Frontiers in Microbiology*, 9(JAN), 1–12. <https://doi.org/10.3389/fmicb.2018.00043>
- Marhan, S., Philippot, L., Bru, D., Rudolph, S., Franzaring, J., Högy, P., Fangmeier, A., & Kandeler, E. (2011). Abundance and activity of nitrate reducers in an arable soil are more affected by temporal variation and soil depth than by elevated atmospheric [CO₂]. *FEMS Microbiology Ecology*, 76(2), 209–219. <https://doi.org/10.1111/j.1574-6941.2011.01048.x>
- McCarthy, H. R., Oren, R., Johnsen, K. H., Gallet-Budynek, A., Pritchard, S. G., Cook, C. W., Ladeau, S. L., Jackson, R. B., & Finzi, A. C. (2010). Re-assessment of plant carbon dynamics at the Duke free-air CO₂ enrichment site: Interactions of atmospheric [CO₂] with nitrogen and water availability over stand development. *New Phytologist*, 185(2), 514–528. <https://doi.org/10.1111/j.1469-8137.2009.03078.x>
- Metzker, M. L. (2010). Sequencing technologies the next generation. *Nature Reviews Genetics*, 11(1), 31–46. <https://doi.org/10.1038/nrg2626>
- Meyer, F., Paarmann, D., D'Souza, M., Olson, R., Glass, E. M., Kubal, M., Paczian, T., Rodriguez, A., Stevens, R., Wilke, A., Wilkening, J., & Edwards, R. A. (2008). The metagenomics RAST server - A public resource for the automatic phylogenetic and functional analysis of metagenomes. *BMC Bioinformatics*, 9, 1–8. <https://doi.org/10.1186/1471-2105-9-386>
- Mollah, M., Norton, R., & Huzzey, J. (2009). Australian grains free-air carbon dioxide

- enrichment (AGFACE) facility: Design and performance. *Crop and Pasture Science*, 60(8), 697–707. <https://doi.org/10.1071/CP08354>
- Moran, M. A., Satinsky, B., Gifford, S. M., Luo, H., Rivers, A., Chan, L. K., Meng, J., Durham, B. P., Shen, C., Varaljay, V. A., Smith, C. B., Yager, P. L., & Hopkinson, B. M. (2013). Sizing up metatranscriptomics. *ISME Journal*, 7(2), 237–243. <https://doi.org/10.1038/ismej.2012.94>
- Morrissey, E. M., McHugh, T. A., Preteska, L., Hayer, M., Dijkstra, P., Hungate, B. A., & Schwartz, E. (2015). Dynamics of extracellular DNA decomposition and bacterial community composition in soil. *Soil Biology and Biochemistry*, 86, 42–49. <https://doi.org/10.1016/j.soilbio.2015.03.020>
- Morton, J. T., Marotz, C., Washburne, A., Silverman, J., Zaramela, L. S., Edlund, A., Zengler, K., & Knight, R. (2019). Establishing microbial composition measurement standards with reference frames. *Nature Communications*, 10(1). <https://doi.org/10.1038/s41467-019-10656-5>
- Moser, G., Gorenflo, A., Brenzinger, K., Keidel, L., Braker, G., Marhan, S., Clough, T. J., & Müller, C. (2018). Explaining the doubling of N₂O emissions under elevated CO₂ in the Giessen FACE via in-field ¹⁵N tracing. *Global Change Biology*, 24(9), 3897–3910. <https://doi.org/10.1111/gcb.14136>
- Mueller, K. E., Blumenthal, D. M., Pendall, E., Carrillo, Y., Dijkstra, F. A., Williams, D. G., Follett, R. F., & Morgan, J. A. (2016). Impacts of warming and elevated CO₂ on a semi-arid grassland are non-additive, shift with precipitation, and reverse over time. *Ecology Letters*, 19(8), 956–966. <https://doi.org/10.1111/ele.12634>
- Müller, C., Rütting, T., Abbasi, M. K., Laughlin, R. J., Kammann, C., Clough, T. J., Sherlock, R. R., Kattge, J., Jäger, H. J., Watson, C. J., & Stevens, R. J. (2009). Effect of elevated CO₂ on soil N dynamics in a temperate grassland soil. *Soil Biology and Biochemistry*, 41(9), 1996–2001. <https://doi.org/10.1016/j.soilbio.2009.07.003>
- Narayanasamy, S., Jarosz, Y., Muller, E. E. L., Heintz-Buschart, A., Herold, M., Kaysen, A., Laczny, C. C., Pinel, N., May, P., & Wilmes, P. (2016). IMP: A pipeline for reproducible reference-independent integrated metagenomic and metatranscriptomic analyses. *Genome Biology*, 17(1), 1–21. <https://doi.org/10.1186/s13059-016-1116-8>
- Narayanasamy, S., Muller, E. E. L., Sheik, A. R., & Wilmes, P. (2015). Integrated omics for the identification of key functionalities in biological wastewater treatment microbial communities. *Microbial Biotechnology*, 8(3), 363–368. <https://doi.org/10.1111/1751-7915.12255>
- Niklaus, P. A., & Falloon, P. (2006). Estimating soil carbon sequestration under elevated CO₂ by combining carbon isotope labelling with soil carbon cycle modelling. *Global*

- Change Biology*, 12(10), 1909–1921. <https://doi.org/10.1111/j.1365-2486.2006.01215.x>
- Norby, R. J. (2011). Ecological and evolutionary lessons from free air carbon enhancement (FACE) experiments. *Annual Review of Ecology, Evolution, and Systematics*, 42. <https://doi.org/10.1146/annurev-ecolsys-102209-144647>
- Norby, R. J., Warren, J. M., Iversen, C. M., Medlyn, B. E., & McMurtrie, R. E. (2010). CO₂ enhancement of forest productivity constrained by limited nitrogen availability. *Proceedings of the National Academy of Sciences of the United States of America*, 107(45), 19368–19373. <https://doi.org/10.1073/pnas.1006463107>
- Ogura, A., Lin, M., Shigenobu, Y., Fujiwara, A., Ikeo, K., & Nagai, S. (2011). Effective gene collection from the metatranscriptome of marine microorganisms. *10th Int. Conference on Bioinformatics - 1st ISCB Asia Joint Conference 2011, InCoB 2011/ISCB-Asia 2011: Computational Biology - Proceedings from Asia Pacific Bioinformatics Network (APBioNet)*, 12(SUPPL. 3). <https://doi.org/10.1186/1471-2164-12-S3-S15>
- Owensby, C. E., Ham, J. M., Knapp, A. K., Bremer, D., & Auen, L. M. (1997). Water vapour fluxes and their impact under elevated CO₂ in a C₄-tallgrass prairie. *Global Change Biology*, 3(3), 189–195. <https://doi.org/10.1046/j.1365-2486.1997.00084.x>
- Palarea-Albaladejo, J., & Martín-Fernández, J. A. (2015). ZCompositions - R package for multivariate imputation of left-censored data under a compositional approach. *Chemometrics and Intelligent Laboratory Systems*, 143, 85–96. <https://doi.org/10.1016/j.chemolab.2015.02.019>
- Pawlowsky-Glahn, V., & Egozcue, J. J. (2006). Compositional data and their analysis: An introduction. *Geological Society Special Publication*, 264, 1–10. <https://doi.org/10.1144/GSL.SP.2006.264.01.01>
- Peano, C., Pietrelli, A., Consolandi, C., Rossi, E., Petiti, L., Tagliabue, L., De Bellis, G., & Landini, P. (2013). An efficient rRNA removal method for RNA sequencing in GC-rich bacteria. *Microbial Informatics and Experimentation*, 3(1), 1–11. <https://doi.org/10.1186/2042-5783-3-1>
- Phillips, R. P., Meier, I. C., Bernhardt, E. S., Grandy, A. S., Wickings, K., & Finzi, A. C. (2012). Roots and fungi accelerate carbon and nitrogen cycling in forests exposed to elevated CO₂. *Ecology Letters*, 15(9), 1042–1049. <https://doi.org/10.1111/j.1461-0248.2012.01827.x>
- Pujol Pereira, E. I., Chung, H., Scow, K., & Six, J. (2013). Microbial communities and soil structure are affected by reduced precipitation, but not by elevated Carbon Dioxide. *Soil Science Society of America Journal*, 77(2), 482. <https://doi.org/10.2136/sssaj2012.0218>

- Qiao, N., Schaefer, D., Blagodatskaya, E., Zou, X., Xu, X., & Kuzyakov, Y. (2014). Labile carbon retention compensates for CO₂ released by priming in forest soils. *Global Change Biology*, 20(6), 1943–1954. <https://doi.org/10.1111/gcb.12458>
- Quinn, T. P., Crowley, T. M., & Richardson, M. F. (2018). Benchmarking differential expression analysis tools for RNA-Seq: Normalization-based vs. log-ratio transformation-based methods. *BMC Bioinformatics*, 19(1), 1–15. <https://doi.org/10.1186/s12859-018-2261-8>
- Quinn, T. P., Erb, I., Richardson, M. F., & Crowley, T. M. (2018). Understanding sequencing data as compositions: An outlook and review. *Bioinformatics*, 34(16), 2870–2878. <https://doi.org/10.1093/bioinformatics/bty175>
- Regan, K., Kammann, C., Hartung, K., Lenhart, K., Müller, C., Philippot, L., Kandeler, E., & Marhan, S. (2011). Can differences in microbial abundances help explain enhanced N₂O emissions in a permanent grassland under elevated atmospheric CO₂? *Global Change Biology*, 17(10), 3176–3186. <https://doi.org/10.1111/j.1365-2486.2011.02470.x>
- Reich, P. B., Hobbie, S. E., & Lee, T. D. (2014). Plant growth enhancement by elevated CO₂ eliminated by joint water and nitrogen limitation. *Nature Geoscience*, 7(12), 920–924. <https://doi.org/10.1038/ngeo2284>
- Reineke, A., & Selim, M. (2019). Elevated atmospheric CO₂ concentrations alter grapevine (*Vitis vinifera*) systemic transcriptional response to European grapevine moth (*Lobesia botrana*) herbivory. *Scientific Reports*, 9(1), 1–12. <https://doi.org/10.1038/s41598-019-39979-5>
- Rivera-Pinto, J., Egozcue, J. J., Pawlowsky-Glahn, V., Paredes, R., Noguera-Julian, M., & Calle, M. L. (2018). Balances: a New Perspective for Microbiome Analysis. *MSystems*, 3(4), e00053-18. <https://doi.org/10.1128/mSystems.00053-18>
- Sharma, R., & Sharma, P. K. (2018). Metatranscriptome sequencing and analysis of agriculture soil provided significant insights about the microbial community structure and function. *Ecological Genetics and Genomics*, 6(September 2017), 9–15. <https://doi.org/10.1016/j.egg.2017.10.001>
- Simonin, M., Le Roux, X., Poly, F., Lerondelle, C., Hungate, B. A., Nunan, N., & Niboyet, A. (2015). Coupling between and among ammonia oxidizers and nitrite oxidizers in grassland mesocosms Submitted to elevated CO₂ and nitrogen supply. *Microbial Ecology*, 70(3), 809–818. <https://doi.org/10.1007/s00248-015-0604-9>
- Song, N., Zhang, X., Wang, F., Zhang, C., & Tang, S. (2012). Elevated CO₂ increases Cs uptake and alters microbial communities and biomass in the rhizosphere of *Phytolacca americana* Linn (pokeweed) and *Amaranthus cruentus* L. (purple amaranth) grown on soils spiked with various levels of Cs. *Journal of Environmental*

- Radioactivity*, 112, 29–37. <https://doi.org/10.1016/j.jenvrad.2012.03.002>
- Sunagawa, S., Mende, D. R., Zeller, G., Izquierdo-Carrasco, F., Berger, S. A., Kultima, J. R., Coelho, L. P., Arumugam, M., Tap, J., Nielsen, H. B., Rasmussen, S., Brunak, S., Pedersen, O., Guarner, F., De Vos, W. M., Wang, J., Li, J., Doré, J., Dusko Ehrlich, S., ... Bork, P. (2013). Metagenomic species profiling using universal phylogenetic marker genes. *Nature Methods*, 10(12), 1196–1199. <https://doi.org/10.1038/nmeth.2693>
- Susin, A., Wang, Y., Lê Cao, K.-A., & Calle, M. L. (2020). Variable selection in microbiome compositional data analysis. *NAR Genomics and Bioinformatics*, 2(2), 5–7. <https://doi.org/10.1093/nargab/lqaa029>
- Tamames, J., & Puente-Sánchez, F. (2019). SqueezeMeta, a highly portable, fully automatic metagenomic analysis pipeline. *Frontiers in Microbiology*, 10(JAN), 1–10. <https://doi.org/10.3389/fmicb.2018.03349>
- Taylor, G., Tricker, P., Graham, L., Tallis, M., Rae, A., Trewin, H., & Street, N. (2006). Managed Ecosystems and CO₂. In *Managed Ecosystems and CO₂* (Vol. 187). <https://doi.org/10.1007/3-540-31237-4>
- Trivedi, P., Delgado-Baquerizo, M., Trivedi, C., Hu, H., Anderson, I. C., Jeffries, T. C., Zhou, J., & Singh, B. K. (2016). Microbial regulation of the soil carbon cycle: Evidence from gene-enzyme relationships. *ISME Journal*, 10(11), 2593–2604. <https://doi.org/10.1038/ismej.2016.65>
- Tsilimigras, M. C. B., & Fodor, A. A. (2016). Compositional data analysis of the microbiome: fundamentals, tools, and challenges. *Annals of Epidemiology*, 26(5), 330–335. <https://doi.org/10.1016/j.annepidem.2016.03.002>
- Van Groenigen, K. J., Gorissen, A., Six, J., Harris, D., Kuikman, P. J., Van Groenigen, J. W., & Van Kessel, C. (2005). Decomposition of ¹⁴C-labeled roots in a pasture soil exposed to 10 years of elevated CO₂. *Soil Biology and Biochemistry*, 37(3), 497–506. <https://doi.org/10.1016/j.soilbio.2004.08.013>
- Vestergard, M., Reinsch, S., Bengtson, P., Ambus, P., & Christensen, S. (2016). Enhanced priming of old, not new soil carbon at elevated atmospheric CO₂. *Soil Biology and Biochemistry*, 100, 140–148. <https://doi.org/10.1016/j.soilbio.2016.06.010>
- Walker, T. S., Bais, H. P., Grotewold, E., & Vivanco, J. M. (2003). Root Exudation and Rhizosphere Biology Root Exudation and Rhizosphere Biology. *Plant Physiology*, 132(1), 44–51. <https://doi.org/10.1104/pp.102.019661>. Although
- Westreich, S. T., Treiber, M. L., Mills, D. A., Korf, I., & Lemay, D. G. (2018). SAMSA2: A standalone metatranscriptome analysis pipeline. *BMC Bioinformatics*, 19(1), 1–11. <https://doi.org/10.1186/s12859-018-2189-z>

- Wohlfahrt, Y., Smith, J. P., Tittmann, S., Honermeier, B., & Stoll, M. (2018). Primary productivity and physiological responses of *Vitis vinifera* L. cvs. under Free Air Carbon dioxide Enrichment (FACE). *European Journal of Agronomy*, 101(February), 149–162. <https://doi.org/10.1016/j.eja.2018.09.005>
- Wohlfahrt, Y., Tittmann, S., Schmidt, D., Rauhut, D., Honer, B., & Stoll, M. (2020). The effect of elevated CO₂ on berry development and bunch structure of *Vitis vinifera* L. cvs. Riesling and cabernet sauvignon. *Applied Sciences (Switzerland)*, 10, 2486. <https://doi.org/10.3390/app10072486>
- Wu, J., Gao, W., Johnson, R. H., Zhang, W., & Meldrum, D. R. (2013). Integrated metagenomic and metatranscriptomic analyses of microbial communities in the meso- and bathypelagic realm of north Pacific ocean. *Marine Drugs*, 11(10), 3777–3801. <https://doi.org/10.3390/md11103777>
- Xie, Z., Cadisch, G., Edwards, G., Baggs, E. M., & Blum, H. (2005). Carbon dynamics in a temperate grassland soil after 9 years exposure to elevated CO₂ (Swiss FACE). *Soil Biology and Biochemistry*, 37(7), 1387–1395. <https://doi.org/10.1016/j.soilbio.2004.12.010>
- Xiong, J., He, Z., Shi, S., Kent, A., Deng, Y., Wu, L., Van Nostrand, J. D., & Zhou, J. (2015). Elevated CO₂ shifts the functional structure and metabolic potentials of soil microbial communities in a C₄ agroecosystem. *Scientific Reports*, 5, 1–9. <https://doi.org/10.1038/srep09316>
- Xu, M., He, Z., Deng, Y., Wu, L., Van Nostrand, J. D., Hobbie, S. E., Reich, P. B., & Zhou, J. (2013). Elevated CO₂ influences microbial carbon and nitrogen cycling. *BMC Microbiology*, 13(1). <https://doi.org/10.1186/1471-2180-13-124>
- Yu, Z., Li, Y., Wang, G., Liu, J., Liu, J., Liu, X., Herbert, S. J., & Jin, J. (2016). Effectiveness of elevated CO₂ mediating bacterial communities in the soybean rhizosphere depends on genotypes. *Agriculture, Ecosystems and Environment*, 231, 229–232. <https://doi.org/10.1016/j.agee.2016.06.043>
- Zelikova, T. J., Blumenthal, D. M., Williams, D. G., Souza, L., LeCain, D. R., Morgan, J., & Pendall, E. (2014). Long-term exposure to elevated CO₂ enhances plant community stability by suppressing dominant plant species in a mixed-grass prairie. *Proceedings of the National Academy of Sciences of the United States of America*, 111(43), 15456–15461. <https://doi.org/10.1073/pnas.1414659111>
- Zhu, K., Chiariello, N. R., Tobeck, T., Fukami, T., & Field, C. B. (2016). Nonlinear, interacting responses to climate limit grassland production under global change. *Proceedings of the National Academy of Sciences of the United States of America*, 113(38), 10589–10594. <https://doi.org/10.1073/pnas.1606734113>

Chapter 2 Elevated atmospheric CO₂ modifies mostly the metabolic active rhizosphere soil microbiome in the Giessen FACE experiment

Research article

Published on Microbial Ecology



Elevated Atmospheric CO₂ Modifies Mostly the Metabolic Active Rhizosphere Soil Microbiome in the Giessen FACE Experiment

David Rosado-Porto^{1,2} · Stefan Ratering¹ · Massimiliano Cardinale³ · Corinna Maisinger¹ · Gerald Moser⁴ · Marianna Deppe⁴ · Christoph Müller^{4,5} · Sylvia Schnell¹

Received: 19 March 2021 / Accepted: 8 June 2021
© The Author(s) 2021

Abstract

Elevated levels of atmospheric CO₂ lead to the increase of plant photosynthetic rates, carbon inputs into soil and root exudation. In this work, the effects of rising atmospheric CO₂ levels on the metabolic active soil microbiome have been investigated at the Giessen free-air CO₂ enrichment (Gi-FACE) experiment on a permanent grassland site near Giessen, Germany. The aim was to assess the effects of increased C supply into the soil, due to elevated CO₂, on the active soil microbiome composition. RNA extraction and 16S rRNA (cDNA) metabarcoding sequencing were performed from bulk and rhizosphere soils, and the obtained data were processed for a compositional data analysis calculating diversity indices and differential abundance analyses. The structure of the metabolic active microbiome in the rhizospheric soil showed a clear separation between elevated and ambient CO₂ ($p = 0.002$); increased atmospheric CO₂ concentration exerted a significant influence on the microbiomes differentiation ($p = 0.01$). In contrast, elevated CO₂ had no major influence on the structure of the bulk soil microbiome ($p = 0.097$). Differential abundance results demonstrated that 42 bacterial genera were stimulated under elevated CO₂. The RNA-based metabarcoding approach used in this research showed that the ongoing atmospheric CO₂ increase of climate change will significantly shift the microbiome structure in the rhizosphere.

Keywords RNA metabarcoding · Elevated CO₂ · Rhizosphere microbiome · Grassland

Introduction

The rise of atmospheric carbon dioxide (CO₂) concentrations and global warming are well-documented processes. Total annual anthropogenic greenhouse gas emissions have continued to increase, comprising CO₂, which represents

around 75% of these emissions [1]. Elevated CO₂ (eCO₂) concentrations have several consequences on plants, such as increased growth in C3, C4, and CAM plants by 41%, 22%, and 15%, respectively [2, 3]; increased plant yield [4]; decreased evapotranspiration of both C3 [5] and C4 plants [6]; augmented photosynthetic capacity [3, 7, 8]; and increased below-ground biomass [9].

Considering that nearly up to 21% of all photosynthetically fixed carbon is transferred to the rhizosphere, roots and root exudates influence the composition and biomass of soil microbiome [10, 11]. Elevated atmospheric CO₂ increases efflux amounts of total soluble sugars, amino acids, phenolic acids, and organic acids in the root exudates [12–14]. Similarly, the rates of organic carbon as energy sources enhance microbial degradation of soil organic matter (SOC), also known as priming effect [14]. Priming effect is defined as an accelerated decomposition of SOC due to an increased supply of labile C to the soil and changes in the microbial activity as a response [15]. The microbial succession is accompanied by the activation of various, previously

✉ Sylvia Schnell
Sylvia.Schnell@umwelt.uni-giessen.de

¹ Institute of Applied Microbiology, Justus Liebig University, Giessen, DE, Germany

² Faculty of Basic and Biomedical Sciences, Simón Bolívar University, Barranquilla, Colombia

³ Department of Biological and Environmental Sciences and Technologies, University of Salento, Via Prov.le Monteroni, 73100 Lecce, Italy

⁴ Institute of Plant Ecology, Justus Liebig University, Giessen, DE, Germany

⁵ School of Biology and Environmental Science and Earth Institute, University College Dublin, Belfield, Dublin, Ireland

dormant microorganisms that respond specifically to the added substrate [15, 16].

The effects of eCO_2 levels on soil ecosystems have been studied in free-air CO_2 enrichment (FACE) experiments, revealing significant effects of rising CO_2 on soil organisms. However, with regard to microbial composition and function related to carbon and nitrogen cycling, mixed results have been obtained. At the BioCON field experiment, it was found that the structure of microbial communities was different between ambient CO_2 (aCO_2) and eCO_2 [17]. Likewise, the abundance of genes involved in labile C degradation and C and N fixation, as RuBisCo, carbon monoxide dehydrogenase (CODH), propionyl-CoA/acetyl-CoA carboxylase (PCC/ACC), *nifH* and *nirS* genes were significantly increased under eCO_2 [18]. Similarly, He et al. [19] and Xiong et al. [20] have reported a shift of soil microbial communities under eCO_2 in a soybean and a maize agro-ecosystem, respectively. These changes included stimulation of key functional genes involved in carbon fixation and degradation, nitrogen fixation, denitrification, methane metabolism, and phosphorus cycling.

Oppositely, some FACE experiments have shown no effects of eCO_2 on soil microbiome structure and activity, as Marhan et al. [21] who described that abundances of both total 16S rRNA genes and nitrate-reducing bacteria were not influenced by CO_2 but by sampling date and depth. Dunbar et al. [22] described that neither bacterial nor fungal community structure nor composition were altered under eCO_2 . Pujol Pereira et al. [23] did not find any significant effects of eCO_2 on bacterial abundance, soil C, and N concentrations. Butterly et al. [24] reported that changes in microbial community structure were not detected, although eCO_2 reduced the abundance of C and N functional genes.

The Giessen free-air CO_2 enrichment (Gi-FACE) experiment in Giessen, Germany, has been running since 1998. It is becoming a good predictor model to assess the effects of long-term increased CO_2 concentrations on soil microbiome structure and function. Some studies carried out in this facility aimed to assess these changes. Regan et al. [25] reported that in the Gi-FACE extractable organic carbon, dissolved organic nitrogen, NH_4^+ , NO_3^- , and abundances of genes involved in ammonia oxidation and denitrification depended more on soil depth and moisture gradient than on eCO_2 . Similarly, also de Menezes et al. [26] described that increases in atmospheric CO_2 may cause only minor changes in Gi-FACE's soil bacterial community composition and that functional responses of the soil community are due to factors like soil moisture rather than CO_2 concentration. Brenzinger et al. [27] reported that the abundance and composition of microbial communities in the topsoil under eCO_2 presented only small differences from soil under aCO_2

(aCO_2), concluding that +20% CO_2 had little to no effect on the overall microbial community involved in N-cycling in the Gi-FACE soil. More recently, Bei et al. [28] described that eCO_2 had significant effects on the functional expression associated to both rhizosphere microbiomes and plant roots; and that abundances of Eukarya relative to Bacteria were significantly decreased in eCO_2 as well.

The question of why some studies reported differences between eCO_2 and aCO_2 while some others did not is still open. Several abiotic and biotic factors could be the reason for the contradictory observations in the different experimental setups described above. However, all such previous studies conducted in the Gi-FACE used a DNA-based metagenomic approach, with the exception of Bei et al. [28], who utilized a metatranscriptomic approach. The disadvantage of using DNA is that, after a cell dies, amplifiable extracellular DNA can remain in soils for weeks to years and may bias DNA-based estimates of the diversity and structure of soil microbial communities [29, 30]. Moreover, Carini et al. [31] reported that DNA from dead cells or free DNA represented a large fraction of microbial DNA in many soils, comprising approximately 40.7% and 40.5% of amplifiable prokaryotic 16S rRNA genes and fungal ITS amplicons, respectively. Therefore, DNA-depending studies may overestimate the richness of the soil microbiome by up to 55% for prokaryotes and 52% for fungi [31] and in consequence may hide the active microorganisms that are involved in soil microbial processes.

A better approach for assessing differences between eCO_2 and aCO_2 is the use of RNA instead of DNA for 16S rRNA metabarcoding analysis. The ribosome numbers are correlated to the metabolic activity of bacteria [32], and different studies showed that, with this approach, the active organisms instead of the dormant ones were assessed [33–35]. Additionally, results of the metatranscriptomic methodological approach on the Gi-FACE soil microbiome reported by Bei et al. [28] demonstrated that RNA instead of DNA is a better predictor of microbiome composition and activity. For this reason, the aims of the present work were (i) to evaluate the effect of long-term eCO_2 concentrations and increased C supply on active soil microbiome through an rRNA-based metabarcoding approach; (ii) to assess the differences between eCO_2 and aCO_2 conditions in rhizosphere and bulk soils; and (iii) to link these differences with environmental factors.

The following questions have been addressed:

1. Is the community structure of active bacteria different between ambient and elevated CO_2 in rhizosphere and/or bulk soil?
2. Which other environmental parameters beside CO_2 shape the community?

Material and Methods

Study Site Description

The Gi-FACE study is located at 50° 32' N and 8° 41.3' E near Giessen, Germany, at an elevation of 172 m above sea level. It consists of three pairs of rings with a diameter of 8 m; each pair consists of an ambient and an elevated CO₂ treatment ring [36]. Since May 1998 until present, elevated CO₂ rings have been continuously enriched by 20% above ambient CO₂ concentrations during daylight hours. Ambient and elevated CO₂ rings are separated by at least 20 m, and each pair is placed at the vertices of an equilateral triangle. The presence of a slight slope within the experimental site (between 0.5 and 3.5°) places the rings on a moisture gradient, such that pair 1 has the lowest mean moisture content (38.8% ± 10.2%) and pair 2 has the highest mean moisture content (46.1% ± 13.2%), whereas pair 3 is intermediate (40.7% ± 11%) [26, 36]. The average annual air temperature and precipitation are 9.4 °C and 580 mm, respectively.

The vegetation is an *Arrhenatheretum elatioris* Br.Bl. *Filipendula ulmaria* subcommunity, dominated by *Arrhenatherum elatius*, *Galium album*, and *Geranium pratense*. At least 12 grass species, 15 non-leguminous herbs and up to 5 legumes with small biomass contributions (<5%) are present within a single plot [37]. The experimental field has not been ploughed for more than 100 years. It has received N fertilization in form of granular mineral calcium ammonium nitrate (40 kg N ha⁻¹ year⁻¹) once a year since 1995 and has been mown twice a year since 1993. The soil at the Gi-FACE site is classified as Fluvisol; its texture is a sandy clay loam over a clay layer, with pH = 6.2 and average C and N contents of 4.5% and 0.45%, respectively, as measured in 2001 [36].

Soil Sampling and Physico-chemical Parameter Measurements

Soil sampling was performed utilizing sawed off 50 ml syringes (11 × 3 cm), and four samples were taken to a depth of ~10 cm within each ring in September 2015. Soil cores were gently shaken by hand to remove loosely attached soil (bulk soil), while the soil that remained attached to the roots was considered as rhizosphere soil. Bulk and rhizosphere soils were sieved (<2 mm) and stored at -80 °C for further analyses. Samples from each soil core were classified in four groups considering the CO₂ conditions (ambient and elevated) and the soil habitat (bulk soil and rhizosphere soil).

Ammonium and nitrate concentrations were measured according to Kandeler et al. [38] and Bak et al. [39]. Water

content, dry matter, and water holding capacity of soil samples were measured gravimetrically [40]. Carbon and nitrogen content of soil were measured by pyrolysis coupled to gas chromatography on a EA 1100 elemental analyzer (ThermoQuest, Milan, Italy) using a TCD detector by the Dumas method according to HBU (1996) [41] and VDLUFA (2012) method [42]. Injected CO₂ and CO₂ soil fluxes were determined from August to September 2015. Injected CO₂ was measured at 60 cm above ground with an infrared gas analyzer (LI-COR 6252) [36]. CO₂ soil fluxes were measured weekly using an automated closed dynamic chamber system (LI-COR 8100, LI-COR Inc., Lincoln, Nebraska, USA). Per ring, 4 PVC soil collars (20.3 cm diameter) were permanently installed as chamber bases in 2006 and held vegetation free since 2008. Fluxes were calculated from the increase in CO₂ concentration in the chamber over the 1–3 min closure time as described by Keidel et al. [43].

Central tendency and dispersion measures were calculated for soil chemical data. CO₂ injection and CO₂ fluxes data were analyzed using growth curve analysis (GCA) [44], with R packages *gazer* version 0.1 [45] and *lme4* version 1.1–23 [46], creating polynomial-transformed predictor variables, fitting them to a linear mixed model by maximum likelihood, and assessing differences between CO₂ conditions with a t-test, using an alpha of <0.05.

RNA Extraction and Reverse Transcription

RNA extraction was performed following a modified protocol of Mettel et al. [47]. For the extraction, 0.3–0.5 g of soil were weighed in reaction tubes containing 100 mg of sterile zirconia beads, added with 700 µl TPM buffer (50 mM Tris-HCl (pH 5), 1.7% [wt/vol] polyvinylpyrrolidone, 20 mM MgCl₂), and vortexed for 30 s. Cells were then disrupted in a cell mill MM200 (Retsch, Haan, Germany) for 2 min at a frequency of 30 Hz. Soil and cell debris were precipitated by centrifugation in a microcentrifuge (Heraeus Fresco, Thermo Fisher Scientific Inc., Waltham) for 5 min at 17,000 g and 4 °C, and then the supernatant was transferred into a fresh reaction tube. To the resulting soil pellet 700 µL of buffer PBL (5 mM Tris-HCl (pH 5), 5 mM Na₂EDTA, and 0.1% [wt/vol] sodium dodecyl sulfate) were added, and the disruption process was performed again as described above. Both supernatants from the lysis processes were pooled in one reaction tube.

The pooled supernatant was immediately extracted, initially with the addition of 500 µl of phenol/chloroform/isoamyl alcohol (25:24:1) and subsequent with chloroform/isoamyl alcohol (24:1). Afterwards, each time the sample was centrifuged for 5 min at 17,000 g and 4 °C. The resulting upper aqueous phase was transferred to a new reaction tube, 800 µl of PEG solution was added (30% [wt/vol]

polyethylene glycol 6000 and 1.6 M NaCl), incubated in ice for 30 min and centrifuged for 30 min at 17,000 g and 4 °C. Subsequently, the DNA/RNA pellet was washed with 800 µl of ice-cold 75% ethanol, dried out and dissolved in 50 µl of nuclease free water.

After extraction, samples were treated for DNA digestion with RNase-Free DNase Set (QIAGEN GmbH — Germany) according to manufacturer instructions; DNase reaction was stopped with 10 µl of 50 mM EDTA. With the DNA-free RNA, a PCR was carried out, using the universal 16S rRNA gene primers 27F (5'-AGAGTTTGATCMTGGATCMTGG CTCAG-3') and 1492R (5'-GGTACCTTGTTACGACT T-3') [48, 49] and checked on agarose gel electrophoresis to verify the absence of remaining DNA in the samples. Subsequently, reverse transcription was performed utilizing AccuScript High Fidelity 1st Strand cDNA Synthesis Kit (Agilent Technologies, Inc., Cedar Creek, TX, USA) following manufacturer instructions.

16S rRNA Ion Torren Sequencing and Metabarcoding Analysis

The 16S rRNA gene hypervariable regions (V4&V5) were PCR amplified using the set of primers 520F (5'-AYT GGGYDTAAAGNG-3') [50] and 907R (5'-CCGTCA ATTCTTTTRAGTTT-3') [51] and sequenced by Ion Torrent technique following the protocol described by Kaplan et al. [52]. The obtained Ion Torrent sequencing output was analyzed using QIIME2 version 2020.6.0 [53], sequences were demultiplexed with the QIIME2 cutadapt command [54] using a barcode error rate of 0 and assigned to specific samples by corresponding barcodes. Later, quality control, denoising, sequences dereplication, and chimera filtering were performed using DADA2 software [55]; the first 15 nucleotides were trimmed, and sequences were truncated at a position of 320 nucleotides. Amplicon sequence variants (ASV) generated with DADA2 were taxonomically affiliated with a trained fitted classifier [56, 57] based on the SILVA 138 database [58, 59].

Alpha and beta diversity analyses were performed using R studio software 1.1.419, R packages Phyloseq 1.22.3 [60] and Vegan 2.4–6 [61]. Before diversity analyses, ASVs were collapsed by genera. For alpha diversity assessment, rarefaction was applied and diversity indices (Observed species, Simpson, Shannon, Fisher) were calculated and compared among CO₂ conditions and soil habitats using the Wilcoxon test [62] with the Bonferroni correction method through 999 permutations. For non-constrained beta diversity analyses, data were transformed using centered log ratio (clr) method [63, 64], using R package Aldex2 1.18.0 [65]. Later, community dissimilarity distance matrices were created using the Aitchison distance [63, 64] and visualized using principal component analysis (PCA) [66]. Statistical differences

among treatments, rings, and CO₂ conditions were assessed by a permutational multivariate analysis of variance using Adonis method and employing 999 permutations [67]. Additionally, the degree of dispersion of the bacterial community composition from the four soil cores taken in each ring was assessed as described above. Redundancy analysis (RDA) was used to explore associations between microbial community structures and environmental parameters, and a permutation test of redundancy analysis using 999 permutations was applied for evaluating their statistical significance [68].

For the analysis of correlation between bacterial genera and environmental parameters, the genera belonging to the core microbiome of each of the soil sample groups were calculated, and their counts were transformed to relative abundance with package Microbiome version 1.8.0 [69]. Later, core microbiomes were calculated including genera with a total relative abundance of $\geq 0.01\%$ and present in $\geq 85\%$ of the corresponding group's samples. A correlation test was performed using Aldex2 1.18.0 [65] and its "aldex.corr" function, utilizing Pearson's correlation coefficient, and p values were corrected using false discovery rate (FDR) method with an alpha of < 0.05 .

Differential abundance of genera from rhizosphere soils was assessed by comparing the core microbiomes of each CO₂ condition utilizing the R packages DESeq2 1.24.0 [70] and Aldex2 1.18.0 [65]. DESeq2 analysis was performed by estimating the size factor and the dispersion using the geometric mean of the core microbiome genera; later, values were fitted with a generalized linear model using negative binomial distribution and applying a Wald significance tests, the option "local" for fitting of dispersions to the mean intensity and an alpha threshold of < 0.05 . Aldex2 analysis was done by performing a centered log ratio (clr) transformation using as denominator the geometric mean abundance of all features and 128 Monte Carlo instances; later, a Welch's t-test with a Benjamini–Hochberg correction and threshold < 0.05 was performed.

Functional capabilities based on the obtained 16S rRNA data were predicted using PICRUSt2 version (v2.3.0 beta) [71]. PICRUSt2 analysis was carried out using the default pipeline option. Afterward, EC number, KO functions, and MetaCyc non-constrained beta diversity and differential abundance analyses were performed as described above.

Quantitative PCR

The quantification of 16S rRNA gene to estimate total bacterial abundance was performed following the protocol described by Kaplan et al. [52], but instead of DNA, cDNA products described above were used for the quantification. Quantitative PCR (qPCR) was conducted on a Rotor-Gene Q (Qiagen, Hilden, Germany) by using Absolute qPCR SYBR Green Mix (Thermo Fisher Scientific). Statistical

comparisons were done with Kruskal–Wallis and Wilcoxon tests with the Benjamini–Hochberg adjustment method using R Package stats version 3.6.3.

Results

Ion Torrent Sequencing

A total of 5,855,099 raw sequences were obtained. After demultiplexing, sequences were assigned to each sample, ranging sequence counts in each sample from 306,675 to 22,410. After quality control, denoising, sequence dereplication, and chimera filtering with DADA2 software, 2,674,159 sequences were removed, resulting in 3,180,940 non-chimeric sequences and 11,587 representative sequences which were grouped into ASVs (Amplicon sequence variations) at a 99% similarity. Later, sequences belonging to chloroplast and mitochondria were removed, resulting in 11,508 ASVs.

Soil Microbial Diversity

Diversity indexes were evaluated to assess differences in soil microbiome between eCO₂ and aCO₂ conditions. In the Gi-FACE, soil active bacterial diversity changed

due to the influence of increased concentrations of CO₂ (Fig. 1). These changes are better appreciated when comparing bulk and rhizosphere soil fractions from aCO₂ and eCO₂ rings separately. In regard to alpha diversity of rhizosphere and bulk soil fractions from aCO₂ rings, significantly higher diversity values were observed in bulk compared to rhizosphere soils with Observed species (p value 0.00036), Shannon (p value 0.0086), and Fisher (p value 0.00036) indexes (Fig. 1). Nevertheless, this difference was not detected between bulk and rhizosphere soil fractions from eCO₂ rings, indicating an evenness between the rhizosphere and bulk soils in eCO₂ rings (Fig. 1). Likewise, eCO₂ rhizosphere soil presented greater diversity values in comparison to its aCO₂ counterpart, according to Observed species (p value 0.0193) and Fisher (p value 0.0193) indexes.

A distance matrix was created using the Aitchison distance and later ordinated using the principal component analysis (PCA) to further analyze the microbiome composition. Initially, the dispersion of the four soil cores taken within each ring and their distance to the centroids was assessed. They indicated a considerably different soil microbiome composition in each soil core, even when soil cores of the same rings were compared (S1). On the other hand, the assessment of differences among the evaluated habitats showed that the strongest effect on the bacterial microbiome

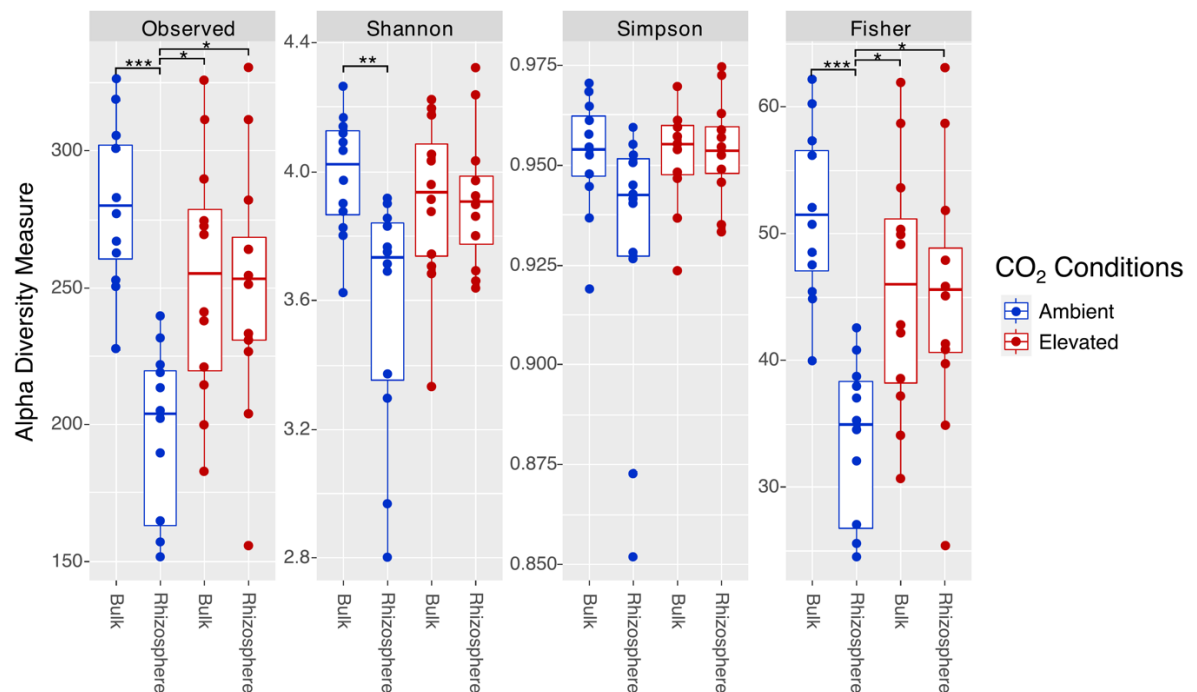


Fig. 1 Alpha diversity metrics. aCO₂, ambient CO₂ conditions; eCO₂, elevated CO₂ conditions. * p smaller 0.01, ** p smaller 0.001, *** p smaller 0.0001

differentiation in the soil was the ring factor, either for rhizosphere or bulk soils (p value 0.001).

Similarly, there were significant differences among the community composition of the four evaluated groups (aCO₂ bulk soil, aCO₂ rhizosphere soil, eCO₂ bulk soil, eCO₂ rhizosphere soil) (p value 0.001). In the same way, the PCA showed a clear differentiation between the microbiome composition of the rhizospheres from eCO₂ and aCO₂ rings (p value 0.002) (Fig. 2a). On the contrary, the separation of the microbial community composition between the bulk soils from aCO₂ and eCO₂ rings was not clear and statistically not significant (p value 0.327) (Fig. 2b).

Effect of Environmental Parameters on Microbial Community

A redundancy analysis (RDA) was carried out to assess the effect of environmental factors on the soil microbiome of the Gi-FACE. The results indicated that continuously higher

environmental CO₂ concentration was a factor that exerted a significant effect on the differentiation of the microbial communities of eCO₂ rings (p value 0.021) (Table 1, Fig. 3a). Furthermore, CO₂ soil fluxes on average were 35% higher in eCO₂ rings in comparison to the aCO₂ ones, and this difference was statistically significant throughout the assessed period of time (p value 0.031) (Fig. 3b). Moreover, increased soil fluxes of CO₂ are associated with the differences that were observed in Gi-FACE soil microbiome (p value 0.001).

Likewise, the ammonium content in the whole soil, rhizosphere and bulk soil fractions had a significant influence on the community composition (Table 1), despite the fact that soil ammonium concentrations were not significantly different between eCO₂ and aCO₂ rings (p value 0.313) (S2). Similarly, the total carbon content had significant influence on the whole soil and bulk soil microbial community structure (Table 1), but likewise ammonium there were no significant differences in carbon content between aCO₂ and eCO₂ rings (p value 0.1304) (S2). On the contrary, the average carbon/nitrogen ratio in the whole soil of the eCO₂ rings (11.1:1) was significantly higher in comparison with aCO₂ rings (10.69:1) (p value 0.0069) and had a significant effect (p value 0.025) on the microbial community composition (Table 1).

Furthermore, when observing each habitat separately, the RDA indicated that in the rhizosphere soil, the CO₂ atmospheric concentration had a significant effect on the microbiome differentiation between the aCO₂ and eCO₂ rings (p value 0.010) (Table 1, Fig. 3c). In contrast, eCO₂ had no substantial influence on the composition of the microbial community's structure of the bulk soils (p value 0.097) (Table 1, Fig. 3d).

Correlation analysis between environmental variables and rhizosphere soil core microbiome demonstrated that the abundance of several bacterial genera was either positively or negatively correlated with environmental CO₂ concentrations and soil CO₂ fluxes. Among the main bacterial families that were significantly positively correlated

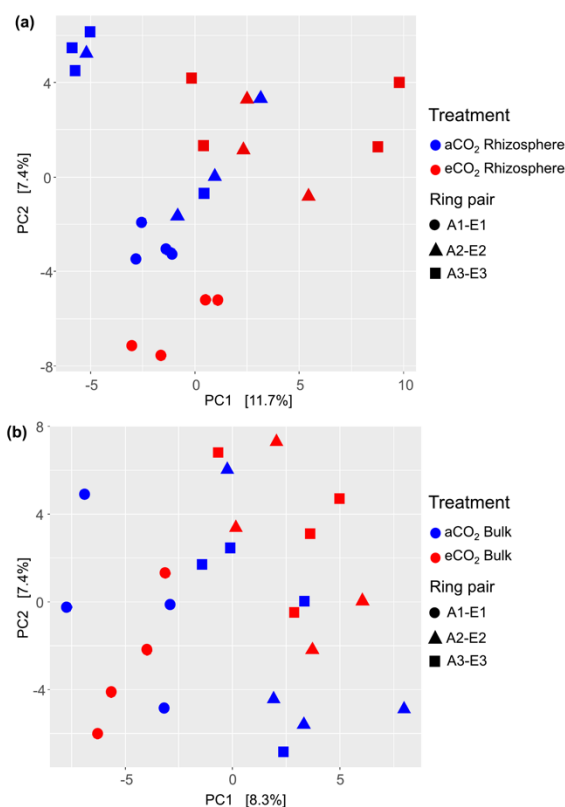


Fig. 2 Principal component analysis (PCA) calculated based on Aitchison community dissimilarity distance matrix of **a** rhizosphere soils from ambient and elevated CO₂ rings and **b** bulk soils from ambient and elevated CO₂ rings. A, ambient CO₂ rings; E, elevated CO₂ rings; aCO₂, ambient CO₂ conditions; eCO₂, elevated CO₂ conditions

Table 1 p values of permutation test for redundancy analysis (RDA) under reduced model using an Aitchison community dissimilarity distance matrix

Environmental parameter	Whole soil	Rhizosphere soil	Bulk soil
C:N	0.025 *	—	0.127
CO ₂ injected concentration	0.021 *	0.010 **	0.097
CO ₂ flux concentration	0.001 ***	0.003 **	0.004 **
NH ₄ ⁺	0.001 ***	0.002 **	0.018 *
Total carbon	0.001 ***	0.007 **	0.001 ***
Water holding capacity	0.006 **	0.024 *	0.100
Total nitrogen	0.141	—	0.688

Significance codes: 0.0001 '***', 0.001 '**', 0.01 '*'

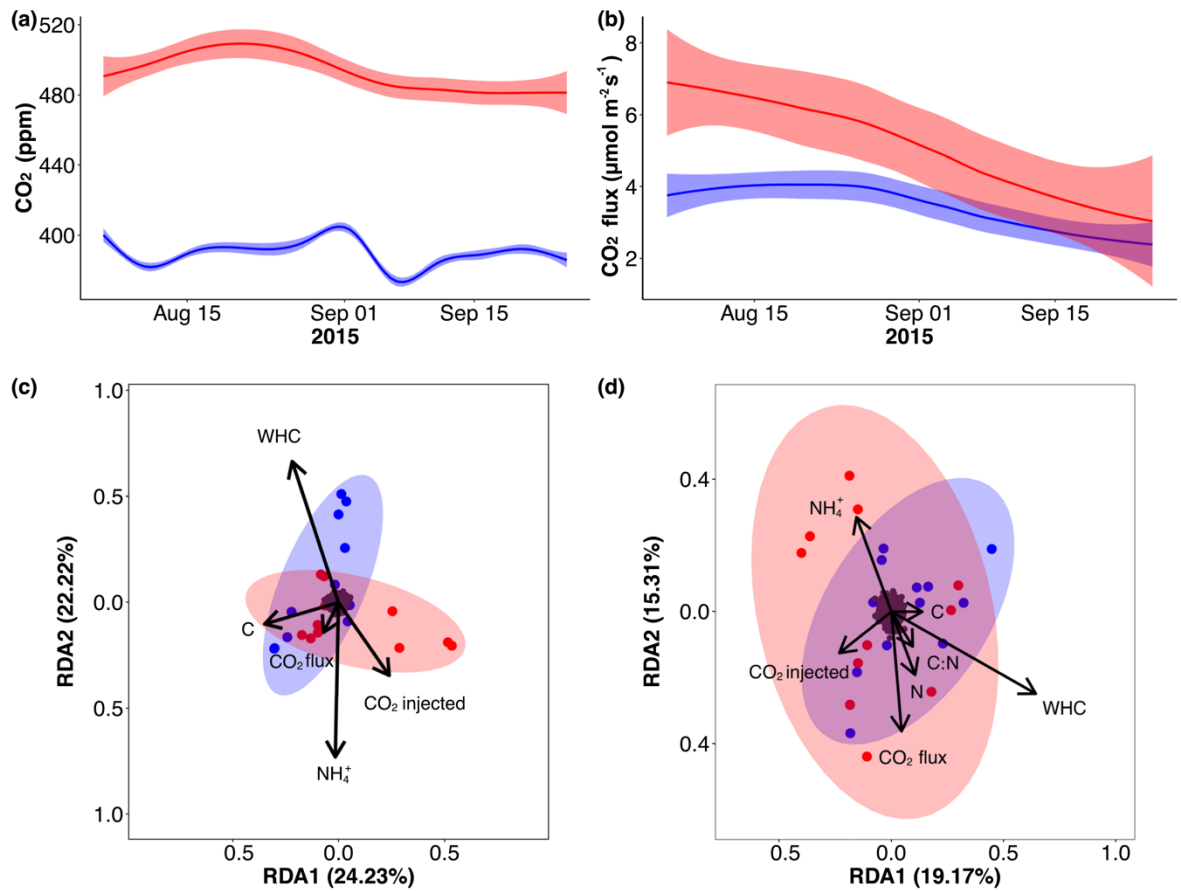


Fig. 3 Time series data from August to September 2015 of **a** average environmental CO₂ concentrations and **b** average soil CO₂ fluxes of ambient (blue) and elevated (red) CO₂ conditions; level of confidence interval of 0.95. Redundancy analysis (RDA) based on Aitchison

community dissimilarity distance matrix of **c** rhizosphere soils from ambient (blue) and elevated (red) CO₂ rings and **d** bulk soils from ambient (blue) and elevated (red) CO₂ rings; black dots indicate soil bacterial genera

with environmental eCO₂ and soil CO₂ fluxes concentrations are Rhodanobacteraceae, “Labraceae,” Xanthomonadaceae, Rhodobacteraceae, Rhizobiaceae, Pseudomonadaceae, Phaselicystidaceae, Haliangiaceae, Bacillaceae, Streptomycetaceae, Xanthobacteraceae, Burkholderiaceae, Devosiaceae, Haliangiaceae, Comamonadaceae and Polyangiaceae (Table S3.1). On the contrary, families “Solibacteraceae,” Caulobacteraceae, Acetobacteraceae, Thermoactinomycetaceae, Beijerinckiaceae, and Blastocatellaceae were negatively correlated with environmental eCO₂ and soil CO₂ fluxes (Table S3.1). Moreover, bacterial orders Nitrospirales, Caulobacterales, “Rokubacteriales,” Vicinamibacterales, “Tistrellales,” and “Rokubacteriales” were significantly correlated with NH₄⁺ content and soil water holding capacity in rhizosphere soils (Table S3.1).

Changes on the Rhizosphere Microbial Community Composition

Differential abundance analyses demonstrated that several rhizosphere soil genera were affected. Both Aldex2 and DESeq2 demonstrated that 42 bacterial genera were stimulated under eCO₂, among those are *Haliangium*, *Phaselicystis*, *Rhizobacter*, *Pseudomonas*, *Rhizobium*, *Phyllobacterium*, *Mesorhizobium*, *Rhodanobacter*, *Labrys*, unidentified genus of the class “Sericytochromatia,” *Dokdonella*, *Massilia*, *Burkholderia*, *Bacillus*, *Novosphingobium*, *Acidibacter*, and *Streptomyces* (Fig. 4a, Fig. 4b). These genera showed Log₂ Fold changes ranging from 0.910 to 9.67. Furthermore, Aldex2 test showed that other 56 genera were significantly stimulated in the rhizosphere soil of eCO₂ rings. These

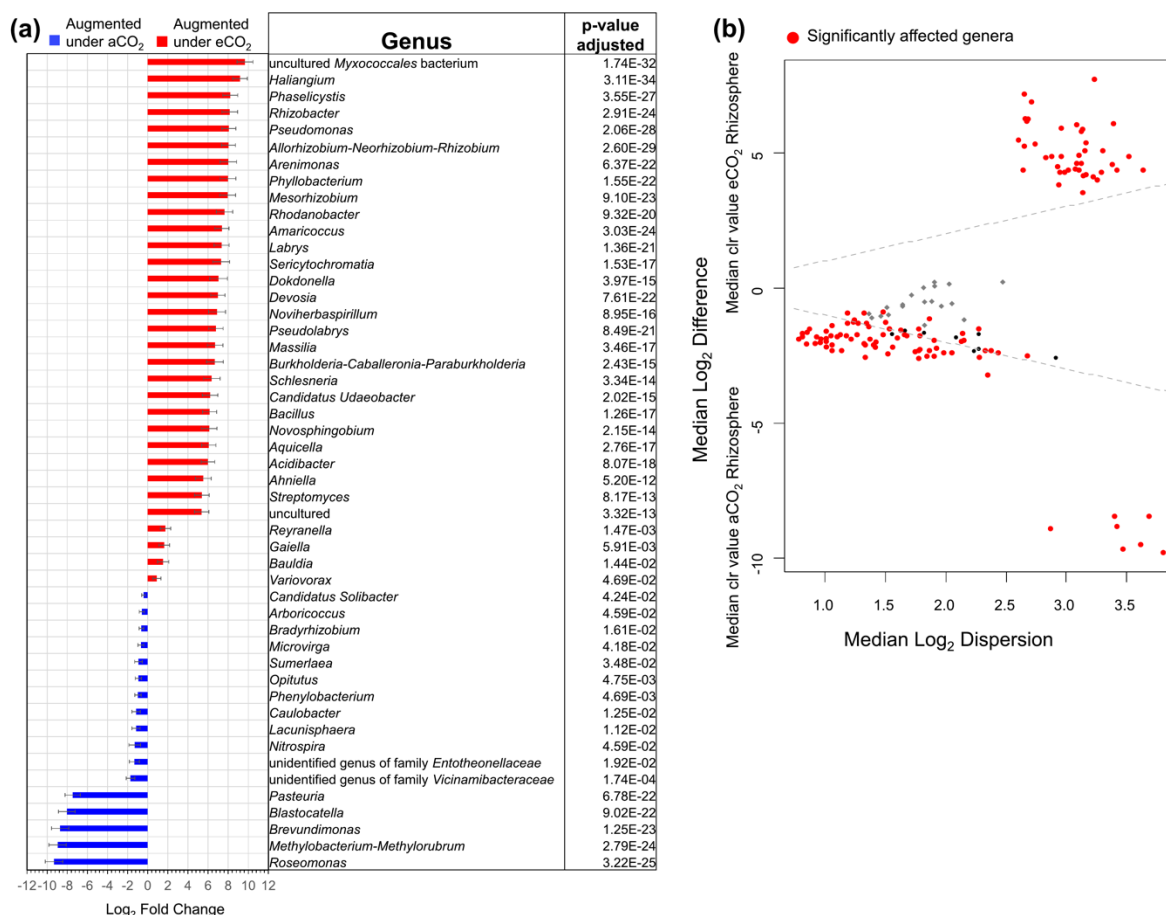


Fig. 4 Differential abundances of core microbiome bacterial genera of rhizosphere soil under elevated and ambient CO₂. **a** DESeq2 test results with an alpha threshold <0.05 and error expressed as standard error of log fold change. **b** Aldex2 results using centered log ratio

(clr) transformation and the geometric mean abundance of all features; red points indicate significantly different genera after Welch's t-test and Benjamini–Hochberg correction with an alpha threshold <0.1

genera belonged mainly to bacterial families Nocardioideae, Beijerinckiaceae, Pyrinomonadaceae, “Koribacteraceae”, “Xiphinematobacteraceae”, Propionibacteriaceae, Dongiaceae, Geminicoccaceae, Solirubrobacteraceae, Blastocatellaceae, Caulobacteraceae, Nitrosomonadaceae, Xanthobacteraceae, Caulobacteraceae, Fibrobacteraceae, Acetobacteraceae, unidentified family of the phylum “Latescibacterota”, Myxococcaceae, “Solibacteraceae”, Rhizobiaceae, and Gemmatimonadaceae (S3).

On the contrary, both differential abundance tests indicated that some genera presented a decreased of abundance under eCO₂ conditions. Among these are unidentified genus of the family Vicinamibacteraceae, *Pasteuria*, *Caulobacter*, unidentified genus of the family “Entotheonellaceae”, *Brevundimonas*, *Methylobacterium-Methylorubrum*, *Sumerlaea*, *Blastocatella*, *Phenyllobacterium*, *Lacunisphaera*,

Roseomonas, and *Opitutus*. These genera had Log₂ Fold changes from −0.421 to −9.31 in eCO₂ ring (Fig. 4a, Fig. 4b, S3).

Functional Metagenomics Prediction

Beta diversity results of functional capabilities based on 16S rRNA data showed significant differences on functional metagenome's composition of rhizosphere soils from aCO₂ and eCO₂ conditions. PICRUSt2 predicted functional metagenome were different regarding Enzyme Commission number (EC number) (p value 0.005), KEGG Orthology (KO) for molecular functions (p value 0.019), and MetaCyc Metabolic Pathways (p value 0.022) (S4). Moreover, similar to taxonomical results, predicted bulk soil's functional metagenomics from aCO₂ and eCO₂ conditions did not show

great differences regarding its beta diversity, neither on EC numbers (p value 0.197), KEGG Orthology (p value 0.179), or MetaCyc Metabolic Pathways (p value 0.317) (S4).

Besides, the analyses of significantly affected predicted enzymes indicated that several enzymes of degradation of carbon compounds were significantly stimulated in rhizospheric soils under eCO₂ conditions. Enzymes involved in carbohydrates, lipids, amino acids, and polycyclic aromatic hydrocarbon degradation were significantly stimulated. Additionally, numerous predicted enzymes and pathways of synthesis of cellular components, membrane transporters, and quorum sensing were significantly higher under eCO₂ conditions (S5). Also, according to KEGG Orthology for molecular functions, several enzymes involved in nitrogen fixation, nitric-oxide synthesis, and nitrite and nitrate reduction were predicted to be more abundant in eCO₂ rhizosphere soil (S5).

Quantitative PCR

Active biomass estimation by 16S rRNA quantification demonstrated changes due to eCO₂ concentrations. A 20% increase of 16S rRNA copy numbers per g dry weight soil in eCO₂ rhizosphere ($2.07 \pm 0.50 \times 10^8$) in comparison to aCO₂ rhizosphere ($1.66 \pm 0.44 \times 10^8$) was observed (p value 0.0001). Nevertheless, when comparing the 16S rRNA copy

numbers per gram dry weight soil of bulk soils from aCO₂ ($2.35 \pm 0.80 \times 10^8$) and eCO₂ ($2.35 \pm 0.79 \times 10^8$) conditions, no significant differences were found (p value 0.9588) (Fig. 5). Moreover, significant differences were found between bulk and rhizosphere soils from aCO₂ (p value 2.1×10^{-5}) with in average 29% more copies per dry weigh in bulk soil compared to rhizosphere soil. Nonetheless, when comparing rhizosphere and bulk soils from eCO₂ rings, this difference is lower and not significant (p value 0.1455), with the bulk soil having 12% more copies than the rhizosphere soil (Fig. 5).

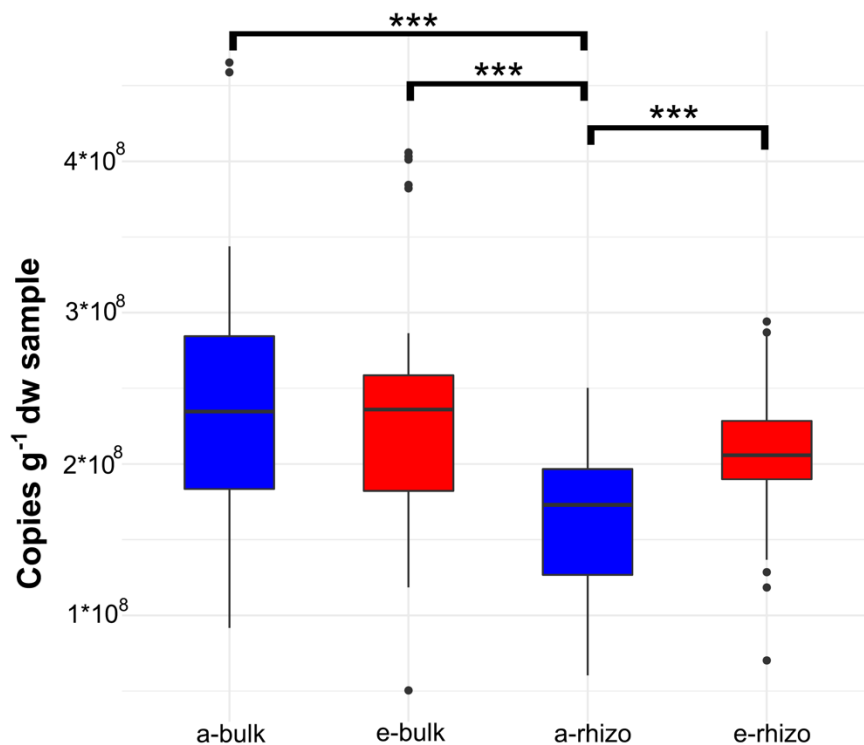
Discussion

Changes in Microbiome Structure and Composition

Elevated CO₂ concentrations affect the composition and biomass of soil microbial communities in the rhizosphere because of greater inputs of labile carbon (C) via root exudation may increase the microbial N demand. This causes an increased competition between plants and soil microorganisms for available N; therefore, N dynamics are likely to change under eCO₂ [10, 11, 14, 72].

Our results showed that eCO₂ had a strong effect in the Gi-FACE on the metabolic active microbiome of the rhizosphere soil, in contrast to the microbiome of the bulk soil

Fig. 5 Boxplot of 16S rRNA quantification of ambient CO₂ rings bulk soil (a-bulk), elevated CO₂ rings bulk soil (e-bulk), ambient CO₂ rings rhizosphere soil (a-rhizo) and elevated CO₂ rings rhizosphere soil (e-rhizo). Significance codes: 0.0001 ***



which remained mostly unaffected. Alpha diversity indices indicate that a shift occurred under eCO₂ conditions, producing an evenness in terms of alpha diversity between rhizosphere and bulk soil. Since significant differences were found between bulk and rhizosphere soil of aCO₂ rings, this evenness represents an increase in alpha diversity of eCO₂ rhizosphere soil (Fig. 1). Furthermore, beta diversity results revealed a different abundance and microbial community composition in the rhizosphere of eCO₂ rings compared to aCO₂ rings (Fig. 2).

These results differ from previous reports of the eCO₂ effects on the Gi-FACE soil microbiome, which stated that only subtle or no effect occurred on microbial communities and that the differences were mostly due to soil conditions and the moisture gradient that occurs at this facility [25–27]. Similarly, to the aforementioned studies, our data confirmed that samples from ring-pair A1-E1 had lower water content in comparison to A2-E2 and A3-E3 samples (S2), and that water holding capacity (WHC) significantly influenced the soil microbiome (Table 1, Fig. 3). This was observable in the effect that the ring-pair factor had on the beta diversity of the Gi-FACE soil microbiome (p value 0.001) (Fig. 2).

Nonetheless, besides the moisture gradient, the observed differences caused by the eCO₂ were likely detected due to the RNA-based metabarcoding approach used in our work, which is able to differentiate the metabolic active microorganisms from the inactive ones, avoiding the biases caused by DNA of dead cell or extracellular DNA, which can comprise approximately 41% of the amplifiable prokaryotic 16S rRNA genes in soil [31]. However, RNA metabarcoding has its limitations as well, mainly due to the fact that RNA conversion to cDNA requires the use of a reverse transcriptase which lacks proofreading activity, creating point mutations in some of the cDNA sequences [73]. Reverse transcriptase also regularly performs template switching, which can lead to the production of chimeric cDNA sequences and the creation of shortened isoform sequences from intramolecular template switching [74, 75]. Nevertheless, in our study these limitations were minimized by using a Moloney murine leukemia virus reverse transcriptase (MMLV-RT) derivative combined with a *E. coli* DNA polymerase III ϵ subunit which lowers the reverse transcription error rate by threefold, and later the resulting cDNA was amplified with a proofreading DNA polymerase which produced up to eightfold fewer errors [76].

The study of Bei et al. [28], which also addressed the active microbial community by using a metatranscriptomic approach, supports our results. For the summer of 2015, the same year that we took the samples for this study, they reported significant effects of eCO₂ on the functional expression related to rhizosphere and plant roots associated microbiomes in the Gi-FACE. Also, similarly to our work, they described that the increase in bacterial abundance was

related to significant enrichment of different taxonomical groups, including Acidobacteria, Actinobacteria, and Proteobacteria, and changes related to a significant decrease in Fungi and increase in Actinobacteria.

However, Bei et al. [28] found no significant eCO₂ effect on the rhizosphere soil and root-associated microbiomes during the summer of 2017. These contrasting results for different years may result from climatic conditions in summer, since the summer 2015 was characterized by prolonged heat waves, while the mean temperature in summer 2017 was closer to the long-term average. The effect of eCO₂ on the soil rhizosphere microbiome we found in our study may be affected by the above average temperatures of this particular year. Additionally, the prediction that heat waves will occur more frequently in the future [77] emphasizes the importance of our findings.

The reason why only the rhizosphere microbiome, in contrast to the bulk soil microbiome, was affected by eCO₂ influx is most probably a consequence of the priming effect of the increased flux of roots exudates and consequently higher availability of carbon compounds. This increased supply of labile C causes an accelerated decomposition of soil organic C [15], which activates previously dormant microorganisms [15, 16].

Effect of eCO₂ Concentration on Microbial Community, C and N Cycles

Our results of the effect of environmental parameters on soil microbiome composition demonstrated that several rhizosphere bacterial families such as Rhodanobacteraceae, “Labraceae,” Xanthomonadaceae, Rhodobacteraceae, Rhizobiaceae, Pseudomonadaceae, Phaselicytidaceae, Haliangiaceae, Bacillaceae, Streptomycetaceae, Xanthobacteraceae, Burkholderiaceae, Devosiaceae, Haliangiaceae, Comamonadaceae, and Polyangiaceae were positively correlated with eCO₂ fumigation and soil CO₂ fluxes. Within these families are found bacterial genera as *Streptomyces*, *Burkholderia*, *Dokdonella*, *Bacillus*, *Pseudolabrys*, *Devosia*, *Mesorhizobium*, *Acidibacter*, *Rhizobacter*, *Rhodanobacter*, *Arenimonas*, *Amaricoccus*, *Phyllobacterium*, *Rhizobium*, *Pseudomonas*, *Phaselicystis*, and *Haliangium*. Furthermore, the aforementioned genera had significant higher counts under eCO₂ conditions according to DESeq2 and Aldex2 results. From other experiments, it was also reported that under eCO₂ conditions the rhizosphere soil microbial communities had changed [78]. Increased atmospheric CO₂ concentrations could also change the competitive ability of *Rhizobium leguminosarum* bv. *trifolii*, probably due to changes in root exudates [79]. In salt marsh systems containing the halophyte *Suaeda japonica*, it was reported that gene abundances and microbial community structures were both affected by eCO₂, and rhizospheric microorganisms

responded to eCO₂ more strongly than those inhabiting the bulk soil [80]. Song et al. [81] described that community composition of soil microbiota associated with *Phytolacca americana* and *Amaranthus cruentus* roots were significantly affected by eCO₂, and numbers of bacteria and fungi, as well as microbial C and N in the rhizosphere soils of both species, were higher at eCO₂.

Greater carbon input due to eCO₂ also explains the increase of 35% in soil CO₂ fluxes and the 20% augmentation in 16S rRNA copy numbers from active bacterial biomass observed in rhizosphere soil under eCO₂ in comparison to aCO₂, which corresponded to an increased soil biological activity in Gi-FACE. Cheng et al. [82] described that eCO₂ affected soil microbial respiration, producing an augmentation of microbial biomass and activities. Similarly, King et al. [83] showed that eCO₂ increased soil respiration at four forest FACE experiments. Blagodatskaya et al. [84] demonstrated that augmented available organic C released by roots at eCO₂ altered the ecological strategy of the soil microbial community, occurring a shift to a higher contribution of fast-growing species. The increased biological activity in eCO₂ rhizosphere soil is supported by the predicted functional metagenome obtained with PICRUSt2, which shows significant increases in several enzymes involved in cellular components biosynthesis such as peptidoglycan, lipopolysaccharide, amino acids, bacterial motility proteins, and lipids synthesis (S5). These results differ from those obtained by Pujol Pereira et al. [23], who reported that on soybean [*Glycine max* (L.) Merr.], eCO₂ decreased 16S rRNA gene abundance in rhizosphere soil by 31%. Also, Marhan et al. [21] described that abundances of total 16S rRNA were not influenced by CO₂ but by sampling date and depth. Likewise, Brenzinger et al. [27] and Bei et al. [28] reported that at the Gi-FACE no differences between aCO₂ and eCO₂ rings were found regarding the 16S rRNA gene. However, Bei et al. [28] described that in summer of 2015 under eCO₂ conditions the functional metagenome of rhizosphere soil presented an increase on amino acids and carbohydrates metabolisms, membrane transporters, and quorum sensing proteins: similar to our study's PICRUSt2 results (S5).

In addition, several genera involved in the degradation of carbon (C) compounds were stimulated under eCO₂ conditions; among these are *Pseudomonas* and *Bacillus* (Fig. 4, S2) that have been previously reported to degrade lignocellulose materials. *Pseudomonas boreopolis* produces a cellulase-free xylanase with a high activity of hemicellulose degradation [85]. Maki et al. [86] reported that *Bacillus* strain (55S5) and a *Pseudomonas* strain (AS1) displayed high potential for lignocellulose decomposition due to a variety of cellulase and xylanase activities. Trujillo-Cabrera et al. [87] described the isolation of cellulolytic bacteria from high humus content soils, as

Bacillus thuringiensis and *Pseudomonas gessardii*. The augmentation of these taxa would agree with the predicted functional metagenome, which indicated an increment of several enzymes involved in lignocellulose materials degradation, as Chitinase (EC:3.2.1.14), Endo-1,3(4)-beta-glucanase (EC:3.2.1.6), Endo-1,4-beta-xylanase (EC:3.2.1.8), and Cellulase (EC:3.2.1.4) (S5). Similar results have been described by He et al. [17, 19], who reported that soils of a soybean agro-ecosystem and a glacial outwash sandplain showed increased abundance of encoding genes for enzymes involved in labile C degradation such as amylase, glucoamylase, pullulanase, fungal arabinofuranosidase, xylanase, endoglucanase, acetylglucosaminidase, and exochitinase. Likewise, Xiong et al. [20] described that alpha-amylase, cellobiase, endoglucanase, vanillin dehydrogenase, endochitinase, and phenoloxidase encoding genes were stimulated under eCO₂ in soybean and maize fields. The above-mentioned increase of C compounds degradation could occur as a response of greater C availability due to an increase of root exudates under eCO₂ conditions.

Moreover, these changes in the C influx could induce a reduction of available N in the soil ecosystem [24], which alters the N cycle and induces significant changes in soil biogeochemical characteristics in the rhizosphere, such as NO₃⁻, available K⁺, soil microbial biomass carbon (SMBC), and available PO₄²⁻ [78]. The aforementioned process could explain the higher carbon/nitrogen ratio found in our study in eCO₂ rings in comparison with ambient ones and might also explain why some genera involved in different processes of the nitrogen cycle were stimulated under eCO₂ conditions. Genera belonging to families Rhizobiaceae and Xanthobacteraceae as *Rhizobium*, *Mesorhizobium*, and *Phyllobacterium* have been extensively reported as nitrogen-fixing bacteria [88–90], and in our study presented Log₂ fold increases ranging from 6.78 to 8.04. Also, PICRUSt2 results indicate that functional orthologs of the enzyme nitrogenase (EC:1.18.6.1) were significantly augmented in eCO₂ rhizosphere soil (S5). This increase in the abundance of nitrogen-fixing bacteria could have occurred as response to N deficiency, which eventually became a limiting factor for biomass production under eCO₂. Similar results were reported by Li et al. [91], who described a 24% increment of ¹⁵N in mine tailing soils under eCO₂ and a dominance of uncultured nitrogen-fixing bacteria.

Aldex2 correlation results demonstrated a significant negative correlation between NH₄⁺ content and *Nitrospira* genus under eCO₂ conditions. Although NH₄⁺ values were not significantly different between aCO₂ and eCO₂, NH₄⁺ content was on average 10% higher in aCO₂ soils, which suggest that nitrification processes could have been affected due to elevated environmental CO₂. Alterations in nitrification process in the Gi-FACE have been already described by Müller et al. [72], who reported that eCO₂ reduced NH₄⁺ oxidation to NO₃⁻ by 25%.

Furthermore, several denitrifying genera as *Streptomyces*, *Rhodanobacter*, *Pseudomonas*, *Burkholderia*, and *Bacillus* were significantly stimulated in $e\text{CO}_2$ rhizospheric soil with Log_2 fold changes between 5.37 and 8.065 [92–96]. Additionally, predicted functional metagenome indicate that several orthologs involved in the denitrification process, as nitric-oxide synthase (NAD(P)H) (EC:1.14.13.165), nitrate reductase (EC:1.7.99.4), nitrite reductase (NO-forming) (EC:1.7.2.1), nitrite reductase (cytochrome; ammonia-forming) (EC:1.7.2.2), periplasmic nitrate reductase NapA (EC:1.7.99.-), and nitric oxide reductase NorD protein, have significantly greater abundance under $e\text{CO}_2$ conditions (S5).

In summary, our results demonstrate that in the Gi-FACE, the rhizosphere soil microbiome was significantly affected due to the influence of increased CO_2 concentrations alongside other environmental factors. The increment of carbon input due to $e\text{CO}_2$ possibly augmented labile carbon degradation in rhizosphere soil reflected by the increment of bacteria biomass and CO_2 soil emissions. The aforementioned processes could cause a nitrogen constraint, observed in the increment of the C:N ratio, and decreased of NH_4^+ , which likely triggered a shift in the rhizosphere soil microbiome with an increment of nitrogen fixing and denitrifying taxa. The observed increase of denitrifier genera might explain the increased N_2O fluxes under $e\text{CO}_2$ conditions, previously described in the Giessen FACE [27, 97, 98]. Similarly, our data support the results described by Moser et al. [98], who reported that under $e\text{CO}_2$ conditions, N_2O emissions were 1.79-fold higher and that the linear interpolations showed a 2.09-fold increase in N_2O emissions mostly because of the oxidation of organic N and incomplete reduction of NO_2^- , emitting N_2O instead of N_2 (Fig. 6).

Our findings suggest that alterations in carbon cycle affects nitrogen cycle dynamics in grassland soils, due to changes on the microorganisms involved on the different processes of these cycles. Nonetheless, further analyses would be necessary to assess the Gi-FACE microbiome metatranscriptome of carbon and nitrogen cycles, how they are affected by $e\text{CO}_2$, and how this effect depends on ambient temperature regimes like summer heat waves.

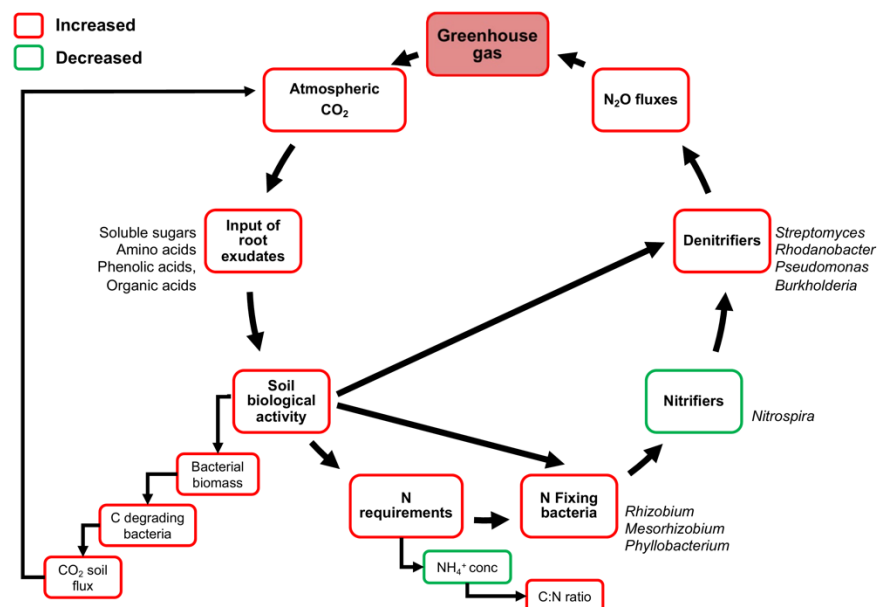
Supplementary Information The online version contains supplementary material available at <https://doi.org/10.1007/s00248-021-01791-y>.

Acknowledgements We thank Professor Bernd Honermeier group for their support to perform soil carbon and nitrogen analyses, and we are grateful to our colleagues Rita Geissler-Plaum and Bellinda Schneider for their excellent technical support. For the long-term funding of the Environmental Monitoring and Climate Impact Research Station Linden that enabled the long-term Gi-FACE experiment, we acknowledge the Hessian Agency for Nature Conservation, Environment and Geology (HLNUG).

Author Contribution DR conducted experiments, data curation, data analysis, and writing of the manuscript. SR contributed with methodology, review and editing. MC contributed with methodology, review and editing. CM conducted experiments and data curation. GM contributed with data curation, review and editing. MD conducted experiments, data curation, review and editing. Ch M contributed with methodology, review and editing. SS contributed with methodology, review and editing.

Funding Open Access funding enabled and organized by Projekt DEAL. This study was partially funded by the Environmental Monitoring and Climate Impact Research Station Linden that enabled the long-term Gi-FACE experiment and the Hessian Agency for Nature Conservation, Environment and Geology (HLNUG).

Fig. 6 Model diagram of the effect of elevated CO_2 on the rhizosphere microbiome of C and N cycles bacterial taxa of the Giessen FACE experiment



Data Availability The authors declare that the data supporting the findings of this study are available within the article and its Supplementary Information. cDNA sequence data are available in the GenBank database under the accession number PRJNA656997.

Code Availability Not applicable.

Declarations

Conflict of Interest The authors declare no competing interests.

Open Access This article is licensed under a Creative Commons Attribution 4.0 International License, which permits use, sharing, adaptation, distribution and reproduction in any medium or format, as long as you give appropriate credit to the original author(s) and the source, provide a link to the Creative Commons licence, and indicate if changes were made. The images or other third party material in this article are included in the article's Creative Commons licence, unless indicated otherwise in a credit line to the material. If material is not included in the article's Creative Commons licence and your intended use is not permitted by statutory regulation or exceeds the permitted use, you will need to obtain permission directly from the copyright holder. To view a copy of this licence, visit <http://creativecommons.org/licenses/by/4.0/>.

References

- IPCC (2014) Climate change 2014: Synthesis report. Contribution of working groups I, II and III to the fifth assessment report of the intergovernmental panel on climate change. IPCC, Geneva, Switzerland
- Idso K (1994) Plant responses to atmospheric CO₂ enrichment in the face of environmental constraints: a review of the past 10 years' research. *Agric For Meteorol* 69:153–203. [https://doi.org/10.1016/0168-1923\(94\)90025-6](https://doi.org/10.1016/0168-1923(94)90025-6)
- He P, Bader KP, Radunz A, Schmid GH (1995) Consequences of high CO₂ concentrations in air on growth and gas-exchange rates in Tobacco mutants. *Z Naturforsch* 50c:781–788
- Kimball BA (1983) Carbon dioxide and agricultural yield: An assemblage and analysis of 430 prior observations. *Agron J* 75:779. <https://doi.org/10.2134/agronj1983.00021962007500050014x>
- Owensby CE, Ham JM, Knapp AK et al (1997) Water vapour fluxes and their impact under elevated CO₂ in a C4-tallgrass prairie. *Glob Chang Biol* 3:189–195. <https://doi.org/10.1046/j.1365-2486.1997.00084.x>
- Kimball BA (2016) Crop responses to elevated CO₂ and interactions with H₂O, N, and temperature. *Curr Opin Plant Biol* 31:36–43. <https://doi.org/10.1016/j.pbi.2016.03.006>
- Habash DZ, Paul MJ, Parry MAJ et al (1995) Increased capacity for photosynthesis in wheat grown at elevated CO₂ - the relationship between electron transport and carbon metabolism. *Planta* 197:482–489. <https://doi.org/10.1007/BF00196670>
- Johnson RM, Pregitzer KS (2007) Concentration of sugars, phenolic acids, and amino acids in forest soils exposed to elevated atmospheric CO₂ and O₃. *Soil Biol Biochem* 39:3159–3166. <https://doi.org/10.1016/j.soilbio.2007.07.010>
- Jongen M, Jones MB, Hebeisen T et al (1995) The effects of elevated CO₂ concentrations on the root growth of *Lolium perenne* and *Trifolium repens* grown in a FACE* system. *Glob Chang Biol* 1:361–371
- Walker TS, Bais HP, Grotewold E, Vivanco JM (2003) Root exudation and rhizosphere Biology root exudation and rhizosphere biology. *Plant Physiol* 132:44–51. <https://doi.org/10.1104/pp.102.019661>. Although
- Li K, Guo XW, Xie HG et al (2013) Influence of root exudates and residues on soil microecological environment. *Pakistan J Bot* 45:1773–1779
- Phillips RP, Meier IC, Bernhardt ES et al (2012) Roots and fungi accelerate carbon and nitrogen cycling in forests exposed to elevated CO₂. *Ecol Lett* 15:1042–1049. <https://doi.org/10.1111/j.1461-0248.2012.01827.x>
- Jia X, Wang W, Chen Z et al (2014) Concentrations of secondary metabolites in tissues and root exudates of wheat seedlings changed under elevated atmospheric CO₂ and cadmium-contaminated soils. *Environ Exp Bot* 107:134–143. <https://doi.org/10.1016/j.envexpbot.2014.06.005>
- Dong J, Hunt J, Delhaize E et al (2021) Impacts of elevated CO₂ on plant resistance to nutrient deficiency and toxic ions via root exudates: a review. *Sci Total Environ* 754:142434. <https://doi.org/10.1016/j.scitotenv.2020.142434>
- Blagodatskaya E, Kuzyakov Y (2008) Mechanisms of real and apparent priming effects and their dependence on soil microbial biomass and community structure: critical review. *Biol Fertil Soils* 45:115–131. <https://doi.org/10.1007/s00374-008-0334-y>
- Di Lonardo DP, De Boer W, Klein Gunnewiek PJA et al (2017) Priming of soil organic matter: chemical structure of added compounds is more important than the energy content. *Soil Biol Biochem* 108:41–54. <https://doi.org/10.1016/j.soilbio.2017.01.017>
- He Z, Xu M, Deng Y et al (2010) Metagenomic analysis reveals a marked divergence in the structure of belowground microbial communities at elevated CO₂. *Ecol Lett* 13:564–575. <https://doi.org/10.1111/j.1461-0248.2010.01453.x>
- Xu M, He Z, Deng Y et al (2013) Elevated CO₂ influences microbial carbon and nitrogen cycling. *BMC Microbiol* 13:124. <https://doi.org/10.1186/1471-2180-13-124>
- He Z, Xiong J, Kent AD et al (2014) Distinct responses of soil microbial communities to elevated CO₂ and O₃ in a soybean agro-ecosystem. *ISME J* 8:714–726. <https://doi.org/10.1038/ismej.2013.177>
- Xiong J, He Z, Shi S et al (2015) Elevated CO₂ shifts the functional structure and metabolic potentials of soil microbial communities in a C4 agroecosystem. *Sci Rep* 5:1–9. <https://doi.org/10.1038/srep09316>
- Marhan S, Philippot L, Bru D et al (2011) Abundance and activity of nitrate reducers in an arable soil are more affected by temporal variation and soil depth than by elevated atmospheric [CO₂]. *FEMS Microbiol Ecol* 76:209–219. <https://doi.org/10.1111/j.1574-6941.2011.01048.x>
- Dunbar J, Gallegos-Graves LV, Steven B et al (2014) Surface soil fungal and bacterial communities in aspen stands are resilient to eleven years of elevated CO₂ and O₃. *Soil Biol Biochem* 76:227–234. <https://doi.org/10.1016/j.soilbio.2014.05.027>
- Pujol Pereira EI, Chung H, Scow K, Six J (2013) Microbial communities and soil structure are affected by reduced precipitation, but not by elevated carbon dioxide. *Soil Sci Soc Am J* 77:482. <https://doi.org/10.2136/sssaj2012.0218>
- Butterly CR, Phillips LA, Wiltshire JL et al (2016) Long-term effects of elevated CO₂ on carbon and nitrogen functional capacity of microbial communities in three contrasting soils. *Soil Biol Biochem* 97:157–167. <https://doi.org/10.1016/j.soilbio.2016.03.010>
- Regan K, Kammann C, Hartung K et al (2011) Can differences in microbial abundances help explain enhanced N₂O emissions in a permanent grassland under elevated atmospheric CO₂? *Glob Chang Biol* 17:3176–3186. <https://doi.org/10.1111/j.1365-2486.2011.02470.x>
- de Menezes AB, Müller C, Clipson N, Doyle E (2016) The soil microbiome at the Gi-FACE experiment responds to a moisture

- gradient but not to CO₂ enrichment. *Microbiology* 162:1572–1582. <https://doi.org/10.1099/mic.0.000341>
27. Brenzinger K, Kujala K, Horn MA et al (2017) Soil conditions rather than long-term exposure to elevated CO₂ affect soil microbial communities associated with N-cycling. *Front Microbiol* 8:1–14. <https://doi.org/10.3389/fmicb.2017.01976>
 28. Bei Q, Moser G, Wu X et al (2019) Metatranscriptomics reveals climate change effects on the rhizosphere microbiomes in European grassland. *Soil Biol Biochem* 138:1–10. <https://doi.org/10.1016/j.soilbio.2019.107604>
 29. Morrissey EM, McHugh TA, Preteska L et al (2015) Dynamics of extracellular DNA decomposition and bacterial community composition in soil. *Soil Biol Biochem* 86:42–49. <https://doi.org/10.1016/j.soilbio.2015.03.020>
 30. Dlott G, Maul JE, Buyer J, Yarwood S (2015) Microbial rRNA: RDNA gene ratios may be unexpectedly low due to extracellular DNA preservation in soils. *J Microbiol Methods* 115:112–120. <https://doi.org/10.1016/j.mimet.2015.05.027>
 31. Carini P, Marsden PJ, Leff JW et al (2016) Relic DNA is abundant in soil and obscures estimates of soil microbial diversity. *Nat Microbiol* 2:1–6. <https://doi.org/10.1038/nmicrobiol.2016.242>
 32. Felske A, Engelen B, Nübel U, Backhaus H (1996) Direct ribosome isolation from soil to extract bacterial rRNA for community analysis. *Appl Environ Microbiol* 62:4162–4167
 33. Duineveld BM, Kowalchuk GA, Keijzer A et al (2001) Analysis of bacterial communities in the rhizosphere of chrysanthemum via denaturing gradient gel electrophoresis of PCR-amplified 16S rRNA as well as DNA fragments coding for 16S rRNA. *Appl Environ Microbiol* 67:172–178. <https://doi.org/10.1128/AEM.67.1.172-178.2001>
 34. Hoshino YT, Matsumoto N (2007) DNA- versus RNA-based denaturing gradient gel electrophoresis profiles of a bacterial community during replenishment after soil fumigation. *Soil Biol Biochem* 39:434–444. <https://doi.org/10.1016/j.soilbio.2006.08.013>
 35. Hunt DE, Lin Y, Church MJ et al (2013) Relationship between abundance and specific activity of bacterioplankton in open ocean surface waters. *Appl Environ Microbiol* 79:177–184. <https://doi.org/10.1128/AEM.02155-12>
 36. Jäger HJ, Schmidt SW, Kammann C et al (2003) The University of Giessen free-air carbon dioxide enrichment study: description of the experimental site and of a new enrichment system. *J Appl Bot Bot* 77:117–127
 37. Andresen LC, Yuan N, Seibert R et al (2018) Biomass responses in a temperate European grassland through 17 years of elevated CO₂. *Glob Chang Biol* 24:3875–3885. <https://doi.org/10.1111/gcb.13705>
 38. Kandeler E, Gerber H (1988) Short-term assay of soil urease activity using colorimetric determination of ammonium. *Biol Fertil Soils* 6:68–72. <https://doi.org/10.1007/BF00257924>
 39. Bak F, Scheff G, Jansen KH (1991) A rapid and sensitive ion chromatographic technique for the determination of sulfate and sulfate reduction rates in freshwater lake sediments. *FEMS Microbiol Lett* 85:23–30. <https://doi.org/10.1111/j.1574-6968.1991.tb04694.x>
 40. Forster JC (1995) Methods in Applied Soil Microbiology and Biochemistry. In: Alef K, Nannipieri P (eds) *Methods in applied soil microbiology and biochemistry*. Academic Press, San Diego, pp 105–106
 41. HBU (1996) *Handbuch der Bodenuntersuchung (HBU), Bodenbeschaffenheit - Bestimmung von organischem Kohlenstoff und Gesamtkohlenstoff nach trockener Verbrennung (Elementaranalyse)*. In: DIN ISO 10. GmbH, Berlin, p 3.4.1.31.1a
 42. VDLUFA (2012) *Methodenbuch- Band I, Die Untersuchung von Böden*, 6. VDLUFA - Verlag, Darmstadt
 43. Keidel L, Kammann C, Grünhage L et al (2015) Positive feedback of elevated CO₂ on soil respiration in late autumn and winter. *Biogeosciences* 12:1257–1269. <https://doi.org/10.5194/bg-12-1257-2015>
 44. Mirman D (2014) Growth curve analysis and visualization using R, 1st ed. Chapman and Hall/CRC in R series, Boca Raton
 45. Geller J, Winn MB, Mahr T, Mirman D (2020) GazeR: a package for processing gaze position and pupil size data. *Behav Res Methods* 52:2232–2255. <https://doi.org/10.3758/s13428-020-01374-8>
 46. Bates D, Mächler M, Bolker BM, Walker SC (2015) Fitting linear mixed-effects models using lme4. *J Stat Softw* 67:1–41. <https://doi.org/10.18637/jss.v067.i01>
 47. Mettel C, Kim Y, Shrestha PM, Liesack W (2010) Extraction of mRNA from soil. *Appl Environ Microbiol* 76:5995–6000. <https://doi.org/10.1128/AEM.03047-09>
 48. Lane DJ (1991) 16S/23S rRNA sequencing. In: Stackebrandt E, Goodfellow M (eds) *Nucleic acid techniques in bacterial systematics*. John Wiley and Sons, New York, pp 115–175
 49. Weisburg WG, Barns SM, Pelletier DA, Lane DJ (1991) 16S Ribosomal DNA amplification for phylogenetic study. *J Bacteriol* 173:697–703
 50. Claesson MJ, O'Sullivan O, Wang Q et al (2009) Comparative analysis of pyrosequencing and a phylogenetic microarray for exploring microbial community structures in the human distal intestine. *PLoS ONE* 4:e6669. <https://doi.org/10.1371/journal.pone.0006669>
 51. Engelbrektson A, Kunin V, Wrighton KC et al (2010) Experimental factors affecting PCR-based estimates of microbial species richness and evenness. *ISME J* 4:642–647. <https://doi.org/10.1038/ismej.2009.153>
 52. Kaplan H, Ratering S, Felix-Henningsen P, Schnell S (2019) Stability of in situ immobilization of trace metals with different amendments revealed by microbial ¹³C-labelled wheat root decomposition and efflux-mediated metal resistance of soil bacteria. *Sci Total Environ* 659:1082–1089. <https://doi.org/10.1016/j.scitotenv.2018.12.441>
 53. Bolyen E, Rideout JR, Dillon MR et al (2019) Reproducible, interactive, scalable and extensible microbiome data science using QIIME 2. *Nat Biotechnol* 37:852–857. <https://doi.org/10.1038/s41587-019-0209-9>
 54. Martin M (2011) Cutadapt removes adapter sequences from high-throughput sequencing reads. *EMBnet J* 17:10
 55. Callahan BJ, McMurdie PJ, Rosen MJ et al (2016) DADA2: High-resolution sample inference from Illumina amplicon data. *Nat Methods* 13:581–583. <https://doi.org/10.1038/nmeth.3869>
 56. Pedregosa F, Varoquaux G, Gramfort A et al (2011) Scikit-learn: machine learning in python. *J Mach Learn Res* 12:2825–2830. <https://doi.org/10.1145/2786984.2786995>
 57. Bokulich NA, Kaehler BD, Rideout JR et al (2018) Optimizing taxonomic classification of marker-gene amplicon sequences with QIIME 2's q2-feature-classifier plugin. *Microbiome* 6:1–17. <https://doi.org/10.1186/s40168-018-0470-z>
 58. Quast C, Pruesse E, Yilmaz P et al (2013) The SILVA ribosomal RNA gene database project: Improved data processing and web-based tools. *Nucleic Acids Res* 41:590–596. <https://doi.org/10.1093/nar/gks1219>
 59. Glöckner FO, Yilmaz P, Quast C et al (2017) 25 years of serving the community with ribosomal RNA gene reference databases and tools. *J Biotechnol* 261:169–176. <https://doi.org/10.1016/j.jbiotec.2017.06.1198>
 60. McMurdie PJ, Holmes S (2013) Phyloseq: an R package for reproducible interactive analysis and graphics of microbiome census data. *PLoS ONE* 8:e61217. <https://doi.org/10.1371/journal.pone.0061217>

61. Oksanen J, Blanchet FG, Friendly M et al (2018) vegan: Community ecology package. R package version 2.5-7. <https://CRAN.R-project.org/package=vegan>
62. Wilcoxon F (1945) Individual comparisons of grouped data by ranking methods. *Biometrics Bull* 1:80–83. <https://doi.org/10.1093/jee/39.2.269>
63. Aitchison J (1982) The statistical analysis of compositional data. *J of the R Stat Soc Ser B* 44:139–177. <https://doi.org/10.1007/978-94-009-4109-0>
64. Aitchison J (1986) Book review, XII. Chapman and Hall, London
65. Fernandes AD, Macklaim JM, Linn TG et al (2013) ANOVA-like differential expression (ALDEx) analysis for mixed population RNA-Seq. *PLoS ONE* 8:e67019. <https://doi.org/10.1371/journal.pone.0067019>
66. Jolliffe IT, Cadima J (2016) Principal component analysis: a review and recent developments subject areas. *PhilTransRSocA* 374:1–16
67. Anderson MJ (2001) A new method for non parametric multivariate analysis of variance. *Austral Ecol* 26:32–46. <https://doi.org/10.1111/j.1442-9993.2001.01070.pp.x>
68. Legendre P, Oksanen J, ter Braak CJF (2011) Testing the significance of canonical axes in redundancy analysis. *Methods Ecol Evol* 2:269–277. <https://doi.org/10.1111/j.2041-210X.2010.00078.x>
69. Lahti L, Shetty S (2019) microbiome R package. <http://microbiome.github.io>
70. Love MI, Huber W, Anders S (2014) Moderated estimation of fold change and dispersion for RNA-seq data with DESeq2. *Genome Biol* 15:550. <https://doi.org/10.1186/s13059-014-0550-8>
71. Douglas GM, Maffei VJ, Zaneveld J et al (2019) PICRUSt2 for prediction of metagenome functions. *Nat Biotechnol* 38:669–673. <https://doi.org/10.1038/s41587-020-0550-z>
72. Müller C, Rütting T, Abbasi MK et al (2009) Effect of elevated CO₂ on soil N dynamics in a temperate grassland soil. *Soil Biol Biochem* 41:1996–2001. <https://doi.org/10.1016/j.soilbio.2009.07.003>
73. Houseley J, Tollervey D (2010) Apparent non-canonical trans-splicing is generated by reverse transcriptase in vitro. *PLoS ONE* 5:e12271. <https://doi.org/10.1371/journal.pone.0012271>
74. Cocquet J, Chong A, Zhang G, Veitia RA (2006) Reverse transcriptase template switching and false alternative transcripts. *Genomics* 88:127–131. <https://doi.org/10.1016/j.ygeno.2005.12.013>
75. Laroche O, Wood SA, Tremblay LA et al (2017) Metabarcoding monitoring analysis: the pros and cons of using co-extracted environmental DNA and RNA data to assess offshore oil production impacts on benthic communities. *PeerJ* 5:e3347. <https://doi.org/10.7717/peerj.3347>
76. Arezi B, Hogrefe HH (2007) *Escherichia coli* DNA polymerase III ϵ subunit increases Moloney murine leukemia virus reverse transcriptase fidelity and accuracy of RT-PCR procedures. *Anal Biochem* 360:84–91. <https://doi.org/10.1016/j.ab.2006.10.009>
77. Russo S, Sillmann J, Fischer EM (2015) Top ten European heat-waves since 1950 and their occurrence in the coming decades. *Environ Res Lett* 10:124003. <https://doi.org/10.1088/1748-9326/10/12/124003>
78. Yu Z, Li Y, Wang G et al (2016) Effectiveness of elevated CO₂ mediating bacterial communities in the soybean rhizosphere depends on genotypes. *Agric Ecosyst Environ* 231:229–232. <https://doi.org/10.1016/j.agee.2016.06.043>
79. Montealegre CM, Van Kessel C, Blumenthal JM et al (2000) Elevated atmospheric CO₂ alters microbial population structure in a pasture ecosystem. *Glob Chang Biol* 6:475–482. <https://doi.org/10.1046/j.1365-2486.2000.00326.x>
80. Lee SH, Kang H (2016) Elevated CO₂ causes a change in microbial communities of rhizosphere and bulk soil of salt marsh system. *Appl Soil Ecol* 108:307–314. <https://doi.org/10.1016/j.apsoil.2016.09.009>
81. Song N, Zhang X, Wang F et al (2012) Elevated CO₂ increases Cs uptake and alters microbial communities and biomass in the rhizosphere of *Phytolacca americana* Linn (pokeweed) and *Amaranthus cruentus* L. (purple amaranth) grown on soils spiked with various levels of Cs. *J Environ Radioact* 112:29–37. <https://doi.org/10.1016/j.jenvrad.2012.03.002>
82. Cheng L, Booker FL, Burkey KO et al (2011) Soil microbial responses to elevated CO₂ and O₃ in a nitrogen-aggrading agroecosystem. *PLoS ONE* 6:e21377. <https://doi.org/10.1371/journal.pone.0021377>
83. King JS, Hanson PJ, Bernhardt ES et al (2004) A multiyear synthesis of soil respiration responses to elevated atmospheric CO₂ from four forest FACE experiments. *Glob Chang Biol* 10:1027–1042. <https://doi.org/10.1111/j.1365-2486.2004.00789.x>
84. Blagodatskaya E, Blagodatsky S, Dorodnikov M, Kuzyakov Y (2010) Elevated atmospheric CO₂ increases microbial growth rates in soil: results of three CO₂ enrichment experiments. *Glob Chang Biol* 16:836–848. <https://doi.org/10.1111/j.1365-2486.2009.02006.x>
85. Guo H, Hong C, Zheng B et al (2018) Biotechnology for bio-fuels improving enzymatic digestibility of wheat straw pretreated by a cellulase - free xylanase - secreting *Pseudomonas boreopolis* G22 with simultaneous production of bioflocculants. *Biotechnol Biofuels* 11:1–10. <https://doi.org/10.1186/s13068-018-1255-0>
86. Maki ML, Idrees A, Tin Leung K, Qin W (2012) Newly isolated and characterized bacteria with great application potential for decomposition of lignocellulosic. *J Mol Microbiol Biotechnol* 22:156–166. <https://doi.org/10.1159/000341107>
87. Trujillo-Cabrera Y, Ponce-Mendoza A, Rivera-Orduña FN, Wang ET (2013) Diverse cellulolytic bacteria isolated from the high humus, alkaline-saline chinampa soils. 63:779–792. <https://doi.org/10.1007/s13213-012-0533-5>
88. Zahran HH (2001) Rhizobia from wild legumes: diversity, taxonomy, ecology, nitrogen fixation and biotechnology. *J Biotechnol* 91:143–153. [https://doi.org/10.1016/S0168-1656\(01\)00342-X](https://doi.org/10.1016/S0168-1656(01)00342-X)
89. Teixeira H, Rodríguez-Echeverría S (2016) Identification of symbiotic nitrogen-fixing bacteria from three African leguminous trees in Gorongosa National Park. *Syst Appl Microbiol* 39:350–358. <https://doi.org/10.1016/j.syapm.2016.05.004>
90. Masson-Boivin C, Sachs JL (2018) Symbiotic nitrogen fixation by rhizobia — the roots of a success story. *Curr Opin Plant Biol* 44:7–15. <https://doi.org/10.1016/j.pbi.2017.12.001>
91. Li Y, Wu Z, Dong X et al (2019) Variance in bacterial communities, potential bacterial carbon sequestration and nitrogen fixation between light and dark conditions under elevated CO₂ in mine tailings. *Sci Total Environ* 652:234–242. <https://doi.org/10.1016/j.scitotenv.2018.10.253>
92. Kester RA, De Boer W, Laanbroek HJ (1997) Production of NO and N₂O by pure cultures of nitrifying and denitrifying bacteria during changes in aeration. *Appl Environ Microbiol* 63:3872–3877
93. Arai H, Kodama T, Igarashi Y (1999) Effect of nitrogen oxides on expression of the *nir* and *nor* genes for denitrification in *Pseudomonas aeruginosa*. *FEMS Microbiol Lett* 170:19–24. [https://doi.org/10.1016/S0378-1097\(98\)00517-5](https://doi.org/10.1016/S0378-1097(98)00517-5)
94. Verbaendert I, Boon N, De Vos P, Heylen K (2011) Denitrification is a common feature among members of the genus *Bacillus*. *Syst Appl Microbiol* 34:385–391. <https://doi.org/10.1016/j.syapm.2011.02.003>

95. Yang XP, Wang SM, Zhang DW, Zhou LX (2011) Isolation and nitrogen removal characteristics of an aerobic heterotrophic nitrifying-denitrifying bacterium, *Bacillus subtilis* A1. *Bioresour Technol* 102:854–862. <https://doi.org/10.1016/j.biortech.2010.09.007>
96. Feng L, Jia R, Zeng Z et al (2018) Simultaneous nitrification–denitrification and microbial community profile in an oxygen-limiting intermittent aeration SBBR with biodegradable carriers. *Biodegradation* 29:473–486. <https://doi.org/10.1007/s10532-018-9845-x>
97. Kammann C, Müller C, Grünhage L, Jäger HJ (2008) Elevated CO₂ stimulates N₂O emissions in permanent grassland. *Soil Biol Biochem* 40:2194–2205. <https://doi.org/10.1016/j.soilbio.2008.04.012>
98. Moser G, Gorenflo A, Brenzinger K et al (2018) Explaining the doubling of N₂O emissions under elevated CO₂ in the Giessen FACE via in-field ¹⁵N tracing. *Glob Chang Biol* 24:3897–3910. <https://doi.org/10.1111/gcb.14136>

Chapter 3 Elevated atmospheric CO₂ concentrations caused a shift of the metabolically active microbiome in vineyard soil

Research article

Submitted to BMC Microbiology

Elevated atmospheric CO₂ concentrations caused a shift of the metabolically active microbiome in vineyard soil

Running title: eCO₂ caused a shift of active microbiome in a vineyard soil

David Rosado-Porto^{a,b}, Stefan Ratering^a, Yvette Wohlfahrt^c, Bellinda Schneider^a, Andrea Glatt^a, Sylvia Schnell^{a#}

^a Institute of Applied Microbiology, Justus Liebig University, 35392 Giessen, Germany

^b Simón Bolívar University, Faculty of Basic and Biomedical Sciences, 080002 Barranquilla, Colombia

^c Department of General and Organic Viticulture, Hochschule Geisenheim University, Von-Lade-Strasse 1, D-65366 Geisenheim, Germany

#Corresponding author: Sylvia Schnell, Heinrich-Buff-Ring 26–32, D-35392 Giessen, Germany

Tel: +49(0)6419937351, Fax: +49(0)6419937359, E-mail: Sylvia.Schnell@umwelt.uni-giessen.de

Abstract

Background: Climate change together with elevated carbon dioxide (eCO₂) has several consequences on both vine and cover plants in vineyards and therefore potentially also on the soil microbiome. Hence, possible changes of the metabolically active microbiome (cDNA of 16S rRNA) were analyzed by metabarcoding from soil samples taken at the Geisenheim Vineyard free-air CO₂ enrichment (VineyardFACE) experiment in the inter-rows with and without cover cropping.

Results: Results from diversity indices and redundancy analysis (RDA) demonstrated that eCO₂ changed the active soil microbiome diversity in grapevine soil with cover crop significantly (p-value 0.007) whereas the microbiome in unplanted soil was unaffected. In addition, the microbial soil respiration (p-values 0.04 - 0.003) and the ammonium concentration (p-value 0.003) were significantly different in the inter-rows with cover crops and eCO₂. qPCR results showed significant decrease in 16S rRNA, and transcripts for enzymes involved in N₂ fixation and NO₂⁻ reduction under eCO₂ conditions. Co-occurrence analysis revealed a shift on the number, strength and patterns of microbial interactions under eCO₂ conditions, mainly represented by a reduction of the number of interacting ASVs and the number of interactions.

Conclusions: The results obtained in this study demonstrate that even within a relative short period of eCO₂ concentrations, soil active microbiome has undergone through changes, which could have future consequences on soil and wine properties and quality.

Keywords: active soil microbiome, carbon cycle, nitrogen cycle, vineyard, rRNA, mRNA quantification, CO₂

Background

Vineyards are important economic and agricultural ecosystems. According to the “Deutsche Wein Statistik”, in 2017 the total amount of vineyard hectares worldwide, in the European Union and in Germany were 7,564,000, 3,312,000 and 102,000 respectively. Grapevines (*Vitis vinifera* L.), as perennial culture grows in a complex and dynamic ecosystem, where climate, soil, microorganisms and management practices are key factors of plant health, plant productivity and wine quality. These complex interactions in the local growing area together with the viticulture and enological techniques lead to the unique taste (the terroir) of the wine in a local area. Alteration of factors in this balance may alter the terroir and lead to less consumer acceptance and

economic losses. Climate change is one of these factors and connected with this increasing CO₂ concentrations that influence plant physiology and microbial communities in vineyards.

Elevated CO₂ (eCO₂) concentrations can modulate plant's transcriptional and metabolic profile, stress responses of C3 plants and consequently affect vegetative and reproductive development. Wohlfahrt et al. [1] reported that under eCO₂ conditions the varieties Riesling and Cabernet Sauvignon presented higher net photosynthesis rates of 32 % and 28 %, respectively. Similarly, it has been demonstrated that under both scenarios eCO₂ plus reduced water availability and eCO₂ plus elevated ambient temperature grapevines presented higher net photosynthetic rates [2, 3]. Additionally, eCO₂ has been proven to affect berry and must properties, increasing berry weights, lateral leaf area, summer pruning fresh weight and yield; and altering malic and tartaric acids concentration [4, 5]. Furthermore, future CO₂ concentrations might alter the way and magnitude of interactions between plants and herbivorous insects, as it was demonstrated by Reineke et al. [6], who described that grapevine plants presented different transcriptional patterns as a response to herbivorous insect *Lobesia botrana* under eCO₂ compared to aCO₂ concentrations.

Different methodologies have been used to assess the effects of elevated atmospheric CO₂ levels on soil ecosystems, with the free-air CO₂ enrichment (FACE) experiments as one of these approaches. In Geisenheim (Germany) in the wine growing region Rheingau the Geisenheim VineyardFACE was started in 2014. Since then, several studies have been conducted in the Geisenheim VineyardFACE, which intend to assess the effects of future CO₂ concentrations on different aspects of grapevine physiology, yield efficiency, grape composition and ecology [1, 5–7].

Regarding grapevine microbiome under normal atmosphere, various research studies addressed this topic from different angles. Some investigations have demonstrated that differences exist between the microbiome of the different grapevine parts and the surrounding soil microbiome, indicating a particular niche adaptation of distinct taxonomic groups to each plant structure, yet soil plays an important role as a major reservoir becoming a bottleneck to microbial abundance in the rest of the grapevine [8–10]. As it was indicated by Nerva et al. [11], who observed that pathogens associated to the chronic and complex wood disease known as ESCA (Black Measle) and grapevine trunk disease pathogens were more abundant in the bulk soils of affected plants, indicating that the soil represents an important source of inoculum. Likewise, studies

have established that independent of the growing region, rootstocks have a core microbiome which influences the taxonomy, structure and the microbial community in grapevine roots [12, 13]. Also, Liu et al.[14] showed that fungal microbiome was influenced by grapevine habitat and plant development stage and the core microbiome members changed through a seasonal community succession.

Nevertheless, eCO₂ effects on the microbiome of vineyard soil have not been studied until now. Taking into account that eCO₂ increases concentrations of sugars, amino acids, and organic acids in plant's root exudates and in consequence having a direct influence on soil microbiome structure and composition [15, 16]. It has been demonstrated in several studies that the structure and function of soil microbiome changed due to eCO₂ conditions [17–21]. Moreover, larger inputs of carbon under eCO₂ may increase the microbial nitrogen demand, therefore, nitrogen dynamics are likely to change under eCO₂ [22].

For the reasons mentioned above, the aims of the present work were: i) to assess the effect of mid-term eCO₂ concentrations on active soil microbiome through an rRNA-based metabarcoding approach; ii) to evaluate differences between eCO₂ and aCO₂ conditions in the vineyard soil; and iii) to study how changes in soil microbiome are connected to environmental variables.

Results

Ion torrent sequencing

A total of 3,903,289 raw sequences were obtained. After demultiplexing, sequences were assigned to each sample, ranging sequence counts in each sample from 135,651 to 34,214. After quality control, denoising, sequence dereplication and chimera filtering with DADA2 software, 2,010,680 sequences were removed, resulting in 1,892,609 non-chimeric sequences that were grouped into 10,708 amplicon sequence variants (ASVs) at a 99% similarity. Later, sequences belonging to chloroplast and mitochondria were removed, resulting in 10,583 ASVs from 1,887,273 total sequences.

Soil microbial diversity

In the Geisenheim VineyardFACE soil the bacterial diversity of the active part of the bacteria has changed as result of elevated atmospheric CO₂ concentration. Our results indicate that under ambient CO₂ (aCO₂) conditions green inter-rows tend to have significantly higher alpha diversity values than open inter-rows, according to indexes of

Observed ASVs (p-value 0.014), Shannon (p-value 0.0074) and Fisher (p-value 0.014) (Fig. 1a). Nevertheless, in eCO₂ rings no statistically difference was observed between green and open inter-rows (Fig. 1a). Even though, alpha diversity values do not show significant differences between green inter-rows from ambient and elevated CO₂ rings, a slight decrease on the values of the different alpha diversity metrics of green inter-rows from elevated CO₂ rings were observed (Fig. 1a).

To evaluate the beta diversity of VineyardFACE, a distance matrix was created using the Aitchison distance and later ordinated using the Principal Components Analysis (PCA). Previous the assessment of differences among the evaluated experimental blocks the dispersion of the soil cores taken within each ring from the different inter-rows and their distance to centroids was measured. The results indicate that soil microbiome composition of each soil core was considerable different from the others, even those taken within the same ring (S1, Fig. S1.1-S1.6, Tab. S1.1-S1.6). Besides, examination of variations on structure of soil bacterial microbiome among the evaluated block indicate that ring, block and row (green or open inter-rows) factors all had statistically significant influence on the microbiome composition of the Geisenheim VineyardFACE according to the performed Adonis test (p-value 0.001). Likewise, CO₂ conditions had also a significant effect on the overall microbiome structure (p-value 0.002), although to a lesser degree than the ones mentioned above. Additionally, when examining green inter-rows diversity from ambient and elevated CO₂ rings, these two habitats have strong statistically differences in terms of beta diversity (p-value 0.001) (Fig. 1b, Fig. 1c). Moreover, the ring factor has a significant impact (p-value 0.001) on the differentiation of microbiomes of green inter-rows under elevated and ambient CO₂ concentrations.

On the other hand, when analyzing the microbiome's beta diversity of open inter-rows from ambient and elevated CO₂ rings, no statistically significant differences were observed between these two soils (p-value 0.123) (Fig. 1d, Fig. 1e). However, the structure of microbiomes in the open inter-rows is essentially influenced by the ring factor (p-value 0.001).

Effect of environmental factors on microbial community

A redundancy analysis (RDA) was performed using a distance matrix based on the Aitchison distance to determine the effect of the different environmental factors that influence the microbiome structure and composition of the Geisenheim VineyardFACE. Results showed that eCO₂ concentration significantly influenced the differentiation of the bacterial microbiome in green inter-rows from ambient and elevated CO₂ rings (p-value

0.007) (Tab. 1, Fig. 2a). Nevertheless, the effect of elevated CO₂ on the differentiation of soil microbiomes of open inter-rows was much weaker in comparison with green inter-rows and not statistically significant (p-value 0.102) (Tab. 1, Fig. 2b). Likewise, correlation analysis performed with Aldex2 showed that ASVs belonging to genera *Bradyrhizobium*, *Marmoricola*, *Nocardioides*, *Ilumatobacter* and *Chthoniobacter* had significant positive correlations with environmental CO₂ concentrations (Tab. S3.1, S3.2).

Table 1. Effect of environmental parameters on microbiome from green and open inter-rows.

Environmental parameter	Green inter-rows soil	Open inter-rows soil
CO ₂ concentration	0.007 **	0.102
NH ₄ ⁺	0.015 *	0.035 *
Water holding capacity	0.003 **	0.240
Soil respiration	0.010 **	0.211
Water content	0.230	0.212
Total carbon	0.005 **	0.164
Total nitrogen	0.001 **	0.222
Carbon/Nitrogen ratio	0.686	0.260

Adjusted p-values of permutation test for redundancy analysis (RDA) based on Aitchison community dissimilarity distance matrix. ** p<0.01, * p<0.05.

Furthermore, RDA showed that ammonium content of soil, had an important effect on the composition of soil microbiome of the VineyardFACE, both in green inter-rows (p-value 0.015) and open inter-rows (p-value 0.035). Moreover, when comparing the ammonium content of inter-rows from ambient CO₂ rings on average higher values on green inter-rows in comparison with open inter-rows (p-value 0.003) were observed (Tab. 2, Fig. 2c). On the contrary, when comparing inter-rows from elevated CO₂ rings, open inter-rows present higher ammonium concentrations than green inter-rows (p-value 0.025), nevertheless, ammonium concentration in general were higher under elevated than ambient CO₂ conditions (Tab. 2, Fig. 2d). Some bacterial taxa presented significant correlations with soil ammonium content as an ASV from the uncultured family “*Entotheonellaceae*” and genus *Phenylobacterium*, which had negative and positive correlation coefficients respectively.

Additionally, water holding capacity (WHC), total nitrogen and total carbon content are all factors that shaped microbiome differentiation of green inter-rows according to the permutation test of canonical axes in redundancy analysis (Tab. 1). In this regard, green inter-rows had significant higher average values of these three environmental parameters in comparison with open inter-rows (S2) and several bacterial ASVs and

genera showed significant correlations with each one of these environmental parameters (S3).

Soil microbial respiration in the Geisenheim VineyardFACE, exhibited that microbial activity, understood as the amount of CO₂ produced by soil organisms is a significant factor shaping the soil microbiome (p-value 0.034). Moreover, soil respiration values were on average higher in eCO₂ rings. In addition, when examining the effect of eCO₂ on green inter-rows soil respiration, a significant higher CO₂ production was observed on basal respiration and with all examined substrates in soils from elevated CO₂ rings in comparison with soils from the ambient ones (Fig. 2e). In contrast in open inter-rows, although soil respiration was higher in soils from eCO₂ rings it was only significantly higher in basal respiration (p-value 0.02), however there were not major statistical differences on the other substrates utilized (Fig. 2f). Additionally, soil microbial respiration was significantly higher in green inter-rows in comparison with open inter-rows, in either elevated or aCO₂ rings, however, these differences were slightly higher under eCO₂ conditions (Fig. S1.7, Tab. S1.7).

Table 2. Average ammonium content of green and open inter-rows from ambient and elevated CO₂ rings.

CO ₂ conditions	Green inter-rows NH ₄ ⁺ [μM g ⁻¹ DW soil]	Open inter-rows NH ₄ ⁺ [μM g ⁻¹ DW soil]	p-value
Ambient	245.66 ± 81.21	161.35 ± 39.3	0.003**
Elevated	370.44 ± 250.86	948.69 ± 628.71	0.025*

Error is expressed as standard deviation of mean values (n=3). P-values significance codes are from a t-test for samples with unequal variances. Significance codes:

** p<0.01, * p<0.05.

Changes on microbial community composition of green inter-rows

Differential abundance analysis confirmed that several core ASVs and genera presented changes in the green inter-rows soil under eCO₂ conditions. In total 44 ASVs and 13 genera showed greater abundance under eCO₂ conditions. Among the highly stimulated ASVs in eCO₂ rings were *Bradyrhizobium*, *Marmoricola*, *Nocardioides mesophilus*, uncultured bacterium clone C10 (JF718671, class *Deltaproteobacteria*), *Nocardioides islandensis* and *Nocardioides caverna*, which presented Aldex effect sizes between 0.86 and 1.29 and fold changes ranging from 1.75 to 366.32 (Fig. 3a, S3). Similarly, core genera *Chthoniobacter*, *Asticcacaulis*, *Phenylobacterium*, *Legionella*, *Candidatus Udaeobacter*, *Luteolibacter* and *Pedosphaeraceae* were positively stimulated under

eCO₂ concentrations, with Aldex effect sizes between 0.78 and 0.5 and fold changes from 1.47 to 44.52 (Fig. 3b, S3).

In contrast, 51 ASVs and 10 genera belonging to the core microbiome showed a decrease under eCO₂ conditions. ALDEx2 results indicated that ASVs identified as *Variovorax*, *Nocardioides islandensis*, uncultured bacterium (EU192989, order *Acidobacteriales*), *Gaiella*, uncultured bacterium (EU134489 family “*Polyangiaceae*”), *Piscinibacter* and *Bryobacter* were the most affected by eCO₂ in the green inter-rows, presenting Aldex effect sizes between -0.8 and -1.18 and fold changes from 13.44 and 189.6 (Fig. 3a, S3). Additionally, genera *Paenibacillus*, *Acidibacter*, *Clostridium sensu stricto* 1, *Hydrocarboniphaga*, uncultured bacterium (order *Azospirillales*), uncultured bacterium (DS-100, class *Blastocatellia*), uncultured bacterium (TRA3-20, order *Burkholderiales*), uncultured bacterium gene (clone SZB85, family “*Nitrosococcaceae*”) showed a reduction under eCO₂ conditions with fold changes between 1.98 and 10 and Aldex effect sizes ranging from -0.723 to -0.54 (Fig. 3b, S3).

Co-occurrence analysis

Co-occurrence analysis results demonstrated changes regarding interactions that happened among soil microorganisms under eCO₂ concentrations. Networks of ASVs with absolute ALDEx effect sizes greater than 0.5, showed a shift on the number, the strength and the patterns of these microbial interactions (Tab. 3). Under eCO₂ conditions a decrease of interacting ASVs and the number of interactions occurred, although the average number of interactions and the network density increased under this condition (Tab. 3, Fig. 4a). Also, the number of negative co-occurrence decreased under eCO₂ among these ASVs, appearing at aCO₂ green inter-rows a total of 26 (28.3%) negative associations in comparison to only 6 (8.8%) at the aCO₂ ones. Moreover, most of the negative interactions at aCO₂ conditions occurred between nodes that are positive and negative affected by the increment of atmospheric CO₂ (Fig. 4a). Oppositely, under eCO₂ interaction patterns changed, occurring mostly among ASVs that were negatively affected (Fig. 4b).

Likewise, co-occurrence analyses performed with SpiecEasi and SPRING packages, showed changes of associations of bacterial genera in the green inter-rows. In terms of interacting genera under aCO₂ and eCO₂, there was no difference between these two conditions, although under eCO₂ there were fewer interactions (Tab. 3). Moreover, the number of positive interactions greater than 0.25 is larger under elevated atmospheric CO₂ (8.7%) in comparison to aCO₂ (4.6%). Furthermore, co-occurrence patterns indicated a shift of bacterial interactions due to eCO₂, as it occurred to genus

Deinococcus, which under aCO₂ conditions, presented positive partial correlations with 13 genera, among which were found *Agromyces*, *Candidatus Nitrososphaera*, *Jatrophihabitans*, *Sphingomonas*, *Azohydromonas*, *Coxiella* and *Novosphingobium* (Fig. 4c). Nonetheless, most of these interaction patterns were no longer present under eCO₂, and in the case of genus *Deinococcus*, it only kept its positive co-occurrence with genus *Azohydromonas* (Fig. 4d).

Table 3. Attributes of co-occurrence analysis from ASVs and genera belonging to green inter-rows.

Co-occurrence attribute	aCO ₂ rings ASVs	eCO ₂ rings ASVs	aCO ₂ rings genera	eCO ₂ rings genera
Number of taxa	79	55	198	199
Number of interactions	92	68	413	393
Average number of interactions	2.33	5.7	4.17	3.95
Negative interactions	26 (28.3%)	6 (8.8%)	132 (32.0%)	144 (36.6%)
Positive interactions	66 (71.7%)	62 (91.2%)	281 (68.0%)	249 (63.4%)
Clustering coefficient	0.056	0.66	0.15	0.116
Network density	0.057	0.44	0.021	0.02

cDNA Real time PCR

The assessment of active bacteria through 16S rRNA quantification demonstrated changes in the soil microbiome due to eCO₂ concentrations. In general, it was observed a decrease of active bacteria under eCO₂ conditions, in both green and open inter-rows. On average aCO₂ green inter-rows had significant higher copy numbers per g dry weight of soil than the eCO₂ ones (p-value 0.015) according to Kruskal-Wallis test, about 36% more in aCO₂ ($1.81 \pm 0.78 \times 10^8$) in comparison to eCO₂ ($1.16 \pm 0.56 \times 10^8$). Also, aCO₂ open inter-rows presented significant higher concentrations of 16S rRNA ($8.93 \pm 2.32 \times 10^7$) in relation their eCO₂ counterparts ($5.24 \pm 4.03 \times 10^7$) (p-value 0.047). Nonetheless, either in aCO₂ and eCO₂ rings, green inter-rows showed higher values of active bacterial biomass compared to the open inter-rows (Fig. 5).

Similarly, to the 16S rRNA, the analysis of mRNA of functional genes involved in nitrogen cycle indicated changes mainly in N₂ fixation and denitrification processes probably because of eCO₂ (Fig. 5). The analysis of the transcribed bacterial nitrogen fixation gene *nifH* showed a significant decrease under eCO₂ in green inter-rows (p-value 0.007), with on average 84% fewer copies of *nifH* in eCO₂ green inter-rows ($2.75 \pm 5.15 \cdot 10^{-4}$) in comparison to aCO₂ ($1.69 \pm 2.17 \cdot 10^{-3}$) (Fig. 5). Likewise, NO₂⁻ reduction gene *nirK* transcription was affected negatively under eCO₂ concentrations in both green and open inter-rows. Under eCO₂ green inter-rows had an average of $2.09 \pm 2.71 \cdot 10^{-2}$ copies expressed as % of 16S rRNA copy numbers, in comparison to $3.11 \pm 3.14 \cdot 10^{-1}$ copies under aCO₂ conditions, which represented a decrease of 93%. Moreover, open inter-rows presented too higher values of *nirK* transcripts under aCO₂ ($2.31 \pm 3.12 \cdot 10^{-1}$) than eCO₂ ones ($1.41 \pm 1.55 \cdot 10^{-2}$) (Fig. 5). Oppositely, NO₂⁻ reduction gene *nirS* transcripts did not show any differences between eCO₂ and aCO₂ conditions, neither between green inter-rows nor open inter-rows. Similarly, also transcripts of *nirS* gene, *amoA* and *nosZ* genes involved in NH₄⁺ oxidation and N₂O reduction respectively, did not presented any differences among the evaluated conditions (Fig. 5).

Discussion

Microbiome structure and diversity

Grapevine (*Vitis spp.*) is one of the most extensively grown and economically important fruit crops and the terroir of wines as main products of the grapes are the outcome of physical (climate), biological (soil, microbiome, grape variety, fauna), viticulture and enological factors. Changes in these factors change the terroir. It is well known that grapevines are particularly sensitive to changes in climatic conditions, on which the increment of atmospheric CO₂ concentrations has several consequences on them [1–3, 5, 6, 23, 24], although it is not well known what the influence is of changed climate conditions on the microbes involved in the microbial terroir [25].

Our results demonstrated that the rise of atmospheric CO₂ concentration altered active soil microbiome structure in a vineyard, in addition to the already reported effects on grapevine physiology, yield efficiency, grape composition and ecology [1–6]. Moreover, our data indicate that changes in soil microbiome occurred mainly in the green inter-rows of eCO₂ rings of the Geisenheim VineyardFACE. Regarding alpha diversity, Observed ASVs, Shannon and Fisher indexes demonstrated that there are differences between green and open inter-rows under aCO₂ conditions; nonetheless, this difference

disappeared under eCO₂. This indicates that under eCO₂ a decrease in terms of alpha diversity in the soil of green inter-rows occurred (Fig. 1a).

Soil microbiome structure and activity were highly affected by eCO₂ in the Geisenheim VineyardFACE, as it is indicated by our beta diversity (Aitchison diversity) outcomes, which showed a change on the structure and composition of Geisenheim VineyardFACE soil microbiome in eCO₂ rings in comparison to the aCO₂ ones (Fig. 1b-e). The increment of atmospheric CO₂ was one of the environmental factors that had a significant influence on the alteration of soil microbiome (Fig. 2a-b). Nevertheless, this change was only observable in the green inter-rows and not in the open ones, very likely due to the presence of vegetation in these inter-rows. Similar results have been reported in crop plants, as wheat and soybean on which eCO₂ altered the structure of soil and rhizosphere microbiomes [26, 27]. Likewise, comparable outcomes have been described on the root and rhizosphere microbiota associated with *Phytolacca americana*, *Amaranthus cruentus* and grassland ecosystems, which described significant changes due to eCO₂ [17, 28, 29]. These changes are probably a consequence of the increment of C and N inputs derived from plant increased rhizodeposition, which influences the composition and biomass of soil microbiome [30, 31].

Our data showed a significant increase of soil heterotrophic respiration on eCO₂ soil samples, with average fold changes ranging from 1.65 to 1.85, a sign of stimulated soil microbial activity. Nonetheless, our quantification of bacterial 16S rRNA through qPCR, demonstrated a decline of bacterial abundance caused by eCO₂ concentrations, which might be explained by an alteration of soil microbial structure in favor of fungal growth. This behavior has been already described in a chaparral ecosystem [32], a scrub-oak ecosystem [33] and a wheat-soybean agroecosystem [26], in which the ratio fungi:bacteria augmented under eCO₂ along with an enhancement of soil microbial heterotrophic respiration.

eCO₂ effect on N cycle, changes in bacterial abundance and microbe-microbe interactions

Greater inputs of labile C under eCO₂ via root exudation increases the microbial nitrogen (N) demand and consequently, N dynamics are likely to change under eCO₂ [22]. Following this train of thought, several studies have investigated and shown the changes that genes, proteins and microorganisms undergo due to eCO₂ conditions, some of which described an enhancement of their amount and/or activity [26, 34–38] and some others did not find any significant differences [39, 40]. In this sense, N₂ fixation at eCO₂ concentrations has been usually reported to increase as a response to higher N demand

due to the excess of C compounds [34, 35, 37, 38]. Nevertheless, our data did not indicate an augmentation in the N_2 fixation because of eCO_2 , on the contrary nitrogenase *nifH* qPCR results demonstrated a diminishing of N_2 fixing activity in the green inter-rows of eCO_2 rings (Fig. 5, Fig. 6).

However, NH_4^+ concentrations are higher in eCO_2 rings than aCO_2 ones, which suggests that although N_2 fixation is downregulated in eCO_2 rings, microorganisms are obtaining NH_4^+ from other sources, probably from soil organic matter (SOM) (Fig. 6). Therefore, the supply of fresh plant derived C into the soil matrix due to eCO_2 may accelerate the decomposition of SOM and decrease soil C stocks [41, 42]; a phenomenon known as “the priming effect”. Also, SOM pools contain significant physically and chemically protected N stocks, therefore the priming effect is a response to the labile C supply by which microorganisms gain access to a reservoir of N to meet their enhanced N demand [43–45]. The aforementioned has been described by Müller et al. [22] who reported that under eCO_2 mineralization of labile organic N became more important. Also occurs an increment in the dissimilatory NO_3^- reduction to NH_4^+ (DNRA) and in the immobilization of NH_4^+ and NO_3^- [22]. Which might explain why some taxa stimulated under eCO_2 conditions are significantly positive correlated with NH_4^+ concentrations (S3), as genus *Phenylobacterium* which has been also reported to perform heterotrophic DNRA [46].

Similar to *nifH*, it has been frequently reported that under eCO_2 occurs an augmentation of transcripts for denitrification genes *nirS*, *nirK* and *nosZ* [34, 35, 37], nonetheless our results did not show an increment on the abundance of mRNAs of these genes, on the contrary our data indicated an alteration of the denitrification process at the step of NO_2^- reduction, by the decrease of *nirK* activity under eCO_2 (Fig. 5, Fig. 6).

Furthermore, the alteration of N cycle related gene transcripts seems to be associated to the decrease of certain bacterial taxa and the shift of the soil microbiome because of the selective pressures imposed by eCO_2 . Our co-occurrence data demonstrated a shift of bacterial taxa and a simplification of microbial interactions under eCO_2 conditions. The aforementioned could be appreciated in the shift of N_2 fixing bacteria with *nifH* genes as *Microbacterium* [47, 48] and *Paenibacillus* [49–53] by genus *Bradyrhizobium* [54–56] in eCO_2 rings, which were negative and positive correlated with atmospheric CO_2 concentrations respectively (S3). Likewise, the decreased abundance of *nirK* transcripts under eCO_2 might be linked to the depletion of bacterial taxa as *Noviherbaspirillum* [57], *Massilia* [58] and *Clostridium sensu stricto* 1 [59] described to perform NO_2^- reduction and possess this gene.

Furthermore, network analysis outputs showed a strong positive co-occurrence between *Noviherbaspirillum* and *Microbacterium* in eCO₂ rings, which demonstrated that the depletion of these two genera is linked. Similarly, the co-occurrence cluster observed among ASVs negatively affected by eCO₂, supports the idea that the increment of atmospheric CO₂ concentrations disrupts soil microbial networks, and the depletion of certain bacterial taxa is entangled to the decrease of others. This cluster included ASVs belonging to genera *Xenophilus* and *Nocardioides* and ASVs from families *Geminicoccaceae* and *Thermoleophilaceae*. Additionally, partial correlation data displayed alterations in the co-occurrence patterns caused by eCO₂, where taxa that were interacting among each other did no longer exhibited these patterns at eCO₂. A good example is genus *Deinococcus*, which at aCO₂ showed positive interactions with 13 genera but it only kept its positive co-occurrence with genus *Azohydromonas* at eCO₂. This modification of interaction patterns is probably connected to alterations of *nirK* mediated denitrification, due to the fact that genus *Deinococcus* has also been described to perform NO₂⁻ reduction and possess this gene [60].

Moreover, it has been reported in field experiments of tea seedlings (*Camellia sinensis* L. 'Baihaozao') that increase in the quantity of *nirK* and *nosZ* genes was linked to the decline of N₂O [61]. This might suggest that in the Geisenheim VineyardFACE eCO₂ might augment N₂O emissions due to alteration of denitrification process reflected in the abundance of *nirK* gene transcripts. Additionally, Moser et al. [62], described that N₂O emissions were 1.79-fold higher in the Giessen FACE under eCO₂ conditions. Nonetheless, it is important to mention that in vineyard fields N₂O emissions depend on its management, including soil type, amount of fertilizers, and humidity along with climate conditions [63], and that correlations with soil properties are likely to be highly system specific [64].

Conclusions

Our results demonstrate that the increase of atmospheric CO₂ concentrations has changed the structure and composition of soil microbiome in the Geisenheim VineyardFACE. This suggests that even with a relative short period of eCO₂ concentration in the VineyardFACE field, alterations in carbon cycle have had an impact on soil nitrogen cycle microbiome, producing a shift of diverse bacterial taxa. These soil microbiome alterations could have in the future more consequences on wine terroir and quality. Nevertheless, additional analyses and timepoints will be needed in order to

assess alterations regarding functional metatranscriptome due to eCO₂ and its impact on wine production and grapevine health and productivity.

Materials and Methods

Study site description

The Geisenheim VineyardFACE facility is located at Hochschule Geisenheim University, Germany (49°59'N, 7°57'E; 96 m above sea level) in the German wine growing region Rheingau on the banks of river Rhine. Geisenheim has a temperate oceanic climate (Köppen-Geiger classification: Cfb) with mild winters and warm summers. The mean annual temperature is 10.5 °C and total annual precipitation averages 543.1 mm (long-term average from 1981 to 2010). The soil at the experimental site is characterized as low-carbonate loamy sand to sandy loam. The VineyardFACE consists of three ring pairs (A1-E1, A2-E2, A3-E3) each with an inner diameter of 12 m, of which three are under elevated CO₂ (eCO₂; E1, E2, E3) and three under ambient CO₂ (aCO₂; A1, E2, E3) concentration. Within eCO₂ rings air was enriched during daylight hours to approximately 18% above the ambient CO₂. Average daily CO₂ concentration of aCO₂ and eCO₂ treatments in June was 409.4 ± 8.6 and 483.2 ± 8.4 (means \pm SD), respectively. Within VineyardFACE rings, vines of *Vitis vinifera* L. cv. Riesling (clone 198–30 Gm) grafted on rootstock SO4 (clone 47 Gm) and cv. Cabernet Sauvignon (clone 170) grafted on rootstock 161–49 Couderc, respectively, were planted in April 2012 as one-year-old potted plants. Each ring contains seven rows of cv. Riesling and cv. Cabernet Sauvignon plants, which were planted alternately across a central divide. Vines were planted with a spacing of 0.9 m within rows and 1.8 m between rows, with a north-south orientation. Cover crop consisted of Freudenberger WB 130 mulch mixture III (10% *Lolium perenne*, 50% *Festuca rubra* and 40% *Poa pratensis*) and was sowed to every second inter-row, identified in this work as green inter-rows; while every other second inter-row was ploughed once in spring and was largely bare or covered with spontaneous vegetation identified in this work as open inter-rows (Fig. 7) [1, 6]

Soil sampling and physico-chemical parameter measurements

Soil sampling was performed utilizing sawed 50 ml syringes (11 x 3 cm) and 12 samples were taken up to a depth of ~10 cm within each ring in June 2018 distributed equally between green inter-rows and open inter-rows; half of the samples were taken to perform molecular biology and chemical analyses, and the other half were utilized to perform soil microbial respiration measurements. Green inter-rows soil cores were by hand gently shaken to remove loosely attached soil (bulk soil) and the soil that remained attached to

the roots was considered as rhizosphere soil. Open inter-rows soil cores were only managed as bulk soil due to no roots were present in them. Bulk and rhizosphere soils were sieved (<2 mm) and stored at -80 °C for molecular biology, at -20 °C for chemical analyses and at 4 °C for soil microbial respiration analyses. Soil samples were classified in four different blocks considering the CO₂ conditions (ambient and elevated) and the inter-rows where they were taken from (green inter-row soil and open inter-row soil).

Ammonium concentrations were measured after soil extractions with 1 M KCl using a colorimetric assay (Kandeler and Gerber 1988). Nitrate was extracted with deionized water and the filtered supernatant was analyzed by ion chromatography (Sykam S5200 chromatograph, Sykam GmbH, Eresing, Germany) according to Bak et al. (1991). Water content, dry matter and water holding capacity of soils samples were measured gravimetrically [66]. Carbon and nitrogen content of soil were measured by pyrolysis coupled to gas chromatography on a EA 1100 elemental analyzer (ThermoQuest, Milan, Italy) using a TCD detector by the Dumas method according to HBU (1996) [67] and VDLUFA (2012) method [68]. In each ring CO₂ concentration was recorded by using an infrared gas analyzer (LI-840A CO₂/H₂O Analyzer, LI-COR Biosciences, Lincoln, NE, USA) mounted at 1.5 m height within the ring center.

Respiration analysis with the MicroResp™ system (James Hutton Ltd, Aberdeen, Scotland UK) was performed following the protocol described by Campbell et al. [69]. Detection plates were prepared mixing agar solution 3% and indicator solution (Cresol Red 12.5 µg ml⁻¹, KCl 150 mM and NaHCO₃ 2.5 mM) in a ration 1:2 (agar:indicator). Soil samples were weighed, added into deep well plates and incubated for 3 days in a sealed box containing wet paper towels. Later, distilled sterile water and substrates (L-Arginine, D-Galactose, D-Glucose and N-Acetyl glucosamine) were added by quadruplicated to each sample at a final concentration of 20 mM. Detection plate's absorbance at time 0 was measured with a TECAN Infinite® M200 multimode Microplate Reader (Tecan Austria GmbH) at 570 nm, immediately assembled with the MicroResp™ seal (James Hutton Ltd) and the deep well plate and incubated for 6 h at 25 °C. After incubation time, detection plate's absorbance was read as described above. For calculation of CO₂ production rate, data were normalized and %CO₂ were calculated with a previously prepared calibration curve using a spline fit with Origin Lab® software (OriginLabCorporation, Northhampton, USA). Later %CO₂ values were converted to CO₂ rate (µg CO₂ – C g⁻¹ DW soil h⁻¹).

For chemical parameter results, measures of central tendency and dispersion were calculated. Ammonium, total carbon, total nitrogen and carbon/nitrogen ratio differences among the four different experimental blocks were assessed using a t-test for groups with similar variances. Differences on respiration results were calculated utilizing a t-test for samples with different variances using Microsoft Excel 2013.

RNA extraction and reverse transcription

RNA extraction was performed following a modified protocol of Mettel et al. [70]. For the extraction, 0.3 – 0.5 g of soil were weighed in reaction tubes containing 100 mg of sterile zirconia beads, added with 700 µL TPM buffer (50 mM Tris-HCl (pH 5), 1.7% [wt/vol] polyvinylpyrrolidone, 20 mM MgCl₂) and vortexed for 30 s. Cells were then disrupted in a cell mill MM200 (Retsch, Haan, Germany) for 2 min at a frequency of 30 Hz. Soil and cell debris were precipitated by centrifugation in a microcentrifuge (Heraeus Fresco, Thermo Fisher Scientific Inc., Waltham) for 5 min at 17,000 g and 4 °C, then the supernatant was transferred into a fresh reaction tube. Buffer PBL (770 µl, 5 mM Tris-HCl (pH 5), 5 mM Na₂EDTA and 0.1% [wt/vol] sodium dodecyl sulfate) were added to the resulting soil pellet and the disruption process was performed again as described above. Both supernatants from the lysis processes were pooled in one reaction tube. The pooled supernatant was immediately extracted, initially with the addition of 500 µl of phenol/chloroform/isoamyl alcohol (25:24:1) and subsequent with chloroform/isoamyl alcohol (24:1). Afterwards, each time the sample was centrifuged for 5 min at 17,000 g and 4 °C. The resulting upper aqueous phase was transferred to a new reaction tube, 800 µl of PEG solution was added (30% [wt/vol] polyethylene glycol 6000 and 1.6 M NaCl), incubated in ice for 30 min and centrifuged for 30 min at 17,000 g and 4 °C. Subsequently, the DNA/RNA pellet was washed with 800 µl of ice-cold 75% ethanol, dried out and dissolved in 50 µl of nuclease free water.

After extraction, samples were treated for DNA digestion with RNase-Free DNase Set (QIAGEN GmbH - Germany) according to manufacturer instructions; DNase reaction was stopped with 10 µl of 50 mM EDTA. With the DNA-free RNA, a PCR was carried out, using the universal 16S rRNA gene primers 27F (5'-AGAGTTTGATCMTGGATCMTGGCTCAG-3') and 1492R (5'-GGTTACCTTGTTACGACTT-3') (Lane, 1991; Weisburg, Barns, Pelletier, & Lane, 1991) and checked on agarose gel electrophoresis to verify the absence of remaining DNA in the samples. Subsequently, reverse transcription was performed utilizing AccuScript High Fidelity 1st Strand cDNA Synthesis Kit (Agilent Technologies, Inc., Cedar Creek – Texas, USA) following manufacturer instructions.

16S rRNA Ion Torrent sequencing and metagenomics analysis

The 16S rRNA gene hypervariable regions (V4&V5) was PCR amplified using the set of primers 520F (5'-AYTGGGYDTAAAGNG-3') [73] and 907R (5'-CCGTCAATTCMTTTRAGTTT-3') [74] and PCRs and sequencing by Ion Torrent technique were done by following the protocol described by Kaplan et al. [75]. The obtained Ion Torrent sequencing output was analyzed using QIIME2 version 2020.6 [76], sequences were demultiplexed with the QIIME cutadapt command [77] using a barcode error rate of 0 and assigned to specific samples by corresponding barcodes. Later, quality control, denoising, sequences dereplication and chimera filtering were performed using DADA2 software [78], the first 15 nucleotides were trimmed and sequences were truncated at a position of 320 nucleotides. Amplicon Sequence Variants (ASV) generated with DADA2 were taxonomic affiliated with a trained fitted classifier [79, 80] based on the SILVA 138 database [81, 82].

Diversity and differential abundance analyses

Alpha and Beta diversity analyses were performed using R studio software 1.1.419, R packages Phyloseq 1.28.0 [83] and Vegan 2.4-6 [84]. For alpha diversity assessment rarefaction was applied and diversity indices (Observed species, Shannon, Fisher) were calculated and compared among CO₂ conditions and soil habitats using the Wilcoxon test (Wilcoxon, 1945) with the Bonferroni correction method through 999 permutations. For non-constrained beta diversity analyses, data were transformed using centered log ratio (clr) method [85, 86], using R package Microbiome version 1.8.0 [87]. Later, community dissimilarity distance matrices were created using the Aitchison distance [85, 86] and visualized using principal components analysis (PCA) [88]. Statistical differences among blocks, rings, CO₂ conditions and ring plus soil habitats, were assessed by a Permutational Multivariate Analysis of Variance using Adonis method and employing 999 permutations [89]. Additionally, it was assessed the degree of dispersion of the bacterial community composition from the soil cores taken in each ring as it is described above. Redundancy analysis (RDA) was used to explore associations between microbial community structures and environmental parameters, and a Permutation test of redundancy analysis using 999 permutations was applied for evaluating their statistical significance [90].

Core microbiome ASVs of green and open inter-row soils were calculated by transforming the ASV counts to relative abundance with Microbiome version 1.8.0 [87]. Later, ASVs with a total relative abundance $\geq 0.01\%$ and present in $\geq 85\%$ of samples

were included as part of the core. For core genera estimation, ASVs were collapsed by genera and analyzed utilizing the settings described above.

Differential abundance of ASVs and genera from green inter-row soils was assessed by comparing the core microbiomes of each one utilizing R package ALDEx2 1.22.0 [91]. ALDEx2 analysis was done by performing a centered log ratio (clr) transformation using as denominator the geometric mean abundance of all features and 128 Monte-Carlo instances; later it was done a Welch's t-test with a Benjamini-Hochberg correction with a threshold of <0.05 . Furthermore, features with absolute Aldex effect sizes of >0.8 and >0.5 were considered to have a significantly greater and a moderate higher abundance respectively.

Microbe-microbe and microbiome-environmental parameters correlation analyses

Network analysis was performed using the core ASVs from aCO₂ and eCO₂ green inter-row soils, which showed an absolute ALDEx effect size >0.5 . Later, ASVs were analyzed utilizing a co-occurrence network with the R package Spiec-easi 1.1.1 [92], using the neighborhood selection method [93], a number of lambda path of 100, a lambda minimum ratio of 10^{-2} and the Stability Approach to Regularization Selection (StARS) using its defaults settings. Subsequently, the network visualization was done on Cytoscape 3.8.2 [94].

Similarly, it was assessed core genera co-occurrence from aCO₂ and eCO₂ green inter-rows with Spiec-easi 1.1.1 [92] and SPRING 1.0.4 [95] using genera with an absolute Aldex effect size >0.1 and using the neighborhood selection method [93], a number of lambda path of 100, a lambda minimum ratio of 10^{-1} and the Stability Approach to Regularization Selection (StARS). Additionally, previous SPRING partial correlation analysis, it was performed a modified central log ratio (mclr) transformation of the genera counts.

Correlation analysis between green inter-rows' ASVs and genera with environmental parameters was done using ALDEx2 1.22.0 [91] and its "aldex.corr" function, utilizing Pearson's and Sperman's correlation coefficients, and obtained p-values were corrected using false discovery rate (FDR) method with a threshold of <0.05 .

cDNA Quantitative PCR

The quantification of 16S rRNA gene to estimate total bacterial abundance was performed following the protocol described by Kaplan et al. [75], but instead of DNA,

cDNA products described above were used for the quantification. Likewise, it was performed the mRNA quantification of transcripts involved in the nitrogen cycle including nitrogen fixation (*nifH*), ammonia oxidation (*amoA*), nitrite reduction (*nirS*, *nirK*) and nitrous oxide reduction (*nosZ*) using primers and amplification protocols described on Tab. 4 and expressed as percentage (%) of 16S rRNA copy numbers. All quantitative PCR (qPCR) were conducted on a Rotor Gene Q (Qiagen, Hilden, Germany) by using Absolute qPCR SYBR Green Mix (ThermoFischer Scientific). Statistical comparisons were done with Kruskal-Wallis and Wilcoxon tests with the Benjamini & Hochberg adjustment method using R Package *stats* version 3.6.3.

Table 4. Primer sets and thermal profiles of transcripts for N cycle functional genes and 16S rRNA.

qPCR target	Primer set	Thermal cycling profile	No. cycles	Reference
16S RNA	520F, 926R complemented	95 °C/45s, 60 °C/45 s, 72 °C/60 s, 84 °C/20 s	40	[73, 74]
<i>amoA</i>	amoA1_F, amoA2_R	95 °C/30 s, 59 °C/30 s, 72 °C/20s, 80 °C/20 s	35	[96]
<i>nifH</i>	IGK3, DVV	95 °C/20 s, 55 °C/30 s, 72 °C/30s, 84 °C/20 s	40	[54]
<i>nirK</i>	nirK876, nirK 5R	95 °C/20 s, 63 °C/25 s, 72 °C/60 s, 80 °C/20 s	40	[97, 98]
<i>nirS</i>	Cd3aF, R3cd	95 °C/20 s, 63 °C/25 s, 72 °C/60 s, 80 °C/20 s	40	[99, 100]
<i>nosZ</i>	nosZ2F, nosZ2R	95 °C/30 s, 63 °C/50 s, 72 °C/50 s, 80 °C/20 s	40	[101]

Declarations

Acknowledgments

We thank Bernd Honermeier for his support to perform soil carbon and nitrogen analyses and Rita Geissler-Plaum for her excellent technical support. For providing the CO₂ data and support of the Vineyard FACE-system we thank Claudia Kammann and Daniel Papsdorf.

Funding

The work was supported partly by the LOEWE excellence cluster FACE2FACE of the Hessian State Ministry of Higher Education, Research and the Arts.

Availability of data and materials

The authors declare that the data supporting the findings of this study are available within the article and its supplementary Information. cDNA sequence data are available in the GenBank database under the accession number PRJNA680929.

Competing interests

The authors declare that they have no competing interests.

Authors' contributions

DR conducted experiments, data curation, data analysis and writing of the manuscript. SR contributed with methodology, review and editing. YW contributed with data curation, review and editing. AG contributed with experiments execution. BS contributed with methodology and experiments execution. SS contributed with methodology, review and editing.

References

1. Wohlfahrt Y, Smith JP, Tittmann S, Honermeier B, Stoll M. Primary productivity and physiological responses of *Vitis vinifera* L. cvs. under Free Air Carbon dioxide Enrichment (FACE). *Eur J Agron.* 2018;101 February:149–62. doi:10.1016/j.eja.2018.09.005.
2. da Silva JR, Patterson AE, Rodrigues WP, Campostrini E, Griffin KL. Photosynthetic acclimation to elevated CO₂ combined with partial rootzone drying results in improved water use efficiency, drought tolerance and leaf carbon balance of grapevines (*Vitis labrusca*). *Environ Exp Bot.* 2017;134:82–95.
3. Edwards EJ, Unwin D, Kilmister R, Treeby M, Ollat N. Multi-seasonal effects of warming and elevated CO₂ on the physiology, growth and production of mature, field grown, Shiraz grapevines. *J Int des Sci la Vigne du Vin.* 2017;51:127–32.
4. Kizildeniz T, Pascual I, Irigoyen JJ, Morales F. Using fruit-bearing cuttings of grapevine and temperature gradient greenhouses to evaluate effects of climate change (elevated CO₂ and temperature, and water deficit) on the cv. red and white Tempranillo. Yield and must quality in three consecutive growin. *Agric Water Manag.* 2018;202:299–310. doi:10.1016/j.agwat.2017.12.001.
5. Wohlfahrt Y, Tittmann S, Schmidt D, Rauhut D, Honer B, Stoll M. The effect of elevated CO₂ on berry development and bunch structure of *Vitis vinifera* L. cvs. Riesling and cabernet sauvignon. *Appl Sci.* 2020;10:2486.
6. Reineke A, Selim M. Elevated atmospheric CO₂ concentrations alter grapevine (*Vitis vinifera*) systemic transcriptional response to European grapevine moth (*Lobesia botrana*) herbivory. *Sci Rep.* 2019;9:1–12. doi:10.1038/s41598-019-39979-5.
7. Schulze-Sylvester M, Reineke A. Elevated CO₂ levels impact fitness traits of vine mealybug *Planococcus ficus* signoret, but not its parasitoid *Leptomastix dactylopii*

howard. *Agronomy*. 2019;9:326.

8. Zarraonaindia I, Owens SM, Weisenhorn P, West K, Hampton-Marcell J, Lax S. The Soil Microbiome Influences Grapevine-Associated Microbiota. *MBio*. 2015;6:e02527-14.

9. Wei YJ, Wu Y, Yan YZ, Zou W, Xue J, Ma WR, et al. High-throughput sequencing of microbial community diversity in soil, grapes, leaves, grape juice and wine of grapevine from China. *PLoS One*. 2018;13:e0193097.

10. Deyett E, Rolshausen PE. Endophytic microbial assemblage in grapevine. *FEMS Microbiol Ecol*. 2020;96:1–11.

11. Nerva L, Zanzotto A, Gardiman M, Gaiotti F, Chitarra W. Soil microbiome analysis in an ESCA diseased vineyard. *Soil Biol Biochem*. 2019;135 January:60–70. doi:10.1016/j.soilbio.2019.04.014.

12. Marasco R, Rolli E, Fusi M, Michoud G, Daffonchio D. Grapevine rootstocks shape underground bacterial microbiome and networking but not potential functionality. *Microbiome*. 2018;6:1–17.

13. Berlanas C, Berbegal M, Elena G, Laidani M, Cibriain JF, Sagües A, et al. The fungal and bacterial rhizosphere microbiome associated with grapevine rootstock genotypes in mature and young vineyards. *Front Microbiol*. 2019;10 MAY:1–16.

14. Liu D, Howell K. Community succession of the grapevine fungal microbiome in the annual growth cycle. *Environ Microbiol*. 2020;n/a n/a. doi:10.1111/1462-2920.15172.

15. Phillips RP, Meier IC, Bernhardt ES, Grandy AS, Wickings K, Finzi AC. Roots and fungi accelerate carbon and nitrogen cycling in forests exposed to elevated CO₂. *Ecol Lett*. 2012;15:1042–9.

16. Jia X, Wang W, Chen Z, He Y, Liu J. Concentrations of secondary metabolites in tissues and root exudates of wheat seedlings changed under elevated atmospheric CO₂ and cadmium-contaminated soils. *Environ Exp Bot*. 2014;107:134–43. doi:10.1016/j.envexpbot.2014.06.005.

17. Bei Q, Moser G, Wu X, Müller C, Liesack W. Metatranscriptomics reveals climate change effects on the rhizosphere microbiomes in European grassland. *Soil Biol Biochem*. 2019;138 July:1–10. doi:10.1016/j.soilbio.2019.107604.

18. Yu Z, Li Y, Wang G, Liu J, Liu J, Liu X, et al. Effectiveness of elevated CO₂ mediating bacterial communities in the soybean rhizosphere depends on genotypes. *Agric Ecosyst Environ*. 2016;231:229–32.

19. Montealegre CM, Van Kessel C, Blumenthal JM, Hur HG, Hartwig U a., Sadowsky MJ. Elevated atmospheric CO₂ alters microbial population structure in a pasture ecosystem. *Glob Chang Biol*. 2000;6:475–82.

20. Lee SH, Kang H. Elevated CO₂ causes a change in microbial communities of rhizosphere and bulk soil of salt marsh system. *Appl Soil Ecol*. 2016;108:307–14.

doi:10.1016/j.apsoil.2016.09.009.

21. Song N, Zhang X, Wang F, Zhang C, Tang S. Elevated CO₂ increases Cs uptake and alters microbial communities and biomass in the rhizosphere of *Phytolacca americana* Linn (pokeweed) and *Amaranthus cruentus* L. (purple amaranth) grown on soils spiked with various levels of Cs. J Environ Radioact. 2012;112:29–37. doi:10.1016/j.jenvrad.2012.03.002.
22. Müller C, Rütting T, Abbasi MK, Laughlin RJ, Kammann C, Clough TJ, et al. Effect of elevated CO₂ on soil N dynamics in a temperate grassland soil. Soil Biol Biochem. 2009;41:1996–2001.
23. Kizildeniz T, Irigoyen JJ, Pascual I, Morales F. Simulating the impact of climate change (elevated CO₂ and temperature, and water deficit) on the growth of red and white Tempranillo grapevine in three consecutive growing seasons (2013–2015). Agric Water Manag. 2018;202 February:220–30. doi:10.1016/j.agwat.2018.02.006.
24. Wohlfahrt Y, Patz C, Schmidt D, Rauhut D, Honermeier B, Stoll M. Responses on Must and Wine Composition of *Vitis vinifera* L. cvs. Riesling and Cabernet Sauvignon under a Free Air CO₂ Enrichment (FACE). Foods. 2021;10.
25. Bokulich NA, Collins T, Masarweh C, Allen G, Heymann H, Ebeler SE, et al. Fermentation Behavior Suggest Microbial Contribution to Regional. MBio. 2016;7:e00631-16.
26. Cheng L, Booker FL, Burkey KO, Tu C, da Shew HD, Rufty TW, et al. Soil microbial responses to elevated CO₂ and O₃ in a nitrogen-aggrading agroecosystem. PLoS One. 2011;6:e21377.
27. Wang P, Marsh EL, Ainsworth EA, Leakey ADB, Sheflin AM, Schachtman DP. Shifts in microbial communities in soil, rhizosphere and roots of two major crop systems under elevated CO₂ and O₃. Sci Rep. 2017;7:1–12. doi:10.1038/s41598-017-14936-2.
28. Simonin M, Le Roux X, Poly F, Lerondelle C, Hungate BA, Nunan N, et al. Coupling between and among ammonia oxidizers and nitrite oxidizers in grassland mesocosms submitted to elevated CO₂ and nitrogen supply. Microb Ecol. 2015;70:809–18.
29. Rosado-Porto D, Ratering S, Cardinale M, Maisinger C, Moser G, Deppe M, et al. Elevated Atmospheric CO₂ Modifies Mostly the Metabolic Active Rhizosphere Soil Microbiome in the Giessen FACE Experiment. Microb Ecol. 2021. doi:10.1007/s00248-021-01791-y.
30. Walker TS, Bais HP, Grotewold E, Vivanco JM. Root Exudation and Rhizosphere Biology Root Exudation and Rhizosphere Biology. Plant Physiol. 2003;132:44–51.
31. Li K, Guo XW, Xie HG, Guo Y, Li C. Influence of root exudates and residues on soil microecological environment. Pakistan J Bot. 2013;45:1773–9.
32. Lipson DA, Wilson RF, Oechel WC. Effects of elevated atmospheric CO₂ on soil

microbial biomass, activity, and diversity in a chaparral ecosystem. *Appl Environ Microbiol.* 2005;71:8573–80.

33. Carney KM, Hungate BA, Drake BG, Megonigal JP. Altered soil microbial community at elevated CO₂ leads to loss of soil carbon. *Proc Natl Acad Sci U S A.* 2007;104:4990–5.

34. Xu M, He Z, Deng Y, Wu L, Van Nostrand JD, Hobbie SE, et al. Elevated CO₂ influences microbial carbon and nitrogen cycling. *BMC Microbiol.* 2013;13.

35. Xiong J, He Z, Shi S, Kent A, Deng Y, Wu L, et al. Elevated CO₂ shifts the functional structure and metabolic potentials of soil microbial communities in a C₄ agroecosystem. *Sci Rep.* 2015;5:1–9.

36. He Z, Xu M, Deng Y, Kang S, Kellogg L, Wu L, et al. Metagenomic analysis reveals a marked divergence in the structure of belowground microbial communities at elevated CO₂. *Ecol Lett.* 2010;13:564–75.

37. He Z, Xiong J, Kent AD, Deng Y, Xue K, Wang G, et al. Distinct responses of soil microbial communities to elevated CO₂ and O₃ in a soybean agro-ecosystem. *ISME J.* 2014;8:714–26.

38. Wang P, Marsh EL, Ainsworth EA, Leakey ADB, Sheflin AM, Schachtman DP, et al. Shifts in microbial communities in soil, rhizosphere and roots of two major crop systems under elevated CO₂ and O₃. *Sci Rep.* 2011;7:1–8. doi:10.1371/journal.pone.0021377.

39. Pujol Pereira EI, Chung H, Scow K, Six J. Microbial communities and soil structure are affected by reduced precipitation, but not by elevated Carbon Dioxide. *Soil Sci Soc Am J.* 2013;77:482. doi:10.2136/sssaj2012.0218.

40. Brenzinger K, Kujala K, Horn MA, Moser G, Guillet C, Kammann C, et al. Soil conditions rather than long-term exposure to elevated CO₂ affect soil microbial communities associated with N-cycling. *Front Microbiol.* 2017;8:1–14. doi:10.3389/fmicb.2017.01976.

41. Fontaine S, Bardoux G, Abbadie L, Mariotti A. Carbon input to soil may decrease soil carbon content. *Ecol Lett.* 2004;7:314–20.

42. Blagodatskaya E, Kuzyakov Y. Mechanisms of real and apparent priming effects and their dependence on soil microbial biomass and community structure: Critical review. *Biol Fertil Soils.* 2008;45:115–31.

43. Derrien D, Plain C, Courty PE, Gelhaye L, Moerdijk-Poortvliet TCW, Thomas F, et al. Does the addition of labile substrate destabilise old soil organic matter? *Soil Biol Biochem.* 2014;76:149–60. doi:10.1016/j.soilbio.2014.04.030.

44. Vestergaard M, Reinsch S, Bengtson P, Ambus P, Christensen S. Enhanced priming of old, not new soil carbon at elevated atmospheric CO₂. *Soil Biol Biochem.* 2016;100:140–8.

45. Liu XJA, Sun J, Mau RL, Finley BK, Compson ZG, van Gestel N, et al. Labile carbon input determines the direction and magnitude of the priming effect. *Appl Soil Ecol.* 2017;109:7–13. doi:10.1016/j.apsoil.2016.10.002.
46. Bleyen N, Hendrix K, Moors H, Durce D, Vasile M, Valcke E. Biodegradability of dissolved organic matter in Boom Clay pore water under nitrate-reducing conditions: Effect of additional C and P sources. *Appl Geochemistry.* 2018;92 June 2017:45–58. doi:10.1016/j.apgeochem.2018.02.005.
47. Gtari M, Ghodhbane-Gtari F, Nouioui I, Beauchemin N, Tisa LS. Phylogenetic perspectives of nitrogen-fixing actinobacteria. *Arch Microbiol.* 2012;194:3–11.
48. Zakhia F, Jeder H, Willems A, Gillis M, Dreyfus B, De Lajudie P. Diverse bacteria associated with root nodules of spontaneous legumes in Tunisia and first report for *nifH*-like gene within the genera *Microbacterium* and *Starkeya*. *Microb Ecol.* 2006;51:375–93.
49. von der Weid I, Duarte GF, van Elsas JD, Seldin L. *Paenibacillus brasiliensis* sp. nov., a novel nitrogen-fixing species isolated from the maize rhizosphere in Brazil. *Int J Syst Evol Microbiol.* 2002;52:2147–53.
50. Padda KP, Puri A, Chanway CP. Plant growth promotion and nitrogen fixation in canola (*Brassica napus*) by an endophytic strain of *Paenibacillus polymyxa* and its GFP-tagged derivative in a long-term study. *Botany.* 2016;94:1209–17. doi:10.1139/cjb-2016-0075.
51. Fernandes G de C, Trarbach LJ, De Campos SB, Beneduzi A, Passaglia LMP. Alternative nitrogenase and pseudogenes: Unique features of the *Paenibacillus riograndensis* nitrogen fixation system. *Res Microbiol.* 2014;165:571–80. doi:10.1016/j.resmic.2014.06.002.
52. Rosado AS, Duarte GF, Seldin L, Van Elsas JD. Genetic Diversity of *nifH* Gene Sequences in *Paenibacillus azotofixans*. *Appl Environ Microbiol.* 1998;64:2770–9.
53. Li Y, Li Q, Chen S. Diazotroph *Paenibacillus tritici* bj-18 drives the variation in bacterial, diazotrophic and fungal communities in the rhizosphere and root/shoot endosphere of maize. *Int J Mol Sci.* 2021;22:1–25.
54. Ando S, Goto M, Hayashi H, Yoneyama T, Meunchang S, Thongra-ar P, et al. Detection of *nifH* Sequences in Sugarcane (*Saccharum officinarum* L.) And Pineapple (*Ananas comosus* [L.] Merr.). *Soil Sci Plant Nutr.* 2005;51:303–8.
55. Ormeño-Orrillo E, Martínez-Romero E. A genomotaxonomy view of the *Bradyrhizobium* genus. *Front Microbiol.* 2019;10:1–13.
56. Hennecke H. Nitrogen fixation genes involved in the *Bradyrhizobium juponicum*-soybean symbiosis. *FEBS Lett.* 1990;268:422–6.
57. Ishii S, Ashida N, Ohno H, Segawa T, Yabe S, Otsuka S, et al. *Noviherbaspirillum denitrificans* sp. nov., a denitrifying bacterium isolated from rice paddy soil and

Noviherbaspirillum autotrophicum sp nov., a denitrifying , facultatively autotrophic bacterium isolated from rice paddy soil and proposal to reclass. Int J Syst Evol Microbiol. 2017;67:1841–8.

58. Zhao X, Li X, Qi N, Gan M, Pan Y, Han T, et al. *Massilia neuiana* sp. nov., isolated from wet soil. Int J Syst Evol Microbiol. 2017;67:4943–7.

59. Xu Z, Dai X, Chai X. Effect of different carbon sources on denitrification performance, microbial community structure and denitrification genes. Sci Total Environ. 2018;634:195–204. doi:10.1016/j.scitotenv.2018.03.348.

60. Zhou S, Zhang Y, Huang T, Liu Y, Fang K, Zhang C. Microbial aerobic denitrification dominates nitrogen losses from reservoir ecosystem in the spring of Zhoucun reservoir. Sci Total Environ. 2019;651:998–1010. doi:10.1016/j.scitotenv.2018.09.160.

61. Zhou S, Zeng X, Xu Z, Bai Z, Xu S, Jiang C, et al. *Paenibacillus polymyxa* biofertilizer application in a tea plantation reduces soil N₂O by changing denitrifier communities. Can J Microbiol. 2020;66:214–27.

62. Moser G, Gorenflo A, Brenzinger K, Keidel L, Braker G, Marhan S, et al. Explaining the doubling of N₂O emissions under elevated CO₂ in the Giessen FACE via in-field ¹⁵N tracing. Glob Chang Biol. 2018;24:3897–910.

63. Nistor E, Dobrei AG, Dobrei A, Camen D, Sala F, Prundeanu H. N₂O, CO₂, Production, and C Sequestration in Vineyards: a Review. Water Air Soil Pollut. 2018;229.

64. Butterly CR, Phillips LA, Wiltshire JL, Franks AE, Armstrong RD, Chen D, et al. Long-term effects of elevated CO₂ on carbon and nitrogen functional capacity of microbial communities in three contrasting soils. Soil Biol Biochem. 2016;97:157–67. doi:10.1016/j.soilbio.2016.03.010.

65. Bak F, Scheff G, Jansen KH. A rapid and sensitive ion chromatographic technique for the determination of sulfate and sulfate reduction rates in freshwater lake sediments. FEMS Microbiol Lett. 1991;85:23–30.

66. Forster JC. Methods in Applied Soil Microbiology and Biochemistry. In: Alef K, Nannipieri P, editors. Methods in Applied Soil Microbiology and Biochemistry. San Diego: Academic Press; 1995. p. 105–6. doi:10.1016/B978-012513840-6/50024-0.

67. HBU. Handbuch der Bodenuntersuchung (HBU), Bodenbeschaffenheit - Bestimmung von organischem Kohlenstoff und Gesamtkohlenstoff nach trockener Verbrennung (Elementaranalyse). DIN ISO 10. Berlin: GmbH; 1996. p. 3.4.1.31.1a.

68. VDLUFA. Methodenbuch- Band I, Die Untersuchung von Böden, 6. Darmstadt: VDLUFA - Verlag; 2012.

69. Campbell CD, Chapman SJ, Cameron CM, Davidson MS, Potts JM. A rapid microtiter plate method to measure carbon dioxide evolved from carbon substrate amendments so as to determine the physiological profiles of soil microbial communities by using whole

soil. *Appl Environ Microbiol*. 2003;69:3593–9.

70. Mettel C, Kim Y, Shrestha PM, Liesack W. Extraction of mRNA from soil. *Appl Environ Microbiol*. 2010;76:5995–6000.

71. Lane DJ. 16S/23S rRNA sequencing. In: Stackebrandt E, Goodfellow M, editors. *Nucleic Acid Techniques in Bacterial Systematics*. New York: John Wiley and Sons; 1991. p. 115–175.

72. Weisburg WG, Barns SM, Pelletier DA, Lane DJ. 16S Ribosomal DNA Amplification for Phylogenetic Study. *J Bacteriol*. 1991;173:697–703.

73. Claesson MJ, O’Sullivan O, Wang Q, Nikkilä J, Marchesi JR, Smidt H, et al. Comparative analysis of pyrosequencing and a phylogenetic microarray for exploring microbial community structures in the human distal intestine. *PLoS One*. 2009;4:e6669.

74. Engelbrektson A, Kunin V, Wrighton KC, Zvenigorodsky N, Chen F, Ochman H, et al. Experimental factors affecting PCR-based estimates of microbial species richness and evenness. *ISME J*. 2010;4:642–7.

75. Kaplan H, Ratering S, Felix-Henningsen P, Schnell S. Stability of in situ immobilization of trace metals with different amendments revealed by microbial ¹³C-labelled wheat root decomposition and efflux-mediated metal resistance of soil bacteria. *Sci Total Environ*. 2019;659:1082–9. doi:10.1016/j.scitotenv.2018.12.441.

76. Bolyen E, Rideout JR, Dillon MR, Bokulich NA, Chase J, Cope EK, et al. Reproducible, interactive, scalable and extensible microbiome data science using QIIME 2. *Nat Biotechnol*. 2019;37:852–7.

77. Martin M. Cutadapt removes adapter sequences from high-throughput sequencing reads. *EMBnet J*. 2011;17:10.

78. Callahan BJ, McMurdie PJ, Rosen MJ, Han AW, Johnson AJA, Holmes SP. DADA2: High-resolution sample inference from Illumina amplicon data. *Nat Methods*. 2016;13:581–3. doi:10.1038/nmeth.3869.

79. Pedregosa F, Varoquaux G, Gramfort A, Michel V, Thirion B, Grisel O, et al. Scikit-learn: machine learning in python. *J Mach Learn Res*. 2011;12 Oct:2825–2830.

80. Bokulich NA, Kaehler BD, Rideout JR, Dillon M, Bolyen E, Knight R, et al. Optimizing taxonomic classification of marker-gene amplicon sequences with QIIME 2’s q2-feature-classifier plugin. *Microbiome*. 2018;6:1–17.

81. Quast C, Pruesse E, Yilmaz P, Gerken J, Schweer T, Yarza P, et al. The SILVA ribosomal RNA gene database project: Improved data processing and web-based tools. *Nucleic Acids Res*. 2013;41:590–6.

82. Glöckner FO, Yilmaz P, Quast C, Gerken J, Beccati A, Ciuprina A, et al. 25 years of serving the community with ribosomal RNA gene reference databases and tools. *J Biotechnol*. 2017;261 February:169–76. doi:10.1016/j.jbiotec.2017.06.1198.

83. McMurdie PJ, Holmes S. Phyloseq: An R package for reproducible interactive analysis and graphics of microbiome census data. PLoS One. 2013;8:e61217.
84. Oksanen J, Blanchet FG, Friendly M, Kindt R, Legendre P, McGlinn D, et al. vegan: Community Ecology Package. 2018. <https://cran.r-project.org/package=vegan>.
85. Aitchison J. The Statistical Analysis of Compositional Data. J of the R Stat Soc Ser B. 1982;44:139–77.
86. Aitchison J. Book review. XII. London - New York: Chapman and Hall; 1986.
87. Lahti L, Shetty S. microbiome R package. 2019. url: <http://microbiome.github.io>.
88. Jolliffe IT, Cadima J. Principal component analysis: a review and recent developments Subject Areas. PhilTransRSocA. 2016;374:1–16.
89. Anderson MJ. A new method for non parametric multivariate analysis of variance. Austral Ecol. 2001;26:32–46. doi:10.1111/j.1442-9993.2001.01070.pp.x.
90. Legendre P, Oksanen J, ter Braak CJF. Testing the significance of canonical axes in redundancy analysis. Methods Ecol Evol. 2011;2:269–77.
91. Fernandes AD, Macklaim JM, Linn TG, Reid G, Gloor GB. ANOVA-Like Differential Expression (ALDEx) Analysis for Mixed Population RNA-Seq. PLoS One. 2013;8:e67019.
92. Kurtz ZD, Müller CL, Miraldi ER, Littman DR, Blaser MJ, Bonneau RA. Sparse and Compositionally Robust Inference of Microbial Ecological Networks. PLoS Comput Biol. 2015;11:1–25. doi:10.1371/journal.pcbi.1004226.
93. Meinshausen N, Bühlmann P. High-dimensional graphs and variable selection with the Lasso. Ann Stat. 2006;34:1436–62.
94. Shannon P, Markiel A, Owen Ozier, Baliga NS, Wang JT, Ramage D, et al. Cytoscape: a software environment for integrated models of biomolecular interaction networks. Genome Res. 2003;13:2498–504.
95. Yoon G, Gaynanova I, Müller CL. Microbial networks in SPRING - Semi-parametric rank-based correlation and partial correlation estimation for quantitative microbiome data. Front Genet. 2019;10 JUN.
96. Rotthauwe JH, Witzel KP, Liesack W. The ammonia monooxygenase structural gene *amoA* as a functional marker: Molecular fine-scale analysis of natural ammonia-oxidizing populations. Appl Environ Microbiol. 1997;63:4704–12.
97. Henry S, Baudoin E, López-Gutiérrez JC, Martin-Laurent F, Brauman A, Philippot L. Quantification of denitrifying bacteria in soils by *nirK* gene targeted real-time PCR. J Microbiol Methods. 2004;59:327–35.
98. Braker G, Fesefeldt A, Witzel KP. Development of PCR primer systems for amplification of nitrite reductase genes (*nirK* and *nirS*) to detect denitrifying bacteria in environmental samples. Appl Environ Microbiol. 1998;64:3769–75.

99. Michotey V, Méjean V, Bonin P. Comparison of methods for quantification of cytochrome cd1-denitrifying bacteria in environmental marine samples. *Appl Environ Microbiol.* 2000;66:1564–71.
100. Throbäck IN, Enwall K, Jarvis Å, Hallin S. Reassessing PCR primers targeting *nirS*, *nirK* and *nosZ* genes for community surveys of denitrifying bacteria with DGGE. *FEMS Microbiol Ecol.* 2004;49:401–17.
101. Henry S, Bru D, Stres B, Hallet S, Philippot L. Quantitative detection of the *nosZ* gene, encoding nitrous oxide reductase, and comparison of the abundances of 16S rRNA, *narG*, *nirK*, and *nosZ* genes in soils. *Appl Environ Microbiol.* 2006;72:5181–9.

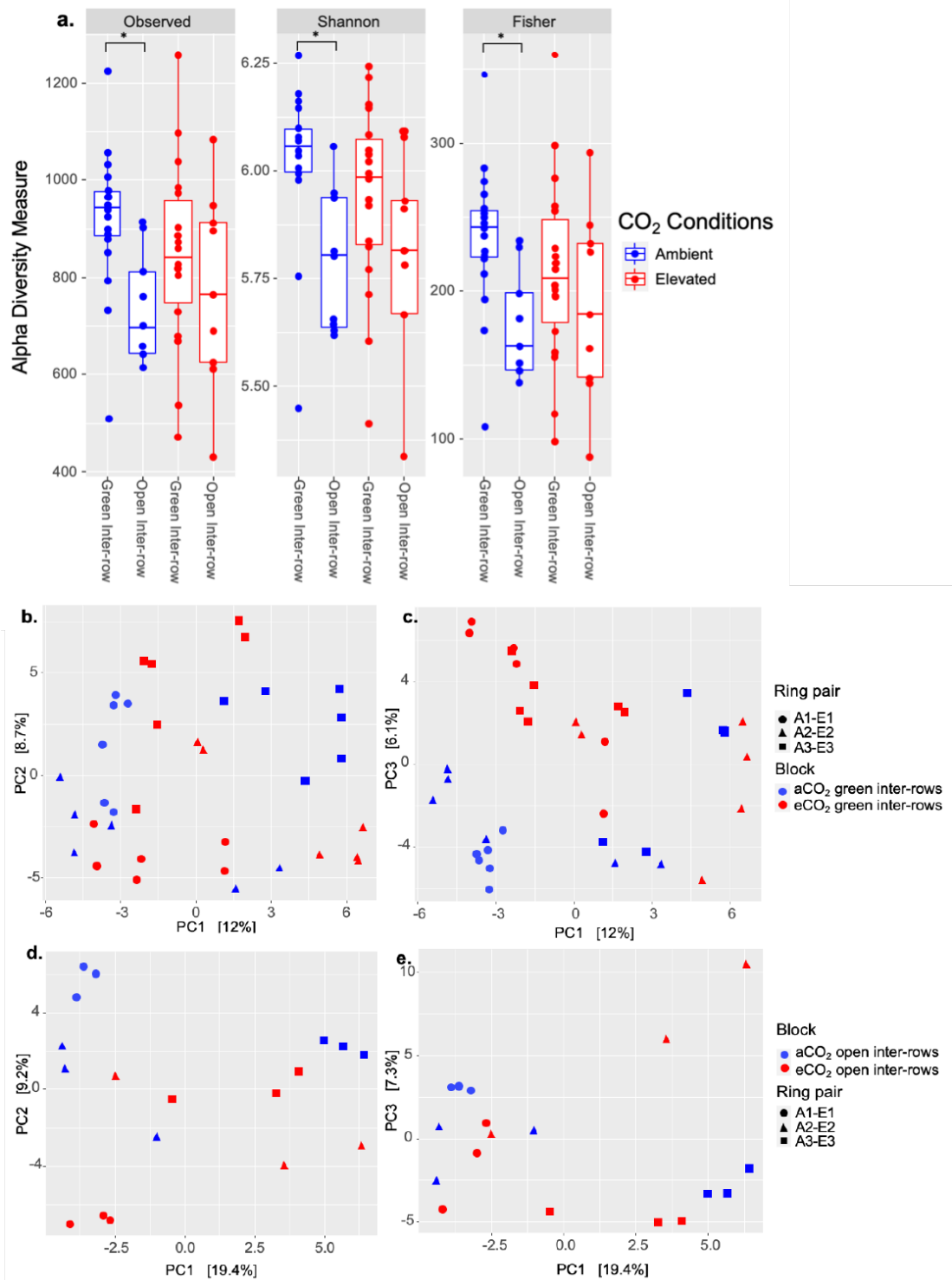


Figure 1. Diversity analysis of Geisenheim VineyardFACE. **(a)** Alpha diversity metrics. aCO₂, ambient CO₂ conditions; eCO₂, elevated CO₂ conditions. * p<0.05. **(b, c)** Principal Components Analysis (PCA) calculated based on Aitchison community dissimilarity distance matrix of axis 1-2 (left) and axis 1-3 (right) of green inter-rows from ambient and elevated CO₂ rings, **(d, e)** Principal Components Analysis (PCA) calculated based on Aitchison community dissimilarity distance matrix of axis 1-2 (left) and axis 1-3 (right) of open inter-rows from ambient and elevated CO₂ rings. A, ambient CO₂ rings; E, elevated CO₂ rings; aCO₂, ambient CO₂ conditions; eCO₂, elevated CO₂ conditions.

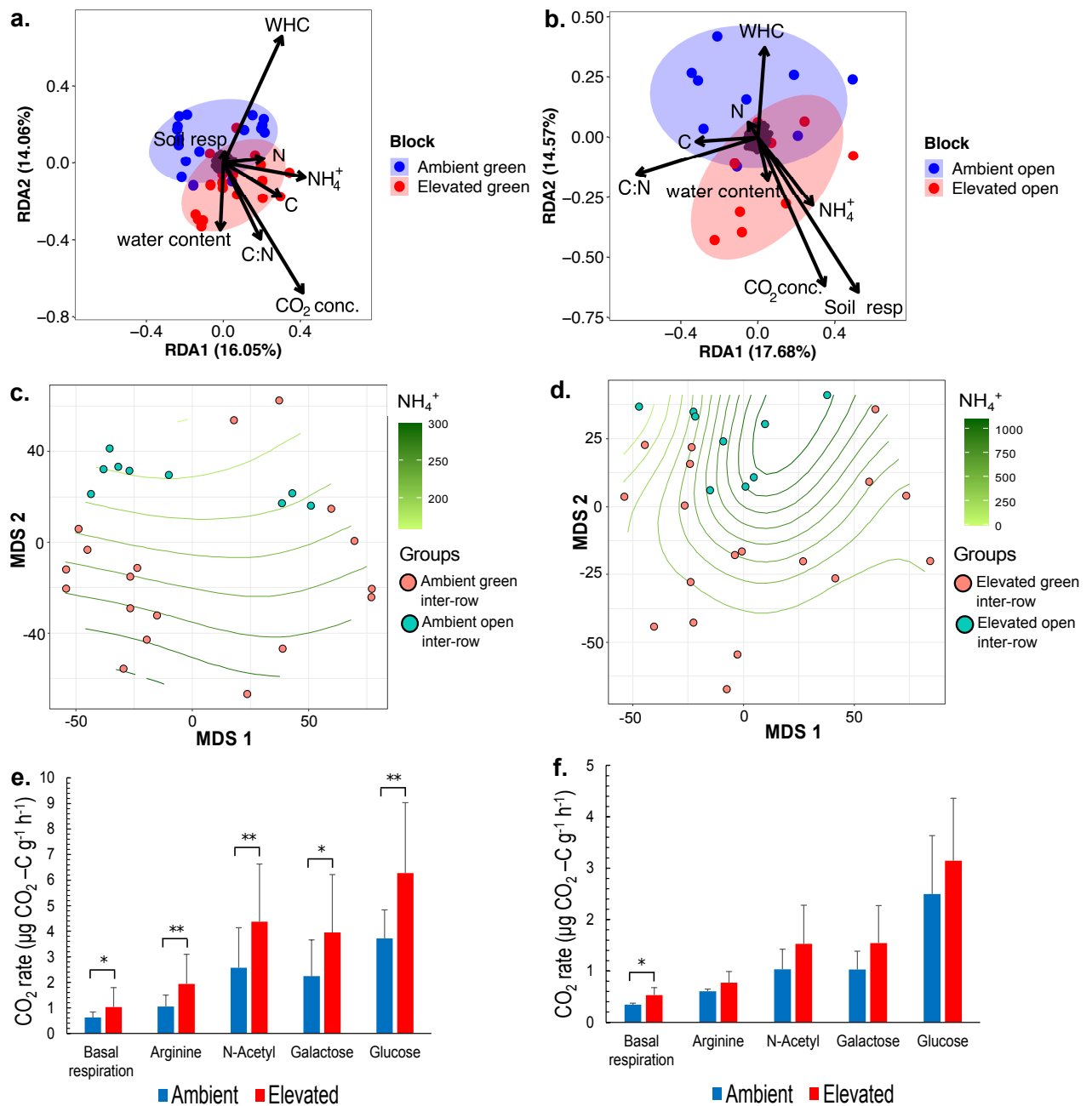


Figure 2. Environmental parameters effect on Geisenheim VineyardFACE microbiome. **(a, b)** Redundancy Analysis (RDA) based on Aitchison community dissimilarity distance matrix of green inter-rows (left) and open inter-rows (right) from ambient (blue) and elevated (red) CO_2 rings. WHC, Water holding capacity; CO_2 Conc., CO_2 concentration; Soil resp., Soil basal respiration; C, Total carbon concentration; N, Total nitrogen concentration; C:N, Carbon-nitrogen ratio; NH_4^+ , Ammonium concentration. **(c, d)** Multidimensional scaling (MDS) with a grid of ammonium concentration expressed as ($\mu\text{M NH}_4^+ \text{g}^{-1}$), using Aitchison community dissimilarity distance matrix of green and open inter-rows from ambient CO_2 rings (left), green and open inter-rows from elevated CO_2 rings (right). **(e, f)** Soil microbial respiration expressed as CO_2 production rate under the addition of different carbon substrates of green inter-rows from ambient and elevated CO_2 rings (left), and open inter-rows from ambient and elevated CO_2 rings (right). Error bars are expressed as variance of mean values

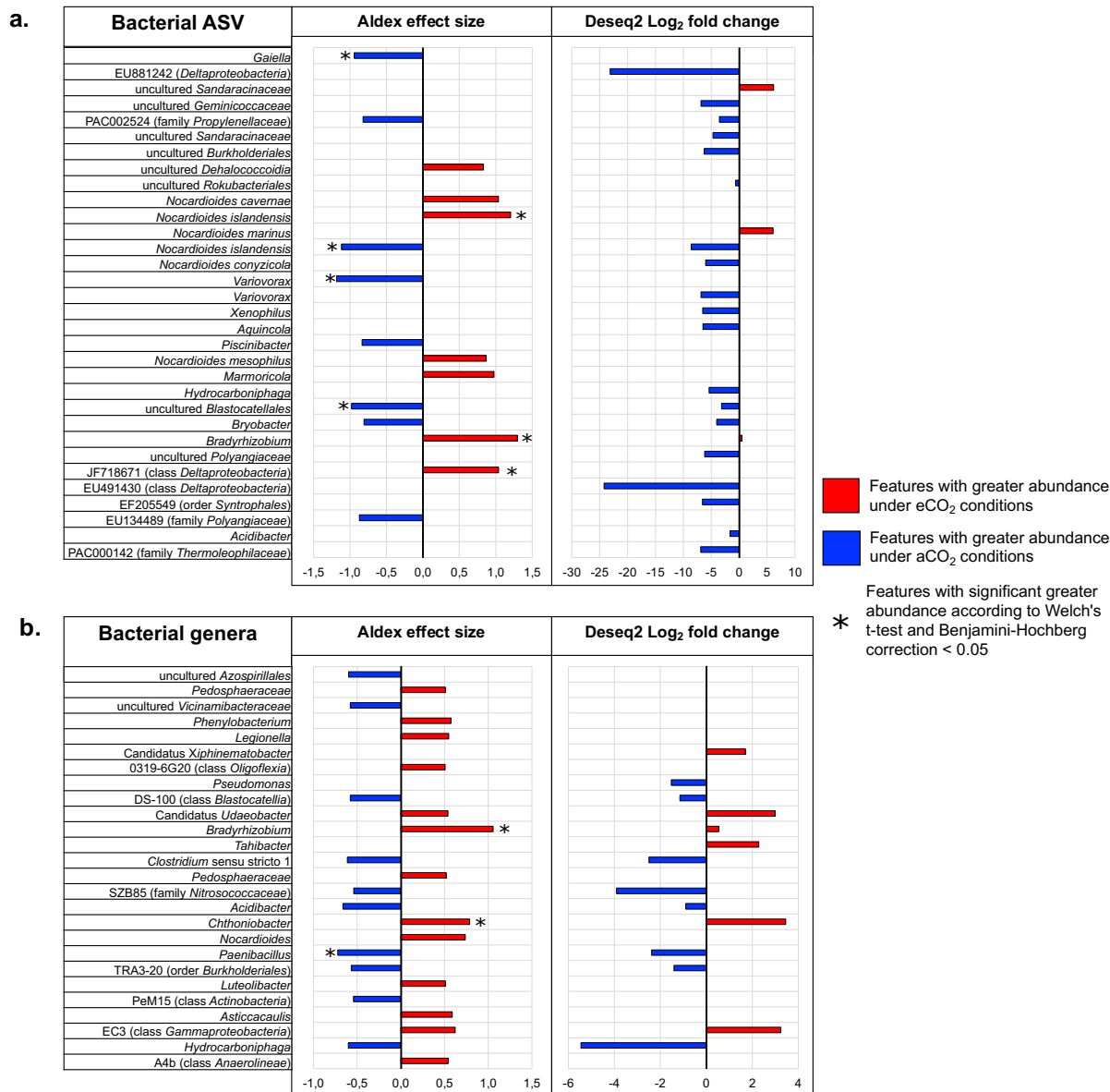


Figure 3. Differential abundances of core microbiome of green inter-rows soil under elevated and ambient CO₂ of **(a)** Bacterial ASVs and **(b)** Bacterial genera. ALDEx2 results of features with an ALDEx effect size > 0.5 using centered log ratio (clr) transformation and the geometric mean abundance of all features.

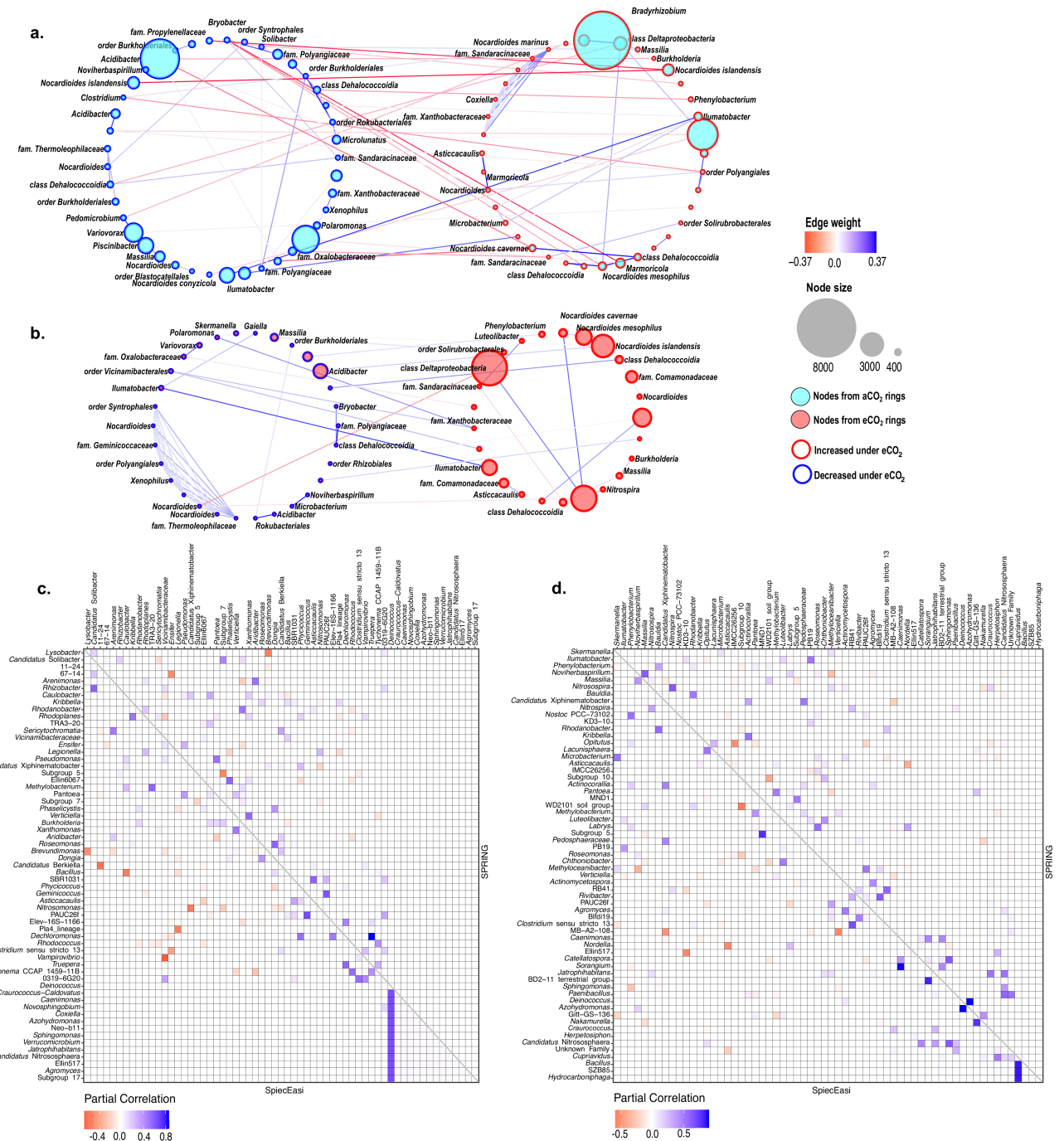


Figure 4. Co-occurrence analysis of features from green inter-rows. **(a)** Network analysis of core ASVs from aCO₂ rings and **(b)** eCO₂ rings. Features with an absolute Aldex effect size > 0.5 were utilized for SpiecEasi analysis applying the Meinshausen & Bühlmann (mb) method with a number of subsamples of 50, n-lambda of 100 and lambda minimum ratio of 0.1; blue and red edges indicate positive and negative co-occurrence respectively; size of the nodes is proportional to the number of ASV reads. Partial correlation analysis of genera with an absolute ALDEx effect size >0.1 from **(c)** aCO₂ and **(d)** eCO₂ green inter-rows using SpiecEasi and SPRING. SpiecEasi run applying the Meinshausen & Bühlmann (mb) method and SPRING with a modified centered log ratio (mclr). Both analyses utilized a number of subsamples of 99, a lambda minimum ratio of 0.1 and the Stability Approach to Regularization Selection (StARS) using co-occurrences with a threshold of <-0.5 and >0.5

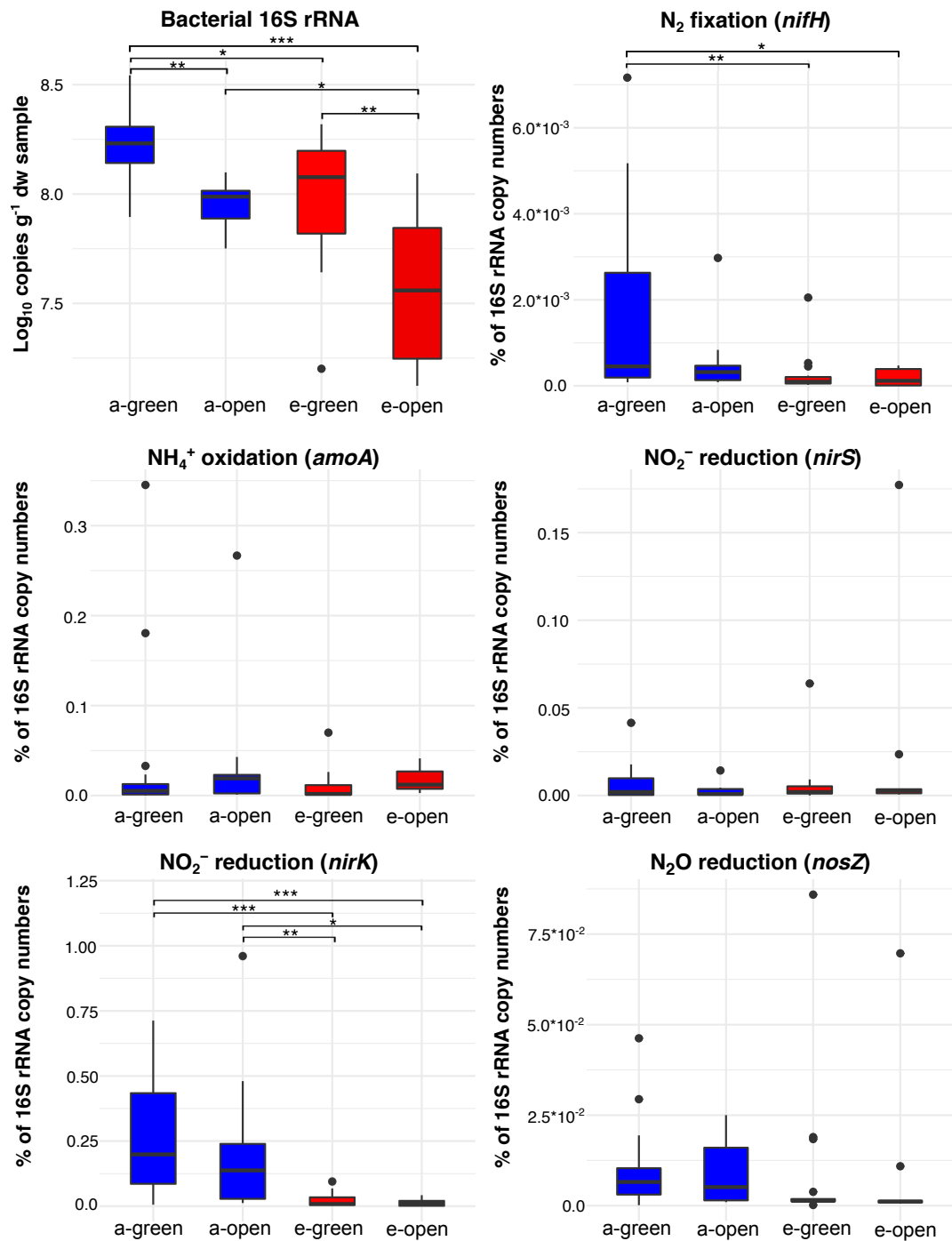


Figure 5. qPCR Boxplots of 16S rRNA, *nifH*, *amoA*, *nirS*, *nirK* and *nosZ* genes from aCO₂ rings green inter-rows (a-green), aCO₂ rings open inter-rows (a-open), eCO₂ rings green inter-rows (e-green), eCO₂ rings open inter-rows (e-open). Significance codes: *** p<0.001, ** p<0.01, * p<0.05.

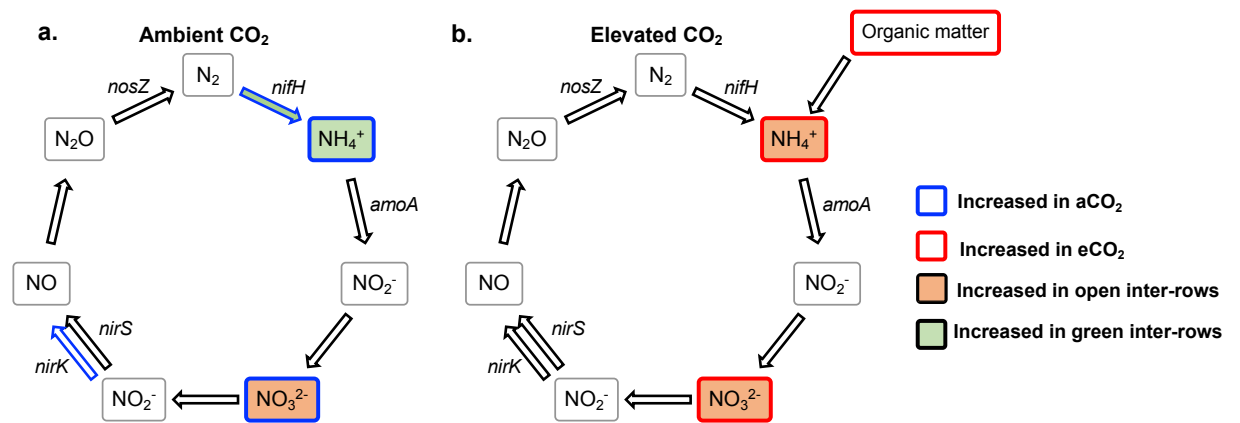


Figure 6. Model diagram of N cycle of Geisenheim Vineyard FACE soil under (a) aCO₂ conditions and (b) eCO₂ conditions.

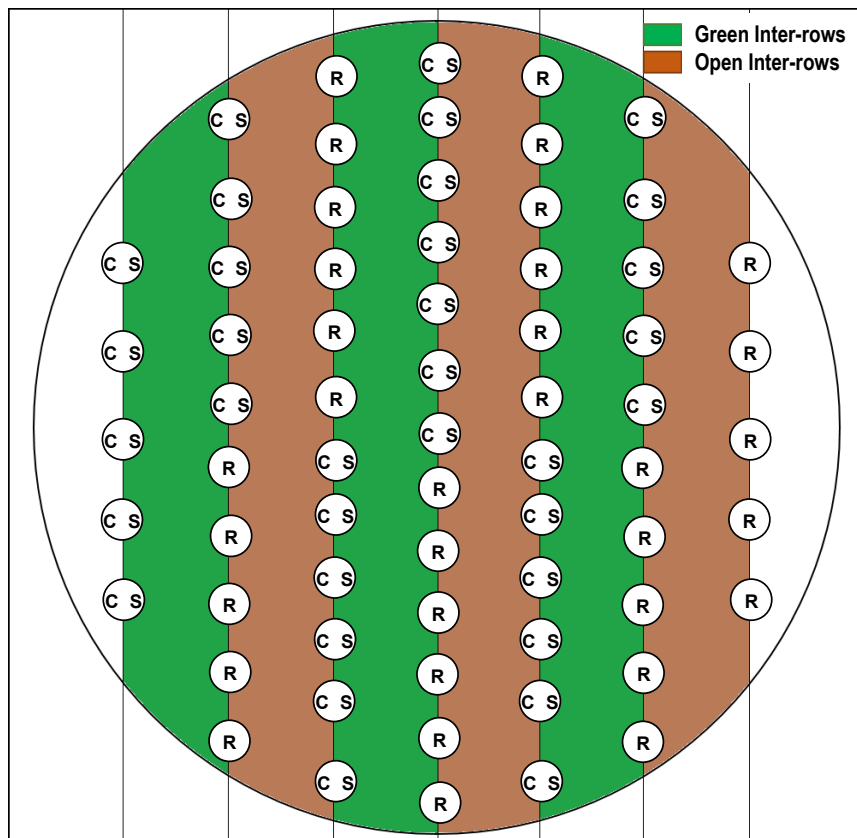


Figure 7. Design of a Vineyard FACE-ring with the two grape varieties Riesling (R) and Cabernet Sauvignon (CS). The vertical lines represent the seven rows per ring of vine plants. Green-colored inter-rows represent the area within the ring with cover crop (green inter-rows) and brown-colored inter-rows represent the areas within the ring where the soil is periodically ploughed (open inter-rows).

Chapter 4 Soil metatranscriptome demonstrates a shift in C, N and S metabolisms of a grassland ecosystem in response to elevated atmospheric CO₂

Research article

To be submitted to Global Change Biology

Chapter 4

Soil metatranscriptome demonstrates a shift in C, N and S metabolisms of a grassland ecosystem in response to elevated atmospheric CO₂

Running Title: Soil metatranscriptome demonstrates a shift in C, N and S metabolisms due to eCO₂

David Rosado-Porto^{1,4}, Stefan Ratering¹, Gerald Moser², Marianna Deppe², Christoph Müller^{2,3}, Sylvia Schnell^{1}*

¹ *Institute of Applied Microbiology, Justus Liebig University, Giessen, DE*

² *Institute of Plant Ecology, Justus Liebig University, Giessen, DE*

³ *School of Biology and Environmental Science and Earth Institute, University College Dublin, Belfield, Dublin, Ireland*

⁴ *Simón Bolívar University, Faculty of Basic and Biomedical Sciences, Barranquilla, Colombia*

**Corresponding author: Prof. Sylvia Schnell, Heinrich-Buff-Ring 26–32, D-35392 Giessen, Germany*

Tel: +49(0)6419937351, Fax: +49(0)6419937359, E-mail: Sylvia.Schnell@umwelt.uni-giessen.de

Abstract

Soil organisms play an important role in the equilibrium and cycling of nutrients. In this sense, because elevated CO_2 (eCO_2) affects plants metabolism including rhizodeposition, it has a direct impact on the soil microbiome and microbial processes. Therefore, eCO_2 influences directly the cycling of different elements in terrestrial ecosystems. Hence, possible changes in the cycles of carbon (C), nitrogen (N) and sulfur (S) were analyzed, alongside with the assessment of changes in the composition and structure of the soil microbiome through a functional metatranscriptomics approach (cDNA from mRNA) from soil samples taken at the Giessen free-air CO_2 enrichment (Gi-FACE) experiment. Results demonstrated changes under eCO_2 in C cycle with augmentation in the uptake and degradation of carbohydrates and amino acids, alongside with the increment of genes for cellulose, chitin and lignin degradation and an increment of prokaryotic carbon fixation. N cycle changes included an impairment of denitrification process, which clarifies the increment of N_2O emissions in the Gi-FACE. Also, occurred a shift in nitrate (NO_3^-) metabolism, with an increment in the dissimilatory NO_3^- reduction to ammonium (NH_4^+) (DNRA) pathway. S metabolism showed an increment in the sulfate (SO_4^{2-}) assimilation under eCO_2 conditions. Furthermore, soil bacteriome, mycobiome and virome were significantly different between ambient and elevated CO_2 conditions. The results obtained in this study demonstrate affectations in the metabolism and cycling of C, N, S and the overall soil microbiome due to eCO_2 , with a direct impact in the emission of greenhouse gases and availability of soil nutrients for the balance of soil ecosystems.

Keywords: functional metatranscriptomics, carbon cycle, nitrogen cycle, sulfur cycle, soil microbiome

Introduction

World atmospheric carbon dioxide (CO_2) has increased by more than 40%, from a pre-industrial level of about 280 parts per million volume (ppmV) to the current concentration of more than 400 ppmV (DOE.2020, 2020), and the current anthropogenic emissions of the greenhouse gases (GHG) are the highest in history (IPCC, 2014). Because terrestrial ecosystems act as a “sink” for a significant portion of global carbon (C), fluctuations in net C exchange between soil and atmosphere impact the CO_2 concentration in the atmosphere profoundly (DOE.2020, 2020). Hence, the response of terrestrial

ecosystems to increasingly higher concentrations of CO₂ under a changing climate has important implications for the global carbon cycle. (Vestergard et al., 2016). In this sense, it has been widely described that elevated CO₂ (eCO₂) concentration affects plants in such a way that decreases evapotranspiration (Kimball, 2016; Owensby et al., 1997), and increases growth (P. He et al., 1995; Idso, 1994), plant yield (Kimball, 1983), photosynthetic capacity (Habash et al., 1995; P. He et al., 1995; Johnson & Pregitzer, 2007), below-ground biomass (Jongen et al., 1995) and the efflux amounts of root exudates (Dong et al., 2021; Jia et al., 2014; Phillips et al., 2012).

Consequently, the supply of fresh plant derived C into the soil matrix due to eCO₂ may accelerate the decomposition of soil organic matter (SOM) and decrease soil C stocks (Blagodatskaya & Kuzyakov, 2008; Fontaine et al., 2004); a process known as “the priming effect”. This alteration of increased decomposition of SOM has been previously reported in different ecosystems as grasslands (Liu et al., 2017; Vestergard et al., 2016), forests (Liu et al., 2017; Phillips et al., 2012; Qiao et al., 2014) and crop fields (Trivedi et al., 2016). Thus, due to the fact that old SOM pools contain significant physically and chemically protected N stocks, the priming effect is a response to the labile C supply by which microorganisms gain access to a reservoir of N to meet their enhanced N demand under conditions of plenty C supply (Derrien et al., 2014; Liu et al., 2017; Vestergard et al., 2016), causing alterations of soil N balance and N cycle. The aforementioned has been described by Müller et al. (2009), who reported that under eCO₂ mineralization of labile organic N became more important. Also occurs an increment in the dissimilatory NO₃⁻ reduction to NH₄⁺ (DNRA) and in the immobilization of NH₄⁺ and NO₃⁻ (Müller et al., 2009). Other alterations in N cycle due to eCO₂ have been described by Kammann et al. (2008), who indicated an increment of N₂O (a potent greenhouse gas) emissions. Likewise, Moser et al. (2018) reported that, N₂O emissions were 1.79-fold higher, and that the linear interpolations showed a 2.09-fold, 1.64-fold and 1.66-fold increase in N₂O emissions from denitrification, nitrification and heterotrophic nitrification respectively. As outcome, these alterations induce significant changes in soil biogeochemical characteristics, such as NO₃⁻, available K⁺, soil microbial biomass carbon (SMBC) and available PO₄²⁻ (Yu et al., 2016).

Likewise, changes in C and N cycles are directly related to the soil microbiome and soil microbial processes, as it has been described by Xu et al. (2013) regarding the abundance of genes involved in labile C degradation and C and N fixation and denitrification processes, which were significantly increased under eCO₂. Similarly, He et al. (2014) and Xiong et al. (2015) have reported a shift of soil microbial communities

under eCO₂ in a soybean and a maize agro-ecosystems, respectively, which included stimulation of key functional genes involved in carbon fixation and degradation, nitrogen fixation, denitrification, methane metabolism and phosphorus cycling. Simonin et al. (2015) reported that shoot biomass, root biomass, and soil respiration were increased under eCO₂ and N supply, and these variables were positively correlated with ammonia-oxidizing bacteria abundance. Le Roux et al. (2016) described that potential nitrite oxidation rate was enhanced in soil by eCO₂. Furthermore, the increase of soil microbial C and N cycling may be accompanied by microbial sulfur (S) and phosphorus (P) demand (Xiong et al., 2015; Yu et al., 2021; Yu et al., 2018). Regarding S cycle alterations under eCO₂ it has been reported by Yu et al. (2021; 2018; 2018), that an increase of S cycling occurs in semiarid grassland soils exposed to eCO₂, indicating too a significant increase in the abundance of *dsrA*, *dsrB* and *sox* genes. Likewise, Padhy et al. (2020), described that several genera as *Desulfatibacillum*, *Desulfotomaculum*, *Desulfococcus*, and *Desulfitobacterium* were more abundant under eCO₂ conditions in a lowland rice field and that several enzymes involved in S assimilation pathways showed higher counts.

Nonetheless, all the aforementioned studies utilized a DNA based approach to assess the changes of C, N and S cycle genes and the microbiome composition under eCO₂ conditions which could lead to biases because DNA from dead cells or free DNA represented a large fraction of microbial DNA in many soils (Carini et al., 2016), which can remain in soils for weeks to years and may opaque DNA-based assessments of microbiome analyses (Dlott et al., 2015; Morrissey et al., 2015). Therefore, the use of RNA instead of DNA for metagenomic studies provides an ideal tool to study the microbial populations that actively participate in various ecological processes (Sharma & Sharma, 2018). In this sense, some studies done in Giessen free-air CO₂ enrichment (FACE) experiment (Gi-FACE) experiment in Giessen Germany, have addressed this issue by performing microbiome metatranscriptomics analyses with rRNA and mRNA, finding that eCO₂ had significant effects on the functional expression associated to both rhizosphere microbiomes and plant roots; and that the structure and composition of the rhizosphere soil microbiome was the most affected by eCO₂ (Bei et al., 2019; Rosado-Porto et al., 2021). These reports demonstrated that through the use of RNA instead of DNA it was possible to assess the effects of eCO₂ on the soil microbiome in the Gi-FACE, contrary to the previous studies which reported little or no effect of it (Brenzinger et al., 2017; de Menezes et al., 2016; Regan et al., 2011).

Nevertheless, in the current literature it has not been described the use of mRNA metatranscriptomics to assess the effects of eCO₂ conditions on C, N and S cycle processes. mRNA metatranscriptomics allows to elucidate accurately which genes are transcribed and to what extent, thereby enabling to demonstrate the functions from a potential range of microorganisms (Franzosa et al., 2014). From such functional data, active metabolic pathways can be identified in the microbiome and can be associated to particular environmental conditions, offering a more informative perspective as it can reveal details about populations that are transcriptionally active (Bashiardes et al., 2016). Therefore, for the aforementioned reasons, the aims of the present study were: i) to assess the effect of long-term eCO₂ concentrations on active soil bacteriome, mycobiome, protistome and virome through an mRNA-based metabarcoding approach; ii) to evaluate the influence of eCO₂ on C, N and S cycle expressed genes in a grassland ecosystem; and iii) to propose an interaction model of C, N and S cycle processes under eCO₂ conditions.

Methods

Study site description

The Gi-FACE study is located at 50°32'N and 8°41.3'E near Giessen, Germany, at an elevation of 172 m above sea level. It consists of three pairs of rings with a diameter of 8 m; each pair consists of an ambient and an elevated CO₂ treatment ring (Jäger et al., 2003). Since May 1998 until present, elevated CO₂ rings have been continuously enriched by 20% above ambient CO₂ concentrations during daylight hours. Ambient and elevated CO₂ rings are separated by at least 20 m, and each pair is placed at the vertices of an equilateral triangle. The presence of a slight slope within the experimental site (between 0.5 and 3.5°) place the rings on a moisture gradient, such that pair 1 has the lowest mean moisture content (38.8% ± 10.2%) and pair 2 has the highest mean moisture content (46.1% ± 13.2%), whereas pair 3 is intermediate (40.7% ± 11%) (de Menezes et al., 2016; Jäger et al., 2003). The average annual air temperature and precipitation are 9.4 °C and 580 mm, respectively.

The vegetation is an *Arrhenatheretum elatioris* Br.Bl. *Filipendula ulmaria* subcommunity, dominated by *Arrhenatherum elatius*, *Galium album* and *Geranium pratense*. At least 12 grass species, 15 non-leguminous herbs and up to 5 legumes with small biomass contributions (<5%) are present within a single plot (Andresen et al., 2018). The experimental field has not been ploughed for more than 100 years. It has received N

fertilization in form of granular mineral calcium-ammonium-nitrate (40 kg N ha⁻¹ year⁻¹) once a year since 1995 and has been mown twice a year since 1993. The soil at the Gi-FACE site is classified as Fluvisol; its texture is a sandy clay loam over a clay layer, with pH= 6.2 and average C and N contents of 4.5% and 0.45%, respectively, as measured in 2001 (Jäger et al., 2003).

Soil sampling, total RNA extraction and ribodepletion

Soil sampling was performed utilizing sawed off 50 ml syringes (11 x 3 cm) and four samples were taken to a depth of ~10 cm within each ring in September 2017. Soil cores were gently shaken by hand to remove loosely attached soil (bulk soil), while the soil that remained attached to the roots was considered as rhizosphere soil. Bulk and rhizosphere soils were sieved (<2 mm) and stored at -80 °C for further analyses.

Total RNA extraction was performed following a modified protocol of Mettel et al. (2010), as described by Rosado-Porto et al. (2021). After extraction, samples were treated for DNA digestion with RNase-Free DNase Set (QIAGEN GmbH - Germany) according to manufacturer instructions; DNase reaction was stopped with 10 µl of 50 mM EDTA. With the DNA-free RNA, a PCR was carried out, using the universal 16S rRNA gene primers 27F (5'-AGAGTTTGATCMTGGATCMTGGCTCAG-3') and 1492R (5'-GGTACCTTGTACGACTT-3') (Lane, 1991; Weisburg et al., 1991) and checked on agarose gel electrophoresis to verify the absence of remaining DNA in the samples. Afterwards, total RNA technical replicates were pooled into a composite sample according to the ring and the soil type they belong to. Afterwards, total RNA samples were ribodepleted using the MICROBExpress™ Kit (Life Technologies, 5791, Carlsbad – California, USA), following manufacturer instructions. Obtained mRNA was reverse transcribed to produce double stranded cDNA.

cDNA Sequencing and metatranscriptomics analysis

cDNA products were sequenced with Illumina MiSeq V3 (2 x 300 bp) - 40 M read pairs / 12 Gb of raw data (LGC Genomics GmbH, Berlin, Germany). After sequenced, all libraries for each sequencing lane were demultiplexed using the Illumina bcl2fastq 2.17.1.14 software (Illumina, 2019), allowing 1 or 2 mismatches in the barcode read when the barcode distances between all libraries on the lane allowed for it. Later, sequencing adapter remnants were removed and reads with final length < 100 bases were discarded. Afterwards, The sequencing outputs were analyzed using SqueezeMeta

version 1.3.1 (Tamames & Puente-Sánchez, 2019). Sequences assembly was performed using Megahit (Li et al., 2015) and the removal of short contigs (<200 bps) was done with Prinseq (Schmieder & Edwards, 2011). Afterwards, RNAs, tRNA/tmRNA and open reading frames (ORFs) were predicted using Barrnap (Seemann, 2014), Aragorn (Laslett & Canback, 2004) and Prodigal (Hyatt et al., 2010) respectively. Subsequently, it was utilized Diamond (Buchfink et al., 2015) to perform the search of similarities in GenBank (Clark et al., 2016), eggNOG (Huerta-Cepas et al., 2016), Kyoto Encyclopedia of Genes and Genomes (KEGG) (Kanehisa & Goto, 2000) databases. Additionally, HMM homology searches were done by HMMER3 (Eddy, 2009) for the Pfam database (Finn et al., 2016). Moreover, additional ORFs were obtained by Diamond BlastX (Buchfink et al., 2015). The read mapping against contigs was performed using Bowtie2 (Langmead & Salzberg, 2012) and the binning was done utilizing MaxBin2 (Wu et al., 2016) and Metabat2 (Kang et al., 2019), later bin statistics were computed using CheckM (Parks et al., 2015).

Diversity and differential abundance analyses

For the analysis of SqueezeMeta output, data were imported into R studio software 1.1.419 with package SQMtools version 0.6.1. (Puente-Sánchez et al., 2020). For diversity assessment of bacteria, archaea, fungi, viruses and protist frequency tables were created and analyzed with package Phyloseq 1.28.0 (McMurdie & Holmes, 2013). Core features for each of the aforementioned taxonomical groups were calculated for eCO₂ and aCO₂ conditions by transforming the frequency table counts to relative abundance with Microbiome package version 1.8.0 (Lahti & Shetty, 2019). Later, features with a total relative abundance $\geq 10 \times 10^{-4}$ % and present in $\geq 95\%$ of samples were included as part of the core. Likewise, for KEGG and GenBank Clusters of Orthologous Groups (COG) protein outputs, features with unknown function or unassigned name were removed from the frequency tables and core features were calculated as described above.

For beta diversity analysis, core datasets were transformed using centered log ratio (clr) method (Aitchison, 1982, 1986), using R package ALDEx2 1.22.0 (Fernandes et al., 2013). Afterwards, community dissimilarity distance matrices were generated using the Aitchison distance (Aitchison, 1982, 1986) and visualized using principal components analysis (PCA) (Jolliffe & Cadima, 2016). Similarly, beta diversity assessment and the identification of features that contributed the most to the clustering of samples was performed with DEICODE (Martino et al., 2019). Core features were transformed with a

robust centered log ratio (rclr) method, organized with robust principal-component analysis (RPCA) and visualized with EMPeror (Vázquez-Baeza et al., 2013). Statistical differences between CO₂ conditions, were assessed by a Permutational Multivariate Analysis of Variance using Adonis method and employing 999 permutations (Anderson, 2001).

Differential abundance analysis of core features was done with R package ALDEx2 1.22.0 (Fernandes et al., 2013) by performing a centered log ratio (clr) transformation using as denominator the geometric mean abundance of all features and 128 Monte-Carlo instance. Subsequently, features with absolute ALDEx effect sizes of >0.8, >0.5 and >0.2 were considered to have a significantly greater, moderate and slightly higher abundance respectively between aCO₂ and eCO₂ rings (Sawilowsky, 2009).

Pathway reconstruction analysis

Pathway prediction for KEGG (Kanehisa & Goto, 2000) and MetaCyc (Caspi et al., 2018) databases was done using MinPath (Ye & Doak, 2009). Pathways reconstruction and assessment of the Log₂ fold change between aCO₂ and eCO₂ rings was performed with SQMtools version 0.6.1. (Puente-Sánchez et al., 2020) and its function “exportPathway” and analyzing feature frequencies as relative abundances.

Results

Sequencing and assembly

In total 23,970,892,090 bases were obtained, comprised in 90,534,066 raw sequences, from which 72,253,754 sequences were mapped and assembled with Megahit, ranging the percentage of sequences successfully mapped per sample between 81.14% and 78.12%. A total of 1,396,973,823 bases from the mapped sequences were retained after short contigs were removed and assembled into 3,997,902 contigs with lengths ranging from 9714 to 200 bases. From the obtained contigs, there were predicted 4,063,836 ORFs, 1,199,550 rRNAs and 2,406 tRNAs/tmRNAs, which subsequently were annotated, producing 92,698 successfully annotated taxa and 483,556 and 1,163,975 KEGG and COG annotations respectively.

Beta diversity and microbe differential abundance

Metatranscriptome results from the Giessen FACE demonstrated changes in the composition and structure of soil microbial communities due to elevated concentrations of atmospheric CO₂. Our data indicated that the soil core bacteriome, mycobiome and virome were the most affected by eCO₂ concentrations, having significantly different compositions between aCO₂ and eCO₂ rings, according to the permutational multivariate analysis of variance using Adonis method (Fig. 1a-c). On the contrary the general structure of the Giessen FACE soil core archaeome and protistome were not significantly affected by eCO₂ (Fig. 1d-e).

Moreover, RPCA output from DEICODE and differential abundance results from ALDEx2 indicated that several taxa were significantly increased or decreased under eCO₂ conditions and that these affected taxa shaped the soil microbiome of the Giessen FACE. Our data showed that the Giessen FACE bacteriome was highly influenced by taxa which were significantly diminished under eCO₂ as is the case of *Alcaligenaceae* bacterium, *Nocardioides oleivorans*, *Patulibacter* sp. and *Geminicoccus roseus* (Fig. 1j, 2a). Moreover, differential abundance results demonstrated that the number of bacterial taxa that were positively stimulated under eCO₂ is greater than the number of taxa which were negatively affected. Among the bacterial taxa which were highly stimulated under eCO₂ conditions are *Flavobacterium*, *Ruminiclostridium*, *Gemmata*, *Dehalococcoides*, *Minicystis*, *Ureaplasma*, *Saccharopolyspora*, *Asaia*, *Nocardioides*, *Defluviimonas*, *Bacillus*, *Nannocystis*, *Glaesserella*, *Pedosphaera*, *Arenimonas*, *Nitrospirae* bacterium, *Blastopirellula*, *Amycolatopsis*, *Tatlockia*, *Povalibacte*, *Thermasporomyces*, *Halolactibacillus*, *Clostridium*, *Pedobacter*, *Aminipila*, *Rhodovastum*, *Pirellula* and *Burkholderia*, which showed ALDEx effect sizes between 1.5 and 0.8 (Fig. 2a, S1).

Likewise, soil mycobiome was shaped by several fungi greatly affected under eCO₂ conditions, most of them belonging to phyla *Basidiomycota*, *Mucoromycota* and *Ascomycota*, as is the case of genus *Aspergillus* (phylum *Ascomycota*), which presented an ALDEx effect size of 1.15 (Fig. 1l, 2b, S1). Additionally, fungi as *Rhizopus*, *Cadophora*, *Gigaspora*, *Histoplasma* and *Aplosporella* were also highly stimulated in eCO₂ rings. Regarding the Giessen FACE soil virome, viruses as Brome mosaic virus, *Panicovirus* and Cocksfoot mild mosaic virus presented a decreased in eCO₂ rings, whereas viruses as *Penicillium discovirus*, unclassified *Picornavirales*, unclassified *Endornaviridae* were positively affected under eCO₂ conditions (Fig. 1k, 2d, S1), and the changes in these viral taxa has had the strongest influence on the Giessen FACE soil virome. Moreover, some viral features belonging to the families *Leviridae*, *Siphoviridae*, *Bromoviridae* and *Dicistroviridae* were affected by eCO₂ as well.

Although, our data did not show that the general structure of the soil archaeome and protistome was significantly influenced by eCO₂, the differential abundance test demonstrated that some archaea and protist taxa were either positive or negative affected under eCO₂ conditions (Fig. 1e, 2c, 2e, S1).

Functional metatranscriptome and differential abundance

Beta diversity analysis of expressed genes mapped against GenBank COG and KEGG databases, exhibited that the functional metatranscriptome was greatly affected under eCO₂ conditions in which the annotations performed to both databases were significantly different in its structure and composition between eCO₂ and aCO₂ conditions (Fig. 1g-h). After the removal from the core of unclassified and non-characterized proteins mapped against the GenBank COG and KEGG databases, 7780 remained for GenBank COG and 8880 for KEGG datasets. Furthermore, our data indicated that the sequences mapped against both databases showed similar results regarding the number of proteins which presented an absolute ALDEx effect size greater than 0.5. In the case of GenBank COG data, 146 features were moderately or greatly stimulated under eCO₂ conditions, in contrast with 161 features which were negatively affected under these conditions. Similarly, KEGG results showed that 147 and 156 mapped proteins were positively and negatively affected, respectively (S2).

Moreover, several COG categories were positively influenced under eCO₂ conditions as is the case of categories for energy production and conversion; inorganic ion transport and metabolism; cell envelope biogenesis, outer membrane; intracellular trafficking; carbohydrate transport and metabolism; and signal transduction mechanisms (Fig. 3, S2). Oppositely, categories for translation, ribosomal structure and biogenesis; transcription; secondary metabolites biosynthesis, transport and catabolism; nucleotide transport and metabolism; DNA replication, recombination and repair; and coenzyme metabolism were negatively affected at eCO₂ concentrations (Fig. 3, S2).

Nitrogen cycle

Concerning N metabolism, the obtained data showed that under eCO₂ conditions a shift in the metabolism of nitrate (NO₃⁻) occurred which involved an increase of the dissimilatory NO₃⁻ reduction to ammonium (NH₄⁺) (DNRA) pathway and a decrease of the assimilatory one (Fig. 4a). In which the expression of the genes for the DNRA enzymes nitrite reductase (NADH) (NirBD) and nitrate reductase (NarGHI) presented

greater abundances under eCO₂ conditions (Fig. 4a-b). Whereas the mapped enzymes nitrate reductase (NAD(P)H) (NR), ferredoxin-nitrite reductase (NirA) and assimilatory nitrate reductase (NasAB) were negatively affected at eCO₂ concentrations (Fig. 4a-b, S2). Similarly, our results exhibited that the denitrification process suffered alterations, presenting the mapped enzymes nitrate reductase/nitrite oxidoreductase (NarGHI/NapAB) and nitric oxide reductase (NorBC) higher levels under eCO₂ conditions, with ALDEx effect sizes of 0.44 and 0.641 respectively; being the first one responsible for the transformation of NO₃⁻ to nitrite (NO₂⁻) and the latter one for the reduction of nitric oxide (NO) to nitrous oxide (N₂O). On the contrary the expressed gene that codes for the enzyme nitrous-oxide reductase (NosZ), which catalyzes the transformation of N₂O to atmospheric nitrogen (N₂), was diminished in the eCO₂ rings (Fig. 4a-b, S2). Likewise, the nitrification process underwent through changes, based on the variations of the expression patterns of the enzymes methane/ammonia monooxygenase (AmoCAB) and nitrate reductase/nitrite oxidoreductase (NrxAB), which were negative and positive affected respectively (Fig. 4a-b, S2). Furthermore, pathway reconstruction and differential abundance analyses did not show any significant changes in the abundance of N fixation enzymes under eCO₂ conditions.

Sulfur cycle

Concerning S cycle alterations due to eCO₂ concentrations, the metatranscriptomics results indicated affectations in the dissimilatory and assimilatory pathways of sulfate (SO₄²⁻) reduction. In the case of the dissimilatory pathway, the mapped enzymes sulfate adenylyltransferase (Sat) and adenylylsulfate reductase (AprAB) were highly decreased under eCO₂ conditions, especially the latter one, which presented an ALDEx effect size of -0.857 and catalyzes the transformation of sulfite (SO₃²⁻) to adenosine 5'-phosphosulfate (APS) (Fig. 5a-b). Similarly, the reduction of SO₄²⁻ to APS in the assimilatory pathway was also decreased, due to the depletion of the enzymes sulfate adenylyltransferase subunit 2 (CysND) and sulfate adenylyltransferase (PAPSS), both depleted under eCO₂, with ALDEx effect sizes of -0.581 and -0.409 respectively (Fig. 5a-b, S2). Nonetheless, the enzymes adenylylsulfate kinase (CysC) and sulfite reductase (NADPH) (CysJI), responsible of the reduction of APS to 3'-Phosphoadenosine-5'-phosphosulfate (PAPS), and the reduction of SO₃²⁻ to sulfide (S²⁻) respectively, were increased at eCO₂ concentrations (Fig. 5a-b, S2). Moreover, our data showed that several enzymes belonging to pathways responsible of the transformation of organic S compounds presented higher abundances at eCO₂, as it is the case of dimethylsulfone monooxygenase, thiosulfate dehydrogenase [quinone] and taurine dioxygenase (Fig. 5b,

S2). Additionally, although the SOX system for the oxidation of S was in general not over expressed under eCO₂ concentrations, the enzyme sulfane dehydrogenase subunit (SoxC) presented a slight increment at these conditions, with an ALDEx effect size of 0.279.

Carbon cycle and ABC membrane transporters

Functional metatranscriptome showed changes in the metabolism of C compounds. The main changes comprised a general increment in the glycolytic and pentose phosphate pathways, which included the augmentation of mapped enzymes phosphoglucomutase; glucose-6-phosphate isomerase; phosphoenolpyruvate carboxykinase (ATP); pyruvate, water dikinase; 2-oxoglutarate, gluconate 2-dehydrogenase; gluconolactonase; transketolase and xylulose-5-phosphate/fructose-6-phosphate phosphoketolase, all with ALDEx effect sizes ranging from 0.795 to 0.524 (Fig. 6a). Likewise, the data demonstrated an increase in the expression of the genes which code for enzymes responsible for the degradation of chitin, cellulose and aromatic compounds, as it is the case of alpha-N-arabinofuranosidase; endo-1,4-beta-xylanase and chitinase (Fig. 6a). Oppositely, the metabolism of fatty acid, starch and sucrose seemed to be negatively affected under eCO₂ conditions, with the most affected features having ALDEx effect sizes from -0,839 to -0,509 (Fig. 6a, S2).

Furthermore, our results indicated a stimulation in the metabolism of aromatic, branched chain and sulfur amino acids. In the case of sulfur amino acids metabolism, an augmentation of expressed enzymes for the metabolisms of homocysteine, taurine and thiol groups occurred (S2). Likewise, the degradation of aromatic amino acids and their degradation pathways presented several enzymes highly stimulated as it is the case of the aminocarboxymuconate-semialdehyde decarboxylase; enoyl-CoA hydratase; amidase; monoamine oxidase; acylpyruvate hydrolase and the gentisate 1,2-dioxygenase, which showed ALDEx effect sizes between 1.105 to 0.538. Moreover, the reconstruction of the prokaryotic carbon fixation pathway known as Arnon-Buchanan cycle, denoted its increase at eCO₂ concentrations, involving the rise of key enzymes as phosphoenolpyruvate carboxykinase (ATP); pyruvate ,water dikinase and pyruvate ferredoxin oxidoreductase, among others (Fig. 6a, S2).

Additionally, the metatranscriptomic data on the ABC membrane transport proteins suggested changes in the uptake and transport of different carbon compounds under eCO₂ conditions. In the case of saccharides, there is an increase of the membrane transporters for glucose/mannose, α-glucoside, ribose/D-xylose, chitobiose. Whereas

there is a decrease in the expression of membrane transporters for raffinose/stachyose/melibiose, rhamnose, galactose oligomer/maltoooligosaccharide, maltose and fructose (Fig. 6b, S2). Similarly, a shift in the ABC transporters for amino acids occurred, with an augmentation of the transporters for general L-amino acids and branched chain amino acids and a diminishing of glutamate/aspartate and oligopeptides transporters (Fig. 6b, S2).

Additionally, some other membrane transport proteins which were over expressed under eCO₂ conditions were transporters for microncin C, osmoprotectant, lipopolysaccharide and iron (II) (Fig. 6b, S2).

Discussion

Soil microbiome response to eCO₂

Our results on the functional metatranscriptome of the Giessen FACE confirm previous reports from Bei et al. (2019) and Rosado-Porto et al. (2021) on the changes of microbiome composition and structure due to eCO₂ concentrations. Additionally, expands our understanding of the consequences of the soil biological processes that involved N, S and C cycles and how these are affected under eCO₂ conditions. Regarding the changes in the soil microbiome composition, our data confirm that the structure of Giessen FACE soil bacteriome was heavily influenced under eCO₂ as it has been already portrayed by Bei et al. (2019) and Rosado-Porto et al. (2021), which have described significant changes in the rhizosphere bacteriome due to eCO₂. Additionally, several bacterial taxa which were found in the present study have been already described to be stimulated under eCO₂ conditions, as it is the case of genera *Bacillus*, *Burkholderia*, *Mesorhizobium*, *Streptomyces*, *Dongia* and *Legionella* (Rosado-Porto et al., 2021).

Besides the soil bacteriome, the results showed that the soil mycobiome was greatly affected too at eCO₂ concentrations and similarly to Bei et al. (2019), our data indicated that the Giessen FACE mycobiome was composed mainly by phyla *Basidiomycota*, *Mucoromycota* and *Ascomycota*, being the latter two the ones with the most significantly affected fungal features (S1). Nevertheless, although it was demonstrated a significant effect of eCO₂ concentrations on the mycobiome composition, the reports of its effect on soil fungal communities vary according to different authors. Some studies have described a decrease of the fungi:bacteria ratio under eCO₂ conditions (Bei et al., 2019;

Carney et al., 2007; Cheng et al., 2011) and some others reported no significant change of the fungal communities (Hayden et al., 2012; Z. He et al., 2010), which indicates that the response of fungal communities to eCO₂ depends on other environmental factors and might be ecosystem specific as well.

In the case of soil archaeome and its variations at eCO₂ concentrations, it hasn't been widely studied by metagenomics nor metatranscriptomics methods, nonetheless some reports described a strong influence from CO₂ on soil archaeal communities (Hayden et al., 2012; Lee et al., 2015; Lee & Kang, 2016). Although, the Giessen FACE archaeome did not show significant differences in its structure or composition in response to eCO₂ concentrations, some taxa presented changes in their abundance, various of them belonging to the family *Nitrosopumilaceae* (phylum *Thaumarchaeota*). In addition, in the present study the core archaeome was mainly composed phylum *Euryarchaeota*, contrary to what Bei et al. (2019) described, who reported the phylum *Thaumarchaeota* as the most abundant one.

Furthermore, our data demonstrated that not only the Giessen FACE soil bacteriome and mycobiome were the ones significantly affected under eCO₂ conditions, but the soil core virome responded to it too. So far, in the current literature there are no reports about the effects of eCO₂ on the soil virome. Moreover, it has been indicated that in general the diversity of the soil virome is highly underestimated, with most of the current information focused on bacterial phages and almost nothing is known about viruses that infect nonbacterial soil microbes, such as the archaea, fungi, and soil protozoa (Pratama & van Elsas, 2018; Williamson et al., 2017). Nevertheless, it has been described the entanglement of viral soil communities with the rest of the soil microbiome and its response to biotic and abiotic properties of soil, highlighting the importance of the virome within the whole soil microbiome (Santos-Medellin et al., 2021). Our results on the differential abundance of the core virome under eCO₂ conditions, suggested that several viral features were reacting to changes in bacterial, archaeal and fungal taxa. As it is the case of the augmentation of features from the families *Leviridae* and *Siphoviridae* (S1), which are viruses that use bacteria and archaea as hosts (Krupovic et al., 2020; "Leviridae," 2012; "Siphoviridae," 2012). Similarly, some fungal viruses as *Mitovirus* and *Penicillium discovirus* have suffered significant changes in their abundance under eCO₂ conditions, which might be linked to the changes of some fungal features as *Penicillium oxalicum* and members belonging to the class *Ophiostomatales* (Hong et al., 1999; Krishnamurthy, 2017).

Changes in C compounds assimilation and priming effect

The obtained data demonstrated changes in several mapped enzymes and reconstructed pathways which involved the metabolism of different C compounds, indicating that C dynamics have suffered alterations due to eCO₂. It has been widely described that eCO₂ increases the efflux of soluble sugars, amino acids, phenolic acids, and organic acids in the root exudates (Dong et al., 2021; Jia et al., 2014; Phillips et al., 2012), which produces the so called “priming effect”, that consists in an acceleration in SOC decomposition (Blagodatskaya & Kuzyakov, 2008; Fontaine et al., 2004). Therefore, the functional metatranscriptomic data demonstrated the occurrence of this aforementioned phenomena in the Giessen FACE soil, presented mainly in an overexpression of glycolysis and pentose phosphates pathways for the metabolism of saccharides and an increment in the metabolism of certain amino acids, alongside with an augmentation of enzymes responsible for the degradation of chitin, cellulose and lignin (Fig. 7). Similar results have been reported by He et al. (2010, 2014), Xiong et al. (2015) and Yu et al. (2018; 2018), who described that functional genes for C compounds degradation, either labile or recalcitrant, were stimulated under eCO₂ conditions, and the increment in the degradation of soil organic polymers as part of the decomposition of older soil C (Niklaus & Falloon, 2006; Van Groenigen et al., 2005; Vestergard et al., 2016; Xie et al., 2005).

Furthermore, the data suggest a shift in the uptake and use of C sources at eCO₂ concentrations, reflected in a shift towards a higher utilization of sugars and amino acids and a decrease in the metabolism of lipids, especially fatty acids (Fig. xxx). Additionally, the analysis of ABC membrane transporters revealed changes on the saccharide compounds that are more often used under eCO₂ conditions, indicating a preference for the uptake of glucose, mannose, α -glucosides, ribose, xylose and chitobiose instead of raffinose, stachyose, melibiose, rhamnose, galactose, maltose and fructose (Fig. xxx). Similarly, pathway reconstruction of amino acids metabolism exhibited a shift towards the utilization of aromatic, sulfur and branched chain amino acids over glutamate, aspartate and oligopeptides.

Besides, functional metatranscriptome revealed that prokaryotic carbon fixation was augmented at eCO₂ concentrations, with the increment of different mapped enzymes as phosphoenolpyruvate carboxykinase, pyruvate water dikinase and pyruvate ferredoxin oxidoreductase accompanied by a decrease of the ribulose-bisphosphate carboxylase (Rubisco) enzyme (Fig. xxx). These results are opposite to the ones reported by He et

al. (2010, 2014), Xu et al. (2013), Xiong et al. (2015) and Yu et al. (2018; 2018), in which all of them described a significant increment of the Rubisco enzyme under eCO₂ conditions. The aforementioned suggests that in the Giessen FACE, the C fixation performed by prokaryotes at eCO₂ concentrations is very likely to be done through the reverse Krebs cycle, also known as Arnon-Buchanan cycle, (Buchanan et al., 2017; Buchanan & Arnon, 1990) instead of the Rubisco pathway.

Shift in N cycle processes

Changes in the N cycle and N compounds metabolism have been previously described in the Giessen FACE (Kammann et al., 2008; Moser et al., 2018; Müller et al., 2009), nonetheless the microbiological underlying mechanisms which were driving these processes were not detected until now. The metatranscriptomic results confirmed a switch on the NO₃⁻ reduction at eCO₂ concentrations, from an assimilatory process to a DNRA, reflected by the increment of mapped enzymes nitrite reductase (NADH) (NirBD) and nitrate reductase (NarGHI), responsible for the transformations of NO₃⁻ to NO₂⁻ and from NO₂⁻ to NH₄⁺ in the DNRA process (Fig. 4a-b, 7). The aforementioned was formerly described by Müller et al. (2009), who through a ¹⁵N labelling approach identified an increment in the DNRA and in the immobilization of NH₄⁺ and NO₃⁻.

Additionally, our functional metatranscriptomic approach clarifies the processes leading to the excess on the production of N₂O under eCO₂ conditions previously described by Kammann et al. (2008) and Moser et al. (2018). According to our data, the abovementioned occurred due to an impairment of the denitrification process with an increase in the production of N₂O, because an over expression of the enzyme nitric oxide reductase (NorBC), alongside a decrease in the transformation of N₂O to N₂ due to a under expression of the enzyme nitrous-oxide reductase (NosZ), which denotes that in the Giessen FACE the excess of produced N₂O has not been totally converted to N₂ (Fig. 7).

Moreover, the results also demonstrated changes in the nitrification process, which are represented by a depletion of the conversion of NH₄⁺ to hydroxylamine (H₃NO) performed by the enzyme methane/ammonia monooxygenase (AmoCAB), accompanied by an increment in the expression of the mapped enzyme nitrate reductase/nitrite oxidoreductase (NrxAB), suggesting an augmentation in the transformation of NO₂⁻ to NO₃⁻ and therefore an increment in the overall nitrification process (Fig. 4a-b, 7). Nonetheless, due to the fact that the first nitrification step is under expressed in the eCO₂

rings, denotes that at these conditions soil organisms are obtaining N from other sources instead of NH_4^+ , which could be explained by Müller et al. (2009) results, in which are described that the mineralization of labile organic N became more important at eCO_2 concentrations. These shift in the use of N sources might have occurred as part of the priming effect, due to old SOM pools contain significant physically and chemically protected N stocks, and therefore the priming effect was a response to the increased C supply in the Giessen FACE by which microorganisms gained access to N reservoirs to meet their enhanced N demand (Derrien et al., 2014; Liu et al., 2017; Vestergard et al., 2016). Moreover, because our results did not show under eCO_2 conditions any increment of N fixation enzymes, contrary to what has been described by He et al. (2010, 2014), Xu et al. (2013), Xiong et al. (2015) and Yu et al. (2018; 2018), supports the idea that in the Giessen FACE, the enhanced N requirements are being met through the uptake of organic sources. Which according to our results might have been the aromatic, sulfur and branched chain amino acids, since their metabolism and uptake were augmented at eCO_2 concentrations (Fig. 7).

S metabolism at eCO_2 concentration

Most research about the effects of eCO_2 on the cycling of nutrients have been focused on C and N cycles, nonetheless the effects of eCO_2 conditions have been also assessed for other elements including S (He et al., 2010, 2014; Padhy et al., 2020; Yu et al., 2018), however, until now there were no reports about the changes in the S cycling and metabolism in the Giessen FACE. The results obtained in the present study demonstrated alterations in the metabolism of SO_4^{2-} , which comprised a lessening of the dissimilatory metabolism of SO_4^{2-} reduction, evidenced by the decrease in the expression of the enzymes sulfate adenylyltransferase (Sat) and adenylylsulfate reductase (AprAB) under eCO_2 conditions (Fig. 5, 7). Similarly, the assimilatory SO_4^{2-} reduction metabolism suffered changes due to eCO_2 , in which the first step that involves the reduction of SO_4^{2-} to APS and is catalyzed by the enzymes sulfate adenylyltransferase subunit 2 (CysND), sulfate adenylyltransferase (PAPSS) and sulfate adenylyltransferase (Sat) presented some degree of depletion. However, the other steps of this pathway, from the reduction of APS up to the production of S^{2-} , were increased under eCO_2 conditions (Fig. 5). This phenomenon could indicate that similarly to N metabolism, due to the augmented C supply, S has become too a limiting element for the development of soil organisms, thus the assimilatory metabolism of S was enhanced at eCO_2 concentrations as a response of this environmental pressure. Although, there are not many reports about the effect of eCO_2 on the S cycle, it has been described by Yu et al. (2018) that under eCO_2 an

increase of S cycling occurred and similar to our data Padhy et al. (2020) reported an increment in the assimilatory metabolism of S under eCO₂ conditions. Moreover, these data also suggested that the obtention of S in the Giessen FACE is not coming from inorganic sources but from organic ones, very likely as consequence of the priming effect and the mining of S from the SOM. One of these sources for the supply of S according to our data, might be sulfur amino acids and molecules with thiol groups, due to the metabolism of these compounds was augmented under eCO₂ conditions (Fig. 5b, 7). Moreover, although our data did not show an overall increment of the SOX system for the obtention of sulfur, it a slight augmentation of the enzyme sulfane dehydrogenase (SoxC) occurred. Which could confirm that in the Giessen FACE, soil organisms have been used organic molecules to supply the S requirements because of eCO₂ concentrations, similar results have been described by He et al. (2014), who reported an increment of sox genes under eCO₂ conditions.

References

- Aitchison, J. (1982). The Statistical Analysis of Compositional Data. *Journal Of the Royal Statistical Society. Series B (Methodological)*, 44(2), 139–177. <https://doi.org/10.1007/978-94-009-4109-0>
- Aitchison, J. (1986). Book review. In *The Statistical Analysis of Compositional Data* (XII). Chapman and Hall. <https://doi.org/10.1007/bf01187862>
- Anderson, M. J. (2001). A new method for non parametric multivariate analysis of variance. *Austral Ecology*, 26, 32–46. <https://doi.org/10.1111/j.1442-9993.2001.01070.pp.x>
- Andresen, L. C., Yuan, N., Seibert, R., Moser, G., Kammann, C. I., Luterbacher, J., Erbs, M., & Müller, C. (2018). Biomass responses in a temperate European grassland through 17 years of elevated CO₂. *Global Change Biology*, 24, 3875–3885. <https://doi.org/10.1111/gcb.13705>
- Bashiardes, S., Zilberman-Schapira, G., & Elinav, E. (2016). Use of metatranscriptomics in microbiome research. *Bioinformatics and Biology Insights*, 10, 19–25. <https://doi.org/10.4137/BBI.S34610>
- Bei, Q., Moser, G., Wu, X., Müller, C., & Liesack, W. (2019). Metatranscriptomics reveals climate change effects on the rhizosphere microbiomes in European grassland. *Soil Biology and Biochemistry*, 138(July), 1–10. <https://doi.org/10.1016/j.soilbio.2019.107604>
- Blagodatskaya, E., & Kuzyakov, Y. (2008). Mechanisms of real and apparent priming effects and their dependence on soil microbial biomass and community structure:

- Critical review. *Biology and Fertility of Soils*, 45(2), 115–131. <https://doi.org/10.1007/s00374-008-0334-y>
- Brenzinger, K., Kujala, K., Horn, M. A., Moser, G., Guillet, C., Kammann, C., Müller, C., & Braker, G. (2017). Soil conditions rather than long-term exposure to elevated CO₂ affect soil microbial communities associated with N-cycling. *Frontiers in Microbiology*, 8, 1–14. <https://doi.org/10.3389/fmicb.2017.01976>
- Buchanan, B. B., & Arnon, D. I. (1990). A reverse KREBS cycle in photosynthesis: consensus at last. *Photosynthesis Research*, 24(1), 47–53. <https://doi.org/10.1007/BF00032643>
- Buchanan, B. B., Sirevåg, R., Fuchs, G., Ivanovsky, R. N., Igarashi, Y., Ishii, M., Tabita, F. R., & Berg, I. A. (2017). The Arnon–Buchanan cycle: a retrospective, 1966–2016. *Photosynthesis Research*, 134(2), 117–131. <https://doi.org/10.1007/s11120-017-0429-0>
- Buchfink, B., Xie, C., & Huson, D. H. (2015). Fast and sensitive protein alignment using DIAMOND. *Nature Methods*, 12(1), 59–60. <https://doi.org/10.1038/nmeth.3176>
- Carini, P., Marsden, P. J., Leff, J. W., Morgan, E. E., Strickland, M. S., & Fierer, N. (2016). Relic DNA is abundant in soil and obscures estimates of soil microbial diversity. *Nature Microbiology*, 2(0), 1–6. <https://doi.org/10.1038/nmicrobiol.2016.242>
- Carney, K. M., Hungate, B. A., Drake, B. G., & Megonigal, J. P. (2007). Altered soil microbial community at elevated CO₂ leads to loss of soil carbon. *Proceedings of the National Academy of Sciences of the United States of America*, 104(12), 4990–4995. <https://doi.org/10.1073/pnas.0610045104>
- Caspi, R., Billington, R., Fulcher, C. A., Keseler, I. M., Kothari, A., Krummenacker, M., Latendresse, M., Midford, P. E., Ong, Q., Ong, W. K., Paley, S., Subhraveti, P., & Karp, P. D. (2018). The MetaCyc database of metabolic pathways and enzymes. *Nucleic Acids Research*, 46(D1), D633–D639. <https://doi.org/10.1093/nar/gkx935>
- Cheng, L., Booker, F. L., Burkey, K. O., Tu, C., da Shew, H. D., Ruffy, T. W., Fiscus, E. L., Deforest, J. L., & Hu, S. (2011). Soil microbial responses to elevated CO₂ and O₃ in a nitrogen-aggrading agroecosystem. *PLoS ONE*, 6(6), e21377. <https://doi.org/10.1371/journal.pone.0021377>
- Clark, K., Karsch-Mizrachi, I., Lipman, D. J., Ostell, J., & Sayers, E. W. (2016). GenBank. *Nucleic Acids Research*, 44, D67–D72. <https://doi.org/10.1093/nar/gkv1276>
- de Menezes, A. B., Müller, C., Clipson, N., & Doyle, E. (2016). The soil microbiome at the Gi-FACE experiment responds to a moisture gradient but not to CO₂ enrichment. *Microbiology*, 162, 1572–1582. <https://doi.org/10.1099/mic.0.000341>
- Derrien, D., Plain, C., Courty, P. E., Gelhaye, L., Moerdijk-Poortvliet, T. C. W., Thomas, F., Versini, A., Zeller, B., Koutika, L. S., Boschker, H. T. S., & Epron, D. (2014).

- Does the addition of labile substrate destabilise old soil organic matter? *Soil Biology and Biochemistry*, 76, 149–160. <https://doi.org/10.1016/j.soilbio.2014.04.030>
- Diott, G., Maul, J. E., Buyer, J., & Yarwood, S. (2015). Microbial rRNA: RDNA gene ratios may be unexpectedly low due to extracellular DNA preservation in soils. *Journal of Microbiological Methods*, 115, 112–120. <https://doi.org/10.1016/j.mimet.2015.05.027>
- DOE.2020, U. S. (2020). *U.S. Department of Energy Free-Air CO₂ Enrichment Experiments: FACE Results, Lessons, and Legacy*. <https://doi.org/10.2172/1615612>
- Dong, J., Hunt, J., Delhaize, E., Zheng, S. J., Jin, C. W., & Tang, C. (2021). Impacts of elevated CO₂ on plant resistance to nutrient deficiency and toxic ions via root exudates: A review. *Science of the Total Environment*, 754, 142434. <https://doi.org/10.1016/j.scitotenv.2020.142434>
- Eddy, S. R. (2009). a New Generation of Homology Search Tools Based on Probabilistic Inference. *Genome Informatics*, 23(1), 205–211.
- Fernandes, A. D., Macklaim, J. M., Linn, T. G., Reid, G., & Gloor, G. B. (2013). ANOVA-Like Differential Expression (ALDEx) Analysis for Mixed Population RNA-Seq. *PLoS ONE*, 8(7), e67019. <https://doi.org/10.1371/journal.pone.0067019>
- Finn, R. D., Coghill, P., Eberhardt, R. Y., Eddy, S. R., Mistry, J., Mitchell, A. L., Potter, S. C., Punta, M., Qureshi, M., Sangrador-Vegas, A., Salazar, G. A., Tate, J., & Bateman, A. (2016). The Pfam protein families database: Towards a more sustainable future. *Nucleic Acids Research*, 44(D1), D279–D285. <https://doi.org/10.1093/nar/gkv1344>
- Fontaine, S., Bardoux, G., Abbadie, L., & Mariotti, A. (2004). Carbon input to soil may decrease soil carbon content. *Ecology Letters*, 7(4), 314–320. <https://doi.org/10.1111/j.1461-0248.2004.00579.x>
- Franzosa, E. A., Morgan, X. C., Segata, N., Waldron, L., Reyes, J., Earl, A. M., Giannoukos, G., Boylan, M. R., Ciulla, D., Gevers, D., Izard, J., Garrett, W. S., Chan, A. T., & Huttenhower, C. (2014). Relating the metatranscriptome and metagenome of the human gut. *Proceedings of the National Academy of Sciences of the United States of America*, 111(22). <https://doi.org/10.1073/pnas.1319284111>
- Habash, D. Z., Paul, M. J., Parry, M. A. J., Keys, A. J., & Lawlor, D. W. (1995). Increased capacity for photosynthesis in wheat grown at elevated CO₂ - the relationship between electron transport and carbon metabolism. *Planta*, 197(3), 482–489. <https://doi.org/10.1007/BF00196670>
- Hayden, H. L., Mele, P. M., Bougoure, D. S., Allan, C. Y., Norng, S., Piceno, Y. M., Brodie, E. L., Desantis, T. Z., Andersen, G. L., Williams, A. L., & Hovenden, M. J.

- (2012). Changes in the microbial community structure of bacteria, archaea and fungi in response to elevated CO₂ and warming in an Australian native grassland soil. *Environmental Microbiology*, 14(12), 3081–3096.
<https://doi.org/10.1111/j.1462-2920.2012.02855.x>
- He, P., Bader, K. P., Radunz, A., & Schmid, G. H. (1995). Consequences of high CO₂-concentrations in air on growth and gas-exchange rates in Tobacco mutants. *Zeitschrift Für Naturforschung*, 50c(11/12), 781–788.
- He, Z., Xiong, J., Kent, A. D., Deng, Y., Xue, K., Wang, G., Wu, L., Van Nostrand, J. D., & Zhou, J. (2014). Distinct responses of soil microbial communities to elevated CO₂ and O₃ in a soybean agro-ecosystem. *ISME Journal*, 8(3), 714–726.
<https://doi.org/10.1038/ismej.2013.177>
- He, Z., Xu, M., Deng, Y., Kang, S., Kellogg, L., Wu, L., Van Nostrand, J. D., Hobbie, S. E., Reich, P. B., & Zhou, J. (2010). Metagenomic analysis reveals a marked divergence in the structure of belowground microbial communities at elevated CO₂. *Ecology Letters*, 13(5), 564–575. <https://doi.org/10.1111/j.1461-0248.2010.01453.x>
- Hong, Y., Dover, S. L., Cole, T. E., Brasier, C. M., & Buck, K. W. (1999). Multiple mitochondrial viruses in an isolate of the Dutch elm disease fungus *Ophiostoma novo-ulmi*. *Virology*, 258(1), 118–127. <https://doi.org/10.1006/viro.1999.9691>
- Huerta-Cepas, J., Szklarczyk, D., Forslund, K., Cook, H., Heller, D., Walter, M. C., Rattei, T., Mende, D. R., Sunagawa, S., Kuhn, M., Jensen, L. J., Von Mering, C., & Bork, P. (2016). eggNOG 4.5: A hierarchical orthology framework with improved functional annotations for eukaryotic, prokaryotic and viral sequences. *Nucleic Acids Research*, 44(D1), D286–D293. <https://doi.org/10.1093/nar/gkv1248>
- Hyatt, D., Chen, G.-L., LoCascio, P. F., Land, M. L., Larimer, F. W., & Hauser, L. J. (2010). Integrated nr Database in Protein Annotation System and Its Localization. *BMC Bioinformatics*, 11(119), 1–11. <http://dx.doi.org/10.1016/B978-0-12-407863-5.00023-5>
[X%5Cnhttp://www.nature.com/doifinder/10.1038/ismej.2009.79](http://www.nature.com/doifinder/10.1038/ismej.2009.79)
[%5Cnhttp://www.nature.com/doifinder/10.1038/nature09916](http://www.nature.com/doifinder/10.1038/nature09916)
[%5Cnhttp://dx.doi.org/10.1038/srep2598](http://dx.doi.org/10.1038/srep2598)
[2%5Cnhttp://dx.doi.org/10.1038/ismej.2010.144](http://dx.doi.org/10.1038/ismej.2010.144)
[%5Cnhttp](http://dx.doi.org/10.1038/ismej.2010.144)
- Idso, K. (1994). Plant responses to atmospheric CO₂ enrichment in the face of environmental constraints: a review of the past 10 years' research. *Agricultural and Forest Meteorology*, 69(3–4), 153–203. [https://doi.org/10.1016/0168-1923\(94\)90025-6](https://doi.org/10.1016/0168-1923(94)90025-6)
- Illumina. (2019). bcl2fastq2 Conversion Software v2.20.
<https://support.illumina.com/downloads/bcl2fastq-conversion-software-v2-20.html>
- IPCC. (2021). Technical Summary. Contribution of Working Group I to the Sixth

- Assessment Report of the Intergovernmental Panel on Climate Change. In V. Masson-Delmotte, P. Zhai, A. Pirani, S. L. Connors, C. Péan, S. Berger, N. Caud, Y. Chen, L. Goldfarb, M. I. Gomis, M. Huang, K. Leitzell, E. Lonnoy, J. B. R. Matthews, T. K. Mycock, T. Waterfield, O. Yelekcy, R. Yu, & B. Zhou (Eds.), *Summary for Policymakers. In: Climate Change 2021: The Physical Science Basis. Contribution of Working Group I to the Sixth Assessment Report of the Intergovernmental Panel on Climate Change* (In Press). Cambridge University Press.
- Jäger, H. J., Schmidt, S. W., Kammann, C., Grunhage, L., Muller, C., & Hanewald, K. (2003). The University of Giessen Free-Air Carbon Dioxide Enrichment study: Description of the experimental site and of a new enrichment system. *Journal of Applied Botany-Angewandte Botanik*, 77(5–6), 117–127.
- Jia, X., Wang, W., Chen, Z., He, Y., & Liu, J. (2014). Concentrations of secondary metabolites in tissues and root exudates of wheat seedlings changed under elevated atmospheric CO₂ and cadmium-contaminated soils. *Environmental and Experimental Botany*, 107, 134–143.
<https://doi.org/10.1016/j.envexpbot.2014.06.005>
- Johnson, R. M., & Pregitzer, K. S. (2007). Concentration of sugars, phenolic acids, and amino acids in forest soils exposed to elevated atmospheric CO₂ and O₃. *Soil Biology and Biochemistry*, 39(12), 3159–3166.
<https://doi.org/10.1016/j.soilbio.2007.07.010>
- Jolliffe, I. T., & Cadima, J. (2016). Principal component analysis : a review and recent developments Subject Areas. *Phil.Trans.R.Soc.A*, 374(20150202), 1–16.
- Jongen, M., Jones, M. B., Hebeisen, T., Blum, H., & Hendrey, G. (1995). The effects of elevated CO₂ concentrations on the root growth of *Lolium perenne* and *Trifolium repens* grown in a FACE* system. *Global Change Biology*, 1, 361–371.
- Kammann, C., Müller, C., Grünhage, L., & Jäger, H. J. (2008). Elevated CO₂ stimulates N₂O emissions in permanent grassland. *Soil Biology & Biochemistry*, 40, 2194–2205. <https://doi.org/10.1016/j.soilbio.2008.04.012>
- Kanehisa, M., & Goto, S. (2000). KEGG: Kyoto Encyclopedia of Genes and Genomes. *Nucleic Acids Research*, 28(1), 27–30. <https://doi.org/10.3892/ol.2020.11439>
- Kang, D. D., Li, F., Kirton, E., Thomas, A., Egan, R., An, H., & Wang, Z. (2019). MetaBAT 2: An adaptive binning algorithm for robust and efficient genome reconstruction from metagenome assemblies. *PeerJ*, 2019(7), 1–13. <https://doi.org/10.7717/peerj.7359>
- Kimball, B. A. (1983). Carbon dioxide and agricultural yield: An assemblage and analysis of 430 prior observations. *Agronomy Journal*, 75(5), 779. <https://doi.org/10.2134/agronj1983.00021962007500050014x>

- Kimball, B. A. (2016). Crop responses to elevated CO₂ and interactions with H₂O, N, and temperature. *Current Opinion in Plant Biology*, 31, 36–43. <https://doi.org/10.1016/j.pbi.2016.03.006>
- Krishnamurthy, S. R. (2017). Expansion of Microbial Virology by Impetus of the Reduction of Viral Dark Matter [Washington University in St. Louis]. In *Arts & Sciences Electronic Theses and Dissertations*. <https://doi.org/10.7936/K7VX0FXS>
- Krupovic, M., Dolja, V. V., & Koonin, E. V. (2020). The LUCA and its complex virome. *Nature Reviews Microbiology*, 18(11), 661–670. <https://doi.org/10.1038/s41579-020-0408-x>
- Lahti, L., & Shetty, S. (2019). *microbiome R package*. url: <http://microbiome.github.io>
- Lane, D. J. (1991). 16S/23S rRNA sequencing. In E. Stackebrandt & M. Goodfellow (Eds.), *Nucleic Acid Techniques in Bacterial Systematics* (pp. 115–175). John Wiley and Sons.
- Langmead, B., & Salzberg, S. L. (2012). Fast gapped-read alignment with Bowtie 2. *Nature Methods*, 9(4), 357–359. <https://doi.org/10.1038/nmeth.1923>
- Laslett, D., & Canback, B. (2004). ARAGORN, a program to detect tRNA genes and tmRNA genes in nucleotide sequences. *Nucleic Acids Research*, 32(1), 11–16. <https://doi.org/10.1093/nar/gkh152>
- Le Roux, X., Bouskill, N. J., Niboyet, A., Barthes, L., Dijkstra, P., Field, C. B., Hungate, B. A., Lerondelle, C., Pommier, T., Tang, J., Terada, A., Tournay, M., & Poly, F. (2016). Predicting the responses of soil nitrite-oxidizers to multi-factorial global change: A trait-based approach. *Frontiers in Microbiology*, 7(MAY), 1–13. <https://doi.org/10.3389/fmicb.2016.00628>
- Lee, S. H., & Kang, H. (2016). Elevated CO₂ causes a change in microbial communities of rhizosphere and bulk soil of salt marsh system. *Applied Soil Ecology*, 108, 307–314. <https://doi.org/10.1016/j.apsoil.2016.09.009>
- Lee, S. H., Kim, S. Y., Ding, W., & Kang, H. (2015). Impact of elevated CO₂ and N addition on bacteria, fungi, and archaea in a marsh ecosystem with various types of plants. *Applied Microbiology and Biotechnology*, 99(12), 5295–5305. <https://doi.org/10.1007/s00253-015-6385-8>
- Leviviridae. (2012). In *Virus Taxonomy* (pp. 1035–1043). Elsevier. <https://doi.org/10.1016/B978-0-12-384684-6.00089-6>
- Li, D., Liu, C. M., Luo, R., Sadakane, K., & Lam, T. W. (2015). MEGAHIT: An ultra-fast single-node solution for large and complex metagenomics assembly via succinct de Bruijn graph. *Bioinformatics*, 31(10), 1674–1676. <https://doi.org/10.1093/bioinformatics/btv033>
- Liu, X. J. A., Sun, J., Mau, R. L., Finley, B. K., Compson, Z. G., van Gestel, N., Brown,

- J. R., Schwartz, E., Dijkstra, P., & Hungate, B. A. (2017). Labile carbon input determines the direction and magnitude of the priming effect. *Applied Soil Ecology*, 109, 7–13. <https://doi.org/10.1016/j.apsoil.2016.10.002>
- Martino, C., Morton, J. T., Marotz, C. A., Thompson, L. R., Tripathi, A., Knight, R., & Zengler, K. (2019). A Novel Sparse Compositional Technique Reveals Microbial Perturbations. *MSystems*, 4(1), e00016-19.
- McMurdie, P. J., & Holmes, S. (2013). Phyloseq: An R package for reproducible interactive analysis and graphics of microbiome census data. *PLoS ONE*, 8(4), e61217. <https://doi.org/10.1371/journal.pone.0061217>
- Mettel, C., Kim, Y., Shrestha, P. M., & Liesack, W. (2010). Extraction of mRNA from soil. *Applied and Environmental Microbiology*, 76(17), 5995–6000. <https://doi.org/10.1128/AEM.03047-09>
- Morrissey, E. M., McHugh, T. A., Preteska, L., Hayer, M., Dijkstra, P., Hungate, B. A., & Schwartz, E. (2015). Dynamics of extracellular DNA decomposition and bacterial community composition in soil. *Soil Biology and Biochemistry*, 86, 42–49. <https://doi.org/10.1016/j.soilbio.2015.03.020>
- Moser, G., Gorenflo, A., Brenzinger, K., Keidel, L., Braker, G., Marhan, S., Clough, T. J., & Müller, C. (2018). Explaining the doubling of N₂O emissions under elevated CO₂ in the Giessen FACE via in-field 15N tracing. *Global Change Biology*, 24(9), 3897–3910. <https://doi.org/10.1111/gcb.14136>
- Müller, C., Rütting, T., Abbasi, M. K., Laughlin, R. J., Kammann, C., Clough, T. J., Sherlock, R. R., Kattge, J., Jäger, H. J., Watson, C. J., & Stevens, R. J. (2009). Effect of elevated CO₂ on soil N dynamics in a temperate grassland soil. *Soil Biology and Biochemistry*, 41(9), 1996–2001. <https://doi.org/10.1016/j.soilbio.2009.07.003>
- Niklaus, P. A., & Falloon, P. (2006). Estimating soil carbon sequestration under elevated CO₂ by combining carbon isotope labelling with soil carbon cycle modelling. *Global Change Biology*, 12(10), 1909–1921. <https://doi.org/10.1111/j.1365-2486.2006.01215.x>
- Owensby, C. E., Ham, J. M., Knapp, A. K., Bremer, D., & Auen, L. M. (1997). Water vapour fluxes and their impact under elevated CO₂ in a C₄-tallgrass prairie. *Global Change Biology*, 3(3), 189–195. <https://doi.org/10.1046/j.1365-2486.1997.00084.x>
- Padhy, S. R., Bhattacharyya, P., Nayak, A. K., Dash, P. K., Roy, K. S., Baig, M. J., & Mohapatra, T. (2020). Key metabolic pathways of Sulfur metabolism and bacterial diversity under elevated CO₂ and temperature in lowland rice: A metagenomic approach. *Geomicrobiology Journal*, 37(1), 13–21. <https://doi.org/10.1080/01490451.2019.1657992>
- Parks, D. H., Imelfort, M., Skennerton, C. T., Hugenholtz, P., & Tyson, G. W. (2015).

- CheckM: Assessing the quality of microbial genomes recovered from isolates, single cells, and metagenomes. *Genome Research*, 25(7), 1043–1055. <https://doi.org/10.1101/gr.186072.114>
- Phillips, R. P., Meier, I. C., Bernhardt, E. S., Grandy, A. S., Wickings, K., & Finzi, A. C. (2012). Roots and fungi accelerate carbon and nitrogen cycling in forests exposed to elevated CO₂. *Ecology Letters*, 15(9), 1042–1049. <https://doi.org/10.1111/j.1461-0248.2012.01827.x>
- Pratama, A. A., & van Elsas, J. D. (2018). The ‘Neglected’ Soil Virome – Potential Role and Impact. *Trends in Microbiology*, 26(8), 649–662. <https://doi.org/10.1016/j.tim.2017.12.004>
- Puente-Sánchez, F., García-García, N., & Tamames, J. (2020). SQMtools: automated processing and visual analysis of ‘omics data with R and anvio. *BMC Bioinformatics*, 21(1), 358. <https://doi.org/10.1186/s12859-020-03703-2>
- Qiao, N., Schaefer, D., Blagodatskaya, E., Zou, X., Xu, X., & Kuzyakov, Y. (2014). Labile carbon retention compensates for CO₂ released by priming in forest soils. *Global Change Biology*, 20(6), 1943–1954. <https://doi.org/10.1111/gcb.12458>
- Regan, K., Kammann, C., Hartung, K., Lenhart, K., Müller, C., Philippot, L., Kandeler, E., & Marhan, S. (2011). Can differences in microbial abundances help explain enhanced N₂O emissions in a permanent grassland under elevated atmospheric CO₂? *Global Change Biology*, 17(10), 3176–3186. <https://doi.org/10.1111/j.1365-2486.2011.02470.x>
- Rosado-Porto, D., Ratering, S., Cardinale, M., Maisinger, C., Moser, G., Deppe, M., Müller, C., & Schnell, S. (2021). Elevated Atmospheric CO₂ Modifies Mostly the Metabolic Active Rhizosphere Soil Microbiome in the Giessen FACE Experiment. *Microbial Ecology*. <https://doi.org/10.1007/s00248-021-01791-y>
- Santos-Medellin, C., Zinke, L. A., ter Horst, A. M., Gelardi, D. L., Parikh, S. J., & Emerson, J. B. (2021). Viromes outperform total metagenomes in revealing the spatiotemporal patterns of agricultural soil viral communities. *ISME Journal*, 15(7), 1956–1970. <https://doi.org/10.1038/s41396-021-00897-y>
- Sawilowsky, S. S. (2009). New Effect Size Rules of Thumb. *Journal of Modern Applied Statistical Methods*, 8(2), 597–599. <https://doi.org/10.22237/jmasm/1257035100>
- Schmieder, R., & Edwards, R. (2011). Quality control and preprocessing of metagenomic datasets. *Bioinformatics*, 27(6), 863–864. <https://doi.org/10.1093/bioinformatics/btr026>
- Seemann, T. (2014). Prokka: Rapid prokaryotic genome annotation. *Bioinformatics*, 30(14), 2068–2069. <https://doi.org/10.1093/bioinformatics/btu153>
- Sharma, R., & Sharma, P. K. (2018). Metatranscriptome sequencing and analysis of

- agriculture soil provided significant insights about the microbial community structure and function. *Ecological Genetics and Genomics*, 6(September 2017), 9–15. <https://doi.org/10.1016/j.egg.2017.10.001>
- Simonin, M., Le Roux, X., Poly, F., Lerondelle, C., Hungate, B. A., Nunan, N., & Niboyet, A. (2015). Coupling between and among ammonia oxidizers and nitrite oxidizers in grassland mesocosms Submitted to elevated CO₂ and nitrogen supply. *Microbial Ecology*, 70(3), 809–818. <https://doi.org/10.1007/s00248-015-0604-9>
- Siphoviridae. (2012). In *Virus Taxonomy* (pp. 86–98). Elsevier. <https://doi.org/10.1016/B978-0-12-384684-6.00004-5>
- Tamames, J., & Puente-Sánchez, F. (2019). SqueezeMeta, a highly portable, fully automatic metagenomic analysis pipeline. *Frontiers in Microbiology*, 10(JAN), 1–10. <https://doi.org/10.3389/fmicb.2018.03349>
- Trivedi, P., Delgado-Baquerizo, M., Trivedi, C., Hu, H., Anderson, I. C., Jeffries, T. C., Zhou, J., & Singh, B. K. (2016). Microbial regulation of the soil carbon cycle: Evidence from gene-enzyme relationships. *ISME Journal*, 10(11), 2593–2604. <https://doi.org/10.1038/ismej.2016.65>
- Van Groenigen, K. J., Gorissen, A., Six, J., Harris, D., Kuikman, P. J., Van Groenigen, J. W., & Van Kessel, C. (2005). Decomposition of ¹⁴C-labeled roots in a pasture soil exposed to 10 years of elevated CO₂. *Soil Biology and Biochemistry*, 37(3), 497–506. <https://doi.org/10.1016/j.soilbio.2004.08.013>
- Vázquez-Baeza, Y., Pirrung, M., Gonzalez, A., & Knight, R. (2013). EMPoror: A tool for visualizing high-throughput microbial community data. *GigaScience*, 2(16), 1–4. <https://doi.org/10.1186/2047-217X-2-16>
- Vestergard, M., Reinsch, S., Bengtson, P., Ambus, P., & Christensen, S. (2016). Enhanced priming of old, not new soil carbon at elevated atmospheric CO₂. *Soil Biology and Biochemistry*, 100, 140–148. <https://doi.org/10.1016/j.soilbio.2016.06.010>
- Weisburg, W. G., Barns, S. M., Pelletier, D. A., & Lane, D. J. (1991). 16S Ribosomal DNA Amplification for Phylogenetic Study. *Journal of Bacteriology*, 173(2), 697–703. <https://doi.org/n.a>.
- Williamson, K. E., Fuhrmann, J. J., Wommack, K. E., & Radosevich, M. (2017). Viruses in Soil Ecosystems: An Unknown Quantity Within an Unexplored Territory. *Annual Review of Virology*, 4, 201–219. <https://doi.org/10.1146/annurev-virology-101416-041639>
- Wu, Y. W., Simmons, B. A., & Singer, S. W. (2016). MaxBin 2.0: An automated binning algorithm to recover genomes from multiple metagenomic datasets. *Bioinformatics*, 32(4), 605–607. <https://doi.org/10.1093/bioinformatics/btv638>

- Xie, Z., Cadisch, G., Edwards, G., Baggs, E. M., & Blum, H. (2005). Carbon dynamics in a temperate grassland soil after 9 years exposure to elevated CO₂ (Swiss FACE). *Soil Biology and Biochemistry*, 37(7), 1387–1395.
<https://doi.org/10.1016/j.soilbio.2004.12.010>
- Xiong, J., He, Z., Shi, S., Kent, A., Deng, Y., Wu, L., Van Nostrand, J. D., & Zhou, J. (2015). Elevated CO₂ shifts the functional structure and metabolic potentials of soil microbial communities in a C₄ agroecosystem. *Scientific Reports*, 5, 1–9.
<https://doi.org/10.1038/srep09316>
- Xu, M., He, Z., Deng, Y., Wu, L., Van Nostrand, J. D., Hobbie, S. E., Reich, P. B., & Zhou, J. (2013). Elevated CO₂ influences microbial carbon and nitrogen cycling. *BMC Microbiology*, 13(1). <https://doi.org/10.1186/1471-2180-13-124>
- Ye, Y., & Doak, T. G. (2009). A parsimony approach to biological pathway reconstruction/inference for genomes and metagenomes. *PLoS Computational Biology*, 5(8), 1–8. <https://doi.org/10.1371/journal.pcbi.1000465>
- Yu, H., Deng, Y., He, Z., Pendall, E., Carrillo, Y., Wang, S., Jin, D., Wu, L., Wang, A., Xu, Y., Liu, B., Tai, X., & Zhou, J. (2021). Stimulation of soil microbial functioning by elevated CO₂ may surpass effects mediated by irrigation in a semiarid grassland. *Geoderma*, 401(April), 115162. <https://doi.org/10.1016/j.geoderma.2021.115162>
- Yu, H., Deng, Y., He, Z., Van Nostrand, J. D., Wang, S., Jin, D., Wang, A., Wu, L., Wang, D., Tai, X., & Zhou, J. (2018). Elevated CO₂ and warming altered grassland microbial communities in soil top-layers. *Frontiers in Microbiology*, 9(AUG), 1–10.
<https://doi.org/10.3389/fmicb.2018.01790>
- Yu, H., He, Z., Wang, A., Xie, J., Wu, L., Van Nostrand, J. D., Jin, D., Shao, Z., Schadt, C. W., Zhou, J., & Deng, Y. (2018). Divergent responses of forest soil microbial communities under elevated CO₂ in different depths of upper soil layers. *Applied and Environmental Microbiology*, 84(1). <https://doi.org/10.1128/AEM.01694-17>
- Yu, Z., Li, Y., Wang, G., Liu, J., Liu, J., Liu, X., Herbert, S. J., & Jin, J. (2016). Effectiveness of elevated CO₂ mediating bacterial communities in the soybean rhizosphere depends on genotypes. *Agriculture, Ecosystems and Environment*, 231, 229–232. <https://doi.org/10.1016/j.agee.2016.06.043>

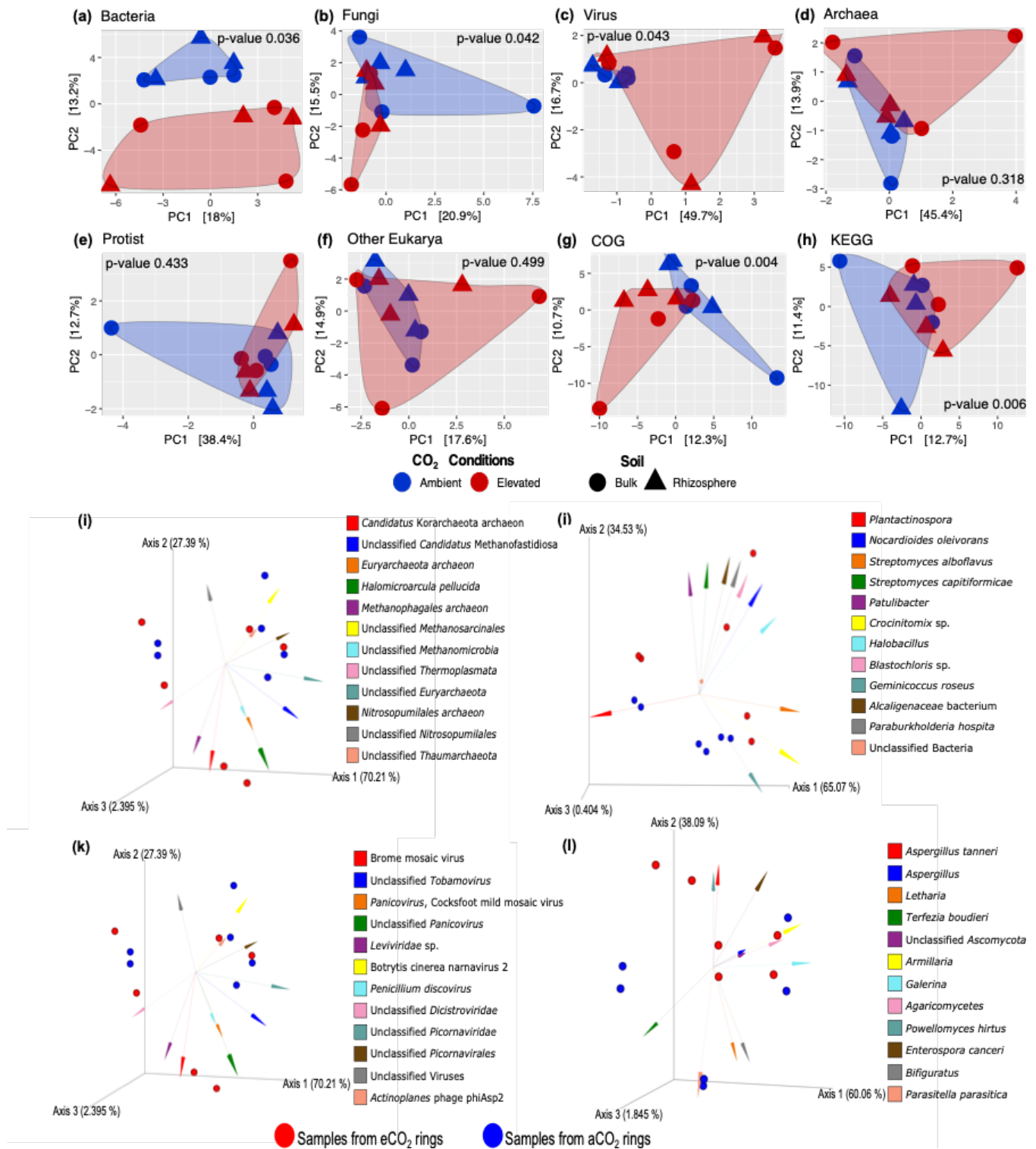


Figure 1. Beta diversity analysis of core features from the Giessen FACE metatranscriptome. Principal Components Analysis (PCA) of (a) archaea, (b) bacteria, (c) virus, (d) fungi, (e) protist, (f) other eukarya, (g) GenBank COG and (h) KEGG functions; p-values obtained from Adonis test. Robust principal-component analysis (RPCA) of (i) archaea, (j) bacteria, (k) virus, (l) fungi. Length and direction of the arrows indicate taxa that contributed the most to the clustering of samples.

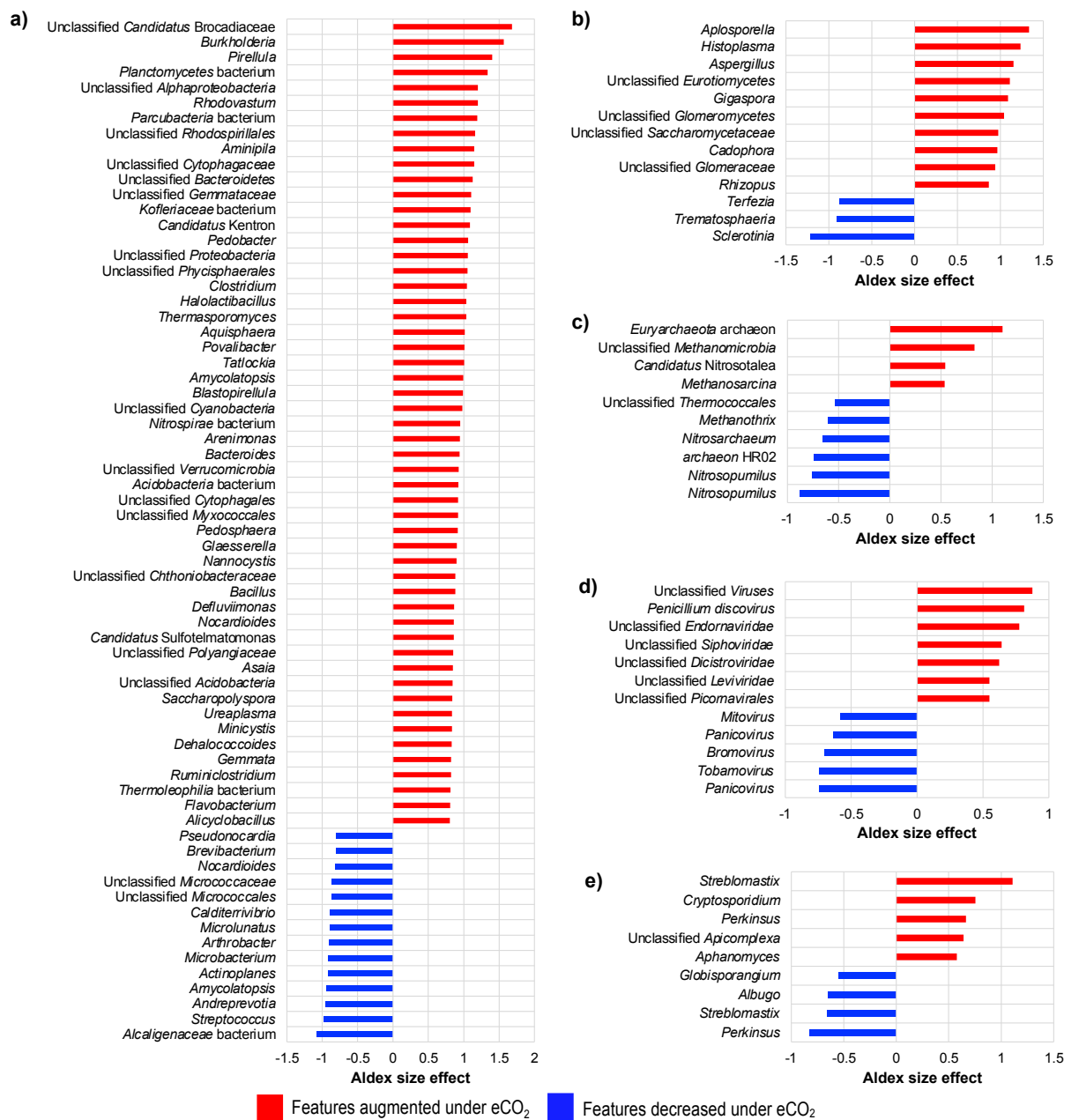


Figure 2. Differential abundances of core features from the Giessen FACE metatranscriptome of (a) bacteria, (b) fungi, (c) archaea, (d) virus and (e) protist. ALDEx2 results of features with an ALDEx effect size > 0.5 using centered log ratio (clr) transformation and the geometric mean abundance of all features.

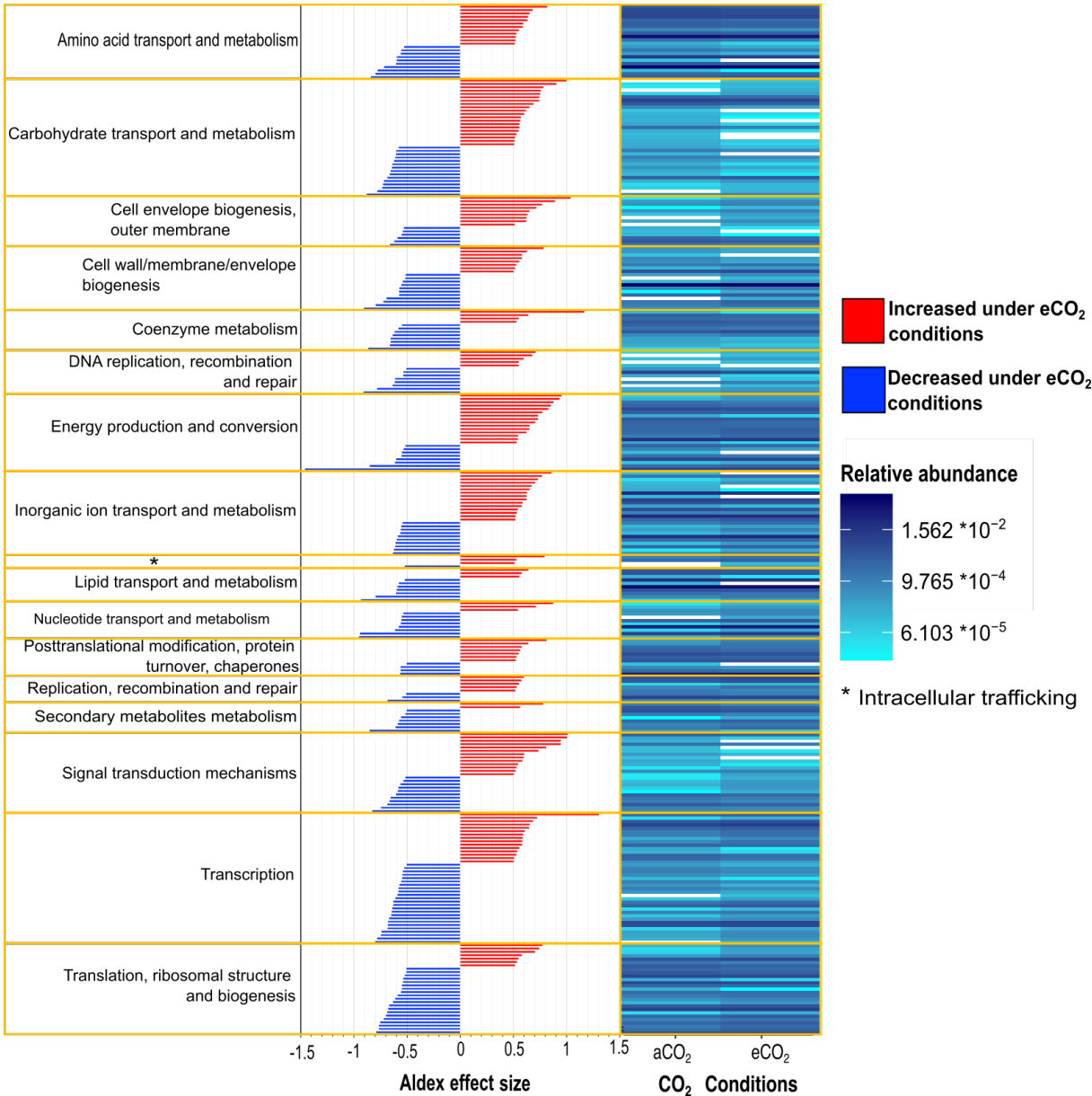


Figure 3. Differential abundance of Giessen FACE metatranscriptome core features annotated against GenBank Clusters of Orthologous Groups (COG) and grouped according COG categories. Results expressed as relative abundance (**right**) and ALDEx effect size (**left**) of features with an ALDEx effect size > 0.5 using centered log ratio (clr) transformation and the geometric mean abundance of all features.

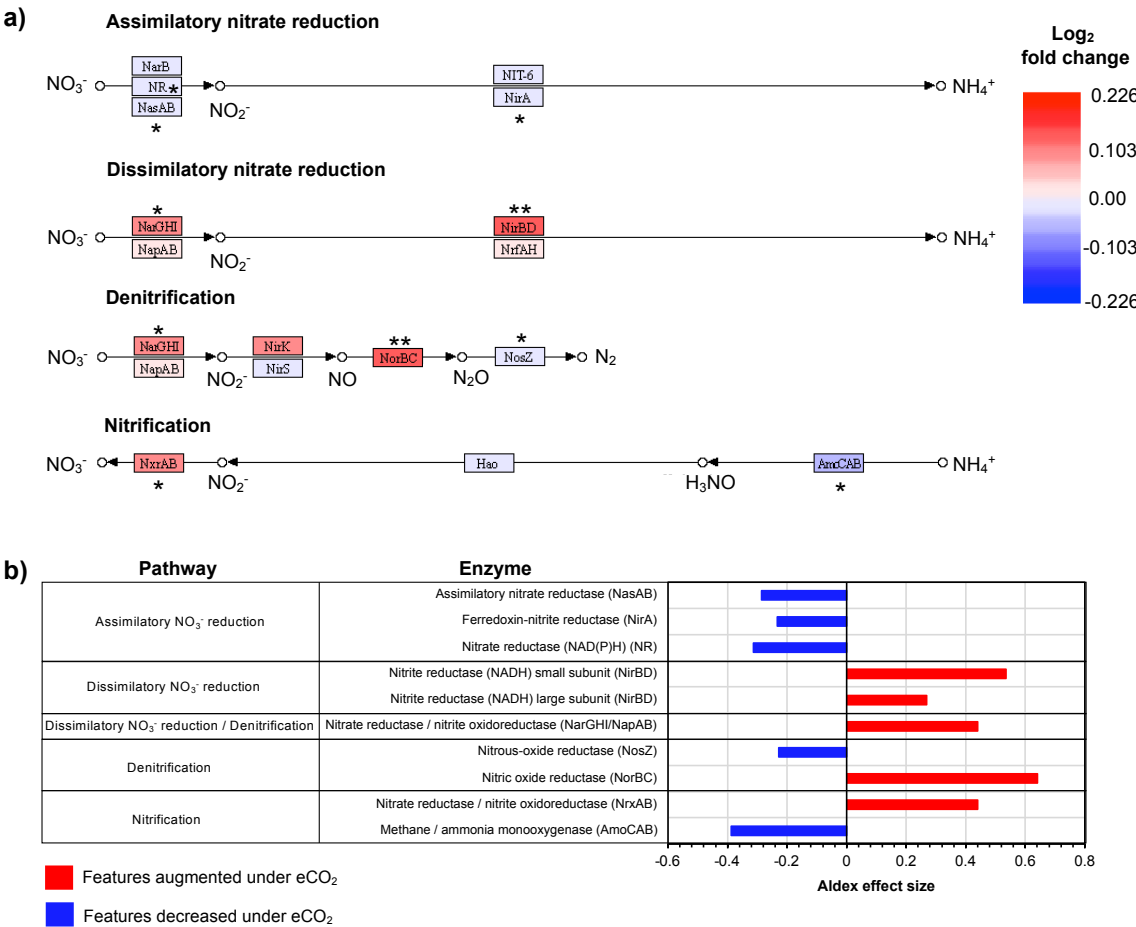


Figure 4. Reconstructed N pathways of NO_3^- assimilatory and dissimilatory reduction, denitrification and nitrification processes. **(a)** N transformations expressed as Log₂ fold change of features as relative abundance. ALDEx effect size: (**) >0.5, (*) >0.2. **(b)** Differential abundance of N cycle enzymes with absolute ALDEx effect sizes > 0.2.

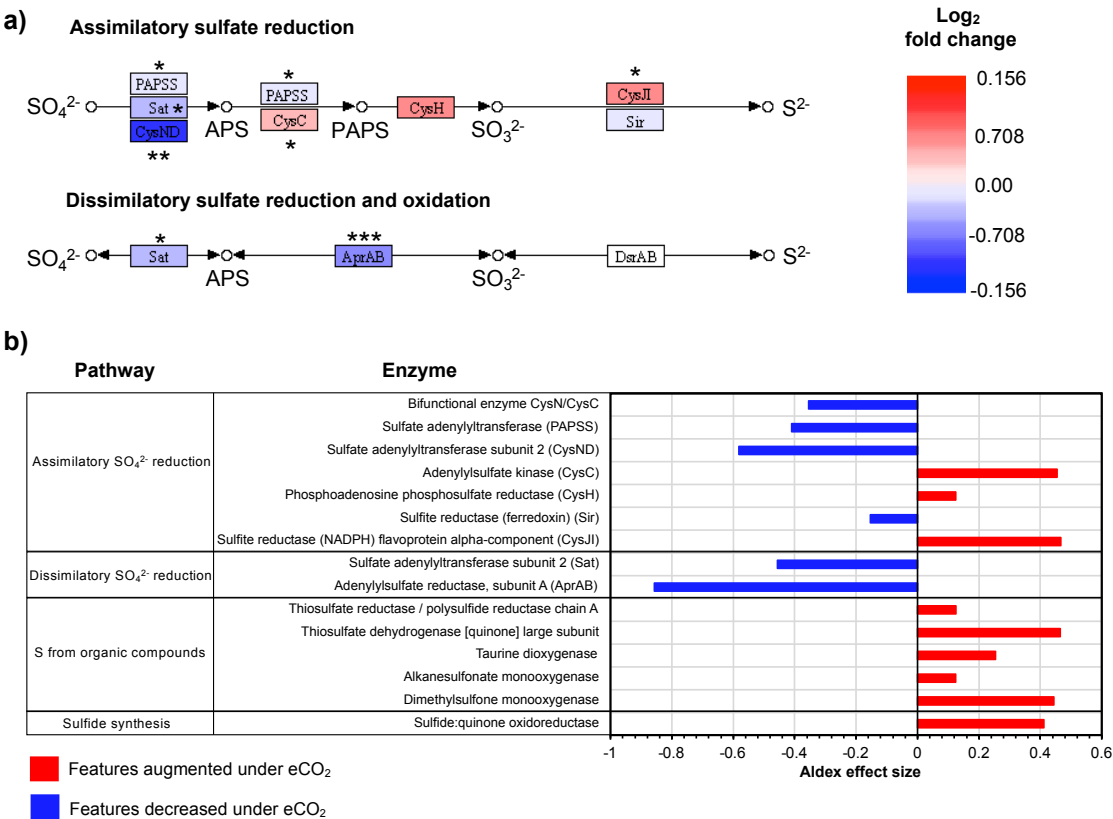


Figure 5. Reconstructed pathways of S metabolism. **(a)** Assimilatory SO₄²⁻ reduction and dissimilatory SO₄²⁻ reduction and oxidation processes expressed as Log₂ fold change of features as relative abundance. ALDEx effect size: (***) >0.8, (**) >0.5, (*) >0.2. **(b)** Differential abundance of S cycle enzymes with absolute ALDEx effect sizes > 0.1 involved in assimilatory SO₄²⁻ reduction, dissimilatory SO₄²⁻ reduction and oxidation, uptake of S from organic compounds and sulfide synthesis

Chapter 4

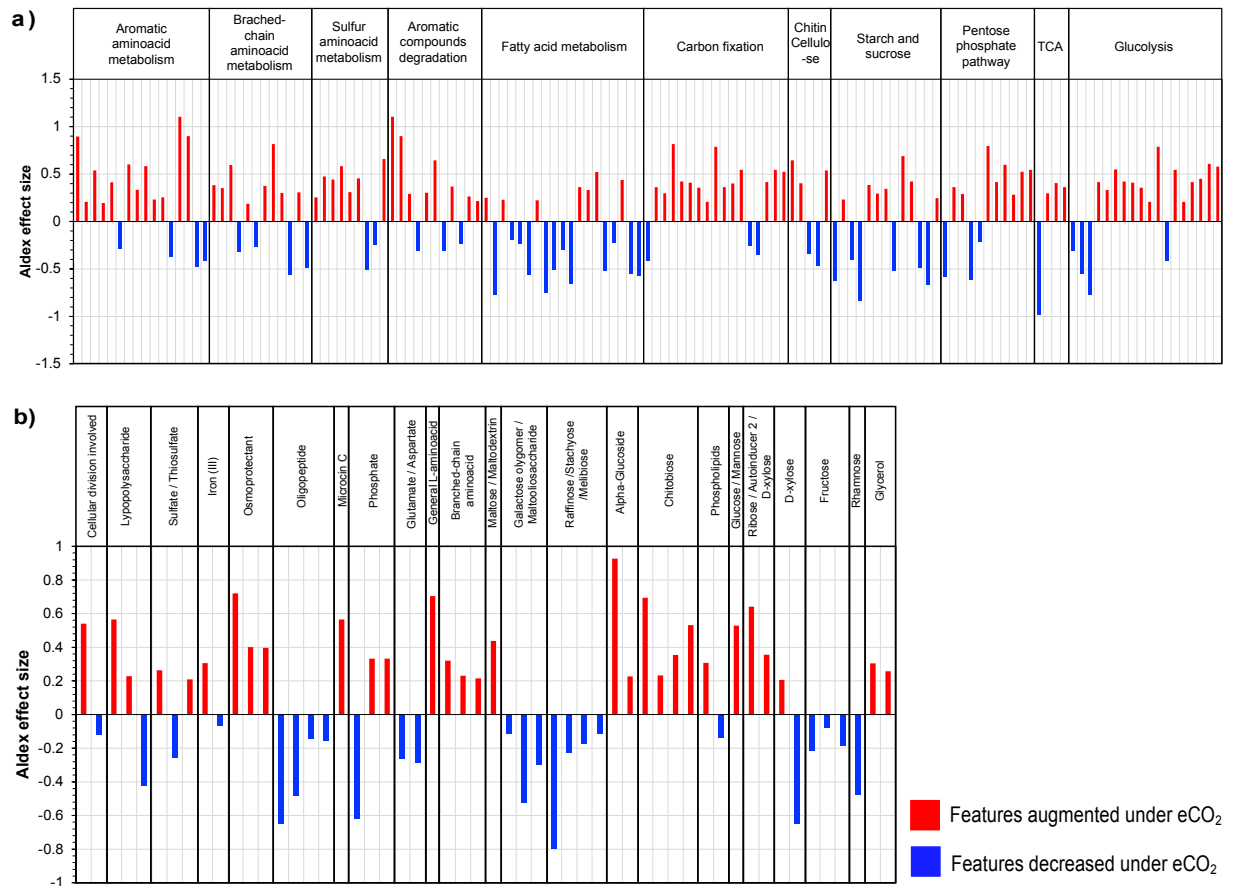
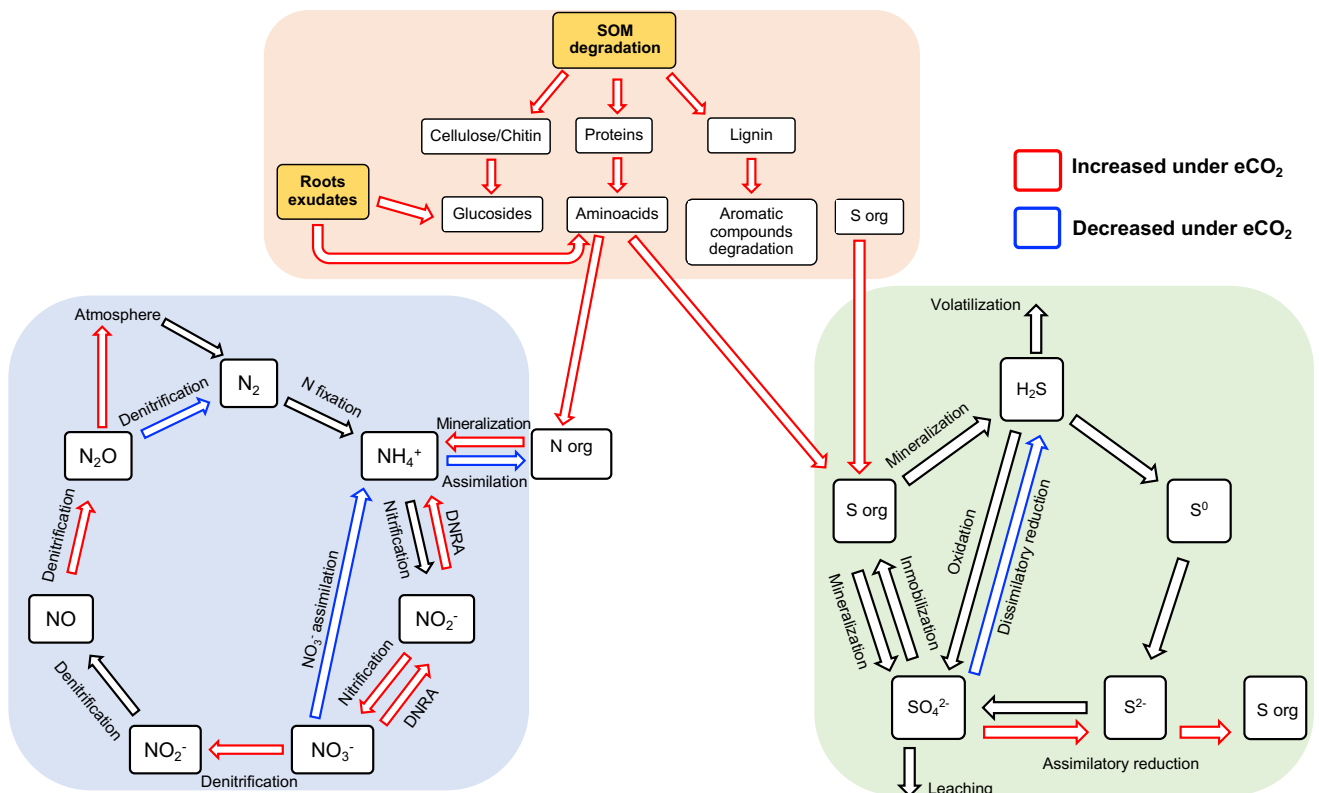


Figure 6. Differential abundance of enzymes grouped by KEGG Orthology (KO) second level of (a) Carbon compounds metabolism and (b) ABC transporters.



Chapter 5 General discussion

The effects of eCO₂ on the soil microbiome have been described in different ecosystems around the globe, demonstrating several changes in its structure and function (Cheng et al., 2011; He et al., 2010, 2014; Simonin et al., 2015; Wang et al., 2017; Xiong et al., 2015; Xu et al., 2013; Yu, Deng, et al., 2018; Yu, He, et al., 2018). Nonetheless, in the Giessen FACE, most of performed research did not show major effects of eCO₂ on the soil microbiome function nor its structure (Brenzinger et al., 2017; de Menezes et al., 2016; Regan et al., 2011), although the changes in soil nutrient dynamics had been already described with great implications in a feedback system which has been causing higher emissions of greenhouse gases as a response to eCO₂ concentrations (Kaleem Abbasi & Müller, 2011; Kammann et al., 2008; Moser et al., 2018; Müller et al., 2009). One key aspect to consider for the detection of how the soil microbiome has been affected by eCO₂ is to target and assess the active soil microorganisms through the utilization of metagenomics analyses based on RNA instead of DNA, as it has been demonstrated by Bei et al. (2019), who was the first to report changes on the microbiome of the Giessen FACE because of eCO₂, applying a metatranscriptomics approach for that purpose. Therefore, in the present work the evaluation of the soil microbiome at the Giessen FACE and Geisenheim VineyardFACE was done through transcriptomics methods, based on 16S rRNA sequencing and the evaluation of functional genes through mRNA sequencing and qPCR.

Moreover, in the current literature about the assessment of soil microbiome changes affected by eCO₂ utilizing NGS technologies have not applied proper methods for the analysis of sequencing outputs, due to a well described fact that is the compositionality of NGS data (Gloor et al., 2017; Susin et al., 2020), for which the procedures proposed by John Aitchison to deal with these kind of data are necessary to be taken into account (Aitchison, 1982, 1986, 2005; Aitchison & Greenacre, 2002; Kaul et al., 2017). Hence, in the present study microbiome's structure of various other environments, differential abundances, correlation with environmental factors and microbe-microbe interactions were mostly evaluated applying compositional data approaches (Fernandes et al., 2013, 2014; Kurtz et al., 2015; Martino et al., 2019; Yoon et al., 2019). Consequently, the use of metatranscriptomics approaches together with proper methods for the analysis of the NGS data permitted to determine several effects of eCO₂ on the soil of the Giessen FACE and Geisenheim VineyardFACE, which included alterations on soil microbiome structure and composition, alongside to changes in the cycling of nutrients (Chapter 2-4).

In both facilities the obtained results showed that the zones under higher influence of vegetation were the ones with the greater changes on the soil microbiome, as it was the case of the Giessen FACE in which the rhizosphere soil structure and composition was significantly affected by eCO₂ (Chapter 2). Likewise, in Geisenheim the green inter-rows were the ones with significant differences between aCO₂ and eCO₂ microbiomes, contrary to the open inter-rows, which did not presented significant changes (Chapter 3). Furthermore, differential abundance analyses from both FACEs performed with ALDEx2 (Fernandes et al., 2014), showed how several taxa were significantly affected, either positively or negatively by eCO₂ (Chapter 2-4). Among the bacterial genera that were stimulated under eCO₂ conditions in both FACEs are *Burkholderia*, *Asticcacaulis*, *Marmoricola*, *Nocardioideis*, *Massilia*, *Bradyrhizobium*, *Acidibacter* and *Legionella*, which might suggest that certain bacterial genera could be more susceptible to increased C supplies to the soil due to eCO₂ concentrations and therefore augmented under these conditions. Moreover, microbe-microbe interaction data obtained from the Geisenheim VineyardFACE demonstrated that eCO₂ produced alterations on bacterial interaction patterns, represented mainly by fewer interactions in eCO₂ rings but more of the strong positive correlations (Chapter 3).

Although initially for both locations it was only evaluated the bacteriome through the amplification of 16S rRNA V4-V5 regions, which showed important differences between aCO₂ and eCO₂ rings (Chapter 2-3). Later, by the sequencing of mRNA the analysis of other taxonomical groups from the Giessen FACE was possible, that included archaea, fungi, virus and protist alongside bacteria as well. A similar approach for the analysis of the functional metatranscriptome was applied by Bei et al. (2019), who described that eCO₂ had significant effects on the functional expression associated to both rhizosphere microbiomes and plant roots; and that abundances of *Eukarya* relative to *Bacteria* were significantly decreased in eCO₂ as well. Nonetheless, the mRNA metatranscriptomic approach used in the present research, allowed to expand the report of Bei et al. (2019), demonstrating that besides the bacteriome, the mycobiome and the virome of the Giessen FACE have undergone through significant changes in their structure and compositions because of eCO₂ concentration, oppositely to soil archaeome and protistome, which were generally not significant affected under these conditions (Chapter 4).

In general terms, the obtained data from both FACEs demonstrated that the soil microbial activity was enhanced under eCO₂ conditions, evidenced in Giessen FACE by a significant increase of CO₂ fluxes in the eCO₂ rings (Chapter 2) and in Geisenheim by

an augmentation of the soil basal respiration but also with the addition of different carbon substrates (Chapter 3). Previous reports of Cheng et al. (2011) and King et al. (2004) have described that eCO₂ affected soil microbial respiration, producing an augmentation of microbial biomass and activities. Nonetheless, 16S rRNA real time qPCR showed different results at both facilities about the way that bacterial populations have been affected by eCO₂ in the areas of higher plant influence, represented by an increment in bacterial 16S rRNA copy number in the Giessen FACE rhizosphere soil but a decrease in Geisenheim green inter-rows at eCO₂ concentrations. These results could reflect the differences in time exposure to eCO₂ conditions in both places, because Giessen FACE and Geisenheim VineyardFACE have been running since 1998 and 2014 respectively, which have given more time to soil bacterial communities in the Giessen FACE to adapt to the environmental pressures which have occurred because of eCO₂, a process that could be still occurring in the VineyardFACE. This trend might also explain the great difference in the number of bacterial taxa significantly correlated with the supplied eCO₂ at both facilities, a total of 119 and 16 genera in Giessen and Geisenheim respectively.

Nonetheless, despite the differences in the way that bacterial taxa have been affected by eCO₂ at both facilities, the data clearly indicated that the overall soil microbial activity has been stimulated under eCO₂ conditions, which denotes that soil microbiomes have been responding to a higher availability of C sources. The aforementioned is supported by the microbial respiration data from Geisenheim, that demonstrated an increased response to the added C substrates L-Arginine, D-Galactose, D-Glucose and N-Acetyl glucosamine. Likewise, functional metatranscriptomics data from Giessen, showed an increment of saccharides and amino acids metabolisms. A direct consequence of this increment of C input is a higher demand for other nutrients especially N, which leads to the phenomenon known as priming effect, that produces an augmentation in the degradation of SOC (Blagodatskaya & Kuzyakov, 2008; Fontaine et al., 2004) (Chapter 1 section 1.3.1). Functional metatranscriptomics results demonstrated that this process has been occurring in the Giessen FACE and the access to protected C sources has become more important in the eCO₂ rings, evidenced by an increment in the expressed genes of enzymes as alpha-N-arabinofuranosidase; endo-1,4-beta-xylanase and chitinase involve in the degradation of cellulose, chitin and lignin as it has been similarly described in other FACE experiments by He et al. (2010, 2014), Xiong et al. (2015) and Yu et al. (2018a; 2018b) (Chapter 4). Although the assessment of enzymes able to degrade complex C sources has not been performed in Geisenheim VineyardFACE, it is very likely that a similar process is occurring in the eCO₂ rings of this facility, supported

also by the observed changes in N metabolism in this FACE, which suggested that soil microorganisms are satisfying their N requirements by mining the SOM.

An obvious consequence of a higher demand of N due to a greater input of C through root exudates and the degradation of the SOM, would be an increment in N₂ fixation rates and metabolism to achieve the enhanced N requirements under eCO₂ conditions. This increment of N₂ fixation genes has been reported by several authors (He et al., 2010, 2014; Xiong et al., 2015; Xu et al., 2013; Yu, Deng, et al., 2018; Yu, He, et al., 2018) and it was hypothesized by Rosado-Porto et al. (2021) (Chapter 2) that a similar process was occurring in the Giessen FACE due to a significant increment in the abundance of certain bacterial genera that belong to families *Rhizobiaceae* and *Xanthobacteraceae* as *Rhizobium*, *Mesorhizobium* and *Phyllobacterium*, which have been widely described as N₂ fixing microorganisms. Nevertheless, the assessment through mRNA of functional genes involved in this process does not support the hypothesis of an increment in N₂ fixation in the Giessen FACE, since the reconstruction of N₂ fixation pathway and differential abundance results from the functional metatranscriptomics outputs did not show significant differences between aCO₂ and eCO₂ conditions (Chapter 4). Comparably, in Geisenheim VineyardFACE the measuring of cDNA from *nifH* mRNA by qPCR, showed that under eCO₂ conditions occurred a significant diminishing of copy numbers of the expression of this gene, indicating no augmentation of N₂ fixing metabolism, but oppositely a decrease of it (Chapter 3). Both data regarding N₂ fixation in both FACE facilities, suggests that similar processes have been happening concerning the sources that soil organisms have been using to fulfill their enhanced N demands. According to the results from both FACEs, the most likely source for N would be the SOM, since the report of Müller et al. (2009) demonstrated that in the Giessen FACE the mineralization of labile organic N became more important under eCO₂ conditions, due to SOM pools contain important protected N stocks, which could indicate that Geisenheim VineyardFACE is undergoing through a similar process. Therefore, the priming effect would be a response to access N reservoirs to meet their greater N demand under conditions of higher C inputs (Derrien et al., 2014; Liu et al., 2017; Vestergard et al., 2016).

The abovementioned would be supported by the results on the analysis of the nitrification process in both FACEs, in which the step from NH₄⁺ oxidation to H₃NO catalyzed by the enzyme ammonia monooxygenase was under eCO₂ conditions either decreased or with no significant changes in the Giessen FACE and the Geisenheim VineyardFACE respectively. This was initially reported by Müller et al. (2009), who portrayed alterations

in the nitrification process under eCO₂, which consisted of a decreased of NH₄⁺ oxidation to NO₃⁻ by 25%. Moreover, pathway reconstruction of the nitrification process in the Giessen FACE (Chapter 4), revealed that although there was a lessening of the mapped enzyme methane/ammonia monooxygenase, responsible for the oxidation of NH₄⁺ to H₃NO, an increment in the expression of the enzyme nitrate reductase/nitrite oxidoreductase occurred, which catalyzes the oxidation of NO₂⁻ to NO₃⁻. These results could be explained by increment of heterotrophic nitrification made by fungi, which has been previously reported by several authors, in which nitrification is mostly performed from the oxidation of organic N as L-asparagine, propionamide, malonylmonohydroxamate and 3-nitropropionate using peroxidase enzymes (Doxtader & Alexander, 1966; Hora & Iyengar, 1960; Marshall & Alexander, 1962). Additionally, more recent studies done by Laughlin et al. 2008 and Zhu et al. 2015 have described in a grassland soil and in subtropical forest respectively, that a significant part of the nitrification was carried out by fungi and that they can simultaneously oxidize NH₄⁺ and organic N. Moreover, many of the fungal taxa able to perform nitrification are members of the genus *Aspergillus* (Doxtader & Alexander, 1966; Hora & Iyengar, 1960; Marshall & Alexander, 1962), one of the most positively affected and with the largest influence in the structure of the Giessen FACE mycobiome (Chapter 4). Therefore, the abovementioned might support the idea of the mining of SOM by soil microorganisms, very likely fungi, in order to fulfill their N requirements under eCO₂, having as consequence alterations in the nitrification process.

Furthermore, metatranscriptomics and qPCR analyses also demonstrated that the denitrification process has undergone through changes in the levels of expression of different genes under eCO₂ conditions, which in the case of the Giessen FACE are directly related with augmentation of N₂O emissions. Initially, Rosado-Porto et al. (2021) based on the prediction of the functional metatranscriptome utilizing PICRUST2 (Douglas et al., 2020), suggested that the increment of different predicted enzymes involved in the denitrification process were linked to the increased emissions of N₂O under eCO₂ conditions (Chapter 2). Which later was confirmed by the reconstruction of the Giessen FACE denitrification pathway, that demonstrated that at eCO₂ concentrations occurred an unbalance between the expression levels of the genes responsible of coding the enzymes nitric oxide reductase (NorBC) and nitrous-oxide reductase (NosZ), in charge of the reduction of NO to N₂O and N₂O to N₂, which lead to the increase in the production of N₂O by denitrifying microorganisms (Chapter 4). This increment of N₂O emissions under eCO₂ conditions was first reported by Kammann et al. (2008) and later by Moser et al. (2018) by applying a ¹⁵N approach detailed the different sources of these increased

emissions. According to Moser et al. (2018), in the case of the denitrification, it occurred a rise of 2.09-fold of N_2O emissions mostly because of the oxidation of organic N and incomplete reduction in NO_2^- , which would support the idea that soil microorganisms are obtaining their N supplies from SOM and leading to greater N_2O emissions. Although, in Geisenheim VineyardFACE the data on the evaluated genes *nosZ*, *nirK* and *nirS*, did not show the same patterns of change in eCO_2 rings as in the Giessen FACE, it did present alterations in the expression of *nirK* gene (Chapter 3). Which suggests that denitrifying metabolism has undergone through some changes that are needed to be clarified to determine if alterations in the expressions of the other genes involved in denitrification process could lead to higher emissions of GHG.

Beyond the alterations of C and N cycles caused by eCO_2 , functional metatranscriptomics data from the Giessen FACE demonstrated that S cycling has undergone through changes as well, represented mainly by modifications in SO_4^{2-} metabolism and the S sources that have been used by soil organisms under eCO_2 conditions (Chapter 4), alterations that have not been detected before the execution of this study. Proving that the use of functional metatranscriptomics is an important tool for the evaluation of the effects of climate change on the soil microbiome and soil microbial processes, due to it allows to determine a broader array of microbial groups and proteins which permit to develop a better understanding of the effects of environmental stressors on soil microorganisms. Therefore, future microbiome research on the Geisenheim VineyardFACE will need to assess the soil functional metatranscriptome as well, with the aims of expanding the data of the effects of eCO_2 on C and N cycles, but also to evaluate changes in the cycling of other nutrients as S and P and to determine what other microbial groups have been disturbed under these conditions in this facility. Additionally, forthcoming investigations will need to perform more sampling events at different time points to assess the effects of seasonal and vegetation changes in order to create a better picture of the alterations that the soil microbiome and soil microbial processes have been undergoing due to eCO_2 .

In general terms, the results obtained in the present study demonstrated that through the use of a metatranscriptomic approach and applying compositional data analysis it was possible to determine that eCO_2 have affected the soil microbiome and the cycling of C and N from two ecosystems with different times of exposure to eCO_2 concentrations. Nonetheless, it is important to consider that future climatic conditions, according to IPCC latest report, also include rise of global temperatures (IPCC, 2021), factor that is indispensable to be evaluated alongside with eCO_2 , in order to have a better

understanding of future climatic conditions on soil microbiome and its associated processes. Some reports have been already performed to assess the effects of these two environmental factors on the soil microbiome, together and separately in different ecosystems, which have showed various effects and alterations on the microbiome structure and/or microbial process (Padhy et al., 2020; Xue et al., 2016; Yu, Deng, et al., 2018). Therefore, future research in temperate European ecosystems will need to focus on the assessment of the eCO₂ and elevated temperature simultaneously, as it is currently happening in the Giessen temperature FACE and from which some initial results will be given in the forthcoming year.

References

- Aitchison, J. (1982). The Statistical Analysis of Compositional Data. *Journal Of the Royal Statistical Society. Series B (Methodological)*, 44(2), 139–177. <https://doi.org/10.1007/978-94-009-4109-0>
- Aitchison, J. (1986). Book review. In *The Statistical Analysis of Compositional Data (XII)*. Chapman and Hall. <https://doi.org/10.1007/bf01187862>
- Aitchison, J. (2005). A Concise Guide to Compositional Data Analysis. *Proceedings of CoDaWork05*, 134. http://ima.udg.edu/Activitats/CoDaWork05/A_concise_guide_to_compositional_data_analysis.pdf
- Aitchison, J., & Greenacre, M. (2002). Biplots of compositional data. *Journal of the Royal Statistical Society. Series C: Applied Statistics*, 51(4), 375–392. <https://doi.org/10.1111/1467-9876.00275>
- Bei, Q., Moser, G., Wu, X., Müller, C., & Liesack, W. (2019). Metatranscriptomics reveals climate change effects on the rhizosphere microbiomes in European grassland. *Soil Biology and Biochemistry*, 138(July), 1–10. <https://doi.org/10.1016/j.soilbio.2019.107604>
- Blagodatskaya, E., & Kuzyakov, Y. (2008). Mechanisms of real and apparent priming effects and their dependence on soil microbial biomass and community structure: Critical review. *Biology and Fertility of Soils*, 45(2), 115–131. <https://doi.org/10.1007/s00374-008-0334-y>
- Brenzinger, K., Kujala, K., Horn, M. A., Moser, G., Guillet, C., Kammann, C., Müller, C., & Braker, G. (2017). Soil conditions rather than long-term exposure to elevated CO₂ affect soil microbial communities associated with N-cycling. *Frontiers in Microbiology*, 8, 1–14. <https://doi.org/10.3389/fmicb.2017.01976>

- Cheng, L., Booker, F. L., Burkey, K. O., Tu, C., da Shew, H. D., Rufty, T. W., Fiscus, E. L., Deforest, J. L., & Hu, S. (2011). Soil microbial responses to elevated CO₂ and O₃ in a nitrogen-aggrading agroecosystem. *PLoS ONE*, 6(6), e21377. <https://doi.org/10.1371/journal.pone.0021377>
- de Menezes, A. B., Müller, C., Clipson, N., & Doyle, E. (2016). The soil microbiome at the Gi-FACE experiment responds to a moisture gradient but not to CO₂ enrichment. *Microbiology*, 162, 1572–1582. <https://doi.org/10.1099/mic.0.000341>
- Derrien, D., Plain, C., Courty, P. E., Gelhaye, L., Moerdijk-Poortvliet, T. C. W., Thomas, F., Versini, A., Zeller, B., Koutika, L. S., Boschker, H. T. S., & Epron, D. (2014). Does the addition of labile substrate destabilise old soil organic matter? *Soil Biology and Biochemistry*, 76, 149–160. <https://doi.org/10.1016/j.soilbio.2014.04.030>
- Douglas, G. M., Maffei, V. J., Zaneveld, J., Yurgel, S. N., Brown, J. R., Taylor, C. M., Huttenhower, C., & Langille, M. G. I. (2020). PICRUSt2 for prediction of metagenome functions. *Nature Biotechnology*, 38(6), 669–673. <https://doi.org/10.1038/s41587-020-0550-z>
- Doxtader, K. G., & Alexander, M. (1966). Nitrification by growing and replacement cultures of *Aspergillus*. *Canadian Journal of Microbiology*, 12(4), 807–815. <https://doi.org/10.1139/m66-109>
- Fernandes, A. D., Macklaim, J. M., Linn, T. G., Reid, G., & Gloor, G. B. (2013). ANOVA-Like Differential Expression (ALDEx) Analysis for Mixed Population RNA-Seq. *PLoS ONE*, 8(7), e67019. <https://doi.org/10.1371/journal.pone.0067019>
- Fernandes, A. D., Reid, J. N. S., Macklaim, J. M., McMurrough, T. A., Edgell, D. R., & Gloor, G. B. (2014). Unifying the analysis of high-throughput sequencing datasets: Characterizing RNA-seq, 16S rRNA gene sequencing and selective growth experiments by compositional data analysis. *Microbiome*, 2(1), 1–13. <https://doi.org/10.1186/2049-2618-2-15>
- Fontaine, S., Bardoux, G., Abbadie, L., & Mariotti, A. (2004). Carbon input to soil may decrease soil carbon content. *Ecology Letters*, 7(4), 314–320. <https://doi.org/10.1111/j.1461-0248.2004.00579.x>
- Gloor, G. B., Macklaim, J. M., Pawlowsky-Glahn, V., & Egozcue, J. J. (2017). Microbiome datasets are compositional: And this is not optional. *Frontiers in Microbiology*, 8(NOV), 1–6. <https://doi.org/10.3389/fmicb.2017.02224>
- He, Z., Xiong, J., Kent, A. D., Deng, Y., Xue, K., Wang, G., Wu, L., Van Nostrand, J. D., & Zhou, J. (2014). Distinct responses of soil microbial communities to elevated CO₂ and O₃ in a soybean agro-ecosystem. *ISME Journal*, 8(3), 714–726. <https://doi.org/10.1038/ismej.2013.177>

- He, Z., Xu, M., Deng, Y., Kang, S., Kellogg, L., Wu, L., Van Nostrand, J. D., Hobbie, S. E., Reich, P. B., & Zhou, J. (2010). Metagenomic analysis reveals a marked divergence in the structure of belowground microbial communities at elevated CO₂. *Ecology Letters*, 13(5), 564–575. <https://doi.org/10.1111/j.1461-0248.2010.01453.x>
- Hora, T. S., & Iyengar, M. R. S. (1960). Nitrification by soil fungi. *Archiv Für Mikrobiologie*, 35(3), 252–257. <https://doi.org/10.1007/BF00446826>
- IPCC. (2021). Technical Summary. Contribution of Working Group I to the Sixth Assessment Report of the Intergovernmental Panel on Climate Change. In V. Masson-Delmotte, P. Zhai, A. Pirani, S. L. Connors, C. Péan, S. Berger, N. Caud, Y. Chen, L. Goldfarb, M. I. Gomis, M. Huang, K. Leitzell, E. Lonnoy, J. B. R. Matthews, T. K. Mycock, T. Waterfield, O. Yelekcy, R. Yu, & B. Zhous (Eds.), *Summary for Policymakers. In: Climate Change 2021: The Physical Science Basis. Contribution of Working Group I to the Sixth Assessment Report of the Intergovernmental Panel on Climate Change* (In Press). Cambridge University Press.
- Kaleem Abbasi, M., & Müller, C. (2011). Trace gas fluxes of CO₂, CH₄ and N₂O in a permanent grassland soil exposed to elevated CO₂ in the Giessen FACE study. *Atmospheric Chemistry and Physics*, 11(17), 9333–9342. <https://doi.org/10.5194/acp-11-9333-2011>
- Kammann, C., Müller, C., Grünhage, L., & Jäger, H. J. (2008). Elevated CO₂ stimulates N₂O emissions in permanent grassland. *Soil Biology & Biochemistry*, 40, 2194–2205. <https://doi.org/10.1016/j.soilbio.2008.04.012>
- Kaul, A., Mandal, S., Davidov, O., & Peddada, S. D. (2017). Analysis of microbiome data in the presence of excess zeros. *Frontiers in Microbiology*, 8(NOV), 1–10. <https://doi.org/10.3389/fmicb.2017.02114>
- King, J. S., Hanson, P. J., Bernhardt, E. S., Deangelis, P., Norby, R. J., & Pregitzer, K. S. (2004). A multiyear synthesis of soil respiration responses to elevated atmospheric CO₂ from four forest FACE experiments. *Global Change Biology*, 10, 1027–1042. <https://doi.org/10.1111/j.1365-2486.2004.00789.x>
- Kurtz, Z. D., Müller, C. L., Miraldi, E. R., Littman, D. R., Blaser, M. J., & Bonneau, R. A. (2015). Sparse and Compositionally Robust Inference of Microbial Ecological Networks. *PLoS Computational Biology*, 11(5), 1–25. <https://doi.org/10.1371/journal.pcbi.1004226>
- Laughlin, R. J., Stevens, R. J., Müller, C., & Watson, C. J. (2008). Evidence that fungi can oxidize NH₄⁺ to NO₃⁻ in a grassland soil. *European Journal of Soil Science*, 59(2), 285–291. <https://doi.org/10.1111/j.1365-2389.2007.00995.x>

- Liu, X. J. A., Sun, J., Mau, R. L., Finley, B. K., Compson, Z. G., van Gestel, N., Brown, J. R., Schwartz, E., Dijkstra, P., & Hungate, B. A. (2017). Labile carbon input determines the direction and magnitude of the priming effect. *Applied Soil Ecology*, 109, 7–13. <https://doi.org/10.1016/j.apsoil.2016.10.002>
- Martino, C., Morton, J. T., Marotz, C. A., Thompson, L. R., Tripathi, A., Knight, R., & Zengler, K. (2019). A Novel Sparse Compositional Technique Reveals Microbial Perturbations. *MSystems*, 4(1), e00016-19.
- Marshall, K. C., & Alexander, M. (1962). Nitrification by *Aspergillus flavus*. *Journal of Bacteriology*, 83(3), 572–578. <https://doi.org/10.1128/jb.83.3.572-578.1962>
- Moser, G., Gorenflo, A., Brenzinger, K., Keidel, L., Braker, G., Marhan, S., Clough, T. J., & Müller, C. (2018). Explaining the doubling of N₂O emissions under elevated CO₂ in the Giessen FACE via in-field ¹⁵N tracing. *Global Change Biology*, 24(9), 3897–3910. <https://doi.org/10.1111/gcb.14136>
- Müller, C., Rütting, T., Abbasi, M. K., Laughlin, R. J., Kammann, C., Clough, T. J., Sherlock, R. R., Kattge, J., Jäger, H. J., Watson, C. J., & Stevens, R. J. (2009). Effect of elevated CO₂ on soil N dynamics in a temperate grassland soil. *Soil Biology and Biochemistry*, 41(9), 1996–2001. <https://doi.org/10.1016/j.soilbio.2009.07.003>
- Padhy, S. R., Bhattacharyya, P., Nayak, A. K., Dash, P. K., Roy, K. S., Baig, M. J., & Mohapatra, T. (2020). Key metabolic pathways of Sulfur metabolism and bacterial diversity under elevated CO₂ and temperature in lowland rice: A metagenomic approach. *Geomicrobiology Journal*, 37(1), 13–21. <https://doi.org/10.1080/01490451.2019.1657992>
- Regan, K., Kammann, C., Hartung, K., Lenhart, K., Müller, C., Philippot, L., Kandeler, E., & Marhan, S. (2011). Can differences in microbial abundances help explain enhanced N₂O emissions in a permanent grassland under elevated atmospheric CO₂? *Global Change Biology*, 17(10), 3176–3186. <https://doi.org/10.1111/j.1365-2486.2011.02470.x>
- Rosado-Porto, D., Ratering, S., Cardinale, M., Maisinger, C., Moser, G., Deppe, M., Müller, C., & Schnell, S. (2021). Elevated Atmospheric CO₂ Modifies Mostly the Metabolic Active Rhizosphere Soil Microbiome in the Giessen FACE Experiment. *Microbial Ecology*. <https://doi.org/10.1007/s00248-021-01791-y>
- Simonin, M., Le Roux, X., Poly, F., Lerondelle, C., Hungate, B. A., Nunan, N., & Niboyet, A. (2015). Coupling between and among ammonia oxidizers and nitrite oxidizers in grassland mesocosms Submitted to elevated CO₂ and nitrogen supply. *Microbial Ecology*, 70(3), 809–818. <https://doi.org/10.1007/s00248-015-0604-9>

- Susin, A., Wang, Y., Lê Cao, K.-A., & Calle, M. L. (2020). Variable selection in microbiome compositional data analysis. *NAR Genomics and Bioinformatics*, 2(2), 5–7. <https://doi.org/10.1093/nargab/lqaa029>
- Vestergard, M., Reinsch, S., Bengtson, P., Ambus, P., & Christensen, S. (2016). Enhanced priming of old, not new soil carbon at elevated atmospheric CO₂. *Soil Biology and Biochemistry*, 100, 140–148. <https://doi.org/10.1016/j.soilbio.2016.06.010>
- Wang, P., Marsh, E. L., Ainsworth, E. A., Leakey, A. D. B., Sheflin, A. M., & Schachtman, D. P. (2017). Shifts in microbial communities in soil, rhizosphere and roots of two major crop systems under elevated CO₂ and O₃. *Scientific Reports*, 7(1), 1–12. <https://doi.org/10.1038/s41598-017-14936-2>
- Xiong, J., He, Z., Shi, S., Kent, A., Deng, Y., Wu, L., Van Nostrand, J. D., & Zhou, J. (2015). Elevated CO₂ shifts the functional structure and metabolic potentials of soil microbial communities in a C₄ agroecosystem. *Scientific Reports*, 5, 1–9. <https://doi.org/10.1038/srep09316>
- Xu, M., He, Z., Deng, Y., Wu, L., Van Nostrand, J. D., Hobbie, S. E., Reich, P. B., & Zhou, J. (2013). Elevated CO₂ influences microbial carbon and nitrogen cycling. *BMC Microbiology*, 13(1). <https://doi.org/10.1186/1471-2180-13-124>
- Xue, K., Xie, J., Zhou, A., Liu, F., Li, D., Wu, L., Deng, Y., He, Z., Van Nostrand, J. D., Luo, Y., & Zhou, J. (2016). Warming alters expressions of microbial functional genes important to ecosystem functioning. *Frontiers in Microbiology*, 7(MAY), 1–13. <https://doi.org/10.3389/fmicb.2016.00668>
- Yoon, G., Gaynanova, I., & Müller, C. L. (2019). Microbial networks in SPRING - Semi-parametric rank-based correlation and partial correlation estimation for quantitative microbiome data. *Frontiers in Genetics*, 10(JUN). <https://doi.org/10.3389/fgene.2019.00516>
- Yu, H., Deng, Y., He, Z., Van Nostrand, J. D., Wang, S., Jin, D., Wang, A., Wu, L., Wang, D., Tai, X., & Zhou, J. (2018a). Elevated CO₂ and Warming Altered Grassland Microbial Communities in Soil Top-Layers. *Frontiers in Microbiology*, 9(AUG), 1–10. <https://doi.org/10.3389/fmicb.2018.01790>
- Yu, H., He, Z., Wang, A., Xie, J., Wu, L., Van Nostrand, J. D., Jin, D., Shao, Z., Schadt, C. W., Zhou, J., & Deng, Y. (2018b). Divergent responses of forest soil microbial communities under elevated CO₂ in different depths of upper soil layers. *Applied and Environmental Microbiology*, 84(1). <https://doi.org/10.1128/AEM>
- Zhu, T., Meng, T., Zhang, J., Zhong, W., Müller, C., & Cai, Z. (2015). Fungi-dominant heterotrophic nitrification in a subtropical forest soil of China. *Journal of Soils and Sediments*, 15(3), 705–709. <https://doi.org/10.1007/s11368-014-1048-4>

Acknowledgements

The accomplishment of this thesis would not have been possible without the contribution of many people and, to all of them, I would like to express my most sincere gratitude.

First of all, to Prof. Dr. Sylvia Schnell, Institute of Applied Microbiology, IFZ, Justus-Liebig University Giessen, for her guidance, patience, support and constant encouraging motivation along the way of this rollercoaster that is the PhD.

To Dr. Stefan Ratering for his advice, comments, and corrections during this process. Also, for introducing me to the wonderful world of bioinformatics and always being open to sharing his knowledge.

To Prof. PhD Christoph Müller and Dr. Gerald Moser and all their research team, for their collaboration, constructive comments, and recommendations with everything related to the Giessen FACE, from the samplings to the revision of the manuscripts.

To the Hochschule Geisenheim University and the Vineyard FACE team, for their help, guidance and, support in the field and data provision.

To Rita Geissler-Plaum and Bellinda Schneider, for their amazing technical assistance. And of course, the staff of the Institute of Applied Microbiology (Renate, Gundula, Katja, Maria, Monika, and Martina).

To Prof. Hernando Sánchez, for giving me the chance and trust of coming to Germany to do this PhD. In the same way, to Pacífico Castro and the Simón Bolívar University for their support.

To Dr. Christian Suárez and Dr. Julián Rojas for their friendship during this road and for making Germany feel as home.

To Santiago Quiroga, Yina Cifuentes, Julia Sacharow, Yulduzhon Abdullaeva, Angel Franco, Corinna Maisinger and all the PhD students that accompanied me during all these years.

To my family in Colombia for their support and words of comfort from the distance. But also, to my adoptive family here in Germany, Ricardo and Babsi, thank you for receiving me into your home.

And last but for sure not least, to my partner “mi compañera galáctica” María Cardenas Alfonso, whom I had the fortune of knowing here in Germany and now I share my life with. Thank you for all your support and trust, even when we both were exhausted, you gave me a lot of strength. Te amo!